

Bench and Large-scale Assessment of Smoke Toxicity.

By

Gabrielle Peck

A thesis submitted in partial fulfilment for the requirements for the degree of
Doctor of Philosophy at the University of Central Lancashire

June 2023

RESEARCH STUDENT DECLARATION FORM

Type of Award: Doctor of philosophy

School: Physical sciences and computing

1. Concurrent registration for two or more academic awards

I declare that while registered as a candidate for the research degree, I have not been a registered candidate or enrolled student for another award of the University or other academic or professional institution

2. Material submitted for another award

I declare that no material contained in the thesis has been used in any other submission for an academic award and is solely my own work

3. Collaboration

Where a candidate's research programme is part of a collaborative project, the thesis must indicate in addition clearly the candidate's individual contribution and the extent of the collaboration. Please state below:

4. Use of a Proof-reader

No proof-reading service was used in the completion of this thesis.

Signature of Candidate

Print name: **Gabrielle Peck**



Abstract

The overall goal of the project was to provide evidence to support the regulation of smoke toxicity in order to reduce death and injury in unwanted fires. This entailed the development of a robust methodology for assessing smoke toxicity on a laboratory bench-scale using the steady state tube furnace (SSTF), ISO/TS 19700, and relating it to the toxicity of large-scale fire tests. A review of the literature relating to bench- and large-scale fire toxicity assessment has been undertaken and is reported.

Research was conducted on a bench-scale to optimise the methodologies developed and assess the current techniques used in smoke toxicity research. In addition, the formation of the main asphyxiants, carbon monoxide (CO) and hydrogen cyanide (HCN), was investigated under different fire conditions. In most cases, where nitrogen was present in the fuel, the formation of HCN mirrored the formation of CO. HCN and CO formation were found to be steady and relatively consistent starting approximately 5 to 7 min after sample ignition. This research was used to test the assumptions related to steady state burning and sampling times stated in ISO/TS 19700.

For smoke toxicity to be regulated as a part of the Construction Product Regulations (CPR), a robust methodology for assessing smoke toxicity for large-scale fires is required as a “reference scenario”. As the current large-scale methods for construction products assess flammability, a revised methodology needed to be developed. In addition, the instrumentation and methodologies for assessing smoke toxicity on a large-scale required development and construction.

To measure the smoke toxicity on a large-scale, gas analysers suitable for operating at large-scale test facilities were required. As no such analysers are commercially available, portable analysers were designed and built. The analysers continuously monitor CO, CO₂ and O₂, with specific sampling of HCN and irritant gases produced during a fire test. The specific sampling was controlled by a mass-flow meter to ensure that equal masses of fire effluent were collected in each sample, and used program-controlled switches for sample collection. To validate the analyser, it was tested alongside the standard SSTF analysers, and used when conducting the research into HCN formation described above.

To identify the fire condition of the test in terms of the equivalence ratio, a phi meter was designed and built for this research, based on modifications to the original design. It was smaller and simpler than the original design, increasing portability and performance. The final apparatus was tested and calibrated using the SSTF where the equivalence ratio is controllable and well-defined. The phi meter was used to investigate the effect of sampling location within the SSTF by studying the equivalence ratio at specific locations inside the apparatus. No significant variation of the equivalence ratio with sampling location was found. The phi meter was successfully used to identify the equivalence ratio during the large-scale fire tests.

The ISO 9705 room corner test was modified to assess smoke toxicity. The novel methodology used either 1 or 2 L-shaped Single Burning Item (SBI) (EN 13823) test rigs placed on a load cell in the centre of the ISO test room. The measurements specified in the ISO 9705 standard from the exhaust duct were recorded throughout the tests. Fire effluent composition was also monitored using the portable gas analysers in the exhaust duct and the doorway of the test room. To enable future gas yield calculations to be made, McCaffrey probes were used with sensitive pressure transducers to estimate the gas flows in and out of the room. The tests aimed to represent a range of fire conditions, from well-ventilated to under-ventilated flaming. Two methods were investigated to replicate different fire conditions: limiting the ventilation; and increasing fuel loading.

Four products, which included non-homogenous and predominantly non-combustible components (plasterboard, OSB, flexible polyurethane foam and electric cables), were burned in the large-scale tests. Under-ventilated flaming occurred in tests with combustible products conducted using two SBI rigs, where well-ventilated flaming had predominated with single SBI rigs. Under-ventilated flaming was not achieved when restricting the ventilation by partially blocking the doorway. These experiments showed that restriction of the ventilation reduced the rate of burning rather than forcing the fire to transition into under-ventilated flaming. This is clearly dependant on the ratio of the heat release from the fuel to the size and heat capacity of the test enclosure.

The fire behaviour of the materials was predicted before testing using ConeTools fire modelling software, using test data from cone calorimetry. As ConeTools had not been written for the novel test layout used, the data was used to create heat release predictions for an SBI test and an ISO room test conducted with the product as a standard wall-lining. ConeTools overestimated the heat release predictions compared to previously reported SBI test data. When used to predict the heat release from products in this study, they were underestimated.

This research has provided key information and methodologies to support the regulation of smoke toxicity within the CPR. It has provided the revised methodologies which would be necessary for ISO/TS 19700 to become a full standard and provided robust research to reinforce existing methodologies. The methodology of testing smoke toxicity on a large-scale has also been enhanced, including details of specific equipment required to assess specific parameters during a large-scale test.

TABLE OF CONTENTS

1	Introduction	1
1.1	Introduction to the project	3
1.2	Layout of the thesis.....	4
1.3	Introduction to Fire toxicity	8
1.3.1	Summary of the subject information provided	8
1.3.2	Characterisation of fires.....	9
1.3.3	Flammability and decomposition process of polymers	13
1.3.4	Fire effluent toxicity.....	17
1.3.5	Expressions of toxicity.....	19
1.3.6	Common toxicants present in fire effluent.....	22
1.3.7	Effect of fire condition on fire toxicity	26
1.3.8	Methods for generating fire effluent.....	27
1.3.9	Methods for quantifying fire effluent.....	34
1.3.10	Comparisons between bench-scale methods.....	35
1.3.11	Fire test regulations within the construction product regulations.....	49
1.3.12	Links between large-scale tests and bench-scale	53
1.4	Choice of bench-scale apparatus	60
2	Method development.....	62
2.1	Selection of materials for study	65
2.2	Method developments for the Steady State Tube furnace	66
2.2.1	Material summary.....	66
2.2.2	Location of standard methodologies used	67
2.2.3	Gap analysis of the ISO/TS 19700	67
2.2.4	Formation of HCN as a function of time during an SSTF run	73
2.2.5	The effects of using supplementary nitrogen to achieve low oxygen environments.	75
2.3	Development of the phi meter	81
2.3.1	Understanding the phi meter.	81
2.3.2	Chemical principles of the phi meter.....	84
2.3.3	Background experimental research.....	84
2.3.4	Schematic designs.....	87
2.3.5	Validation of the phi meter.....	89
2.4	Equivalence ratio inside the SSTF combustion tube.....	93
2.4.1	Results and discussion	93

2.5	Portable gas analysis system.....	96
2.5.1	Description of analysers.....	96
2.5.2	Design and construction	96
2.6	HCN analysis using ion chromatography	98
2.6.1	Generation of HCN samples.....	98
2.6.2	Analysis of HCN in solution	98
2.6.3	Results and comparison	99
2.7	large-scale test design.....	102
2.7.1	Description of the 9705 test.	102
2.7.2	Aims and objectives of the large-scale testing	104
2.7.3	Materials and testing	105
2.7.4	Test layout and fuel load.....	106
2.7.5	Cable test layout	109
2.7.6	Controlling the ventilation of the test	112
2.7.7	Ignition source	114
2.7.8	Predicted parameters	115
2.8	Large-scale test measurements	121
2.8.1	Measurements at the doorway	122
2.8.2	Measurements in the duct.....	126
2.8.3	Measurements in the room	128
2.8.4	Measurement procedure.....	129
3	Results and Discussion	133
3.1	Heptane and propane calibrations	135
3.1.1	Test layout and summary.....	135
3.1.2	Data summary	135
3.2	Plasterboard.....	137
3.2.1	Test layout.....	137
3.2.2	Description of test:.....	137
3.2.3	Heat release measurements:	138
3.2.4	Mass loss measurements:.....	139
3.2.5	Temperature measurements	140
3.2.6	Fire condition	141
3.2.7	O ₂ measurements	142
3.2.8	CO ₂ measurements	143
3.2.9	CO measurements.....	144
3.2.10	CO/CO ₂ ratio.....	145

3.2.11	Summary of test data.....	146
3.3	Oriented strand board (OSB)	147
3.3.1	well-ventilated	147
3.3.2	Under-ventilated with door	156
3.3.3	Under-ventilated (using 2x fuel load)	166
3.3.4	OSB: Data comparison	176
3.4	Cables.....	178
3.4.1	Test layout.....	178
3.4.2	Well-ventilated.....	179
3.4.3	Under-ventilated.....	188
3.4.4	Comparison	195
3.5	Polyurethane.....	196
3.5.1	Test layout.....	196
3.5.2	Well-ventilated.....	196
3.5.3	Under-ventilated.....	205
3.5.4	Comparison of data.....	213
3.6	Summary of tests	214
3.6.1	Time to flashover:	214
3.6.2	Equivalence ratio.....	215
3.6.3	Heat release	216
3.7	Summary of fire effluent toxicity measurement	216
4	Conclusions and future work.....	218
4.1	Steady state tube furnace.....	218
4.2	Phi meter.....	219
4.3	Box analysers	220
4.4	Large-scale test design.....	221
4.5	Large-scale testing: future work	221
4.6	Summary of conclusions	222
	Appendices.....	i

List of abbreviations

AGI = A series of terms for each acid gas irritant

CACC = Controlled Atmosphere Cone Calorimeter

CH₂O = Formaldehyde

CO = Carbon Monoxide

CO₂ = Carbo Dioxide

COHb = Carboxyhaemoglobin

CNS = Central Nervous System

CPR = Construction Product Regulations

C₃H₄O = Acrolein

FEC = Fractional Effective Concentration

FED = Fractional Effective Dose

FPA = Fire Propagation Apparatus

FR = Fire Retardants

FTIR = Fourier Transform Infrared Spectroscopy

HBr = Hydrogen Bromide

HCl = Hydrogen Chloride

HCN = Hydrogen Cyanide

HF = Hydrogen Fluoride

HNO₂ = Nitrous

HNO₃ = Nitric Acid

HPLC = High-Performance Liquid Chromatography

HPIC = High-Performance Ion Chromatography

HRR = Heat Release Rate

IC = Ion Chromatography

K_p = Equilibrium Constant

LFL = Lower Flammable Limit

MCC = Microscale Combustion Calorimetry

MFC = Mass Flow Controller

MetHb = Methaemoglobin
NaOH = sodium hydroxide
NDIR = Non-Dispersive Infrared Analyser
NFX = Non-Dynamic Tube Furnace
NIST = National Institute of Science and Technology
NO = nitrogen oxide
NO₂ = Nitrogen dioxide
N₂ = nitrogen
NO_x = nitrogen Oxides
OI = Organic Irritants
PAH = Polycyclic Aromatic Hydrocarbons
PA6 = Polyamide 6
PA6.6 = Polyamide 6.6
PIR = Polyisocyanurate
PMMA = Polymethylmethacrylate
PPM = Parts Per Million
PVC = Polyvinyl chloride
SBI = Single-Burning Item Test
SDC = Smoke Density Chamber
SO₂ = Sulphur Dioxide
SSTF = Steady State Tube Furnace
THR = Total Heat Release
 ϕ = Equivalence Ratio
CaSi = Calcium silicate

List of figures

Figure 1: Great Britain Fire Deaths (1955-2019) ²	2
Figure 2: A simplified graph of a typical fire growth curve over time ¹⁶	14
Figure 3: Flow diagram for methane combustion in a stoichiometric methane-air flame at atmospheric pressure ¹	15
Figure 4: 30 min lethal FED (ISO 13344) from burning 1 kg with the effluent dispersed in a volume of 50 m ³ for a range of materials under different fire conditions, indicated by ISO fire stage (2, 3a, 3b). PF to PF3 are different commercial Phenolic foam insulation ⁶³	26
Figure 5: Schematic diagram of the Controlled Atmosphere Cone Calorimeter ⁷⁰	29
Figure 6: Diagram of the Non-dynamic tube furnace ⁷³	30
Figure 7: : Diagram of the Steady State Tube Furnace ⁷⁵	31
Figure 8: Schematic diagram of the Fire Propagation Apparatus ⁷⁸	32
Figure 9: Schematic diagram of the Radiant Test Apparatus ⁸¹	33
Figure 10: Comparisons of CO yield as a function of equivalence ratio from bench-scale tests and large-scale tests ¹⁰¹	54
Figure 11: Comparison of NO _x and HCN yields produced by the SSTF and ISO room test as a function of equivalence ratio ¹¹³	55
Figure 12: Comparison of CO yields as a function of equivalence ratio produced by: SSTF, CACC and FPA with ISO room data.....	56
Figure 13: Comparison of HCN yields as a function of equivalence ratio produced by: SSTF and CACC with ISO room data ¹⁰⁶	57
Figure 14: CO yields produced by various apparatus under well-ventilated and under-ventilated conditions ¹⁰⁶	59
Figure 15: Example gas concentration data obtained from the duration of testing plasterboard in the SSTF.....	69
Figure 16: HCN concentrations generated over the duration of testing PA6.6 in the SSTF at 650 °C (under-ventilated flaming) ran in duplicate to test the repeatability of the methodology.	74
Figure 17: Average HCN concentrations measured over the duration of testing PA6.6 in the SSTF at 650 °C (under-ventilated flaming) VS CO concentration measured throughout the test.	74
Figure 18: Reynolds number calculated at different air flows using the SSTF as a function of temperature and distance from the centre of the SSTF furnace.....	76
Figure 19: CO yields obtained at varying oxygen concentrations for tests conducted using PA6	76
Figure 20: HCN yields obtained when conducting tests on PA.6 at varying oxygen concentrations ...	77
Figure 21: CO ₂ yields obtained from tests conducted using PA6 at varying oxygen concentrations ...	78
Figure 22: CO yields obtained at varying oxygen concentrations at 650, 750 and 850 °C, conducted using PA6.6.....	78
Figure 23: HCN yields quantified from testing PA6.6 in the SSTF under a range of oxygen concentrations using 3 different temperatures: 650, 750 and 850° C.	79
Figure 24: Yield of CO ₂ produced from Microscale combustion calorimetry as a function of time, tested at a range of oxidiser temperatures	85
Figure 25: CO yields obtained from Polystyrene produced from Microscale Combustion calorimetry as a function of time, tested at a range of oxidiser temperatures.....	85
Figure 26: CO yields obtained from PMMA tested on the SSTF at an equivalence ratio of 1.5 using varying secondary furnace temperatures.....	86
Figure 27: Final schematic design of phi meter created for this project, where MFC is a mass flow controller, NDIR is used for monitoring CO ₂ and CO.	87
Figure 28: Simple, schematic flow diagram of the simplified phi meter designed for this thesis.	88
Figure 29: Picture of the ceramic tube used in the phi meter.....	88

Figure 30: Labelled picture of the ceramic tube and air inlets and sample mixture outlets in the phi meter.....	89
Figure 31: Oxygen percentage measured by the phi meter at varying ratios of oxygen and nitrogen	89
Figure 32: Comparison of the CO ₂ yields measured using the phi meter and the SSTF at an equivalence ratio of 0.5 using PMMA.....	91
Figure 33: Comparison of the equivalence ratio measured using the phi meter and SSTF when testing PMMA at a range of equivalence ratios in the SSTF using different air to effluent ratios in the phi meter.....	92
Figure 34: Equivalence ratio at varying distances in the SSTF tested in 650 °C under-ventilated flaming conditions.....	94
Figure 35: Equivalence ratio at varying distances in the SSTF tested in 650° C well-ventilated flaming conditions.....	95
Figure 36: Schematic design of the portable box analysers designed and constructed for this research.	97
Figure 37: Comparison between HCN concentrations detected by HPIC and spectrophotometric analysis from samples obtained from testing PA6 in the SSTF	99
Figure 38: HCN concentrations detected by HPIC from samples obtained from testing PA6 in the SSTF	100
Figure 39: HCN concentrations detected by spectrophotometry from samples obtained from testing PA6 in the SSTF.	101
Figure 40: Diagram of the ISO 9705 room corner test ⁹⁹	103
Figure 41: SBI rig design with triangular burner that was used in the large-scale testing.	107
Figure 42: Picture of the final SBI rig set up inside the ISO 9705 test room.....	108
Figure 43: Frame position in room for the cable tests in the ISO 9705 room (Plan view – from above and side view).	110
Figure 44: Picture of the final cable test set up in the ISO 9705 room.....	111
Figure 45: Diagram and picture of the door used to control the ventilation during under-ventilated tests.....	113
Figure 46: Diagram of the triangular fuel pan used to hold the ignition source during the ISO 9705 tests.....	114
Figure 47: Dimensions of small-scale flashover box test.....	116
Figure 48: Dimensions of the internal layout of small-scale flashover box test.....	117
Figure 49: Picture of the reduced scale SBI rig set up in the flashover box.....	118
Figure 50: Picture of the reduced scale cable set up used in the flashover box	118
Figure 51: Layout of sampling set up for monitoring the equivalence ratio and gasses in the door during testing.....	123
Figure 52: Diagram and picture of the placement of McCaffrey probes and thermocouple tree for air velocity and temperature measurements	125
Figure 53: Picture of the sampling system and additional gas line set up to the ISO room corner exhaust duct.....	126
Figure 54: Standard gas analysis set up inside the ISO 9705 room corner exhaust duct ⁹⁹	126
Figure 55: Layout of the gas analysis system sampling from the ISO room corner exhaust duct taken from ISO 9705 ⁹⁹	127
Figure 56: Picture of the camera set up to record the inside of the ISO room corner test protected by Rockwool and heat proof glass.....	128
Figure 57: Heat Release rate data obtained from testing samples in the cone calorimeter at 50 kW.	131
Figure 58: Heat release data measured in the ISO 9705 room corner when testing plasterboard. ...	138

Figure 59: Mass loss measurements measured on the scale in the ISO 9705 room when testing plasterboard.....	139
Figure 60: Temperature measurements taken in the doorway of the ISO room when testing plaster board (2 x SBI with no door). The measurements are taken from thermocouples labelled 'Thermo pile 1' with the final number indicating the distance from the ceiling in cm (e.g. Thermo pile 1 40, meaning thermocouple 1, 40 cm from the ceiling).	140
Figure 61: Equivalence ratio measured in the doorway of the ISO 9705 room when testing plasterboard.....	141
Figure 62: Oxygen concentrations measured in the doorway and exhaust duct of the ISO room when testing plasterboard.....	142
Figure 63: CO ₂ concentrations measured in the doorway and exhaust duct of the ISO room when testing plasterboard.....	143
Figure 64: CO concentrations in the doorway and exhaust duct of the ISO room when testing plasterboard.....	144
Figure 65: CO/CO ₂ ratio calculated for the doorway and exhaust duct of the ISO room when testing plasterboard.....	145
Figure 66: Heat release measurements taken when testing OSB (1x SBI rig with the door open) in the ISO 9705 room corner.....	148
Figure 67: Mass loss measurements taken using the scale in the ISO room corner test, when testing OSB (1x SBI with the door open).....	149
Figure 68: Temperature measurements taken in the doorway of the ISO room when testing OSB (1x SBI with no door). The measurements are taken from thermocouples labelled 'Thermo pile 1' with the final number indicating the distance from the ceiling in cm (e.g. Thermo pile 1 40, meaning thermocouple 1, 40 cm from the ceiling).	150
Figure 69: Equivalence ratio monitored using a phi meter when testing OSB (1x SBI no door) in the ISO room corner.....	151
Figure 70: Oxygen measurements taken in both the door and duct of the ISO room corner when testing OSB (1x SBI no door).	152
Figure 71: CO ₂ measurements taken in duct of the ISO room corner when testing OSB (1x SBI no door) shown with a predicted CO ₂ concentration of the doorway measurement.....	153
Figure 72: CO measurements taken in the exhaust duct of the ISO room when testing OSB (1x SBI no door), shown with a calculated doorway concentration found by using the duct measurement multiplied by the dilution factor (4x).....	154
Figure 73: Calculated CO/CO ₂ ratios in the exhaust duct and door when testing OSB in the ISO room (1x SBI no door).....	155
Figure 74: Heat release measurements taken in the ISO room when testing OSB (1x SBI with door)	157
Figure 75: Mass loss measured using the scale in the ISO room when testing OSB (1x SBI with door).	158
Figure 76: Mass loss measured by the ISO room scale when testing OSB (1 x SBI with door), with a reduced scale axis.	159
Figure 77: Temperature measurements taken in the doorway of the ISO room when testing OSB (1x SBI with door). The measurements are taken from thermocouples labelled 'Thermo pile 1' with the final number indicating the distance from the ceiling in cm (e.g. Thermo pile 1 40, meaning thermocouple 1, 40 cm from the ceiling).	160
Figure 78: Equivalence ratio measured when testing OSB (1x SBI with door) in the ISO room.	161
Figure 79: Oxygen measurements taken in the doorway and duct of the ISO room when testing OSB (1x SBI with door).....	162

Figure 80: CO ₂ measurements taken in the door and exhaust duct of the ISO room when testing OSB (1x SBI with door using a calculated doorway measurement value).....	163
Figure 81: CO measurements taken in the door and exhaust duct of the ISO room when testing OSB (1x SBI with door).....	164
Figure 82: CO/CO ₂ ratio calculated when testing OSB (1x SBI with door) in the ISO room.....	165
Figure 83: Heat release measurements taken in the ISO room when testing OSB (2x SBI no door)..	167
Figure 84: Mass loss measured using the scale in the ISO room when testing OSB (2x SBI no door).	168
Figure 85: Equivalence ratio monitored in the ISO room when testing OSB (2x SBI no door).....	169
Figure 86: Temperature measurements taken in the doorway of the ISO room when testing OSB (2x SBI no door). The measurements are taken from thermocouples labelled 'Thermo pile 1' with the final number indicating the distance from the ceiling in cm (e.g. Thermo pile 1 40, meaning thermocouple 1, 40 cm from the ceiling).	170
Figure 87: Oxygen measurements taken in the door and exhaust duct of the ISO room when testing OSB (2x SBI no door).	171
Figure 88: CO ₂ measurements taken in the door and exhaust duct of the ISO room when testing OSB (2x SBI no door).....	172
Figure 89: CO measurements taken in the door and exhaust duct of the ISO room when testing OSB (2x SBI no door).....	173
Figure 90: CO/CO ₂ ratio calculated from the measurements taken in the doorway and exhaust duct of the ISO room when testing OSB (2x SBI no door).....	174
Figure 91: Picture of the cable trays set up on a stainless steel holder for testing in the ISO 9705 room corner. The ISO 9705 propane burner, while not visible, is below the end of the cable trays in the corner.	178
Figure 92: Heat release measurements taken when testing cables in the ISO room with no door...	179
Figure 93: Mass loss measurements taken by the scale in the ISO room when testing cables with no door.....	180
Figure 94: Mass loss measured in the ISO room when testing cables (no door), with a reduced, zoomed in scale.....	181
Figure 95: Temperature measurements taken in the doorway of the ISO room when testing Cables with no door. The measurements are taken from thermocouples labelled 'Thermo pile 1' with the final number indicating the distance from the ceiling in cm (e.g. Thermo pile 1 40, meaning thermocouple 1, 40 cm from the ceiling).	182
Figure 96: Equivalence ratio measured when testing cables with no door in the ISO room.	183
Figure 97: Oxygen concentrations measured in the door and exhaust duct of the ISO room when testing cables with no door.....	184
Figure 98: CO ₂ concentrations logged in the exhaust duct of the ISO room when testing cables with no door.....	185
Figure 99: CO concentration measured in the exhaust duct of the ISO room when testing cables with no door.....	186
Figure 100: Calculated CO/CO ₂ ratio in the exhaust duct of the ISO room when testing cables with no door.....	187
Figure 101: Heat release measurements taken in the ISO room when testing Cables with a door...	188
Figure 102: Mass loss measured using the scale in the ISO room when testing cables with a door.	189
Figure 103: Temperature measurements taken in the doorway of the ISO room when testing Cables with a door. The measurements are taken from thermocouples labelled 'Thermo pile 1' with the final number indicating the distance from the ceiling in cm (e.g. Thermo pile 1 40, meaning thermocouple 1, 40 cm from the ceiling).	190

Figure 104: Equivalence ratio measured in the ISO room when testing cables with a door.....	191
Figure 105: Oxygen measurements taken in the door and exhaust duct of the ISO room when testing cables with a door.....	192
Figure 106: CO ₂ measurements taken in the exhaust duct of the ISO room when testing cables with a door.....	193
Figure 107: CO/CO ₂ ratio calculated from measurements taken in the exhaust duct of the ISO room when testing cables with a door.....	194
Figure 108: Heat release measured in the ISO room when testing polyurethane (1 x SBI).	197
Figure 109: Mass loss measured by the scale in the ISO room when testing polyurethane (1x SBI). 198	
Figure 110: Temperature measurements taken in the doorway of the ISO room when testing polyurethane (1x SBI) with no door. The measurements are taken from thermocouples labelled 'Thermo pile 1' with the final number indicating the distance from the ceiling in cm (e.g. Thermo pile 1 40, meaning thermocouple 1, 40 cm from the ceiling).	199
Figure 111: Equivalence ratio when testing polyurethane (1x SBI) in the ISO room.....	200
Figure 112: Oxygen measurements taken in the door and exhaust duct of the ISO room when testing polyurethane with no door.....	201
Figure 113: CO ₂ concentrations measured in the doorway and exhaust duct of the ISO room when testing polyurethane (1x SBI no door).....	202
Figure 114: CO concentration measured in the exhaust duct and doorway of the ISO room when testing polyurethane (1x SBI no door).	203
Figure 115: CO/CO ₂ ratio calculated for the doorway and exhaust duct in the ISO room when testing polyurethane (1x SBI no door).	204
Figure 116: Heat release rate measured in the ISO room when testing polyurethane (2x SBI).....	205
Figure 117: Temperature measurements taken in the doorway of the ISO room when testing polyurethane (2x SBI) with no door. The measurements are taken from thermocouples labelled 'Thermo pile 1' with the final number indicating the distance from the ceiling in cm (e.g. Thermo pile 1 40, meaning thermocouple 1, 40 cm from the ceiling).	206
Figure 118: Picture taken approximately 300 seconds into the polyurethane (2x SBI) ISO 9705 room test.	207
Figure 119: Equivalence ratio measured in the doorway of the ISO room when testing polyurethane (2x SBI)	208
Figure 120: Oxygen measurements taken when testing polyurethane (2x SBI) in the ISO room.	209
Figure 121: CO ₂ concentrations measured in the exhaust duct and doorway of the ISO room when testing polyurethane (2x SBI).....	210
Figure 122: CO concentrations measured in the doorway and exhaust duct of the ISO room when testing polyurethane (2x SBI).....	211
Figure 123: CO/CO ₂ ratio calculated for the doorway and exhaust duct of the ISO room when testing polyurethane (2x SBI).....	212

List of tables

Table 1: Stages of a fire (adapted from ISO 19706) ²	9
Table 2: Hazards from fire, typical origins, and their effect on humans ²⁰	17
Table 3: Factors affecting toxic product yield ^{18,20}	18
Table 4: Summary of the conditions tested, showing applied heat flux and ventilation condition ⁸⁴ . 35	
Table 5: Summary of results reported from SDC tests used for comparison in NIST technical note 1763.	44
Table 6: Summary of the CO and CO ₂ yields obtained from all tests conducted in NIST reports 1760, 1761, 1762 and 1763.	47
Table 7: Description of the Euro classification system for fire tests conducted on construction products ⁹⁷	51
Table 8: Classifications for smoke production and burning droplet ⁹⁷	52
Table 9: A table summarising the different bench-scale test methods for assessing smoke toxicity, containing practical information and advantages and disadvantages of each technique	61
Table 10: Summary of the materials used for SSTF assessments.	66
Table 11: Long-term and short-term trend calculated using ISO/TS 19700 for plasterboard tested at 900 °C under-ventilated conditions in the SSTF.	68
Table 12: Summary of the time intervals plotted with the time intervals used.....	73
Table 13: A comparison of the data obtained from the SSTF (ϕ sec-SSTF) and phi meter (ϕ phi-meter) at varying flow ratios and equivalence ratios using PMMA.	90
Table 14: Validation of the phi meter using the SSTF at set equivalence ratios set for well-ventilated and under-ventilated flaming at 650 °C and 850 °C using a 1:1 ratio of fire effluent to fresh air in the phi meter.....	90
Table 15: Summary of tests to conduct in the ISO 9705 room.....	105
Table 16: Estimated height of opening for specific equivalence ratios ¹⁰⁴	112
Table 17: TOXFire project data: Actual equivalence ratios obtained from the door heights used ¹⁰⁴ . 112	
Table 18: Summary of the results obtained from the reduced scale ISO 9705 room tests.....	120
Table 19: Summary of the heights where the McCaffrey probes were placed during testing. The distance was measured from the ceiling.	124
Table 20: Predicted parameters for 2 SBI rigs produced using cone tools and data obtained from cone calorimetry tests conducted at 50 kW.	132
Table 21: Comparison of predicted parameters and actual SBI data ⁸²	132
Table 22: Summary of the calibration data collected in the ISO 9705 room corner test.	136
Table 23: A summary of the test data obtained when testing plasterboard in the ISO room.	146
Table 24: A comparison of the data obtained from testing OSB in the ISO room using several different test configurations for different fire conditions.	176
Table 25: A comparison of the data obtained from testing cables two different ways in the ISO room.	195
Table 26: Summary of the test data obtained when testing Polyurethane in the ISO room in two different test conditions.	213
Table 27: A summary table of test conditions, time to flashover, the mass of fuel and comments on each test conducted in the ISO 9705 room corner.....	214
Table 28: Summary of the maximum equivalence ratio reached for each test conducted in the ISO 9705 room corner.	215
Table 29: Summary of the peak heat release in each test conducted in the ISO 9705 room corner. 216	

Table 30: Summary of the average HCN data obtained in the doorway of the ISO room when testing polyurethane, where the sample number is indicative of sample duration (where 1: 0 to 5 min, 2: 5 to 10 min, 3: 10 to 15 min, 4: 15 to 20 min, 5: 20 to 25 min and 6: 25 to 30 min)..... 217

ACKNOWLEDGEMENTS

Firstly, to my supervisor Professor Richard Hull. Thank you for your support and guidance. I am incredibly grateful for all of the opportunities and support you have given me over the years. You helped me develop into the scientist, and person that I am today. I hope you know how much this is appreciated.

I would also like to thank the wonderful team at EiFC in Denmark for your time, support and hard work. This project would not have been possible without such a fantastic team. I am incredibly grateful to have had the pleasure of working with you all. I would also like to thank Fire Safe Europe (FSEU) for funding this project and making the work possible.

To my fantastic colleagues and dear friends Dr Sean McKenna and Dr Nicola Jones. Words can not express my gratitude to you both. Although we have all parted ways, your continuous support has meant the world to me. I would also like to extend a special note of appreciation to Dr Clare Bedford for assisting with sample analysis after the large-scale tests.

To everyone who has helped and supported me over the years; thank you. I hope you know how deeply it is appreciated.

1 INTRODUCTION

Despite being the largest cause of fatality in unwanted fires¹, smoke toxicity is unregulated within the UK and EU (except for mass-transport industries). The UK fire death statistics, shown in *Figure 1*², show a rise in the number of fatalities due to smoke inhalation and a combination of smoke inhalation and burns from 1970. Between 1955 and 1980, materials such as cotton, wool, and wood were gradually replaced with synthetic plastics, including polyurethane-foam filled furniture³. This was accompanied by the rise in deaths caused by smoke inhalation.

In 1988, UK furniture flammability regulations became more restrictive, leading to the incorporation of fire retardants in furniture. At the same time, low-cost smoke alarms were introduced, with 90% of UK homes having a smoke alarm. In addition, significant causes of fire, such as smoking in bed and indoors, slowly transitioned to smoking outdoors and using open flame heating in homes (including paraffin heaters, which provided heating but could easily be tipped over) decreased. This offers some explanation as to why the number of fatalities from fires has generally decreased, although the biggest cause of fatality results from smoke. Despite this, there is no current requirement to limit the toxicity of the smoke produced from any domestic or construction products.

Indeed, it could be argued that regulating smoke toxicity in the mass transport industries is a major reason for so few fire deaths in transport. While regulators are unwilling to dictate what people can have in their homes, they can control the fire behaviour of the building itself. In particular, people living in multi-occupancy buildings such as apartment blocks should be as safe as those in traditional two-storey homes. The lack of regulation of smoke toxicity is more concerning for high-rise buildings and buildings with limited escape routes, particularly if the insulation and external coverings are combustible and produce toxic smoke.

In 2017, a fire broke out in an apartment in the Grenfell tower block in London, ultimately killing 72 people. The fire ignited the external rain screen façade system of the newly refurbished building and rapidly spread via the façade, producing very large volumes of smoke⁴. Although the materials used in the façade appear to have passed regulatory tests, the fire propagated across the building, igniting a large proportion of apartments in the process. Tower blocks are designed with compartmentation to prevent a fire from spreading from one compartment to another, both vertically and horizontally. However, the safety of the compartmentation design of high-rise buildings is undermined when the external façade can spread the fire.

The use of combustible materials not only allows for fire spread across the external façade, it may also produce a significant quantity of toxic smoke that can enter the rooms of the building. Many of the occupants were overcome with toxic smoke as a result. Smoke exposure will typically incapacitate the victim, removing their ability to escape from a fire unaided before causing death. The use of combustible materials poses serious risk in terms of ignitability and a potential hazard in terms of flame spread and smoke toxicity.

Despite this risk, few robust studies are available whereby smoke toxicity is measured on a large scale and even less for bench-to-large-scale comparisons. As large-scale tests are expensive and time consuming, a bench-scale methodology that can assess material smoke toxicity and correlates to large-scale testing would provide necessary information to reduce injuries and loss of life from unwanted fires.

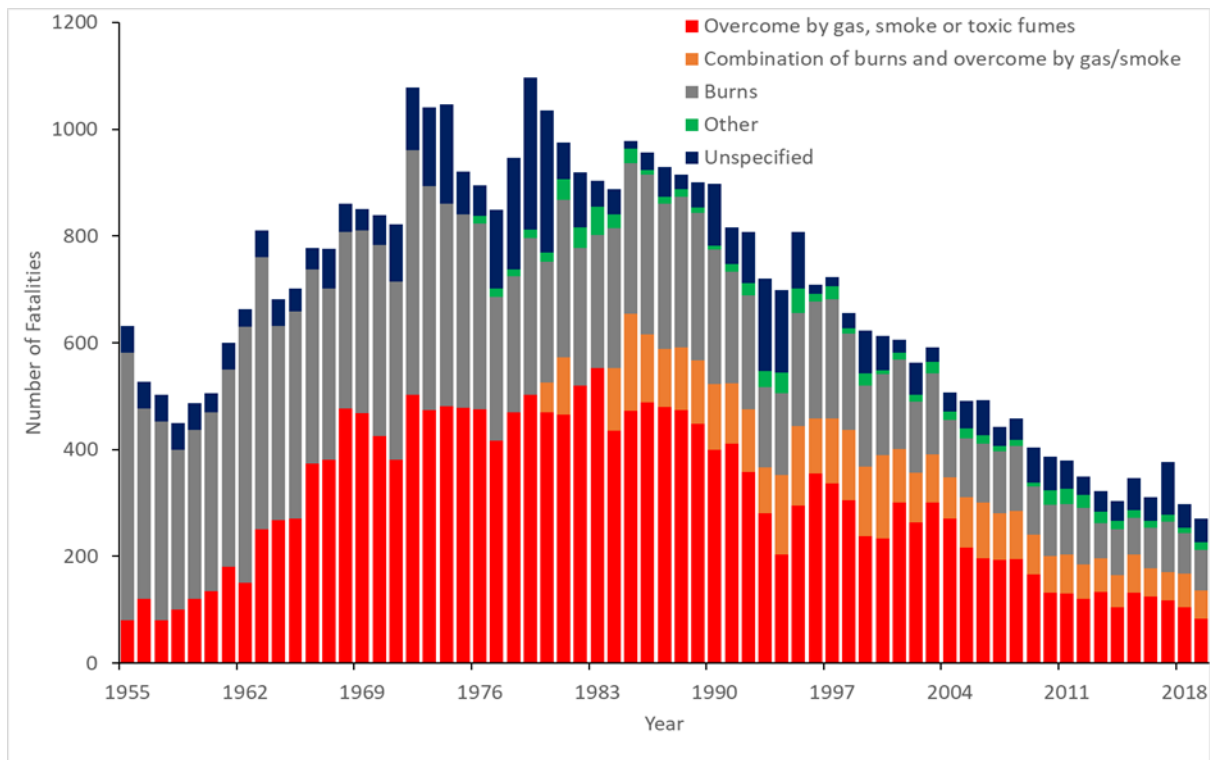


Figure 1: Great Britain Fire Deaths (1955-2019)².

1.1 INTRODUCTION TO THE PROJECT

This research aims to provide the necessary tools and information to implement smoke toxicity into fire safety regulations applying to construction products. This will allow national regulators, architects, and building specifiers to differentiate products with high smoke toxicity from those with less toxic smoke. To allow for the regulation of smoke toxicity, this project aims to provide the experimental data and methodology to assess the smoke toxicity of construction products and provide the necessary information on the factors affecting smoke toxicity to be more widely understood.

The first objective was to produce a critical review of studies relating to smoke toxicity. This review has included an overview of smoke toxicity, followed by a review of current assessment techniques on both bench and large-scale. A gap analysis was also undertaken to identify areas where further research was needed prior to the incorporation of smoke toxicity into a regulatory framework.

The second objective was to undertake large-scale toxicity assessments of a range of construction products and refine the methodology for doing so. It is hoped that bench-scale toxicity assessments can be made in the future for direct comparisons, and the chosen apparatus will undergo an inter-laboratory reproducibility assessment after completion of this project to demonstrate the methodology's reproducibility to ensure it is a suitable test method for the construction product regulations.

The methodologies developed in this project can be used to undertake comparative studies on bench-scale toxicity assessments for the use in regulating smoke toxicity.

1.2 LAYOUT OF THE THESIS

The thesis has been sectioned into four core chapters. These chapters are briefly outlined below. Details of each chapter are described at the beginning of each chapter, providing more information regarding the chapter's content and following sub-chapters.

Chapter 1: Introduction

The thesis begins by providing an introduction to the concept of smoke toxicity. This introduction aims to provide background information surrounding fire stages and conditions and the thermal decomposition process of combustible construction products. Details regarding the characterization of fires linked to the ISO 19706 fire stages are also provided. This is followed by a description of the process of decomposition of polymeric materials. This provides an insight into how and why a decomposing material will produce volatile fuel, which may produce some toxic smoke. Common decomposition products are identified, and their mechanisms of toxicity within humans are evaluated.

This section then looks into the apparatuses available for generating toxic smoke, identifying each method's strengths, weaknesses and repeatability. This is followed by an explanation of what is happening to particular materials during the test, reasoning as to why one test method may be superior to another. This is then directly linked to the means of testing construction products in relation to the Construction Product Regulations and Euroclass system used to quantify the fire behaviour of construction products. This is followed by a description of the analytical techniques for quantifying individual toxic components in smoke. The links between bench-scale assessments made for smoke toxicity and their links to large-scale tests are discussed, and a critical review of the approaches used for bench-to-large-scale comparisons is provided.

This chapter then critiques the literature surrounding the apparatuses used in this work, identifying the positives and negatives of the available fire test methods and explaining why specific apparatuses were chosen over others.

Chapter 2: Method development

This chapter contains details of all the experimental method developments undertaken in this research. The results obtained from each individual method development have been reported according to the appropriate section. This allows the reader to follow the method development steps that were based on the data and results obtained.

This chapter is separated into eight core sections: Selection of materials, two separate sections regarding method development using the steady state tube furnace (SSTF), phi meter, portable gas analysers, analysis of the equivalence ratio in the SSTF, and two sections regarding the development of the large-scale test design. Each section contains relevant background information followed by details of the method developments and research conducted to conclude the final methodology used. The results and discussion from each

method development are found at the end of each section they pertain to, except the large-scale test results and discussion.

Chapter 3: Large-scale results and discussion

Due to the amount of data obtained from the large-scale testing conducted in the ISO 9705 room, the results and discussion were separated from the large-scale method development. The results and discussion of the large-scale test data are separated into materials tested.

Chapter 4: Conclusions and future work

The final conclusions found from this research are compiled in this section. Details of the key information identified and a discussion on its significance and potential applications are also provided. The potential applications are also discussed in terms of future work applicable to the findings from this project.

Appendices

All standard methodologies used in this research have been placed in the appendix. Due to the extensive amount of data produced in this project, detailed results have been placed in an appendix. The results are separated into those obtained on a bench-scale and large-scale.

The appendices are as follows:

Appendix 1: Sampling and analysis of acid gases in fire effluent

This appendix contains information regarding the procedures used for acid gas sampling in fire effluent, and analysis of the samples collected. The analysis contains the methodologies for making standard solutions for calibration and the set up of the equipment used for analysis.

Appendix 2: Sampling and analysis of Hydrogen cyanide

This appendix contains information regarding the chemical theory behind wet chemical analysis of HCN, details of sampling methodologies and information on how to calculate the concentration of HCN in solution. It also details ion chromatography methodologies for sample analysis.

Appendix 3: ISO/TS 19700 Steady State Tube Furnace Standard methodology

This appendix contains information regarding the set up of the SSTF and details regarding sample preparation. It also contains instructions on how to calculate the equivalence ratio for a test, information regarding the calibration of the apparatus as well as information pertaining to equipment maintenance and test modifications.

Appendix 4: ISO 5660 Cone calorimetry testing: standard methodology used

This appendix contains the methodology used for the cone calorimeter and details regarding the sample preparation for testing.

Appendix 5: Microscale Combustion Calorimetry: Standard testing methodology

This appendix contains details regarding calibration testing and the methodologies used for sample testing.

Appendix 6: Using the McCaffrey probe data to calculate air velocity

This appendix contains information and details about the pressure transducers used for the measurement of air velocity in the McCaffrey probes, as well as details regarding the calculations from the voltage measurements to air velocity.

Appendix 7: Calculation of volume flow of gas using McCaffrey probe measurements.

This appendix contains information regarding the use of air velocity measurements alongside temperature measurements to calculate volume flow of gas in an opening.

Appendix 8: ISO/TS 19700 Steady State Tube Furnace manual and user guide

This appendix contains the SSTF user manual written and created for this work.

Appendix 9: Box analyser

This appendix contains information about the program designed for the analysers, the details of sampling times and a set of instructions created for operation of the analysers. Final photographs of the analyser are also shown.

Appendix 10: Bench-scale data

This appendix contains the validity assessments of the data obtained during SSTF testing of proposed round robin materials, calculated using the original methodology in the ISO/TS 19700 standard, as well as the assessment made using the longest steady state period possible.

Appendix 11: Large-scale test data

This appendix contains the smoke toxicity data obtained from the large-scale tests. This includes the acid gas analysis and HCN analysis conducted using HPIC.

1.3 INTRODUCTION TO FIRE TOXICITY

1.3.1 Summary of the subject information provided

This chapter provides the information required to investigate smoke toxicity and its measurement. It starts with the characterization of fire stages and then explains the key characteristics of fire scenarios and how they transition from one to another. The stages are also described in terms of fire toxicity and explain why one scenario may produce more toxicants than another. The equivalence ratio is then explained in terms of combustion efficiency and its importance concerning smoke toxicity and is linked to the aforementioned fire stages. As the equivalence ratio is such an important concept in smoke toxicity, the chapter then explains how this can be continuously monitored during experiments (both bench and large-scale) via a phi-meter.

There follows a detailed explanation of the chemistry of combustion. This is used to explain how to measure smoke toxicity accurately, based on the chemistry behind the combustion reactions occurring. This was provided to allow the reader to understand the process of toxic gas generation and apply this when attempting to select the most appropriate test method for smoke toxicity analysis.

The estimation of toxicity is then reviewed in greater detail, providing explanations for common expressions of toxicity (Fractional Effective Dose (FED) and Fractional Effective Concentration (FEC)) for common toxicants produced during a fire. An in-depth explanation of the adverse effects of the major toxicants (sub-categorised into acute and chronic toxicants) is provided. As smoke toxicity is greatly influenced by fire condition, an explanation for this and a review of relevant data is provided.

The methods of generating smoke for toxicity analysis are then introduced and reviewed. An explanation of each apparatus and a discussion of its capabilities are provided. In addition, the means of analysing fire effluent are also outlined. This is linked to published studies on large-scale toxicity testing and a review summary is provided. This study has been used to identify weaknesses within certain test methods for specific materials and to compare data sets obtained from different bench-scale methods.

An explanation and review of the Construction Product Regulations are provided, linking the literature review to real-life applications. A review of the suitability of the ISO 9705 room test and EN 13823 single burning item test for smoke toxicity analysis is also provided. Frequently, bench-to-large-scale comparisons are made to reduce the number of large-scale tests conducted. ISO 29903 details the methodology for such comparisons and is one of few available resources. The ISO 29903 has been reviewed in relation to smoke toxicity comparisons and suggestions for improvement before smoke toxicity regulations are introduced have been provided.

1.3.2 Characterisation of fires

Each fire stage will exhibit different combustion conditions, often characterised by monitoring the presence of a flame, ventilation condition, oxygen concentration and heat flux. The fire's condition will directly affect the toxicity of the smoke produced, so the corresponding smoke toxicity will vary accordingly as the fire grows. A fire is typically defined by its combustion efficiency⁵.

The most widely recognised classification system for combustion conditions can be found in ISO 19706⁶. It details four fire stages relevant to this project: non-flaming, well-ventilated, under-ventilated and post flashover. The categories of fire conditions can be found in Table 1. Most unwanted fires are stages 1b, stage 2 (well-ventilated), and 3a and 3b (under-ventilated).

Table 1: Stages of a fire (adapted from ISO 19706)²

Fire stage	Max temp / °C		Equivalence ratio ϕ	CO/CO ₂ ratio
	Fuel	Smoke		
Non-flaming				
1a. Self-sustained smouldering	450-800	25-85	-	0.1-1
1b. Oxidative, external radiation	300-600		-	
1.c Anaerobic external radiation	100-500		-	
Well-ventilated flaming				
2. Well-ventilate flaming	350-650	50-500	0.5-0.7	<0.05
Under-ventilated flaming				
3a. low-ventilation room fire	300-600	50-500	1.5-2	0.2-0.4
3b. Post flashover	350-650	>600	1.5-2	0.1-0.4

1.3.2.1 Non-flaming fires:

ISO 19706 details 3 sub-categories within non-flaming combustion; stage 1a, stage 1b and stage 1c. These are typically dependent on oxygen availability, air supply rate, and the heat applied to the material. Stage 1a is representative of self-sustaining smouldering combustion, although this only occurs with porous solids, where decomposition is typically driven by exothermic oxidation. Reaction with oxygen takes place on the surface of the material.

Stage 1b is most relevant to oxidative external radiation (pyrolysis), one of the more common forms of decomposition in fires. The thermal decomposition drives reactions at the material's surface within the gas phase and is often a precursor to flaming combustion. The presence of a flame greatly accelerates the thermal decomposition and often, the transition between fire stages 1b to 2 generally produces complete combustion products such as water and CO₂. It is most relevant to scenarios such as smoking in bed as the victim may be overcome by the smoke produced in the close vicinity, leading to fatality without flaming combustion occurring³.

Stage 1c describes the conditions of anaerobic external radiation. If the material has sufficient heat applied to it, decomposition begins to occur in the absence of oxygen, often yielding large volumes of CO from oxygen-containing materials³.

1.3.2.2 Well-ventilated fires

Well-ventilated stage 2 fires describe the flaming combustion of a material under a normal (20.95%) oxygen environment. They often have a high combustion efficiency, resulting in them being generally regarded as less hazardous than other fire stages in terms of fire toxicity. This type of fire is usually observed in the early stages of flaming combustion and typically builds up a hot smoke layer in an enclosure.

As the fire transitions to under-ventilated flaming, the yield of toxic products generally increases by a factor between 5 and 25, resulting in large volumes of CO and HCN and many other incomplete combustion products. The observed increases correlate to changes in the equivalence ratio (fuel-to-air ratio)⁷.

Provided sufficient fuel, well-ventilated fires almost always become ventilation controlled and develop into under-ventilated fires. As flames pyrolyse more fuel, they need more air to oxidise it. Even in open air, the rate of burning will be controlled by the access of air to the fire. Indoors, the presence of windows and doorways will often mean that the size of the vent is fixed for the duration of the fire. This is typical of a fire in a larger compartment. The well-ventilated fire will grow significantly until most of the oxygen available is consumed, causing it to develop into a ventilation-controlled or under-ventilated fire.

1.3.2.3 Under-ventilated fires

Under-ventilated fires are sub-categorized as stage 3a, low-ventilated room fires and Stage 3b post-flashover fires. Stage 3a under-ventilated fires occur when the air supply to the fire is limited (in comparison to the mass of fuel available for combustion) and arguably represent the most hazardous scenario in terms of fire toxicity as a much larger volume of toxic smoke is produced during these fires, provided there is sufficient fuel. Small under-ventilated fires are responsible for most fire fatalities in the UK and Europe⁸ due to the typical layout of domestic dwellings (e.g. small rooms, not open plan).

1.3.2.3.1 Stage 3a: Small under-ventilated

As the fire grows within a room, the hot smoke layer will gradually build, filling the upper layer of the room. This accelerates the fire growth rate, often resulting in the fire growing rapidly as the smoke layer descends. As this happens, a large proportion of the flame burns within an oxygen-depleted atmosphere making the burning zone more inefficient. The unavailability of oxygen prevents complete combustion, increasing the amount of fuel present in the smoke. This yields larger quantities of toxic species such as CO, HCN and volatile organic compounds and reduces the quantity of complete combustion products such as CO₂ and water. As the fire grows, the air supply will be approximately constant, but the mass of fuel pyrolyzed will increase, causing the fire to continue with insufficient oxygen.

In some cases, fresh air is continuously supplied to the lower layer of the under-ventilated fire allowing the fire to consume all the available fuel. The fire growth rate typically stabilizes and is unlikely to self-extinguish and will continue to produce toxic species until either the fuel runs out or the fire is quenched. In these conditions, the CO yield observed is commonly around 0.2 g/g^{9,10}.

1.3.2.3.2 Stage 3b: Post-flashover

Flashover occurs when the total thermal radiation (from the combination of the fire plume, the hot walls and ceilings of the compartment and hot gases) induces the radiative ignition of the exposed combustible materials within a compartment with sufficient levels of ventilation. A rapid change in heat is often observed before flashover¹¹. The hot gases in the upper ceiling areas are often seen to ignite, forming red streaks before flashover, an occurrence commonly referred to by firefighters as “angel’s fingers” because of the imminent danger. The main distinguishable features between fire stages 3b and 3a are the temperature and fire size¹². Fire stage 3b produces large volumes of highly toxic smoke and is associated with most major fire disasters.

1.3.2.4 Equivalence ratio

The equivalence ratio (ϕ) is a common parameter used to identify the ventilation condition during a fire and aids the identification of the stage of a fire as described in ISO 19706². It is defined as the comparison between the actual fuel-to-air ratio and the stoichiometric fuel-to-air ratio, shown in Equation 1.

$$\phi = \frac{\dot{m}_{fuel} / \dot{m}_{oxygen}}{(\dot{m}_{fuel} / \dot{m}_{oxygen})_{Stoic}} \quad \text{Equation 1}$$

When $\phi = 1$, the combustion is stoichiometric (where all oxygen is consumed). ISO 19706 defines the borders between well-ventilated flaming and under-ventilated flaming as $\phi < 1$, the combustion is well-ventilated, and when $\phi > 1$, the combustion is under-ventilated. However, there is generally clear separation in the values of equivalence ratios.

Early well-ventilated flaming will typically show $\phi = 0.5-0.7$. As the fire grows, ϕ will be significantly greater than 1.0 as the concentration of oxygen reaching the flame reduces, causing the fire to become under-ventilated. Equivalence ratios will typically reach 1.5 to 2.0 (and above) as it becomes under-ventilated. The equivalence ratio has a direct effect on smoke toxicity due to the changes in the availability of air. When a fire is well-ventilated, the likelihood of complete combustion occurring is higher. During complete combustion, the only products of decomposition are CO₂ and H₂O. While this is generally not attainable in a real-fire scenario, well-ventilated combustion will produce higher volumes of CO₂ and H₂O than its under-ventilated counterpart¹³. In environments of reduced oxygen and hence an increase in equivalence ratio, combustion efficiency decreases. This is often coupled with increased yields of CO and HCN (from nitrogen-containing fuel).

For equivalence ratios to be accurately measured, steady burning is typically required¹⁴. The equivalence ratio can be calculated in tests where the fuel to air ratio is known or measured using a phi meter¹⁵.

1.3.3 Flammability and decomposition process of polymers

Most unwanted fires are fuelled by combustible materials based on some form of organic polymeric material that decomposes to form gas phase fuel upon heating. When sufficient heat is applied to a material, the bonds within the polymer chain begin to break, eventually producing volatile molecules. This will occur at the points where the bonds are weakest. This will happen progressively, with the chains becoming smaller and smaller. This is often a free radical process. When the temperature is sufficient, small molecular fragments such as hydrocarbons will evolve.

There are three processes by which a polymer will decompose: end-chain scission, random-chain scission, and chain stripping¹⁶. With end-chain scission, groups found on the end of the polymeric chain (usually resulting in a stable fragment (monomer)) are released, leaving a reactive shortened chain end. When the polymeric chain breaks at random points along the chain, it is known as random-chain scission. If good leaving groups are present along the side chains of the polymer, it will typically decompose in a chain-stripping manner where these groups are stripped first. The resultant chain will be unsaturated (containing double bonds), leading to char formation. Chain scission mechanisms are the most common mechanism for polymer decomposition¹⁷, with random chain scission being far more common than end chain scission¹⁸.

The chemical composition of the polymer will dictate the volatile fragments produced during thermal decomposition. The fragments produced must be small if they are to be volatile at the temperatures of decomposition. Larger fragments will typically remain in the condensed phase before being further decomposed into smaller fragments when higher temperatures are reached.

These volatiles will diffuse from the surface of the material due to their higher temperature, making them buoyant and lifting off the surface. This results in the formation of a fuel/air mixture above the surface of the material. When the concentration of volatile fuel present in the fuel/air mixture reaches the lower flammable limit (LFL: defined as the concentration at which a flammable mixture can be ignited with sufficient temperature), the fuel/air mixture can ignite if an ignition source is present. Alternatively, in the absence of an ignition source (flame or spark), as the temperature rises, reactions with oxygen will produce more free radicals until a sufficient concentration is reached, resulting in spontaneous ignition. In this case, for a particular liquid fuel, its vapour pressure will rise with temperature, and the point at which flaming occurs is known as the spontaneous or self-ignition temperature.

Upon ignition, the combustion process will result in flaming where visible and infrared radiation is emitted. This will transfer some of the heat back to the polymer's surface, aiding the production of more volatile fragments and sustaining the burning of the material. When the heat required to cause volatilisation of the solid is exceeded by the heat, feedback from the flame combustion will stabilize¹⁹. This is the criteria for sustained ignition.

As the fire progresses, burning will become more stable and usually be ventilation controlled, leading to a steady state of burning. The typical progression of a ventilation-controlled fire is shown in Figure 2²⁰. After this point, the effluent given off is approximately constant (in terms of production and rate), and the fire condition is usually easily definable. For this reason, and because the ventilation-controlled flaming is more toxic, the steady burning period is the most important for assessing smoke toxicity.

Soot formation will occur as a result of progressive dehydrogenation of fuel molecules leading to the generation of species with conjugated double bonds. The conjugated double bonds undergo cyclisation and aromatization to form polycyclic aromatic hydrocarbons (PAH). This is illustrated in

Figure 3¹⁶. As this occurs, the combustion products move away from the flame zone and the heat source. The decreasing temperature induces a phase change in the gas molecules where they become solid and begin to aggregate.

Soot particles are the main absorbers and emitters of infrared radiation, conducting heat from the flame back to the fuel surface (a Bunsen flame with the airhole open is premixed, forms little soot and radiates very little; a yellow Bunsen flame allows soot to form and radiates much more heat sideways causing greater flame spread). Many PAHs are carcinogenic and when they agglomerate into particles approximately 1 μm in diameter, they diffuse less and penetrate deeper into the lungs. These particulates in fire effluents and diesel exhausts are responsible for around 40000 deaths a year in the UK²¹. In well-ventilated flaming fires, polymers containing purely aliphatic structural units produce relatively little smoke, while polymers with aromatic groups in the side chains produce the largest amounts of smoke. In under-ventilated fires, almost all fuels produce large amounts of smoke.

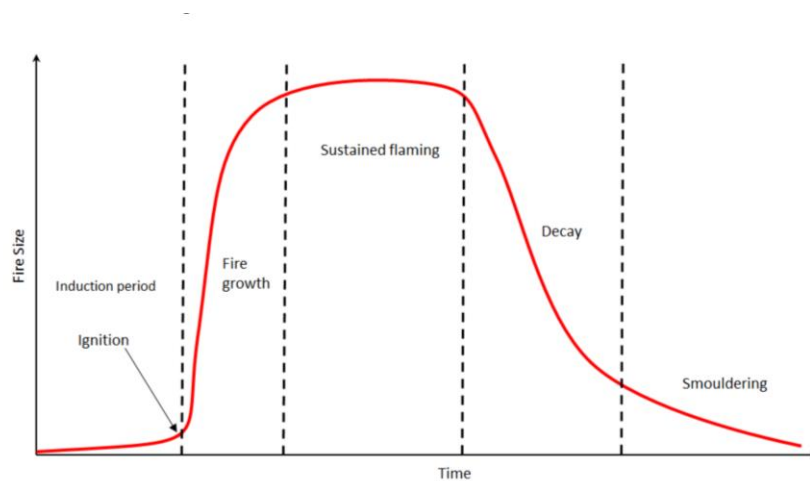


Figure 2: A simplified graph of a typical fire growth curve over time¹⁶.

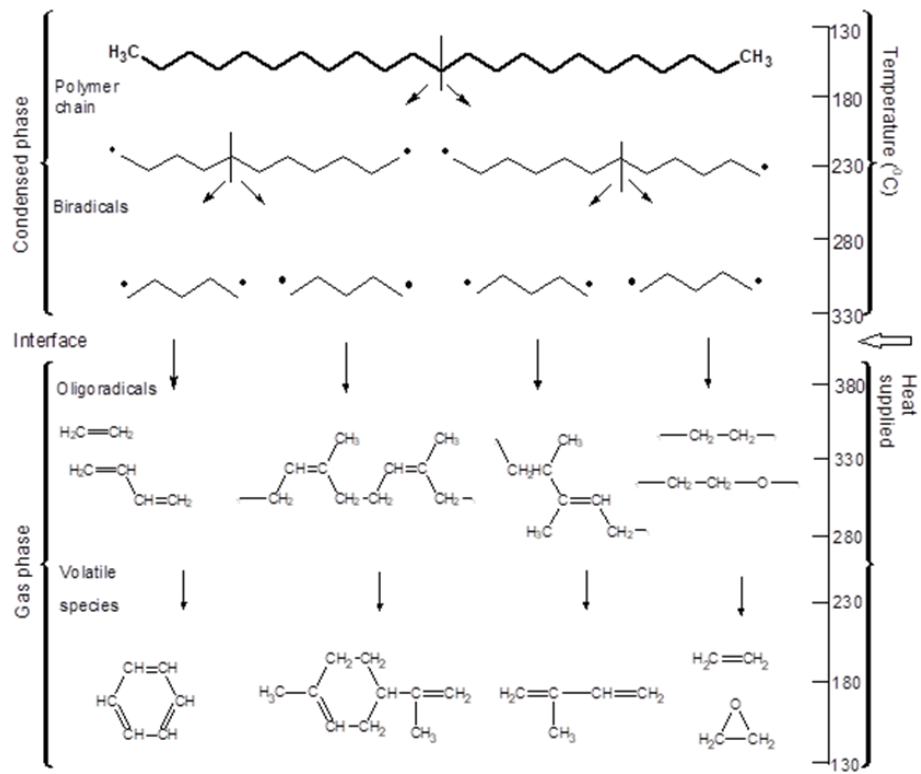
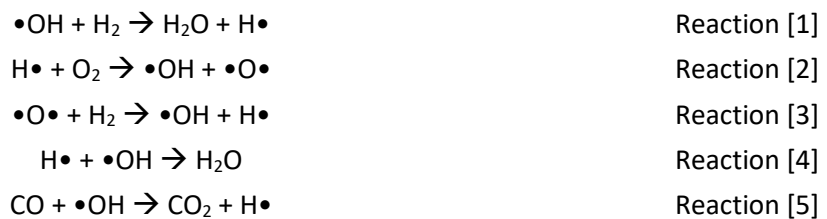


Figure 3: Flow diagram for methane combustion in a stoichiometric methane-air flame at atmospheric pressure ¹.

1.3.3.1 Gas phase Free radical reactions

Free radical reactions are one of the main processes of flaming combustion. Their reaction rates are millions of times faster than stable molecule reaction rates. While the life of an individual radical is relatively short, the rapid chain reactions that occur lead to continuous regeneration of radical species and the formation of a flame. Their reactions are responsible for fuel consumption and heat production during combustion. The chemistry of a methane flame is complex, including over 50 free radical reactions²². However, only a few of these reactions dominate the overall reaction rate.

Some common free radical reactions occurring within a flame have been shown in reaction schemes [1] through [5]. Although these only relate to hydrogen reacting with oxygen, they are present in almost every flame. Upon generation of a free radical species (shown with ●), the radical quickly goes on to react with other molecules present, such as H₂. The radical can react with either a non-radical species in a propagation reaction leading to further radical generation such as in [1] or react with another radical in a termination reaction such as in [4]. Termination requires the removal of a large amount of energy and can usually only occur when a third molecule is present to absorb the excess energy. The individual reactions release a significant amount of energy while processes such as [2] generate more radical species that propagate further reactions, allowing the flame to grow rapidly.



Of the hundreds of documented reactions of free radicals in a flame, reaction [2] is one of the most significant, as one radical can produce three unpaired electrons in a single reaction. This will lead to three times more radicals and hence more reactions with other molecules present when compared to reactions 1, 3 and 5, furthering the decomposition process and hence referred to as a branching reaction. Reaction 4 results in a decrease in the radical concentration.

Hydrocarbon radicals will rapidly react with atmospheric oxygen, ultimately producing heat that radiates back to the fuel source, aiding the generation of volatile fuel, resulting in flame spread. The most common hydrocarbon radical reaction and the most important for this thesis is reaction 5. This reaction is the main heat release step in fires.

During steady combustion, the concentration of radical species is approximately constant as the rate of recombination of radicals is equal to the rate of radical formation. During this time, the components evolved will be released at a constant rate. This means that toxic species, such as CO or HCN, should be formed at an approximately steady rate during the period of steady burning.

1.3.4 Fire effluent toxicity

Fire effluent toxicity largely depends on the fire condition, with smoke toxicity increasing by up to a factor of 50 with the fire becoming under-ventilated²⁴. As the fire grows and becomes more under-ventilated ($\phi > 1$), the yield of CO significantly increases. If the fuel contains nitrogen, this is accompanied by an increase in HCN yields²³. Table 2²⁴ shows the effects and threshold limits of some common toxicants in smoke. While the fire condition and ventilation directly affect the yields of toxicants, additives, such as gas-phase flame retardants, also affect yields.

Table 2: Hazards from fire, typical origins, and their effect on humans²⁰.

Toxic products	Origin	Effects	Tenability/Threshold Limits (within 30 minutes)
Halogenated acids	Polyvinyl chloride, halogenated flame retardants	Respiratory tract irritation	100 ppm to 1000 ppm
Nitrogen dioxide	High-temperature combustion- severe fires, car exhaust	Respiratory tract irritation, mucus membrane irritation	170 ppm
Smoke	Organic material forming tar droplets or soot particles	Airways obstruction, visual obstruction	0.33 ODm ⁻¹ (OD is optical density)
Oxygen depletion	Combustion/ pyrolysis	Asphyxia, laryngotracheitis	10-12%
Carbon monoxide	Incomplete combustion of any organic material	Functional asphyxia, narcosis tissue hypoxia, organ failure, death	1000 ppm
Hydrogen cyanide	Polyurethane, polyamides, polyacrylonitrile, wool etc.	Cellular asphyxia, tissue hypoxia, organ failure, death	100 ppm

1.3.4.1 Effect of fire retardants on smoke toxicity

A large proportion of construction products and furniture are flammable, posing a hazard when used in occupied buildings. To meet fire safety regulations, fire retardants are typically added to the material to decrease its flammability and formulate a product capable of passing regulatory tests, allowing it to be used for construction applications. Unfortunately, while the addition of fire retardants may reduce the ignitability or initial flame spread, the toxicity of the smoke produced can increase. In the construction product industry, smoke toxicity is rarely, if at all, considered.

Fire retardants have been shown to significantly increase the toxicity of the smoke produced during a fire^{17, 25}. For example, the presence of halogenated molecules not only leads to the evolution of halogenated species in the smoke, but they also suppress the free radical reactions leading to the formation of CO₂ and water and increase the yields of CO and HCN (without the OH radical, neither CO nor HCN can be oxidised to CO₂ and N₂). Fire retardants (FR) acting in the gas phase (such as chlorinated, brominated, and some phosphorus compounds) will quench the flame reaction, increasing the products of incomplete combustion, including CO, HCN and organo-irritants.

A summary of the factors affecting smoke toxicity can be shown in Table 3. It is important to understand that while non-flaming conditions produce more toxic effluent than flaming conditions per gram of material burnt, flaming fires consume fuel at a much greater rate, producing much larger volumes of toxic smoke.

Table 3: Factors affecting toxic product yield^{18,20}

Lower toxicity	Higher toxicity
Flaming	Non-flaming
Well-ventilated	Under-ventilated
Nitrogen absent	Nitrogen present in the fuel
Gas-phase FR absent	Gas-phase FR present

1.3.5 Expressions of toxicity

Toxicants present in smoke have been shown to be approximately additive in experiments measuring lethality using laboratory rats²⁶. The toxicity of smoke to a living organism can be estimated in terms of a Fractional Effective Dose (FED). An FED can be calculated in terms of the fraction of the measured dose required to induce incapacitation or cause death in 50% of the exposed population. Dose is calculated by using Equation 2. These are expressed as FED for incapacitation and FED for lethality.

$$[Dose = concentration \times time] \quad \text{Equation 2}$$

1.3.5.1 Estimation of incapacitation

ISO 13571²⁷ provides guidance for estimating incapacitation. Taking the four hazards of asphyxiant gases (CO and HCN), irritant gases (HCl, HBr, NO₂ etc), obscuration by smoke, and effects of heat, it gives equations to estimate when incapacitation will occur. It assumes each incapacitation hazard acts independently. Incapacitation by asphyxiants is calculated as an FED (concentration x time). Incapacitation by irritants is assumed to be instantaneous and is calculated as a fractional effective concentration (FEC).

1.3.5.2 Incapacitation by asphyxiants

The FED for incapacitation by asphyxiants is calculated by taking into consideration the concentrations of CO and HCN (in terms of Fractional Effective Concentrations (FEC)) that will impede escape.

The equation for calculating FED for incapacitation, taken from ISO 13571²⁷, is shown in Equation [3].

$$FED = \sum_{t_1}^{t_2} \frac{[CO]}{35000} \Delta t + \sum_{t_1}^{t_2} \frac{[HCN]^{2.36}}{1.2 \times 10^6} \Delta t \quad \text{Equation 3}$$

Equation [3] uses the concentration-time product effects of CO by taking the incapacitating dose of CO (35 000 µl L⁻¹min) with the length of exposure (Δt at each concentration). This is added to the effects of HCN. HCN asphyxiation does not follow a linear relationship because HCN causes hyperventilation and is calculated using an exponential relationship. In the most recent ISO 13571, Equation 3 is expressed with a phi (φ) symbol. Square brackets have been used to express concentration in this equation for this thesis to avoid confusion based on the use of phi as an expression of equivalence ratio.

1.3.5.3 Incapacitation by irritants

In a fire, it is difficult to distinguish between the unpleasantness of smoke and the toxicity, particularly when irritants are present. The FED for incapacitation by irritants is calculated by taking into consideration the concentrations of irritants (typically HCl, HBr, HF, SO₂, NO₂, etc.) in terms of Fractional Effective Concentrations (FEC) which will impede escape. The FEC is quantified as the fraction of the measured concentration of each toxicant (e.g. [CO], [HCN], etc. in the equation) over

the concentration required to induce death in 50% of the population over 30 minutes of exposure²⁴ (e.g. $LC_{50, CO}$, $LC_{50, HCN}$, etc.). Each toxicant will have an LC_{50} value expressed as a gas concentration. FEC can be calculated using Equation 4. ISO 13571:2012 expresses FEC by use of f-values in place of LC_{50} values. Both values can be used to calculate FEC. This thesis uses the LC_{50} value as it is more common in chemistry to express values in terms of their concentrations. As the thesis focus is towards the chemistry involved in fire, the FEC has been chosen to be expressed in terms of concentration.

The effects of incapacitation by irritants are concentration dependant rather than dose-dependent due to their additive effects. Should the FEC be over 1, 50% of exposed persons will be at risk of incapacitation

$$FEC = \frac{[HCl]}{LC_{50,HCl}} + \frac{[HBr]}{LC_{50,HBr}} + \frac{[HF]}{LC_{50,HF}} + \frac{[SO_2]}{LC_{50,SO_2}} + \frac{[NO_2]}{LC_{50,NO_2}} + \frac{[irritant]}{LC_{50,irritant}} \quad \text{Equation 4}$$

1.3.5.4 Fractional effective dose for lethality

As CO_2 enhances respiration rate, all the fractional contributions are augmented by a V_{CO_2} factor (Equation 5 and 6). Summing the LC_{50} contributions of individual toxicants will yield a fractional effective dose²⁸. This is a measure of the lethality of fire effluent. Fractional effective dose can be calculated in terms of incapacitation and lethality. Many people will be unable to escape during a fire due to incapacitation from inhalation of fire effluent containing irritants and asphyxiants, described in ISO 13344²⁹.

$$FED = \left\{ \frac{[CO]}{LC_{50,CO}} + \frac{[HCN]}{LC_{50,HCN}} + \frac{[AGI]}{LC_{50,AGI}} + \frac{[OI]}{LC_{50,OI}} \dots \right\} \times V_{CO_2} + A + \frac{21-[O_2]}{21-5.4} \quad \text{Equation 5}$$

$$V_{CO_2} = 1 + \frac{\exp(0.14[CO_2]) - 1}{2} \quad \text{Equation 6}$$

Where $[CO_2]$ and $[O_2]$ are expressed in terms of percentage by volume, $[AGI]$ represents a series of terms for each acid gas irritant. $[OI]$ represents a series of terms for each organic irritant. A is the acidosis factor equal to $[CO_2] \times 0.05$. FED values allow for comparing the toxicity of different effluents generated under comparable conditions. However, only an FED value of 1 can be considered meaningful. An FED of 2 can only be interpreted as if that effluent were diluted to twice its volume, it would still be lethal to 50% of the population. ISO 13571 takes the approach of 'consensus estimates' based on an agreed value, whereas ISO 13344 is based on rat exposure data.

1.3.5.5 Material LC-50

The FED values can be used to calculate a material LC_{50} , calculated using Equation 7. The material LC_{50} value represents the toxic potency of the effluent (as an FED of 1 inside a volume of 1 m^3)

yielded from the mass of material burning at a specific fire condition. A higher material LC_{50} indicates lower toxicity for that specific fire condition, and a lower value indicates more toxic smoke.

$$\text{Material } LC_{50} = \frac{M}{FED \times V} \quad \text{Equation 7}$$

Where M is mass in (g), V is volume (m^3).

1.3.6 Common toxicants present in fire effluent

Toxicants in fire effluent can be separated into acute and chronic toxicants.

1.3.6.1 Acute toxicants

Acute toxicants have been separated into two categories: Asphyxiant gases and irritant gases.

1.3.6.1.1 Asphyxiant gases

Asphyxiant gases are generally classified into two sub-categories: simple and chemical³⁰. Simple asphyxiants prevent the victim from acquiring oxygen by displacing the oxygen from the surrounding environment. Chemical asphyxiants, such as HCN or CO, deprive cells of oxygen. They can do this by occupying the haemoglobin responsible for oxygen transport or preventing oxygen uptake by interfering with specific elements used in the metabolic processes of cells. Only three asphyxiant gases are likely to be present in fire effluent: HCN, CO and CO₂.

1.3.6.1.1.1 Hydrogen Cyanide

Hydrogen cyanide (HCN) is a significantly toxic asphyxiant gas produced during the combustion of nitrogen-containing materials. When inhaled, hydrogen cyanide passes through the blood-gas barrier in the lungs and forms cyanide ions in the blood. The cyanide ions bind to the trivalent iron moiety of Cytochrome oxidase C. Cytochrome oxidase C is an enzyme located within the mitochondria membranes of cells. The enzyme is used in the electron transport chain where it aids the process of ATP synthesis. However, as CN⁻ binds to the enzyme, forming Cytochrome oxidase-CN, the enzyme can no longer transport electrons to oxygen in the respiratory chain, stopping cellular respiration from occurring³¹. This essentially prevents cells from utilizing oxygen to release energy within the body³². Many tissues are dependent on such aerobic respiration, including the heart and central nervous system (CNS), meaning, at sufficient concentrations, HCN can induce rapid loss of cellular functions, resulting in CNS depression and cardiac irregularities, ultimately leading to death^{33, 34}.

1.3.6.1.1.2 Carbon Monoxide

Carbon monoxide (CO) is one of the most abundant asphyxiant gases formed during the combustion of organic materials. While it is not as toxic as HCN, the greater volume of CO produced during a typical fire result in it being one of the major hazards in most fire atmospheres. When inhaled, carbon monoxide combines with haemoglobin to form carboxyhaemoglobin (COHb) within the red blood cells. CO has a 220% greater affinity to haemoglobin than oxygen, resulting in cellular hypoxia due to a reduction in haemoglobin's oxygen capacity. CO also causes tissue hypoxia by inducing a leftwards shift in the oxygen disassociation curve, further preventing oxygen delivery. An oxygen dissociation curve is a sigmoid-shaped plot of the partial pressure of oxygen in the blood against oxygen saturation. The pressure difference in oxygen entering and leaving the lungs allows oxygen to bind to haemoglobin more easily³⁵. When the oxygen dissociation curve shifts, it is harder for oxygen to bind to haemoglobin. In addition, CO also inhibits mitochondrial respiration by binding to the haem moiety found in Cytochrome oxidase C (an essential component of the electron transport chain used in mitochondrial respiration)³⁶.

1.3.6.1.1.3 Carbon Dioxide

Carbon dioxide (CO₂) is present in air at around 400 ppm and is a product of combustion and respiration. CO₂ will be at their highest levels when the fire is small and well-ventilated, with levels decreasing slightly as the fire grows and develops into an under-ventilated fire. At low concentrations, CO₂ has very few toxicological effects. The major threats CO₂ poses is as a simple asphyxiant since its presence will result from the replacement of oxygen in the smoke. To ensure

continuous respiration, the accumulation of CO₂ triggers a panic reaction to stimulate breathing, therefore resulting in it having a synergistic relationship with other toxicants.

Upon inhalation, CO₂ dissolves into the water within the lungs³⁷. Once dissolved, it diffuses across the alveolar membranes into the bloodstream. Carbonic acid forms when the dissolved CO₂ is in equilibrium with carbonic acid in the blood. A saturated solution of CO₂ in water has a pH of 5.5, inducing acidosis of the blood (lowered pH < 7.5) at excessive levels of CO₂³⁸. Once this occurs, the body begins to increase levels of plasma proteins in the blood. This is due to plasma proteins being one of the major components in CO₂ regulation in the blood. Severe acidosis of the blood is thought to interfere with the hydrolysis of acetylcholine, a major neurotransmitter in the body, and increase parasympathetic nervous activity. This results in depression of the respiratory system and potentially the circulatory system, which is typical of inhalation of higher levels of CO₂³⁹. The increased concentration of CO₂ stimulates breathing, increasing respiration rates as well as the volumes inhaled, which can increase by up to 50% (when the CO₂ is at 2%)⁴⁰. Blood pressure also increases, and blood vessels begin to constrict, reducing the blood flow in the body.

1.3.6.1.2 Irritants

Irritant gases typically induce sensory and respiratory irritation upon exposure and often prevent escape from fires as a result of this (the effects will vary accordingly with concentration)⁴¹. The most common irritant gases are nitrogen oxides, sulphur oxides and hydrogen halides. Hydrogen halides (HCl, HBr and HF) are evolved from burning materials containing halogens, such as PVC, fluoropolymers, or polymers with flame retardants. Organo-irritants are also produced. However, their yields depend more on the fire's ventilation and the original composition of the decomposing polymer.

1.3.6.1.2.1 Acrolein

Acrolein's toxicological effects result from its high reactivity towards biological nucleophiles, resulting in rapid irreversible binding to cellular components. Its toxicity is thought to be due to reactions occurring with sulphhydryl groups that are present in proteins, disrupting membrane functions. Upon initial inhalation, acrolein is thought to bind to neural receptors located in the mucus membranes of nasal passages and within the cornea, resulting in rapid depolarization of the affected neurons, causing severe irritation. Acrolein has been reported to induce a 50% reduction in respiratory rate (RD₅₀) in mice at 1.7ppm⁴².

1.3.6.1.2.2 Formaldehyde

Similarly to acrolein, formaldehyde is a highly irritating gas formed during the combustion of cellulosic materials. Exposure to low concentrations can induce rapid throat and nasal irritation, chest pain and coughing due to formaldehyde binding to cellular components. Vapours can induce lacrimation and irritation of the eyes if exposed⁴³. Exposure to high concentrations of formaldehyde will result in inflammation of the lungs and windpipe and often result in fluid accumulation in the lungs⁴⁴. While the toxicokinetic mechanism of formaldehyde is not entirely clear, it is believed that when inhaled, it interacts with cell membranes and molecules in body fluids, disrupting cellular functions⁴⁵. The irritant effects of formaldehyde can be felt as low as 2 ppm⁴⁶.

1.3.6.1.2.3 Hydrogen Chloride

Hydrogen chloride gas (HCl) is produced when the burning material contains chlorine or materials containing a chlorine-based fire retardant. It is also commonly produced from burning materials such as PVC⁴⁷, used to make electrical cables, window frames, synthetic leathers, wallpapers, wall linings (bathroom/shower) and plastic articles.

HCl causes severe irritation at approximately 100 ppm⁴⁸ and can cause death at high concentrations (5500 ppm in mice for 30 minutes of exposure, with incapacitation occurring at 1000 ppm). Due to HCl's high water solubility, rapid adsorption occurs on mucous membranes within the upper respiratory tract after inhalation. After the HCl has been adsorbed by the mucous layers, it will then dissociate into chloride ions and hydrogen ions. The hydrogen ions then produce hydronium ions from their reactions with water within the body. These ions go on to react further with the organic molecules within the body. These reactions are thought to be responsible for the cellular injury and cell death that is commonly observed in HCl exposure (in high concentrations)⁴⁹. The sites where this occurs often accumulate fluid resulting in pulmonary oedema⁵⁰. Rather than causing a direct effect, the chloride ions are thought to be distributed around the body due to them being common electrolytes⁵¹. Typical concentrations of chloride ions are not thought to be high enough to affect the body's electrolyte balance⁵².

1.3.6.1.2.4 Hydrogen Bromide

Bromine-based flame retardants are common additives in construction products, especially electrical and furnishing products. When burnt, large quantities of HBr can be produced. Like HCl, HBr's toxicity is largely due to its high water solubility and potent oxidising abilities. Upon inhalation, HBr causes irritation to the upper respiratory tract⁵³. The HBr is then absorbed into the mucous membranes of the respiratory tract and disassociates into bromide ions and hydrogen ions. If chronic exposure occurs, the bromide ion can potentially displace the Cl ion present in plasma (found within extracellular fluid) or from cells within the body⁵⁴. In an attempt to control a constant total halide ion concentration, the kidneys then begin to increase the elimination of chloride ions. This causes impairment of the central nervous system.

1.3.6.1.2.5 Nitrogen oxides

Nitrogen oxides (NO and NO₂) are formed during fires by the combination of nitrogen and oxygen from the burning of nitrogen-containing materials. Upon inhalation, NO and NO₂ can react with water to form nitrous (HNO₂) and nitric acids (HNO₃), respectively. They interact with the mucous membranes within the respiratory tract. The NO_x ions can either remain in the lungs or be transported around the body via the bloodstream. Once in the bloodstream, NO₂⁻ or NO₃⁻ will oxidise the haem iron in haemoglobin to its ferric state to form methaemoglobin (MetHb), which has a higher affinity for oxygen but is less available haems to bind to oxygen and hence decreases the oxygen carrying abilities of the blood⁵⁵. This will reduce the oxygen supplied to tissues in the body. At low concentrations, NO can induce vasodilation and lower blood pressure in the body⁵⁶.

1.3.6.2 Chronic Toxicants

1.3.6.2.1 Polycyclic aromatic hydrocarbons

Polycyclic aromatic hydrocarbons (PAHs) are volatile organic compounds commonly produced during unwanted fires. Individual PAHs attach themselves to other PAHs by loosely attaching to them, or by fusing to form structures with more rings⁵⁷. When more PAHs stick together and accumulate, the gas phase molecules ultimately become tar droplets and soot particles⁵⁸.

PAHs are typically lipophilic, so when inhaled, they easily cross cell membranes via passive diffusion. This also allows them to be bio-accumulative in fatty tissue⁵⁹. The PAHs then go on to be metabolized by enzymes within the cells into phenols and quinones, eventually producing radical cations, redox-active molecules and diol-epoxides⁶⁰. These react with DNA producing DNA adducts which interrupt the process of DNA replication, leading to mutations⁶¹.

1.3.6.2.2 Isocyanates

Isocyanates are a common product used in manufacturing and are released during the decomposition of polyurethanes. They are defined by their isocyanate functional group ($-N=C=O$), which is often connected to an aromatic moiety⁶². The capacity of isocyanates to act as respiratory sensitizers, leading to asthma after a single exposure in sensitive individuals, was first identified during their manufacture and when making polyurethanes. This functional group is highly reactive, especially towards nucleophiles such as amines or hydroxyls, including water. Another exposure route to isocyanates is through inhalation of fire effluents.

Initial exposure to low concentrations will typically induce irritation of the eyes, airways, and skin. Exposure to high concentrations can result in swelling of the lungs. This can occur upon exposure or several days after exposure. Isocyanate exposure is commonly associated with long-term respiratory problems⁶³, most commonly asthma^{64,65}. Isocyanates are thought to induce long-term respiratory problems by directly binding to epithelial cell proteins when inhaled, confirmed by the detection of isocyanates in the epithelial cells in the airways of exposed workers and animals⁶⁰. Isocyanates present a significant hazard in fire effluents but can be difficult to quantify because of their high reactivity.

1.3.6.2.3 Halogenated dioxins and furans

Halogenated dioxins (also referred to as dibenzo-p-dioxin) and furans (referred to as dibenzo furan) are highly toxic cyclic aromatic hydrocarbons. While little is known about their initial toxicity, their long-term effects are widely reported. Both dioxins and furans are bio-accumulative and are well-absorbed by body tissues, predominantly in adipose tissues and the liver. Some dioxins have shown a half-life in the body of between 7 and 12 years⁶⁶.

1.3.6.2.4 Volatile Organic Compounds

VOCs are a product of incomplete combustion. Their generation is dependent on the fuel composition, as well as the fire condition. Due to this, they are considered potential fuel markers. However, over time the volatility of the VOCs changes making it difficult and unrealistic to assign VOC profiles to specific fuels⁶².

1.3.7 Effect of fire condition on fire toxicity

Fire condition has a direct impact on smoke toxicity. In a fuel-rich fire, the only factor limiting fire growth is oxygen availability. Hence, as the fire progresses and consumes more oxygen, it drives the fire to change from well-ventilated to under-ventilated, reducing the combustion efficiency (the percentage conversion of fuel to fully oxygenated products). As the fire shifts from well-to-under-ventilated, the combustion products change, typically becoming more toxic. Studies have found that CO yields dramatically increase as the equivalence ratio changes.

As the fuel-rich fire grows, the amount of available oxygen will decrease. The lack of oxygen will cause the equivalence ratio to increase and an increase in smoke production. The smoke will often contain a cocktail of toxicants, including the main asphyxiants, CO and HCN, whilst particulates reduce visibility within the smoke. Figure 4⁶⁷ shows the contribution of toxicants from different materials under different fire conditions for a range of materials, expressed as Fractional Effective Dose (FED) ⁶⁷. An increase in CO and HCN can be seen when the fire condition shifts from well-ventilated to under-ventilated. As these materials also contain gas-phase flame retardants, the CO and HCN yields are higher for well-ventilated flaming. This is particularly prevalent in PIR foams. In each material tested, the FED contributions from the material increases as the ventilation decreases.

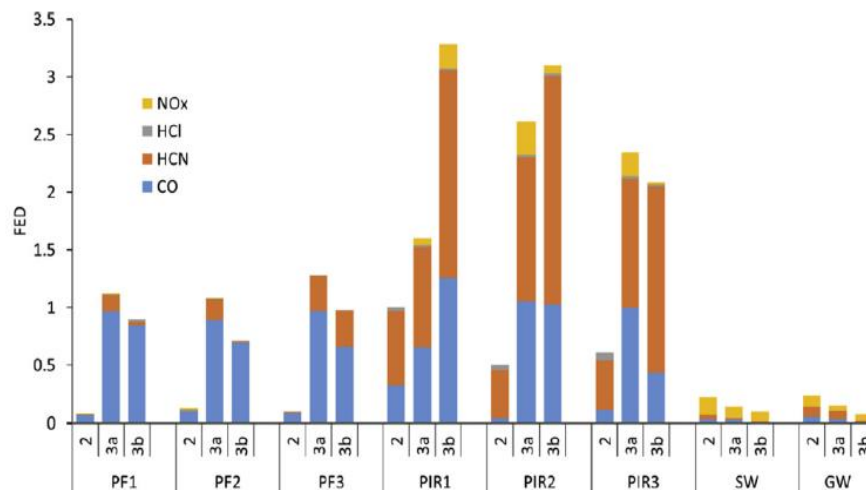


Figure 4: 30 min lethal FED (ISO 13344) from burning 1 kg with the effluent dispersed in a volume of 50 m³ for a range of materials under different fire conditions, indicated by ISO fire stage (2, 3a, 3b). PF to PF3 are different commercial Phenolic foam insulation⁶³.

1.3.8 Methods for generating fire effluent

Smoke toxicity results from a combination of both the combustion conditions and the materials' chemistry. For smoke toxicity to be assessed appropriately, it is essential that the apparatus used to generate the smoke can accurately replicate the fire stages and conditions the material is exposed to. Flammability tests typically use the atmospheric concentration of oxygen (21%) as the likely worst case for flammability but the least bad case for fire toxicity. The worst-case scenario is when the oxygen concentration has fallen below 10%, causing yields of carbon monoxide (CO) and hydrogen cyanide (HCN) to increase exponentially. However, few test apparatuses are able to force combustion under these conditions. Some flammability tests, such as the cone calorimeter, have been modified to attempt to quantify smoke toxicity but are generally unable to replicate the toxic product yields of under-ventilated flaming.

The difficulty in replicating real fire conditions results from several practical problems originating with the apparatus design. Firstly, toxic product yield depends on the fuel-to-air ratio; this is often unknown for flammability test methods. Secondly, if products are recirculated into the flame zone, the toxicity measured may change. Thirdly, uncertainties and errors will arise in apparatuses where the fuel-to-air ratio changes rapidly as this will alter the effluent composition, placing an artificially short limit on the time available for sampling and taking mass loss measurements. As most of these tests were originally designed to assess flammability, they use a fixed heat flux and allow the sample flammability to dictate the burning rate. The applied heat flux must be sufficient to force burning at low oxygen concentrations to avoid these problems. Forcing a sample to burn at a fixed rate, independent of flammability, by varying the applied heat flux has been shown to replicate different ventilation conditions accurately³.

Various apparatuses for assessing smoke toxicity exist, though some are more representative of real fires than others. ISO 16312-1⁶⁸ details the criteria for assessing the validity of fire test apparatuses. One of the most important principles described in the standard is model validity. The test method must accurately reproduce toxicant yields found in real fires (i.e. be representative of large-scale data). According to ISO 16312-1, the ideal apparatus will be able to attain constant combustion conditions and prolonged steady-state periods for toxic smoke analysis. The apparatus must accurately define the fire condition to provide relevant smoke toxicity data.

1.3.8.1 *Smoke Density Chamber*

One apparatus commonly adopted for smoke toxicity assessment is the smoke density chamber (SDC) (ISO 5659-2)⁶⁹. The smoke density chamber was designed for smoke obscuration measurements. A sample (75 mm ± 1 mm) is placed in the sample holder inside the chamber and exposed to radiative heat after closing the door. A spark ignitor or pilot flame can be placed near the sample to induce ignition depending on the test condition required. The SDC offers a range of test conditions, although they are not linked to a particular specific fire scenario. ISO 16312-2⁶⁴ notes the SDC is only representative of fire stages 1b (oxidative pyrolysis) and 3a (well ventilated flaming).

Upon testing, the chamber fills with gaseous fire effluent as the sample burns, which is drawn through a sampling port located at the top of the chamber. The extent of the mixing of the smoke with air in the chamber depends on the burning behaviour of the fuel. A fuel with a high heat release rate will cause more complete mixing than one with a low heat release rate. Smoke obscuration measurements are also taken using a light source and detector within the chamber.

Despite its adoption by mass transport industries as a means of toxicity assessment^{70,71,72}, the SDC is unable to replicate under-ventilated flaming, ultimately preventing the test from being able to distinguish between materials that produce very toxic fire effluent and those whose toxicity is much less. Due to the design of the apparatus, the sample thickness and combustible fuel content will dictate the ventilation condition the material is exposed to, meaning both the burning behaviour and toxic product yields will vary depending on sample preparation. An attempt to force under-ventilated burning in the SDC by increasing the sample mass resulted in premature extinction of the larger samples, once the oxygen concentration in the chamber fell significantly⁷³. As the SDC is currently unable to produce reproducible data that has a definitive fire scenario, there is difficulty in comparing SDC data with real fire data.

1.3.8.2 Cone Calorimeter

The cone calorimeter (ISO/TS 5660-5:2020)⁷⁴, shown in Figure 5⁷⁴, is one of the world's most widely used fire testing apparatuses. A sample (typically 100 mm x 100 mm) is placed on the sample holder and exposed to radiative heat with a removable spark ignition source above the sample. Upon ignition, the spark ignition source is moved away from the material. Parameters such as the sample's heat release and mass loss are measured throughout the test. A series of modifications have been made to the apparatus for smoke toxicity measurement, including enclosing the combustion zone and providing controlled ventilation to the chamber. This modified controlled atmosphere cone calorimeter (CACC) has been shown to replicate early well-ventilated flaming⁷⁵ where the fire would be of insufficient size to generate enough toxicants to cause harm.

Laboratory tests have previously shown⁷⁶ that the fire effluent produced tends to continue to burn as it emerges from the chamber, giving ambiguous data about the ventilation condition. To mitigate this, a longer chimney was added to the test design in attempt to handle the after-burning effects that were noted to have occurred previously. However, ambiguity of the combustion conditions and equivalence ratio ultimately means that the toxicity data produced cannot be confined to a specific fire condition, increasing the difficulty in comparing CACC data to real fire data.

The standard cone calorimeter design (without the controlled atmosphere) has difficulties in replicating specific fire conditions, the test is widely accepted as a means of determining the flammability of a material and obtaining data regarding a materials heat release rate, mass loss, and ignitability. The information about a material obtained through cone calorimetry can provide a basis for predicting how a material will behave on a large scale.

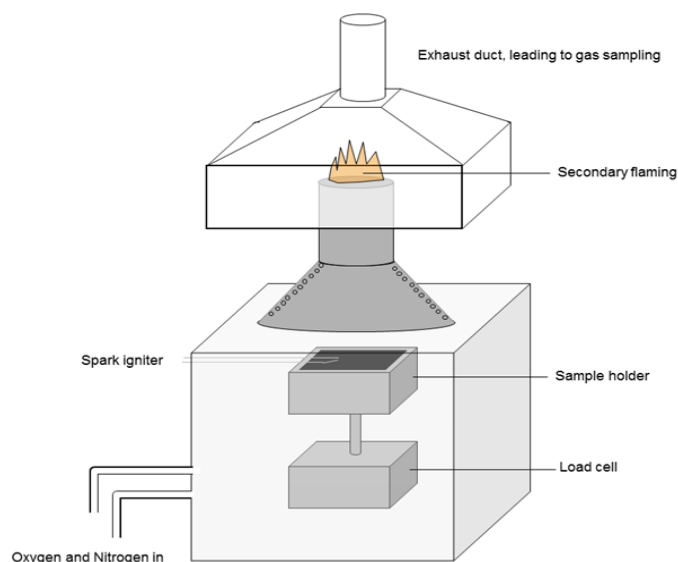


Figure 5: Schematic diagram of the Controlled Atmosphere Cone Calorimeter⁷⁰

1.3.8.3 Non-dynamic Tube Furnace (NF X 70-100)

The non-dynamic tube furnace (NFX)⁷⁷, shown in Figure 6, is also commonly used for smoke toxicity assessment. It forces the thermal decomposition of a small static specimen (~1 g) in a furnace with metered airflow (2 L min^{-1}), driving the effluent into a sampling system. The sample is introduced into a quartz tube inside a furnace heated by external heaters. Air is fed through the tube at a fixed rate. The effluent is then drawn and collected at the other end of the tube and sampled for toxic gases.

The equivalence ratio can only be determined when the rate of pyrolysis is known, which requires additional on-line analysis. The rate of pyrolysis is material dependent, so testing at the same air flow will result in equivalence ratios that vary with materials and furnace temperatures. The French standard (NF X 70-100) allows for applying three different conditions; 400°C, 600°C and 800°C. These conditions do not correlate with the exact fire stage; however, it could be assumed that 400°C corresponds to pyrolysis without ignition representing oxidative pyrolysis, 600°C corresponds to well-ventilated flaming, and 800°C corresponds to under-ventilated flaming. The results obtained from the test are susceptible to differences in furnace design⁷⁸. In addition, a sample that is close to ignition will not always ignite, and there is no requirement to report whether flaming occurred. This leads to problems of reproducibility and reliability of the data obtained, meaning several replicate tests are often required to obtain a sufficient volume of sample for effluent analysis.

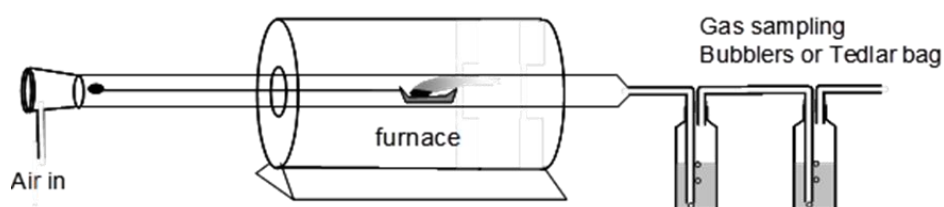


Figure 6: Diagram of the Non-dynamic tube furnace⁷³.

1.3.8.4 Steady State Tube Furnace

The steady state tube furnace (SSTF) (ISO/TS 19700⁷⁹), shown in Figure 7, forces samples to sustain burning at a steady rate in ventilation-controlled conditions, replicating the individual stages of real fires. The instrument offers a range of conditions, including under-ventilated and well-ventilated fires at different temperatures by forcing combustion by driving a sample at a fixed rate into a ventilation-controlled furnace of increasing heat flux. The SSTF is the only fire test that can accurately replicate each fire stage by steady burning. In addition, toxic product yields can be quantified from a combination of mass feed rate and gas concentrations during steady burning, which can be correlated to a specific fire condition. The ability to define the specific fire condition and equivalence ratio makes the SSTF particularly useful when comparing large-scale data.

The SSTF can also accurately quantify products such as HCN, CO/CO₂, NO_x and acid gasses. Using test methods ISO 13344²⁵ and ISO 13571²³, the test can generate data for input to fire hazard assessments in relation to the ISO fire stages. These reasons have resulted in its use for this project. The SSTF has routinely been shown to produce reliable and reproducible data that shows good agreement between laboratories^{80, 81}. The SSTF has also proven to be the most reliable apparatus for toxicity testing, being one of the only methods to replicate under-ventilated flaming accurately.

The apparatus introduces the sample at a fixed rate, typically around 1g per minute. As the sample is introduced into a pre-heated furnace, the temperature of the sample rises and eventually induces ignition. This process repeats as each 1g is fed into the furnace, resulting in the flame spreading and occurring at a relatively fixed rate, similarly to how a fire behaves in real life. As this happens, the fire effluent rises from the sample and is forced into the mixing chamber by the flow of air passing over the sample. The effluent is then drawn from the mixing chamber for analysis. The effluent is typically well mixed due to the secondary air flow forcing mixture in the mixing chamber. The primary air flow can easily be altered, allowing for easy alterations to the equivalence ratio, enabling a range of conditions to be tested.

At low flow rates (around 2 L min⁻¹), the fire effluent can flow back from the mixing chamber and back into the quartz tube. To avoid this, a plug with a small hole through it is often used to prevent the effluent from re-entering the quartz tube but still allows effluent into the chamber. Nitrogen balancing can also be used to prevent this from occurring. This involves the addition of nitrogen gas to the primary air flow so that no effluent flows back into the tube, but the gas flow has little to no effect on the chemistry of the effluent.

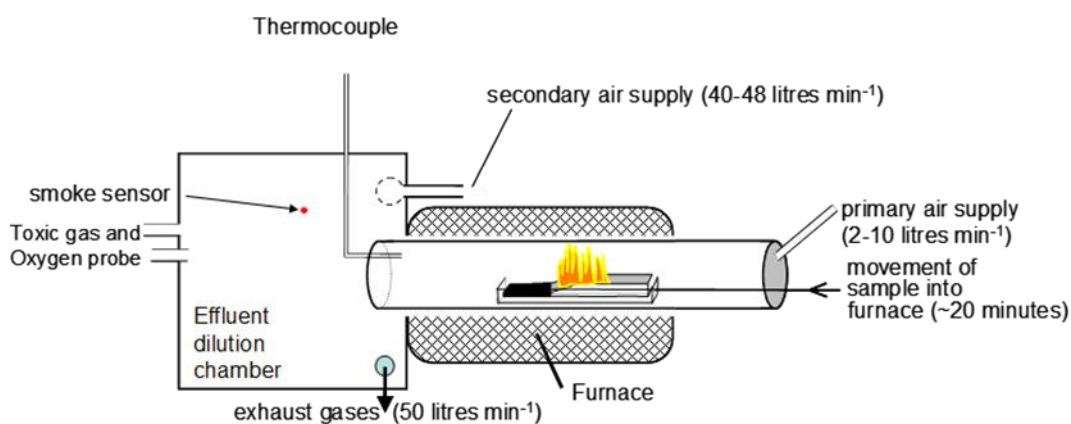


Figure 7: : Diagram of the Steady State Tube Furnace ⁷⁵.

1.3.8.5 The Fire Propagation Apparatus

The fire propagation apparatus (FPA) (ISO 12136)⁸², shown in Figure 8, consists of a vertical cylindrical tube which contains the fire zone. Four external radiant heaters force pyrolysis until the material is ignited with the pilot flame. They continue to drive flaming, adding to the radiant flux from the burning material. The method was designed to measure heat release rate, sample mass, oxygen depletion and CO/CO₂ yields throughout the test. The data generated can be used to calculate the equivalence ratio of the test and identify the fire stage. ASTM E2058⁸³ notes the apparatus is capable of reproducing fire stages: 1b, 1c, 2 and 3. The test has been used previously for fire effluent analysis, with CO data being shown to be representative of real fire scenarios⁸⁴. However, no data has been reported for HCN.

The ability of the apparatus to generate toxic gases has not been formally assessed for its inter-laboratory reproducibility. Currently, the test method is limited to flammability measurements, heat release rate and smoke measurements. The test is relatively unsuited for smoke toxicity measurements as the flame zone is typically present in the cylindrical quartz tube, with measurements typically taken from the top. As the flame reactions may not be complete before the effluent leaves the quartz tube, the effluent composition may change in the analysis chain.

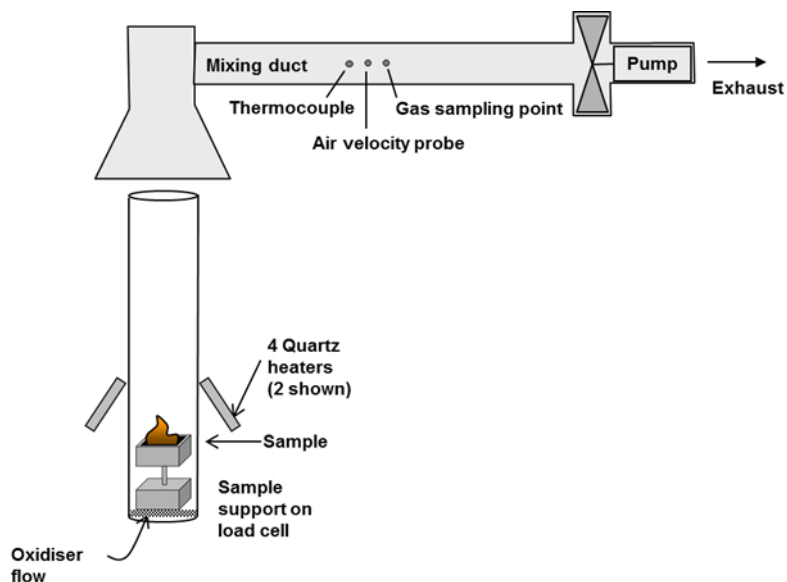


Figure 8: Schematic diagram of the Fire Propagation Apparatus⁷⁸.

1.3.8.6 Radiant test apparatus

The NFPA 269/ASTM E 1678 Radiant test apparatus⁸⁵, shown in Figure 9, was designed for smoke toxicity assessment. Test materials are typically prepared in configurations to approximate the full material.

Fire effluent is drawn through Port C through a 6.5 mm cooled coiled copper tube, followed by a cooled impinger (placed in dry ice) with glass wool and a glass fibre filter before going through an non-dispersive infrared analyser (NDIR) and paramagnetic analysers for continuous monitoring of CO, CO₂ and O₂. After analysis, the effluent is returned to the chamber through port F. Sampling is typically maintained at 1 L min⁻¹ for O₂, CO and CO₂ measurements.

Additional sampling lines can be set up in port E for Fourier Transform Infrared Spectroscopy (FTIR) analysis. The effluent is drawn through Port E through a heated copper tube (approximately 170 ± 5°C) piercing a rubber stopper placed in a sampling port at a flow rate of approximately 10 L min⁻¹ (variation in the flow rate is common due to smoke deposits fouling the sampling line). The effluent is then returned to the chamber through Port A.

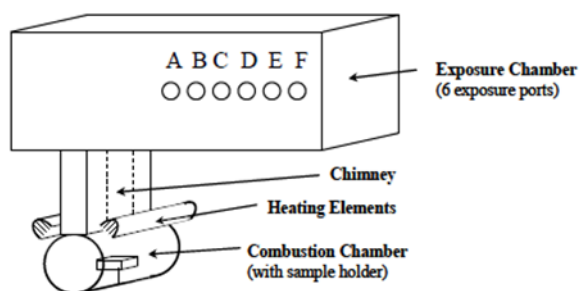


Figure 9: Schematic diagram of the Radiant Test Apparatus⁸¹.

1.3.9 Methods for quantifying fire effluent

There are three key components to successfully quantifying smoke toxicity. First, the fire effluent must be generated in a consistent manner which can be related to a particular fire stage. As discussed, smoke toxicity depends on a material's chemistry and the combustion conditions the material is exposed to. This means that to quantify smoke toxicity accurately, one must identify the combustion conditions to assess the most relevant fire scenarios.

Smoke toxicity increases with lowered ventilation, so a bench-scale method must be able to replicate this scenario to assess the worst case for a material. Many current apparatuses were not designed to achieve this, with some tests unable to sustain flaming at oxygen concentrations below 12%. Oxygen concentrations in dwelling fires have been shown to drop below 10%, a concentration many apparatuses would not be able to sustain flaming. Secondly, the fire effluent must be sampled consistently and without loss.

Effluent is typically sampled for a specified time during a test and represents that particular period during the test. Steady burning often presents the best opportunity for sampling as the effluent produced should be relatively consistent for the steady period. The smoke produced during combustion consists of various components, including many condensable water- and water-soluble species. So, it is important to choose a sampling method to minimise losses due to condensation. Cold sampling lines can result in water droplets forming, which will trap water-soluble gases. Gases can also adsorb onto solid matter such as metal or plastics.

Thirdly, once the sample has been generated and sampled, the gases need to be analysed. Smoke is complex and made up of a wide variety of components, so, unsurprisingly, no single method or combination of methods can accurately identify all toxicants present in the smoke. "Permanent" gases, such as O₂, CO₂, and CO have well-known, robust methods for sampling and analysis using methods such as paramagnetic analysers, electrochemical cells and non-dispersive infrared analysers. These gases are less susceptible to sampling issues and are typically easy to measure robustly. Analysis of most other toxic components can be undertaken by trapping fire effluent in bubblers after passing a known volume. The volume must be known to calculate the concentration of toxicants in the gas phase.

HCN is typically trapped in a solution of weak sodium hydroxide and quantified by derivatising the solution using chloramine T. The chloramine T reacts with cyanide present in samples producing cyanogen chloride. This then goes on to react with the reagents 1-phenyl-3-methylpyrazole-5-one and isonicotinic acid, yielding a blue solution⁸⁶. The cyanogen chloride breaks the aromatic ring in isonicotinic acid, producing carboxy-glutaconic aldehyde, which can then react with 1-phenyl-3-methylpyrazole present in the reagents to produce the polymethine dye. Hydrochloric acid and cyanamide are also produced as by-products. The intensity of the solution will increase with increasing cyanide concentration which can be measured colourimetrically as the dye follows the Beer-Lambert law, whereby the concentration of cyanide ions in solution is directly proportional to absorbance. This method is described in ISO 19701⁸⁷.

Toxicants such as acid gases are water soluble and can be trapped in a water solution. The solution can then be analysed using techniques such as High-Performance Liquid Chromatography (HPLC).

Techniques such as FTIR can be used to identify a wider range of gases with a single method. While FTIR is a powerful means of gas analysis, complex mixtures can cause peak overlap in the spectra, requiring challenging, detailed interpretation. A large proportion of chromatographic techniques (such as gas chromatography-mass spectroscopy) are commonly used to identify further toxic

species but are much harder to use for quantitative analysis, although similarly to peaks overlapping, toxicants can obscure the presence of other toxicants. Each mode of analysis will have its own positives and negatives, with some techniques being more sensitive to one toxicant than others. For this reason, it is unsurprising that analysis typically involves a wide range of analytical methods.

1.3.10 Comparisons between bench-scale methods

Blomqvist and Sandinge⁸⁸ investigated four bench-scale methods for assessing fire toxicity: the Steady State Tube Furnace (ISO/TS 19700) (SSTF), the non-standard Controlled Atmosphere Cone Calorimeter (CACC), the Fire Propagation Apparatus (ASTM E2058 and ISO 12136) (FPA), and the Smoke Density Chamber (EN ISO 5659-2) (SDC) with the effluent analysis in accordance with the EN 45545-2 test procedure. 12 materials were tested using three bench-scale methods, SSTF, CACC and SDC, with the FPA test limited to a single material (PMMA). The remaining materials tested were thermal insulation products, comprising five polymeric foams, two organic fibre insulation materials and four mineral fibre insulation materials. All gas analysis was carried out using FTIR. A summary of the conditions tested throughout this literature is shown in Table 4.

Each material was tested under several conditions. In the CACC, the oxygen concentrations varied from 10 or 15% to 18% to achieve the desired condition.

Table 4: Summary of the conditions tested, showing applied heat flux and ventilation condition⁸⁴.

Condition	Abbreviation	SSTF	FPA	CACC
Non-flaming	N-F	350 °C Low air flow	50 kW m ⁻² ; 21% O ₂	50 kW m ⁻² ; 10-15% O ₂
Well-ventilated	W-V	650 °C High air flow	50 kW m ⁻² ; 21% O ₂	50 kW m ⁻² ; 21% O ₂
Under-ventilated	U-V	825 °C Low air flow	50 kW m ⁻²	50 kW m ⁻² ; 15-18% O ₂

The conditions used for the SDC tests are classified as mixed conditions, largely due to the SDC's inability to replicate specific fire scenarios. Instead, the conditions tested were: mixed condition 1 (MC1) 25 kW m⁻² with pilot ignition and mixed condition 2 (MC2) 50 kW m⁻² without pilot ignition. Since the pilot flame does not guarantee the sample will ignite, and its absence does not prevent it from igniting.

The interpretation of equivalence ratio for the CACC for the tests conducted was based on the theoretical temporal global equivalence ratio which calculated by using a combination of: the mass loss measurements, oxygen concentration measurements, the total oxygen flow rate through the box and the theoretical oxygen demand for complete combustion (found from elemental composition analysis), taken throughout the test.

1.3.10.1 Discussion of the results obtained from the report:

The results obtained from the report have been summarised in sections for the different materials tested.

1.3.10.1.1 PMMA:

PMMA was tested using all four apparatuses and the conditions described above. All apparatuses produced high yields of CO₂ during the well-ventilated tests. The SSTF produced the highest CO₂ yields showing near-complete combustion of the material. For under-ventilated flaming, the SSTF produced a yield of CO typical of under-ventilated flaming. The three other under-ventilated tests showed high yields of CO₂ and much lower yields of CO, suggesting under-ventilated flaming had not occurred. This is consistent with other studies showing similar results⁸⁹. The elemental analysis conducted in the study showed the material contained less than 0.05% nitrogen, insufficient to produce detectable nitrogen-containing decomposition products. However, the SDC and CACC generated detectable concentrations of NO_x and HCN, suggesting there are contributions from N₂ oxidation in the test atmosphere (methane gives 15ppm of HCN burning in air⁹⁰). In the oxygen-depleted CACC tests, after-burning occurs outside of the combustion chamber from early on in the tests, invalidating the under-ventilated condition.

As the SDC pilot flame contributed to CO₂ and NO_x yields, all data obtained using the pilot flame tests required correction. Such correction adds to the uncertainty of the data, raising questions on the validity of other experimental data that have not taken the gases produced by the pilot flame into consideration.

1.3.10.1.2 Polymeric Foam:

Based on the information supplied in the report, the polymeric foams are likely to have included phenolic, polyurethane/polyisocyanurate and expanded polystyrene foams. Generally, the SSTF was found to adequately replicate the desired fire scenarios, with some well-ventilated tests showing CO₂ yields that were 99% of the theoretical yield indicating very well-ventilated flaming. The CACC consistently reported lower CO yields during under-ventilated tests compared to the other apparatuses suggesting the under-ventilated condition was not always achieved. The inability of many fire test apparatuses to replicate under-ventilated flaming has been a common observation throughout literature⁹¹.

In the PF₄ tests, the SDC struggled to sustain flaming throughout. The test was conducted at 25 kW m⁻² (with pilot flame) and sustained flaming combustion for only 2 minutes of the 20-minute test time. The contributions from the pilot flame meant the data produced needed to be corrected. However, this resulted in a very high CO₂ yield of 3305 mg g⁻¹. In addition, in most of the CACC and SDC tests (e.g. PF₃), there is seemingly a lack of differentiation between test conditions. In some CACC tests, the CO yield decreases as the ventilation is reduced. CO yields typically increase with decreasing ventilation.

1.3.10.1.3 Organic fibre tests:

Organic fibre insulation products are predominantly cellulosic and will be expected to burn, producing CO₂, H₂O, CO and char. For the well-ventilated tests, both the CACC and SSTF showed high yields of CO₂ and low yields of CO, suggesting well-ventilated flaming was achieved. In the case of under-ventilated flaming, the SSTF was the only test to show the high CO yields associated with this condition. The CACC showed lower yields of CO₂ and higher yields of CO during under-ventilated flaming but did not generate high yields of CO₂ during well-ventilated flaming tests. In both the SDC tests at 25 kWm⁻² and 50 kWm⁻², results were similar, showing the SDC did not distinguish between the conditions. The 25 kW m⁻² test also showed higher yields of CO than the 50 kW m⁻² test. As cellulosic materials produce a lot of CO during non-flaming (smouldering) combustion, this suggests

erratic flaming or extinguishment. In the case of non-flaming tests, the CACC and SSTF generally showed relatively high yields of CO and low yields of CO₂, with similar results.

1.3.10.1.4 Mineral fibre tests:

The organic (combustible) content of the mineral fibres was reported to vary from 2-4%, generally too low a proportion of fuel to support flaming combustion. For the tests using mineral fibre materials, the CACC generally did not detect CO₂ in measurable yields in well-ventilated tests. In some cases, the CO yields produced by the CACC matched those of the SSTF, although the CO yields produced by the CACC were found to decrease with under-ventilation. During under-ventilated tests, the SSTF generated both NO_x and SO₂. In some SDC tests, the CO₂ concentration produced by the pilot flame was several times higher than that from the sample, but as the yields of CO₂ were low, correcting the CO₂ yield left the value lower than the error limits. The CACC and SSTF produced similarly low yields of CO throughout the tests. The SSTF generated quantifiable amounts of HCN during most tests. Elemental analysis showed the materials contained between 0.05% to 0.57% nitrogen. It was also reported that at a particular fuel-to-air ratio, yields varied as the volume of air flowing through the SSTF varied, showing that the current protocol needs to be extended to cover non-combustible materials.

The differences observed in yields of toxicants produced during the tests can be attributed to the differences in test methods.

For each product, the SSTF could distinguish between under-ventilated flaming and well-ventilated flaming. The CO yields were most representative of the fire condition and permitted comparison with other test methods. It was noted that obtaining and maintaining steady burning was difficult, particularly in the polymeric foam tests. In non-flaming tests, the protocol needs to be adapted to better replicate this condition. For mineral fibres with very low fuel content, where flaming combustion does not occur, the protocol must also be adapted to reduce the dependence on air flow.

The CACC seemed to replicate an intermediate between well-ventilated and under-ventilated flaming. When testing PMMA, low yields of CO₂ were produced alongside higher yields of CO, indicating less than complete combustion. Generally, a mix of fire conditions was observed rather than a particular O₂% replicating a particular fire stage. Reducing the chamber O₂ concentration did not always increase the CO and HCN yields. There was also the recurring problem of flaming occurring outside of the combustion chamber.

In the SDC, the pilot flame in the 25 kW m⁻² tests added a significant uncertainty, particularly when low yields of CO₂ were produced. Pyrolysis products also accumulated in the chamber, potentially affecting the measured gas yields within the chamber. This adds to the uncertainty of the test. The SDC also generated quantities of NO_x from materials such as PMMA, where nitrogen was absent from the material. This was believed to result from oxidation of the atmospheric nitrogen present in the chamber.

From the test methods used, the SSTF was able to replicate both well-ventilated flaming and under-ventilated flaming. While the report recommends the SSTF as a useful method for non-flaming behaviour, it is apparent that modification to the protocol would be beneficial. It is also apparent that the ISO/TS 19700 standard may require a modified protocol for non-combustible materials where flaming does not occur.

1.3.10.2 NIST Study on Smoke toxicity generation

The US National Institute for Science and Technology (NIST) produced a series of technical reports (1760⁹², 1761⁹³, 1762⁹⁴ and 1763⁹⁵) to assess correlations between bench-scale smoke toxicity measurements with those from a large-scale test for both pre- and post-flashover conditions. The reports focused on three products: a bookcase with a PVC finish, a sofa with a chlorine-based fire retardant, and household cables lined with PVC and nylon. The report explains that sample sizes were chosen to produce a fractional effective dose (FED) of near 1.

1.3.10.2.1 Technical report 1760

NIST technical report 1760⁸⁸ focuses on assessing the smoke toxicity of a series of materials using the Radiant Test apparatus. Sofa materials were prepared in 7.5 cm x 7.5 cm x 1 cm squares with a single 7.5 cm x 7.5 cm piece of fabric on the top, bookcase materials were prepared in 7.5cm x 10 cm lengths with the vinyl surfaces facing the heaters, and cable materials were prepared into 3 x 7.5 cm lengths.

A total of 12 toxicants were sampled for in each test: CO (minimum detection limit: 20 uL/L), CO₂ (minimum detection limit: 800 uL/L), NO₂ (minimum detection limit: 40 uL/L), NO (minimum detection limit: 70 uL/L), HCN (minimum detection limit: 35 uL/L), HCl (minimum detection limit: 20 uL/L), C₃H₄O (acrolein) (minimum detection limit: 20 uL/L) and CH₂O (formaldehyde) (minimum detection limit: 40 uL/L). As no bromine or fluorine was present in the samples being tested, HBr and HF formation were not monitored. Toxicants were continuously monitored using NDIR gas analyser (used for CO₂ and CO), paramagnetic oxygen analysers and FTIR.

Fire effluent was drawn through a port using a 6.5 mm cooled coiled copper tube, followed by a cooled impinger (placed in dry ice) with glass wool and a glass fibre filter before going through the NDIR and paramagnetic analysers. After analysis, the effluent was returned to the chamber through port F. Sampling was maintained at 1 L min⁻¹ for O₂, CO and CO₂ measurements. An additional sampling line was set up in the end port (E) for FTIR analysis. Initially, the effluent was drawn through Port E via a heated copper tube (approximately 170 ± 5°C) piercing a rubber stopper placed in a sampling port at flow rate of approximately 10 L min⁻¹ (variation in the flow rate was observed due to smoke deposits fouling the sampling line). The effluent was then returned to the chamber through Port A. However, to improve the data obtained by the FTIR, the sampling point was moved to the side of the chimney (approximately 7 cm from the top). After moving the FTIR sampling position, an increase in the measured effluent volume fractions was observed before diluting the effluent with 200 L of air. Based on these findings, samples were drawn through the chimney from the point of ignition to when flaming ceased and sampled from Port E in the chamber. It was assumed that the ratio of the volume fractions measured in the chimney to the ratio of CO/CO₂ was the same as the ratio of volume fractions measured in the chamber. Average volume fractions in the chimney measured throughout the sample burn were used and related to the final volume fraction measured in the collection chamber. In several tests, flames were noted to extend past the sampling point.

Preliminary tests showed the bookcase specimens continued to smoulder after flaming ceased, and cable materials continued to pyrolyse. The effluent produced during this time was not included in the toxicity analysis as it was thought to be potentially misleading of the pre- and post-flashover flaming. In addition to standard testing, variations to the standard procedure were also examined. This involved altering the oxygen volume fraction from 0.21 to 0.17 and varying the sample preparation from intact to diced samples (cables cut into 1 cm lengths).

The cable specimens were the only material to produce quantifiable yields of HCl. The increase in HCl yields from the diced cables was attributed to the exposure of the PVC interior. No HCl was detected from the sofa foam with a Cl-based fire retardant or the bookcase with PVC finish. HCN yields were calculable from both the sofa and cable specimens but at yields close to the detection limits. The bookcase showed no HCN above the limits of detection. All other toxicants present in the effluent were below the detection limit. Before calculating fractional effective concentrations (FEC) and FEDs for acrolein, the incapacitation limits of acrolein were suggested to be unnecessarily conservative as a direct result of the incapacitation limits being close to the limits of detection. Based on an animal study⁹⁶, humans were said to be expected to be able to withstand nearly instantaneous exposure of a minimum of 300 µL/L without incapacitation. The FEC value used for acrolein was reduced to <0.1.

The recorded CO yields (g/g) throughout all tests were below 0.2 g/g (a yield of 0.2 g/g would be expected from under-ventilated fires), and no significant effect on CO₂ and CO yields was found when changing initial oxygen volume fractions. Diced specimens produced higher yields of CO (in the case of the bookcase) and higher yields of HCl (in the case of cable specimens). All other toxicants remained below the limits of detection in all tests. This was deemed to be a result of using a short optical path length (115 mm) in the FTIR, limiting both the precision and sensitivity.

The yields of CO showed low repeatability for all three materials, with the bookcase prone to unpredictable transitions from flaming to smouldering, generating a disproportionate volume of CO. The variance in CO yields was attributed to the differences in the burning behaviour of the materials after dicing. For example, the veneer on the un-diced particleboard irregularly peeled and blistered, altering the initial heat flux. This did not occur on the diced specimens as more particle board surface was exposed to the ignition source as opposed to exposure of the veneer.

Calculations of the contribution of the gases to incapacitation show that:

- From the bookcase material, incapacitation would result from CO and CO₂ inhalation.
- For the cable material, incapacitation would result from HCl exposure.
- For the sofa material, incapacitation would result from HCN inhalation.

1.3.10.2.2 Technical report 1761

NIST technical report 1761⁸⁹ focussed on assessing the use of the ISO/TS 19700 SSTF⁹⁷ for smoke toxicity analysis. In addition, they aimed to study the effects of varying: air flow rate, fuel feed rate, fuel load and sample preparation. The study focussed on two fire conditions: well-ventilated flaming at 650°C and under-ventilated flaming at 825°C. All tests were run in triplicate.

A total of 12 toxicants were sampled for in each test: CO (minimum detection limit: 20 uL/L), CO₂ (minimum detection limit: 800 uL/L), NO₂ (minimum detection limit: 40 uL/L), NO (minimum detection limit: 70 uL/L), HCN (minimum detection limit: 35 uL/L), HCl (minimum detection limit: 20 uL/L), C₃H₄O (acrolein) (minimum detection limit: 20 uL/L) and CH₂O (formaldehyde) (minimum detection limit: 40 uL/L). As no bromine or fluorine was present in the sample materials, HBr and HF formation were not monitored. CO, CO₂ and O₂ were analysed throughout the test using an NDIR and paramagnetic analysers. All other toxicants were monitored during the chosen sampling period during the test.

Fire effluent was continuously drawn from the mixing chamber through a 6.5 mm cooled coiled copper tube, followed by a cooled impinger (placed in dry ice) with glass wool and a glass fibre filter before going through the NDIR and paramagnetic analysers. A flow of 1 L min⁻¹ to the NDIR was maintained, and a flow of 0.2 L min⁻¹ was maintained throughout the test to the paramagnetic analysers. All other toxicants were monitored using an FTIR, with effluent drawn at 4 L min⁻¹ (the flow varied due to smoke deposits fouling the sampling line) from the mixing chamber through a heated line to the FTIR (using a 100 mm optical path length).

Gas samples were collected between 4 to 12 minutes from the start of the test. In this study, the data at 200 s (approximately 3 min) were used for calculating average gas concentrations.

Similarly to work described in technical note 1760⁸⁸, the preparation of samples was varied (samples were left intact and diced, cable specimens were separated into their constituent layers), air flow rates were varied (increasing by 30% for well ventilated conditions and decreasing by 30% for post-flashover conditions), the feed rate was increased by 50% (with the primary air flow adjusted to maintain equivalence ratio) and mass loads were doubled (adding additional length to the specimen and increasing the primary air flow to maintain equivalence ratio). Sofa specimens were cut in half (with the air flow adjusted) due to being too dimensionally large for the furnace.

The tests used a range of air flows to alter the ventilation conditions of the test. While the actual method of calculating the air flows used in the tests was not shared, the necessary primary air flow was said to be calculatable by using the oxygen depletion (e.g. for an equivalence ratio of 2, the formula $P = DO_2 \times 1.193$ was used to calculate the air flow required (where P is the primary air flow, DO₂ is the oxygen depletion). For the bookcase specimens, the air flows used for testing ranged from 23.1 L min⁻¹ to 1.76 L min⁻¹. For the sofa specimens, the air flows ranged from 14.4 L min⁻¹ to 1.18 L min⁻¹. Tests conducted on the cable specimens ranged from 23.1 L min⁻¹ to 1.54 L min⁻¹.

The sofa material produced quantifiable yields of HCN in both conditions, with post flashover tests showing HCN at yields five times higher than the minimum detection limits. In well-ventilated tests, HCN was only observable after the primary air flow was increased by 30%. However, this was only observed in two of the three replicate tests at concentrations just above the minimum limits of detection. Data for the diced sofa specimens were not included as the diced pieces blew out of the sample boat and into the hot part of the furnace. During some of the tests conducted on the sofa specimen, once ignited, the flame spread rate exceeded the feed rate going into the furnace, causing flaming to occur just outside the furnace. Two flame zones existed during some tests, one upstream

of the furnace (said to be due to the combustion of TDI, a decomposition product of polyurethane foams) and one well within the furnace.

Cables were the only material to produce calculatable yields of HCl. Well-ventilated tests showed yields between 0.2 g/g and 0.3 g/g HCl, close to the calculated notional yields. Cables that had been separated into their constituent parts showed the highest yields of HCl, likely due to the increased exposure of the cable innards. The lowest yields were observed when the fuel load was doubled. A 40 % reduction in HCl yield was observed under post-flashover conditions. All other toxicants were below the limits of detection.

Altering the equivalence ratio (from approximately 0.3-0.7 to 1.5-2) decreased CO₂ yields throughout the tests (by a factor of 3 to 4) and was shown to cause substantial increases in CO yields for both the bookcase and sofa specimens. During well-ventilated conditions, CO yields were found to be below the limits of detection and around 0.05 g/g for post-flashover conditions. CO yields were consistently below 0.2 g/g, suggesting under-ventilated flaming was not achieved during the tests (CO yields of 0.2 g/g and above indicate under-ventilated burning). Significant variation was found between tests, particularly regarding CO₂ yields during pre-flashover tests, with around 20% variability observed in the bookcase tests, 20 to 40% variation for sofa tests, and 10% variation for cable tests.

Overall, the operators struggled to obtain steady burning in samples, which necessitated verification that their steady state sampling selection did not bias the results. Despite the difficulty in reaching steady burning, the tests yielded fairly repeatable CO₂ yields during their well-ventilated tests. The lowest fraction of carbon conversion was observed in cable specimens and, as a result, obtained higher yields of CO from incomplete combustion. A reduction in CO₂ yields was observed in post-flashover conditions, with only 10 to 30% of carbon in the specimen being converted to CO₂. CO yields were far less repeatable. Overall, calculations from the gas yields showed that:

- Incapacitation would occur from CO and CO₂ regarding the bookcase material.
- Incapacitation would occur from CO and HCN regarding the sofa material.
- Incapacitation would occur from HCl exposure regarding the cable specimen.

1.3.10.2.3 Technical report 1762

NIST technical report 1762⁹⁰ focussed on assessing the use of the ISO 5660-1 CACC⁹⁸ for smoke toxicity analysis. This study aimed to test specimens under normal and reduced oxygen conditions, two heat fluxes and two gas inlets. The apparatus consists of a load cell, specimen holder, heater, spark igniter, canopy hood and exhaust ductwork inside an aluminium framed polycarbonate walled enclosure with a gas delivery system. The gas delivery system could deliver 25 L s⁻¹ of air mixed with nitrogen.

Gas samples were taken from the exhaust duct using a heated line and analysed using an FTIR spectrometer with a 1000 mm optical path length and an internal volume of 0.2 L (maintained at 170°C ± 5°C). The optical path length used in this study was longer than that used in the reports mentioned earlier. The sample flow rate was approximately 4 L min⁻¹. However, this varied due to smoke deposits fouling the sampling line and reducing the flow rate.

CO and CO₂ concentrations were measured using an NDIR placed in the exhaust duct and calculated using the air flow in the exhaust duct, the exhaust temperature, the fuel consumed mass, and the ideal gas law. The effluent was drawn at 3 Lmin⁻¹ through a large volume cartridge filter and two parallel Hepa filters before passing through an electrical chiller (set to -2°C). The effluent was then drawn through a bed of calcium sulphate desiccant before passing over a bed of silica coated in sodium hydroxide. All other toxicants were sampled from a stainless steel tube placed in the exhaust duct and connected to a heated line that fed directly to the FTIR.

The research aimed to obtain fire effluent composition data with variations to the standard operating procedure to examine potential improvements in the relationship between yield data from room-scale tests and provide an insight into the sensitivity of the gas yields at specific operating conditions. The incident heat flux was varied between 20 kW m⁻² and 50 kW m⁻² to identify its significance on the gases evolved. The inlet oxygen fraction was also varied from 21% to 14% in an attempt to produce post-flashover conditions. The overall gas flow rate varied from 25 L s⁻¹ to 12.5 L s⁻¹ to increase the sensitivity of gas measurements.

Similar to previous tests, the bookcase continued to pyrolyze after flaming ceased. However, as the CACC is a continuous-flow apparatus, no physical steps were necessary to isolate the pyrolysis results from the flaming results and it was observed as a sudden drop in the mass loss rate characterized the transition from burning to pyrolyzing.

Test specimens were prepared to approximate the full item. However, the size was limited by the sample holder. Cable specimen size and layout were chosen to produce similar gas concentrations to those produced by the other materials tested. Bookcase specimens were 10 cm x 10 cm, with the vinyl surface facing upward and the particle board beneath. Sofa specimens were 10 cm x 10 cm x 1 cm single pieces of foam covered with a single oversized piece of fabric (polyester/cotton cover) tucked around the edges of the foam in the sample holder. Cable specimens were cut into five sets of 10 cm strips and placed side by side with aluminium foil over the bottom of the specimen holder and on the ends of the specimens. No diced samples were tested in the cone calorimeter because it had little to no effects during tests conducted on other radiative apparatuses.

HCN was detected only from sofa specimens and HCl from cable specimens. All other toxicants were below the limits of detection. Alterations to the oxygen concentration had little effect on CO₂ yields. Sofa specimen tests showed increased variability within CO₂ yields, particularly when reducing oxygen concentration. This increased variability was thought to be a result of the low heat flux and the low oxygen failing to sustain combustion of the sofa specimen. This resulted in non-flaming

pyrolysis, where the specimen failed to oxidise to CO or CO₂ and escaped as unreacted hydrocarbon, which was not measured.

No test produced yields of CO higher than 0.073 g/g, suggesting under-ventilated burning was not achieved in any test conducted.

At heat fluxes of 50 kW m⁻² with a flow rate of 25 L s⁻¹, decreasing the oxygen concentration to 16% was found to cause an increase in CO yields by a factor of 2 for the bookcase, 0.6 increase for the sofa specimen and a 0.3 increase for the cable specimens. Reducing the oxygen concentration to below 16% resulted in a large increase in CO yields for all specimens. Reducing the airflow to 12.5 L s⁻¹ produced consistently lower CO yields. It was suggested that this was due to the lower flow increasing the residence time of the effluent near the cone heater, allowing more time for oxidation.

HCN yields were not repeatable for the sofa tests, with one test resulting in a yield of roughly half the value of the other two tests conducted. An overall variability of 33% was obtained. Due to the large variation, one test was disregarded from the overall results, so the uncertainty was reported as 0.2%. Variation in the oxygen volume fractions (decreasing from 0.21 to 0.16) produced a linear increase in HCN yields with decreasing oxygen. However, the lowest volume fraction of oxygen produced a very low yield of HCN. HCl was only detected in the cable tests. These findings were relatively consistent, with their yields varying by 3.8%. The yields of CO in all tests ranged from 0.01 to 0.06 g/g.

Overall, it was concluded that an incident heat flux of 25 kW m⁻² did not provide any information beyond that found at 50 kW m⁻²; it only increased variability between tests due to slow ignition and early extinction. It was also concluded that toxic gas yields increased with decreasing initial oxygen concentrations. However, at fractions of 0.14, results were unpredictable for both toxic gas yields and burn behaviour, so it was not recommended to conduct tests at this oxygen fraction. It was also found that reducing the flow rate during testing to 12.5 L s⁻¹ reduces the limits of detection for gases by a factor of 2 and produces lower oxygen environments, but consistently measured lower yields of gases when compared to the higher flow rate. In real fires, oxygen concentrations fall below 10%, producing large quantities of CO and HCN.

Overall, calculations from gas yields showed:

- Incapacitation would occur primarily from CO regarding the bookcase specimens.
- Incapacitation would occur from a combination of CO and HCN regarding the sofa specimen.
- Incapacitation would occur from HCl initially and CO (after 15 minutes) regarding the cable specimen.

1.3.10.2.4 Summary of data used from bench-scale tests for large-scale comparisons.

The results from Technical Notes 1760, 1761 and 1762 were used to compare data obtained from room scale fire tests for pre- and post-flashover tests. Additional bench-scale test data⁹⁹ obtained in the SDC was included in the comparison. The SDC was operated at three conditions: 50 kWm⁻² with and without pilot flame and 25 kWm⁻² with the pilot flame.

No test conducted on the SDC produced gas yields representative of under-ventilated flaming. The highest yield of CO did not surpass 0.073 g/g. The data reported from tests conducted on the SDC can be found in Table 5.

Table 5: Summary of results reported from SDC tests used for comparison in NIST technical note 1763.

Material	Condition	CO ₂ yield g/g	CO yield g/g	HCL yield g/g	HCN yield g/g
Bookcase	50 kWm ⁻² unpiloted ignition	0.2	7.3 x10 ⁻²	<5x10 ⁻⁴	<6x10 ⁻⁴
	50 kWm ⁻² piloted ignition	1.06	<4 x10 ⁻⁴	<5x10 ⁻⁴	<6x10 ⁻⁴
	25 kWm ⁻² piloted ignition	No data reported			
Sofa	50 kWm ⁻² unpiloted ignition	1.65	1.9 x10 ⁻²	< 3 x10 ⁻³	< 4 x10 ⁻³
	50 kWm ⁻² piloted ignition	1.33	6.6 x10 ⁻³	< 3 x10 ⁻³	< 4 x10 ⁻³
	25 kWm ⁻² piloted ignition	1.76	4.3 x10 ⁻³	< 4 x10 ⁻³	< 6 x10 ⁻³
Cables	50 kWm ⁻² unpiloted ignition	1.12	3.0 x10 ⁻²	0.18	< 2 x10 ⁻³
	50 kWm ⁻² piloted ignition	1.18	2.8 x10 ⁻²	0.05	< 2 x10 ⁻³
	25 kWm ⁻² piloted ignition	0.77	1.2 x10 ⁻²	0.10	< 3 x10 ⁻³

Both the SDC and radiant apparatus initially expose the test specimen to a radiant heat flux of 50 kW m⁻², which was thought to be similar to well-ventilated conditions in the room corner test. The ISO/TS 19700 SSTF standard defined the corresponding fire conditions to the test procedures, which were used for the direct comparison. All test specimens in the bench-scale apparatus were cut from the same products tested in the room tests, so any differences in gas yields were attributed to the specimen preparation and combustion environment. As the specimen preparation for the radiant apparatus, SDC and CACC are similar, good agreement between the yields obtained by the two tests was observed.

The oxygen volume percentage was found to decline to approximately 0.17 during a test, and it was decided that the bench-scale tests should be performed at an oxygen volume percentage of 17% and an irradiance level of 25 kWm⁻². However, the duration of the test exceeds the flaming portion of the test, so attempts were made to decrease the inclusion of oxidative pyrolysis products from the final gas yields. This was not possible for the SDC, and significant proportions of CO were generated post-flaming.

The ISO/TS 19700 SSTF standard defines two operating conditions for two fire stages to simulate well-ventilated combustion, achieving an equivalence ratio of 0.75, and under-ventilated combustion, achieving an equivalence ratio of 2.0. These were assumed to correspond to radiation temperatures of 40 kW m^{-2} and 80 kW m^{-2} , which were considered high for the irradiance for post-flashover scenarios in the room test. The cone calorimeter was placed in an enclosure to produce a CACC to simulate post-flashover combustion at oxygen levels as low as 14%. Each apparatus was run to its corresponding standard. Modifications were made to identify changes that would improve agreement with the results obtained on a large scale.

1.3.10.2.5 Room-scale tests

The room-scale tests used a propane burner as an ignition source and were conducted in a burn room 2.44 m wide, 2.44 m high and 3.66 m long (8ft x 8ft x 12 ft), with an attached corridor of 9.75 m (32 ft) with the downstream end being left fully open, and a central doorway 0.76 m wide and 2.0 m high.

The materials were tested under two different conditions: pre-flashover and post-flashover conditions. Non-flaming fire stages were not included. Sofa materials were centred along the room's rear wall (facing the doorway) with a match used to initiate the fires. Bookcases were placed in a "V" formation. A TB133 burner was used in furniture tests following California Technical Bulletin 133¹⁰⁰, facing upwards underneath the lower shelves. Cables were placed in trays hooked to shelves, with two trays in total. Each tray supported a total of 65 kg of cable. The trays were parallel to the room's rear, with two propane ignition burners centred under the bottom tray of each. All tests obtained pre-flashover data for approximately 2 minutes after flaming was established. Post-flashover data was obtained for a similar length of time after flames filled the test room.

In the room-scale cable tests, the pre-flashover yields of CO_2 were found to be well below 10% of the calculated notional yields. This was attributed to the likelihood of the PVC pyrolyzing and emitting HCl, substantially decreasing the mass of cable residue while generating no CO_2 . More vigorous burning was observed in post-flashover tests, increasing the CO_2 yields measured. Flames were not particularly vigorous, so it was suggested that much of the pyrolysate was unoxidized. Pre-flashover sofa tests produced CO_2 yields just below the theoretical yield, while post-flashover CO_2 yields were only half the theoretical values.

CO yields were significantly lower than the typical value of post-flashover fires (0.2 g/g). During some post-flashover tests, flames were seen to exit the test door. It was thought that hot effluent was reigniting upon contact with fresh air, causing a proportion of the CO to oxidize and reduce the yields measured downstream. As a result, it was recommended that a CO yield of 0.2 g/g was used for the fire hazard calculations rather than the measured value, as it has been established as being indicative of under-ventilated conditions.

HCl yields were low, approximating one-fifteenth of the theoretical yield for pre-flashover tests. For bookcase materials, HCl yields were slightly lower than the theoretical yields. Sofa specimens differed significantly from the calculated values, and cable specimen tests yielded HCl at much lower than theoretical values.

No NO_2 , acrolein or formaldehyde were detected during the large-scale tests. The lower pre-flashover concentrations of toxicants just outside the door indicated that effluent concentrations would not reach incapacitating levels outside of the fire room.

1.3.10.2.5.1 Radiant apparatus:

During the bookcase tests, CO₂ yields were not sensitive to variations made to the initial oxygen volume fraction regardless of specimen preparation. Yields from both pre- and post-flashover tests were very low but within the large variability of the room tests. Sofa specimens showed CO₂ yields around 15% lower than the notional yields, regardless of the variations made to the initial oxygen fractions. Bench-scale yields were almost double the post-flashover value obtained in room tests. Cable tests were also unaffected by variations made to the initial oxygen fraction and specimen preparation. CO₂ yields were said to agree with post-flashover room tests, although the bench-scale method did not reflect the conditions of the pre-flashover room tests. The bench-scale values largely over predicted CO₂ yields.

CO yields were in agreement with pre-flashover room data (within experimental repeatability) for the bookcase and sofa material tests but were greatly over-predicted for the cable materials. Variations made to the operating procedure did not affect the agreement to room data.

In the case of HCl, no test reached yields close to those generated in room test data in the case of all materials. Yields were also inconsistent with the closed room (post-flashover) values.

No HCN was detected from the bookcase materials. The radiant apparatus was the only test to detect HCN from cable specimens. The HCN yields obtained from sofa specimens were said to be in good agreement with pre-flashover and closed room yields, but lower values were obtained during post-flashover tests. Reductions made to the initial oxygen concentration did not affect the HCN yields during the test. HCN yields from cable material tests were much higher than those in pre-flashover room tests. Reductions to the initial oxygen fraction reduced the HCN yields substantially, reducing the agreement with room test data yields.

1.3.10.2.5.2 Smoke density chamber:

Sofa specimens exposed to 50 kW m⁻² yielded CO₂ yields that agreed (within the experimental uncertainty) with the post-flashover room data for all three sofa tests. The bookcase and sofa materials exposed to 50 kW m⁻² pilot flame generated CO₂ yields that agreed with pre-flashover room data within the experimental variability.

CO yields from cable specimens exposed to 50 kW m⁻² with pilot flame greatly over-predicted pre-flashover yields. Both the sofa and bookcase materials were severely under-predicted. Tests with and without pilot flame were unrepresentative of CO yields from room data.

In the case of HCl, no test reached yields close to those generated in room test data in the case of all materials. No HCN was detected from the bookcase materials. No NO₂, acrolein, or formaldehyde were detected during the test.

1.3.10.2.5.3 Steady State Tube Furnace:

At 650°C well-ventilated conditions, CO₂ yields were generally over-predicted (by a factor of 3 for the bookcase materials and 10 for the cable). Post-flashover conditions in the tube furnace (825°C) accurately reflected the room data. Alterations made to the airflow and mass (while maintaining equivalence ratio) led to under prediction of the pre-flashover yields for sofa specimens. No changes were observed in bookcase and cable tests.

For well-ventilated tests (650°C), CO yields for the bookcase were severely under predicted. Other data sets were in agreement with the room data. In pre-flashover conditions, the CO yield was predicted accurately for the cable fires and slightly over predicted the yields from sofa tests. Improvements to the agreement of yield data with the cable and sofa specimens was achieved when

the airflow was increased. Overall, the tube furnace generated the nearest yield to under-ventilated flaming out of all tests.

Yields of HCl generated from bookcase specimens were in relative agreement with pre-flashover and post-flashover room test values. Sofa specimen and cable specimen tests also agreed with room test yields. Testing with a 30% reduction (under well-ventilated operating conditions) in equivalence ratio led to good agreement with HCN yields produced in room tests. Post-flashover tests slightly under-predicted HCN yields when compared to room test data. HCN yields were higher than the yields produced during closed room sofa tests.

1.3.10.2.5.4 Cone Calorimeter:

Alterations made to the initial volume fraction (reducing it to 0.14) had no effect on data agreement with room tests. Bench-scale yields were greatly over-predicted for pre-flashover conditions and greatly under-estimated for the post-flashover conditions for both the bookcase and cable materials. Sofa tests were said to agree within experimental uncertainty.

When operated at 50 kW m⁻², very low CO yields were generated during the bookcase tests, which did not agree with room data. This agreement was improved by decreasing the radiant flux to 25 kW m⁻². High yields of CO were obtained during cable and sofa tests at 50 kW m⁻² and were within an agreement of a factor of 2 with the pre-flashover CO yields from the room test data. Lowering the heat flux for these materials (to 25 kW m⁻²) had no improvement on the room test agreement. At the lower heat flux of 25 kW m⁻², many materials did not ignite.

The upper limits of the HCl yields for the bookcase specimens were said to approach pre- and post-flashover room test data. In all other tests, HCl yields did not agree with room data. No HCN was detected from the bookcase materials. Pre-flashover HCN yields were said to agree with room tests but over-predicted regarding the closed room sofa tests. For post-flashover, yields were substantially lower than those generated in room tests, although reducing the radiant heat flux increased the yield to a value approaching the post-flashover yield.

A summary table showing the CO and CO₂ yields obtained from all tests conducted across NIST technical notes 1760, 1761, 1762 and 1763 are shown in Table 6.

Table 6: Summary of the CO and CO₂ yields obtained from all tests conducted in NIST reports 1760, 1761, 1762 and 1763.

Test	Condition	Material	CO ₂ yield g/g	CO yield g/g
Room corner	Pre-flashover	Bookcase	0.5	2.4 x10 ⁻²
		Sofa	1.59	1.4x10 ⁻²
		Cables	0.12	5.5x10 ⁻³
	Post-flashover	Bookcase	1.89	4.6 x10 ⁻²
		Sofa	1.13	5.1x10 ⁻²
		Cables	1.38	1.48x10 ⁻¹
	Closed room	Bookcase	No data available	
		Sofa	0.92	3.6x10 ⁻²
		Cables	No data available	
Radiant furnace	Initial O ₂ concentration	Bookcase	0.88	1.8x10 ⁻²
		Sofa	1.68	2.8x10 ⁻²
		Cables	1.16	5.8x10 ⁻²

	of 0.21 (sample intact)				
	Initial O ₂ concentration of 0.17 (sample intact)	Bookcase	0.84	1.8x10 ⁻²	
		Sofa	1.64	3.6x10 ⁻²	
		Cables	1.05	6.2x10 ⁻²	
Smoke density chamber	50 kWm ⁻² unpiloted	Bookcase	0.2	7.3x10 ⁻²	
		Sofa	1.65	1.9x10 ⁻²	
		Cables	1.12	3.0x10 ⁻²	
	25 kWm ⁻² piloted	Bookcase	No data available		
		Sofa	1.76	4.3x10 ⁻³	
		Cables	0.77	1.2x10 ⁻²	
Cone calorimeter	50 kWm ⁻² with 25 Lmin ⁻¹ airflow with 0.21 oxygen	Bookcase	1.11	1.0x10 ⁻²	
		Sofa	1.41	2.7 X10 ⁻²	
		Cables	1.04	5.4x10 ⁻²	
	50 kWm ⁻² with 25 Lmin ⁻¹ airflow with 0.16 oxygen	Bookcase	1.06	1.9x10 ⁻²	
		Sofa	1.41	4.4x10 ⁻²	
		Cables	1.11	7.1x10 ⁻²	
	50 kWm ⁻² with 12.5 Lmin ⁻¹ airflow with 0.21 oxygen	Bookcase	1.02	0.6x10 ⁻²	
		Sofa	1.36	2.4X10 ⁻²	
		Cables	1.02	5x10 ⁻²	
	50 kWm ⁻² with 12.5 Lmin ⁻¹ airflow with 0.16 oxygen	Bookcase	1.03	0.9x10 ⁻²	
		Sofa	1.38	3.5X10 ⁻²	
		Cables	1.02	6.1x10 ⁻²	
	25 kWm ⁻² with 25 Lmin ⁻¹ airflow with 0.21 oxygen	Bookcase	1.14	1.9x10 ⁻²	
		Sofa	1.55	2.4x10 ⁻²	
		Cables	1.13	5.1x10 ⁻²	
	25 kWm ⁻² with 25 Lmin ⁻¹ airflow with 0.16 oxygen	Bookcase	0.85	2.7x10 ⁻²	
		Sofa	1.36	2.9x10 ⁻²	
		Cables	0.68	4.2X10 ⁻²	
	SSTF	650 well-ventilated (samples intact)	Bookcase	1.3	<1x10 ⁻³
			Sofa	1.87	2.6x10 ⁻²
			Cables	1.43	8.8x10 ⁻²
		825 under-ventilated (sample intact)	Bookcase	0.36	6.2x10 ⁻²
			Sofa	0.56	1.43x10 ⁻¹
			Cables	0.33	4.3x10 ⁻²

1.3.11 Fire test regulations within the construction product regulations

The Construction Products Regulations¹⁰¹ necessitate the testing and labelling of the fire performance of construction products according to their Euroclass. The Euroclassification system was implemented in 2000 to create a universal platform that allowed for comparing fire properties of construction products between countries¹⁰². This allowed for harmonized trade of building products by removing differences in test methods and classification systems. The classification system is based on a material's ability to conform to relevant reference scenarios based on standardized tests, originally described in Guidance Document G as the ISO 9705 room corner test¹⁰³. The Euroclass predominantly focuses on a product's ignitability, flame spread, non-combustibility and the development of smoke and burning droplets.

Due to the impracticality of testing individual construction products in the ISO 9705 corner test, intermediate-scale test methods were developed to replicate large-scale fire behaviour on a smaller scale, most commonly using the EN 13823 single burning item test (SBI)¹⁰⁴.

The SBI test has been shown to accurately represent the fire behaviour observed in the ISO 9705 room corner test for 18 typical construction products. It uses an L-shaped configuration of 1 m x 1.5 m tall and 0.5 m x 1.5 m sample to provide a better correlation to full-scale fire development. As such, the Euro classification system is based on material performance in the SBI test for Euroclasses A2 to D. The classifications given are described in Table 7 and *Table 8*.

A series of round robin tests were carried out to provide evidence of the repeatability and reproducibility of the SBI test. The first interlaboratory reproducibility test took place in 1997¹⁰⁴, testing 30 products, followed by the second in 2004, where a further 70 products were tested. The products were also tested using the ISO 9705 room corner test to establish a correlation between the SBI test and the ISO 9705 room corner reference scenario.

Of the 30 products tested in the first round robin, 26 were found to have a good correlation with the reference scenario. The four un-correlated products were: steel-clad expanded polystyrene sandwich panels, PVC water pipes, PVC-covered electric cables and fire retarded polycarbonate panels. The polycarbonate and polystyrene sandwich panels showed large variation in the SBI test. Messerschmidt¹⁰⁰ reported that the SBI test was unsuitable for PVC cables and water pipes. Sundström¹⁰⁵ showed that when using FIGRA as the main parameter for classification, the SBI was a suitable test method for predicting fire hazard.

While the SBI test is an accurate representation for flammability, it is not suitable for the assessment of smoke toxicity. One of the reasons for this is the SBI test is an open-configuration only able to replicate well-ventilated flaming and unable to replicate the most toxic under-ventilated fire scenario.

In addition, the exhaust duct draws a large quantity of air through it, diluting the fire effluent. While this is necessary for the test operator's safety, it renders most toxicants present in the fire effluent below the detection limits. Unfortunately, the SBI test is not designed to assess external products for building facades or layered products such as aluminium composite panels. In addition to the Euroclass A-F, construction products can also be classified on their smoke development. A construction product can be given a classification ranging from s1, through s2 to s3, along with their dripping behaviour on a scale of d0, d1 to d2.

For smoke toxicity to be incorporated into the construction product regulations, a method capable of accurately predicting smoke toxicity should be used. This method would also need to be

correlated to the reference scenario, possibly by being used in conjunction with the SBI or a test method that can measure similar parameters as the SBI on a bench scale.

A rationale for the present work is to provide the data necessary to incorporate an additional classification (tox 1, tox 2, tox 3) into the Euroclass system to highlight the smoke toxicity of burning products.

Table 7: Description of the Euro classification system for fire tests conducted on construction products⁹⁷.

Classification	Description	Fire Scenario	Heat attack	Examples of products	Example product
A1	No contribution to fire	Fully developed fire in a room	At least 60kW/m ²	Products of natural stone, concrete, bricks, ceramic, glass, steel and many metallic products	Stonewool, Gypsum board
A2	No contribution to fire	Fully developed fire in a room	At least 60kW/m ²	Products similar to those of class A1, including small amounts of organic compounds	Similar to A1
B	Very limited contribution to fire	Single burning item in a room	40kW/m ² on a limited area	Gypsum boards with different (thin) surface linings. Fire retardant wood products	Painted gypsum board
C	Limited contribution to fire	Single burning item in a room	40kW/m ² on a limited area	Phenolic foam, gypsum boards with different surface linings (thicker than in class B)	Gypsum board with paper-based wallpaper.
D	Acceptable contribution to fire	Single burning item in a room	40kW/m ² on a limited area	Wood products with thickness ≥ about 10mm and density ≥ about 400 kg/m ³ (depending on end use)	Wood
E	Acceptable contribution to fire	Small flame attack	Flame height of 20 mm	Low density fibreboard, plastic based insulation products	Fire-retarded EPS
F	No performance requirements	-	-	Product not tested (no requirements)	Non-tested materials, EPS

Table 8: Classifications for smoke production and burning droplet ⁹⁷.

Classification	Description given
s1	Structural element emits a very limited amount of combustion gases
s2	Material emits a limited amount of combustion gases
s3	No requirement for restricted production of combustion gases
d 0	No burning droplets or particles emitted from material
d 1	Burning droplets or particles are released in limited quantities.
d 2	No restriction of burning droplets and particles

1.3.12 Links between large-scale tests and bench-scale

The main purpose of bench-scale fire testing is to predict the behaviour and smoke toxicity of a fire in a real-life scenario. To do this adequately, the bench-scale test must reflect the fire behaviour observed in a large-scale test and must have a means of comparing the data obtained by the method used to the data generated on a large scale.

ISO 29903¹⁰⁶ provides the guidance that should be followed to compare toxic gas yields produced on a bench-scale to those produced on a large scale and compare bench-scale methods with each other. It notes the need to define the combustion condition in which the bench-scale test is conducted. This also enables two or more bench-scale test methods to be compared. Without this, an accurate comparison is not possible.

During the combustion process, if more than one fire stage is encompassed, then the duration of the combustion stage used for comparison will need to be known. The most reliable means of identifying combustion conditions on a large scale is by measuring the equivalence ratio during the test once a period of steady burning is reached. At the steady point of burning, it is often assumed that the heat release rate (HRR) remains relatively constant regardless of the ventilation. Most fires are in enclosures, and the geometry remains fixed for the duration of the fire. Exceptions include windows breaking, which would change the steady burning rate and end that period of steady burning.

Agreement between bench and large-scale data is affirmed when all toxicant yields measured are reflective of each other. All toxicants measured must be in agreement. If one toxicant outliers, an explanation must be given as to why the particular toxicant is not in agreement –an explanation can often be found after conducting repeat experiments evaluating the sampling and mode of analysis. If the outlier results from differences in combustion conditions, the comparison is rendered invalid. The bench-scale method used in the comparison must therefore be able to accurately and repeatably generate smoke under definitive fire conditions. The criteria for assessing the validity of a test method are described in ISO 16312-1. This does mean that the bench-scale method used needs to be able to accurately measure smoke toxicity for the data produced to be valid in terms of the bench to large-scale comparisons.

1.3.12.1 *Equivalence ratio comparisons.*

The equivalence ratio can be measured using a phi meter¹⁰⁷, as used in the TOXFIRE project¹⁰⁸. The fire effluent is drawn over a heated catalyst (platinum) and mixed with a known amount of oxygen to quantify the amount needed for complete combustion. Using a phi meter allows for easy, direct scale comparisons with bench-scale methods that can provide accurate equivalence ratio data. Direct equivalence ratio measurements also allow more understanding of the fire stage during the experiment. This is particularly useful for large-scale tests.

The equivalence ratio is one of the easier means of comparing bench to large-scale data and is recommended in ISO 29903. Using the equivalence ratio is also the best means for comparing bench to large-scale toxicity data as the combustion condition is known (if the combustion condition varies during the test then the toxic gas yields produced at a specified equivalence ratio for a specific time limit are compared). However, ISO 29903 notes the invalidity in identifying equivalence ratio during stage 1a fires (smouldering) (as the equivalence ratio concept is only valid for flaming fires) but provides no guidance for alternative means of data comparisons.

ISO 29903 identifies the potential problems in using the equivalence ratio for smoke toxicity comparisons when $\phi < 0.5$. At ratios below 0.5, it is difficult to ensure that the ϕ value is genuine. If half of the air measured is not part of the fire phase, then the ϕ value is underestimated. At low ϕ values, some toxicants begin showing insensitivity to equivalence ratio changes, inferring that below this level, alternative methods of comparison should be used. This is not an issue for higher equivalence ratios ($\phi > 1$) as the toxicants have shown to still be sensitive to equivalence ratio changes.

The TOXFIRE project¹⁰⁸ published data expressing the comparison of CO yields as a function of equivalence ratio to compare bench to large-scale data. This is shown in Figure 10¹⁰⁸.

The apparatuses used were: the SSTF, CACC (as a function of equivalence ratio and the corrected equivalence values- values were required to be corrected due to flaming occurring outside of the combustion area) and the FPA, all compared with ISO room data. The tests were conducted using Polyamide 6.6 (PA 6.6) with conditions ranging from well-ventilated to under-ventilated. As the fire progressed from well-ventilated to under-ventilated, the CO yields produced by all tests showed more scatter.

As the equivalence ratio increases, the yield of CO is seen to increase due to the lower combustion efficiency and availability of oxygen. The SSTF and FPA showed general agreement with the ISO room data during well- and under-ventilated conditions.

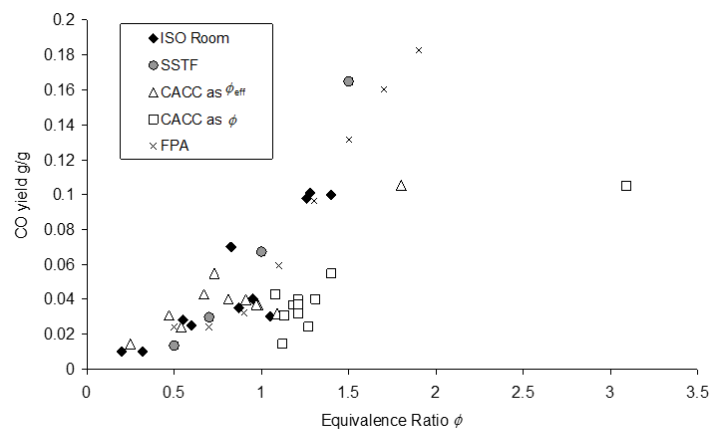


Figure 10: Comparisons of CO yield as a function of equivalence ratio from bench-scale tests and large-scale tests¹⁰¹

The CACC struggled to replicate high yields of CO, particularly in under-ventilated tests. The CACC was only able to produce yields reflective of under-ventilated burning at a single equivalence ratio ($\phi = 3.2$), suggesting the test cannot routinely replicate under-ventilated conditions. This has been shown by several studies that focused on bench-to large-scale comparisons using the CACC.

NIST Technical Note 1762 showed that at no point in the study could the CO yields reach what is reflective of under-ventilated combustion. Technical note 1763 also indicated the CACC's struggles to accurately reflect data obtained in their room corner tests, particularly for under-ventilated conditions.

The CACC's inability to replicate under-ventilated flaming was reported by Blomqvist and Sandinge¹⁰⁹, who noted the common issue of after-burning and burning occurring outside of the

enclosure, similar to NIST technical note 1762. More often than not, the apparatus required adjustment of oxygen concentrations for each product tested and rarely produced toxicants above the detection limits. Perhaps further modification might enable the apparatus to replicate under-ventilated flaming so that it may be used for smoke toxicity assessment. It is currently only able to replicate well-ventilated combustion, the best-case scenario for smoke toxicity.

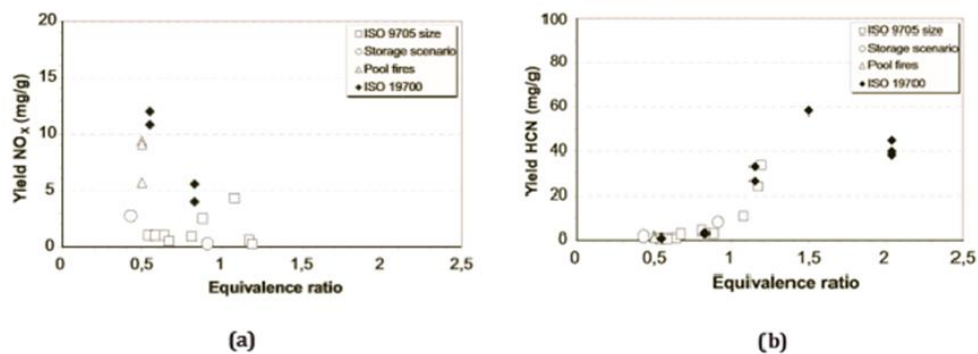


Figure 11: Comparison of NO_x and HCN yields produced by the SSTF and ISO room test as a function of equivalence ratio¹¹³.

NO_x (a) and HCN (b) yields produced by the SSTF were also plotted as a function of equivalence ratio as a means of bench-to-large-scale comparison, shown in Figure 11. The data show a strong correlation between bench-scale and large-scale, with the SSTF showing expected trends for the NO_x yields (increased yields with increasing ventilation). This was also true for HCN, with yields increasing with lowered ventilation. The data showed the best correlation with the pool fire, particularly for the NO_x yields when compared with the more scattered yields obtained near the ISO room opening.

Several bench-to-large-scale data comparisons have been made. Figure 12¹¹⁰ shows a comparison of CO yields published from ISO room data from various materials and apparatus. Four data sets were obtained from the SSTF by a) Blomqvist using PA 6.6 (the same material and batch as used in the TOXFIRE project), b) Stec using PA 6.6 (the same material but different batch used in the TOXFIRE project) and c) Purser using polyamide 6 (PA 6)^{108,111,112}. All methods showed an increased scatter as the fire reaches higher equivalence ratios but show a general trend of increasing CO yields as the equivalence ratio increases. The CACC produced the lowest yields of CO of all tests conducted, regardless of the increase in equivalence ratio. The SSTF showed higher yields of CO at higher temperatures with increasing equivalence ratios, producing a more accurate representation of the ISO room data. The FPA shows dramatic increases in CO yields as the equivalence ratio approaches 1 and only shows agreement with ISO room data at the lower equivalence ratios.

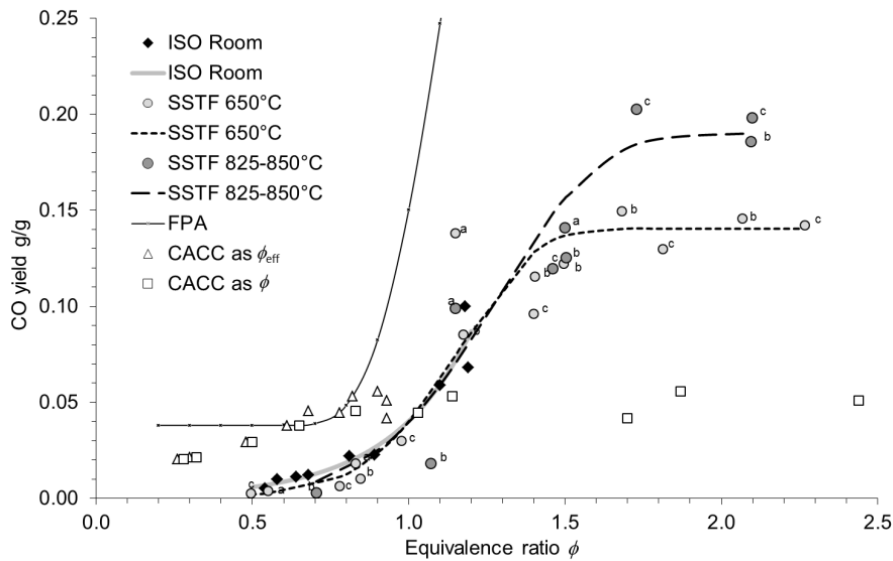


Figure 12: Comparison of CO yields as a function of equivalence ratio produced by: SSTF, CACC and FPA with ISO room data

While the TOXFIRE project did not predominantly focus on insulation materials, it is one of few reliable large-scale datasets. The study tested five different materials in the ISO 9705 room corner test, using FTIR for gas analysis. In addition, the equivalence ratio was also monitored during the tests, with the size of the door varying in an attempt to simulate under-ventilated flaming. Gas sampling was taken from the upper layer of the room close to the doorway and in the main ventilation duct.

The TOXFIRE project is currently the only large-scale testing that monitored the equivalence ratio throughout. The equivalence ratio is a means of describing the fire condition. Rapid changes in equivalence ratio will result in non-consistent yields of toxicants being produced throughout the test.

During large-scale testing, there is much less control over the burning conditions your material is subject to in comparison to bench-scale assessments. The project used a phi-meter, an apparatus specifically designed to quantify equivalence ratio, to monitor this parameter¹¹³. This allowed the project to identify the fire scenarios throughout their tests and provide an insight into the yields of toxicants measured. For the experiments, the air was sampled from the upper part of the door opening. This was the out going air from the combustion occurring in the room. This was used to calculate the equivalence ratio during the tests.

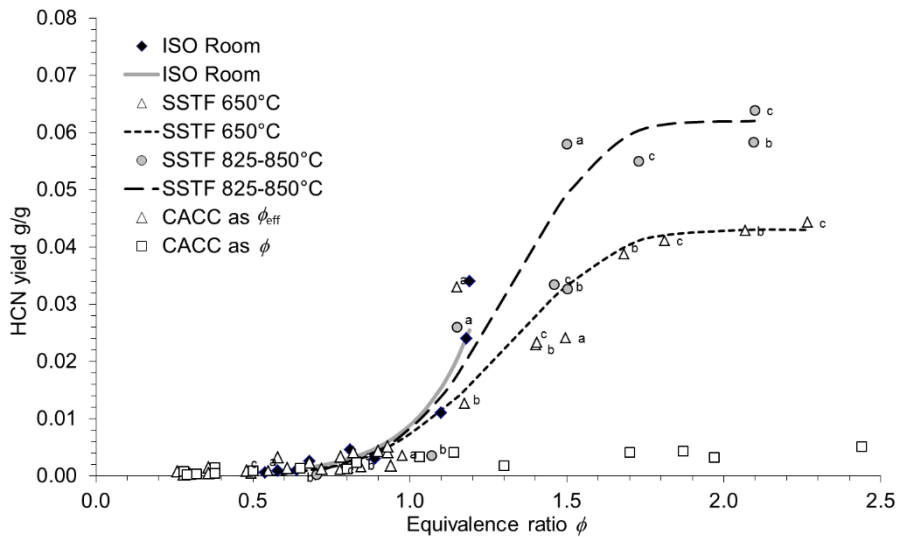


Figure 13: Comparison of HCN yields as a function of equivalence ratio produced by: SSTF and CACC with ISO room data¹⁰⁶.

Figure 13¹⁰⁶ shows the same comparison of HCN yields produced in the ISO room with those produced by the SSTF and CACC. The CACC fails to replicate the yields produced in both the SSTF and ISO room, with very small changes in HCN yield occurring as the reported equivalence ratio increases, further illustrating the CACC's inability to replicate under-ventilated conditions. At $\phi=1$, the CACC was able to predict similar HCN yields as produced in the ISO room, suggesting it can replicate well-ventilated flaming it struggles as the ventilation decreases. The SSTF shows good agreement with the ISO room yields, with HCN yields increasing as the equivalence ratio increases and can hence replicate large-scale burning.

In three of the five tests, flashover was reached. The toxicants measured at this point were representative of under-ventilated conditions, with high yields of CO and HCN being produced. In one test, the equivalence ratio reached levels surplus of 2.5 (extremely under-ventilated). The fire was manually extinguished early for the operator's safety. However, high yields of toxicants were found before extinguishing. Although flash-over was achievable in these cases, it proved difficult to maintain a constant equivalence ratio once under-ventilation was reached, suggesting irregular burning during the tests. In some tests, additional burning outside of the opening occurred. In these cases, a lower equivalence was measured with more complete combustion products. The additional flaming will cause further changes to the chemistry of the effluent, causing the measurements to be less reliable than in tests where no secondary flaming occurred. For this reason, large-scale tests must be careful to control the occurrence of secondary flaming as this could produce misleading data suggesting the toxicity of the test is lower than it actually is. For this reason, it would be useful for any large-scale tests to report any instances of secondary flaming.

The uncertainties and variation observed in some results of this study can be explained by the high intensity of the fires. The intensity of the fire caused turbulence in the air flow both in and out of the room, affecting the air flow and mass loss measurements. In tests where the fire was noticeably intense, a very noisy mass loss signal was obtained. This turbulence would affect the yields measured as the yields depend on the air flow and the mass loss throughout the test. It would also affect how representative the gas sampling was throughout the tests. Tests with significant water

and soot production were so detrimental to the analysis that they were rendered useless and not included in the overall data set.

The data reported for these tests were used to make bench-scale comparisons to highlight the bench-scale test that is most representative of large-scale fire behaviour. As the equivalence ratio was monitored during these large-scale tests, this could be used as a basis for comparing the data, as suggested in ISO 29903.

1.3.12.2 CO/CO₂ ratio

ISO 29903 provides guidance for comparing bench to large-scale fire tests by using CO/CO₂ ratio - this is not the preferred basis of comparison and is only suitable for materials which do not contain halogens or other gas-phase flame retardants. The CO/CO₂ ratio is representative of the oxygen availability, providing details of the fire's combustion condition. Valid comparisons cannot be made when the burning material contains additives that interfere with gas-phase combustion. Halogenated flame retardants have also been shown to interfere with the production of CO₂^{114, 115} irrespective of combustion conditions, so it is understandable that this renders comparisons from bench to large-scale using CO/CO₂ ratios unusable. It should also be noted that combustion temperatures also influence the production of toxic species and should be considered when using CO/CO₂ ratio as a comparison method. The sampling position can also affect the yields measured. This further complicates the comparison process, so using CO/CO₂ ratio for bench- to large-scale comparisons is not recommended.

Figure 14 shows CO yields produced by various apparatus under different combustion conditions. Both the SSTF and FPA have shown the most agreement with the CO yields produced in the ISO room, particularly during well-ventilated tests. However, they both typically over-estimate yields in under-ventilated conditions. The SDC consistently under-predicts CO yields regardless of ventilation. In contrast, the NFX typically overestimates CO yields. The variability of the CO yields between each test reinforces the difficulty in using CO yields as a comparison between bench and large-scale.

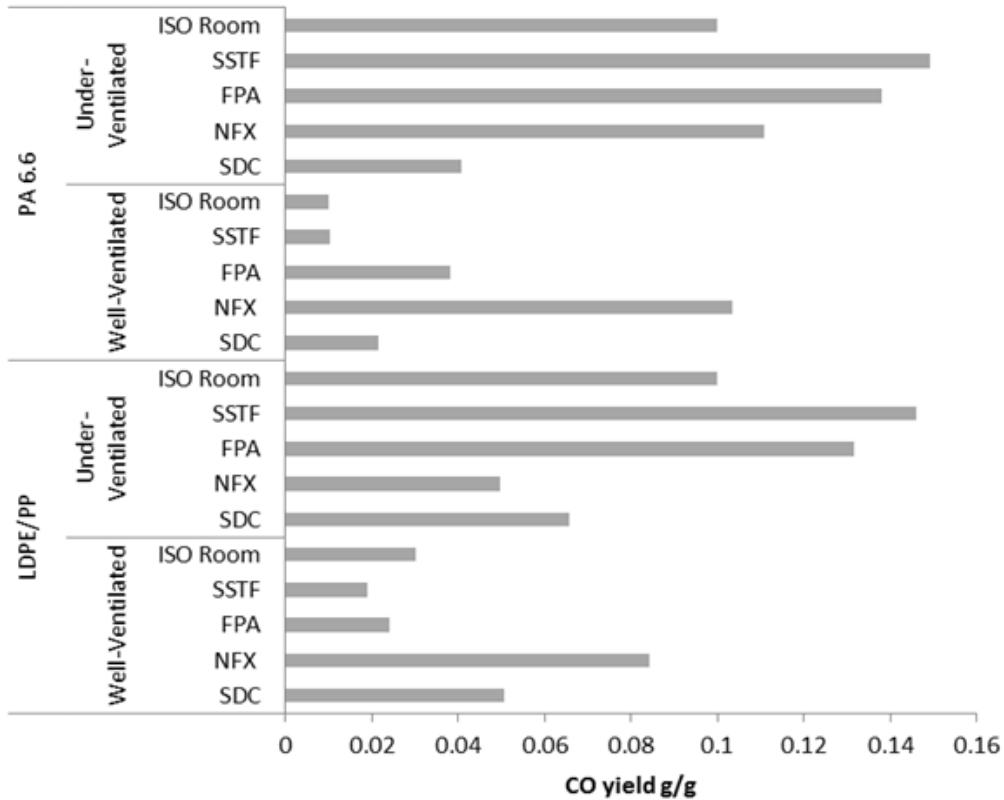


Figure 14: CO yields produced by various apparatus under well-ventilated and under-ventilated conditions¹⁰⁶.

1.3.12.3 Effect of sampling position and method of analysis on smoke toxicity data

The sampling position chosen during both large-scale and bench-scale tests will influence the data obtained. The position chosen should typically represent the desired degree of combustion of the effluent where it has been well-mixed and fallen to temperatures low enough to prevent further reactions but warm enough to prevent condensation of the effluent.

While many bench-scale methods dictate the sampling position, there are a variety of positions to choose from in most large-scale tests. However, most enclosure tests recommend sampling in a hood/duct (which would be representative of cool, diluted effluent). This is not ideal for early well-ventilated, small enclosure fires as the dilution can result in toxicants falling below the detection limits.

Sampling should occur at the top of the doorway to catch the undiluted effluent, although the gases may not be sufficiently oxidized in this area before sampling. Points chosen at alternative positions around the fire are deemed unsuitable for bench- to large-scale comparisons and are only relevant for that specific test. Although, it may be sensible to choose a sampling position for large-scale testing that will represent the scenario the bench-scale method aims to reproduce.

1.4 CHOICE OF BENCH-SCALE APPARATUS

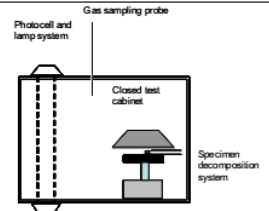
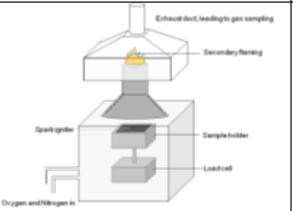
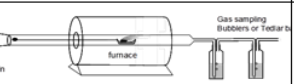
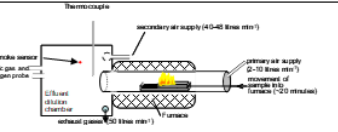
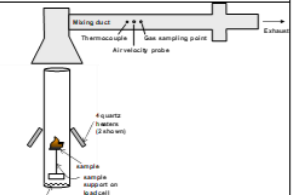
The advantages and disadvantages of each method available, alongside a comparison between available test conditions and parameters, have been created and shown in Table 9. This was used to directly compare available methodologies to select the apparatus used in this research.

For smoke toxicity to be measured accurately, the sample must be able to burn in a steady state. During steady burning, the rate of generation of effluent is equal to the rate of decomposition. This means that at this point, any toxicants produced by the material will be produced at a steady rate, making measurements much more reliable and repeatable.

The generation of gaseous species also depends on the fire condition, meaning the test method selected must be able to differentiate between fire stages to enable data to be obtained for the best-case and worst-case fire scenarios.

Therefore, the research's focal point was based on the ISO/TS 19700 SSTF, a bench-scale apparatus designed to determine a material's smoke toxicity. As the apparatus has previously demonstrated its ability to generate fire effluent consistently that is representative of individual fire scenarios, it was selected as the main bench-scale assessment method.

Table 9: A table summarising the different bench-scale test methods for assessing smoke toxicity, containing practical information and advantages and disadvantages of each technique

Name	The Smoke Density Chamber (SDC)	Controlled Atmosphere Cone Calorimeter (CACC)	The Non-dynamic Tube Furnace (NFX)	Steady State Tube Furnace (SSTF) BS7990 & ISO/TS 19700	Fire Propagation Apparatus ISO 12136
Schematic					
Heat regimes	25, 50 kW m ⁻²	25, 35, 50 kW m ⁻²	400, 600, 800°C	350, 650, 825°C (15 to 80 kW m ⁻²)	Up to 100 kW m ⁻²
Design	Closed box	Flow-through	Flow-through	Flow-through	Flow-through
Mass loss rate	Variable, sample dependent	Variable, sample dependent	Variable, sample dependent	Fixed	Variable, sample dependent
Sample requirement	75 x 75 mm ² results only valid for thickness tested	100 x 100 mm ² results only valid for thickness tested	0.1 to 1.0 g	800 x 25 x 25 mm ³ (Maximum size)	100 x 100 mm ² results only valid for thickness tested
Smouldering	Y	Y	Y	Y	Y
Well-ventil'd	Y	Y	Y	Y	Y
under-vent'd	N	N	?	Y	Y
Post-flashover	N	N	?	Y	Y
Advantages	Widely available Currently used for toxicity assessment	Modification to widely used standard test; measures flammability as well as toxicity	Simple and low cost	Designed for smoke toxicity assessment; ideal for linear of homogeneous products; correlates with large scale tests for all conditions.	Able to replicate high CO yields for under-ventilated flaming
Disadvantages	Poor interlaboratory reproducibility; unable to force under-ventilated flaming; fire stage unknown; sample probe can miss toxic plume	No standard equipment exists; unable to go above 50 kW m ⁻² ; toxic product yields do not correlate to large scale fire tests; equivalence ratio only known after test	Conditions not related to fire stages; does not distinguish between flaming and non-flaming; limited volume of effluent for analysis.	Not proven for layered materials; not widely adopted (~10 apparatuses, globally); Standard needs modification for testing non-combustible materials.	Expensive, not widely used

2 METHOD DEVELOPMENT

This chapter describes experimental work undertaken as part of this project to support the development of the steady state tube furnace and a robust assessment of smoke toxicity. The chapter has been divided into eight key sections. Details of each sub-section are as follows:

Section 2.1: Selection of materials for study

This section provides an overview of the selection process used to identify materials used for the research. It provides the origin of each material used.

Section 2.2: Steady State Tube Furnace

All methods used on the Steady State Tube Furnace have been detailed in this section. The section is introduced with a summary of all materials used and selected for assessment, followed by a detailed gap analysis of the ISO/TS 19700 standard. This gap analysis was used to develop specific methodologies required for the SSTF to reach full standard. The methodology was used to provide revisions to the standard and generate data for bench-to-large scale comparisons.

The SSTF was also used to monitor the formation of specific acute toxicants over time to refine gas sampling techniques used on a bench scale. In addition, the SSTF was modified and studied to determine whether the SSTF can force steady burning in low oxygen environments (< 5%) and tested to identify its effects on smoke toxicity analysis.

Section 2.3: Phi meter

A phi meter describes instruments designed to quantify the equivalence ratio from fire effluent measurements. All bench-scale research and development using the phi meter can be found in this section. The section provides a background for understanding the phi meter, including a derivation of the equivalence ratio calculation used to develop the phi meter and an overview of the chemical principles behind the apparatus.

The section then provides details of the background research conducted to identify operating conditions and procedures for the equipment, as well as validation for the modifications made to the original design to produce the phi meter used in this research. Schematic designs are provided. The background research contains experimental data from microscale combustion calorimetry (MCC) and the SSTF. The SSTF was used to validate the data obtained from the phi meter. In addition to validation, the phi meter was used to study the equivalence ratio at several locations within the SSTF to identify how the equivalence ratio changes within the apparatus and how this would affect sampling using the phi meter.

Section 2.4: Equivalence ratio in the Steady State combustion tube

This section details research conducted using the phi meter designed in **Section 2.3** to monitor the equivalence ratio throughout the combustion tube of the ISO/TS Steady State Tube Furnace.

Section 2.5 Portable gas analysers

This section describes the analysers designed and constructed for gas analysis on a large-scale, with details of the design and construction of the analysers and schematic diagrams.

Section 2.6 Analysis of HCN using ion chromatography

This section contains information about the available techniques for HCN quantification as described in ISO 19701. Ion chromatography was used to analyse HCN samples obtained from SSTF testing and compared to wet chemical techniques to identify the best means of HCN analysis for this research.

Section 2.7 Large-scale test design

Due to the scale of the tests and planning required, the large-scale test method development has been divided into eight sections:

Section 2.6.1: Test description

This section describes the standard ISO 9705 room corner test. Details of the modifications to the test are outlined in the subsequent sections.

Section 2.6.2: Aims and objectives

This section provides the overall aims and objectives of the large-scale testing and details the measurements needed from the tests to meet the aims and objectives. This provides background information and reasoning for the modifications made to the ISO 9705 test procedure for this research.

Section 2.6.3: Materials and tests

All materials selected for large-scale testing are detailed in this section, alongside a summary of the desired test conditions for each.

Section 2.6.4: Test layout and fuel loading

This section details the test layouts chosen for the large-scale experiments for all materials. The modified layout was designed to meet the aims and objectives of the research.

Section 2.6.5: Controlling ventilation

This section describes the proposed methodology for controlling the ventilation to create under-ventilated flaming during the large-scale tests based on literature.

Section 2.6.6: Ignition source

Due to the test design modifications, the standard ISO burner could not be used for all tests conducted in the room corner test. Modifications to the ignition source, fuel pan geometry and calculations on fuel loading are detailed in this section.

Section 2.6.7: Predicted parameters

This section contains two sets of experiments conducted to predict the proposed large-scale test designs and test the proposed methodologies. Details of cone calorimetry tests conducted on a bench-scale inputted into Cone Tools to create predictive models of the HRR output from the large-scale tests can be found in this section. Details of a reduced-scale model of the 9705 room used to test the proposed test layout designs and ignition source can also be found in this section.

Section 2.8: Large-scale test measurements

All measurements and methodologies used for large-scale testing can be found in this section. Due to the scale of the experiments, the measurements have been sectioned into location: measurements at the door, measurements in the exhaust duct, measurements inside the room and the overall test procedures used.

2.1 SELECTION OF MATERIALS FOR STUDY

One of the key aims of this research is to provide the methodology to allow the ISO/TS 19700 SSTF technical standard to become a full standard.

The standard requires revisions to enable this to happen. These revisions must also be tested for their inter-laboratory reproducibility. Before conducting reproducibility assessments, areas for improvement of the standard were identified. These were identified through preliminary practical assessments on a series of non-homogenous and non-combustible materials and identified from the literature.

The selected materials were chosen to be typical of the wide range of substances used in construction and represent the diverse set of materials the SSTF is capable of assessing. As the ISO/TS 19700 standard is limited to homogenous materials, the preliminary assessments aim to prove that the test method can be used repeatably for testing a wider array of materials, including non-homogenous thermoplastics and non-combustible materials

Once preliminary assessments were made, specific guidance and methodologies were developed to enable the SSTF to undergo an interlaboratory reproducibility assessment to prove the data and methodology is repeatable. This would enable the SSTF to reach full standard status.

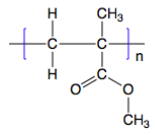
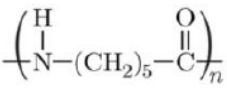
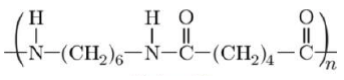
A series of four materials were proposed for testing: plasterboard (gypsum board), chipboard, flexible polyurethane foam and cables.

2.2 METHOD DEVELOPMENTS FOR THE STEADY STATE TUBE FURNACE

2.2.1 Material summary

As the ISO/TS 19700 standard only covers homogenous thermoplastic materials, this work aimed to prove the SSTF could be used for non-homogenous thermoplastics, complex materials and non-combustible materials. Therefore, four materials were selected for additional bench-scale testing to represent what the standard is missing. Additional assessments were made to the SSTF using simple polymeric materials to refine the operating procedures. These materials and their codes used have been summarised in *Table 10*. Details of the materials densities and elemental composition are unfortunately unavailable.

Table 10: Summary of the materials used for SSTF assessments.

Material code	Product name	Description	Chemical structure (if applicable)	Supplier details
PMMA	Polymethylmethacrylate	Simple polymer tested in the form of strips and pellets		Lucite International, Accrington, Lancashire, UK 2 mm sheet.
PA6	Polyamide 6	Simple polymer (also known as Nylon 6) tested in the form of pellets		Lucite International, Accrington, Lancashire, UK
PA 6.6	Polyamide 6.6	Simple polymer (also known as Nylon 6.6) tested in the form of pellets		Lucite International, Accrington, Lancashire, UK
PB	Plaster board	Standard construction product		Wicks, Preston, Lancashire, UK
MDF	MDF	Standard construction product		Wicks, Preston, Lancashire, UK
W	Wood	Untreated wood strips		Wicks, Preston, Lancashire, UK
PW	Plywood	Standard construction product (2.6 mm thick)		Wicks, Preston, Lancashire, UK

PU	Polyurethane	Flexible polyurethane (density approximately 0.35 cm ³). Standard product.	Not combustion modified. Typical foam supplied in Europe for domestic furniture.	
Cables	Data cables	Standard data cables used in university buildings	Standard Cat7 Ethernet Cable	Obtained from ELand cables.

2.2.2 Location of standard methodologies used

All standard methodologies used in this research have been placed in the appendices. This contains methodologies developed specifically for the work conducted for this project. Any methodology used that is standard and readily available has therefore been placed into its own appendix and referenced specifically where needed.

2.2.3 Gap analysis of the ISO/TS 19700

The current methodology in the ISO/TS 19700 works well for most materials which undergo flaming combustion. Where flaming does not occur, changes to the protocol are proposed to enable valid and reproducible data to be obtained for smoke toxicity assessment. The protocol must also address situations when a non-combustible material has a combustible coating or binder. During these tests, flaming is not observed from the material itself, but the surface paint may support a flame.

Each material chosen was tested per the current ISO/TS 19700 standard in triplicate. Modifications were then made to the operating procedure to improve the steady period of burning when testing the material and establish the best means of testing the material in the SSTF.

Plasterboard was tested both with the outer-paper layer. The flexible polyurethane did not contain fire retardants. The cables tested were a mixture of household and data cables to identify which would provide the best steady burning period.

2.2.3.1 Revisions to the standard based on experimental data.

Currently, if no flaming occurs during the test, the operator is instructed to increase the temperature in 25 °C increments until flaming is observed. Increasing temperature increments ceases when consistent flaming occurs (with a minimum steady burning period of 5 minutes) or the maximum temperature is reached (900 °C). While this methodology works for materials where flaming is possible, materials where flaming is not possible (such as with plasterboard), must follow a simpler methodology as increasing tests in increments of 25 °C will cost a lot of time. Similarly, there is no guidance for materials where there is difficulty obtaining steady burning. A minimum period of 5 minutes of steady burning during the test is required to be valid.

The validity of the data obtained was checked against criteria in the ISO/TS 19700 standard.

During dynamic steady-state conditions, the volume fractions of carbon dioxide and oxygen depletion in the mixing and measurement chamber shall remain approximately constant, such that both

a) for any long-term trend, the average rate of change of volume fraction divided by the average value of the volume fraction over the 5 min period shall be less than $\pm 0,020 \text{ min}^{-1}$;

b) for any short-term fluctuations, the standard deviation of the volume fraction divided by the average value of the volume fraction, over the 5 min period shall be less than 0.20.

Several problems regarding calculating validity using the standard were noticed, particularly when testing non-combustible materials.

An example of this can be seen when testing plasterboard in the SSTF. Plasterboard was tested at 900 °C under-ventilated conditions. The variance in the data obtained, combined with a pass/fail according to the ISO/TS 19700 standard, is shown in *Table 11*. The calculation for the long-term trend does not take non-combustibility into account. As a result, the test data is considered invalid when using the current variation calculation methodology. A clear example of this can be seen when looking at CO yields.

CO concentrations measured were between 0.00013 % and 0.000015 %. However, using the current methodology, the range of the data is not taken into account. Due to the data showing significant variation at five decimal places, the data is invalid when using the current calculation and so fails the assessment on every attempt despite negligible volumes of CO being produced. Therefore testing non-combustible materials, such as plasterboard, will consistently result in ‘invalid’ data.

An example of the validity calculations made to the gas concentration data obtained from testing plasterboard in the SSTF is shown in *Figure 15*. Despite little change being observed in the gas yields during the test, the variation between the small changes in gas concentrations causes the test to fail on validity assessments.

Table 11: Long-term and short-term trend calculated using ISO/TS 19700 for plasterboard tested at 900 °C under-ventilated conditions in the SSTF.

Material	Gas identified	Long-term trend per min		Short-term trend per min	
		Value	Result	Value	Result
plasterboard	O ₂	0.00	Pass	0.0004	Pass
		-0.001	Pass	0.0011	Pass
	CO ₂	1.6287	Fail	0.0178	Pass
		0.0512	Fail	0.0193	Pass
	CO	0.125	Fail	0.0513	Fail
		-0.156	Fail	0.0532	Fail

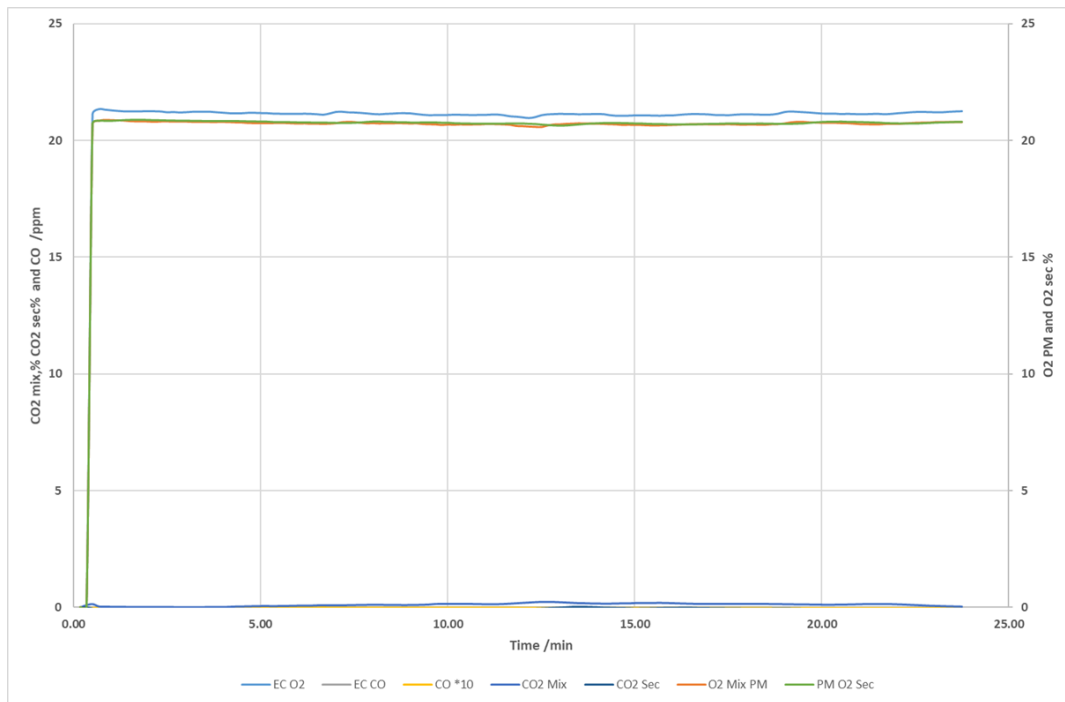


Figure 15: Example gas concentration data obtained from the duration of testing plasterboard in the SSTF.

2.2.3.2 Revised methodology

Section 10.3 a. in the ISO/TS 19700 standard currently assumes the standard deviation and average is a linear relationship that is evenly distributed. Using the gradient assumes that the standard deviation is also constant and the rate of change to be a straight line. This section aims to assess variation within the data, meaning the standard deviation is most likely not constant throughout the test.

One proposed methodology is to conduct a Shapiro-Wilk test to assess the normality of the data, then conduct a one-tailed t-test using a 95% confidence interval. Using confidence intervals (such as 95%) allows for the sample range and potential variation within the data set to be examined. It is a test of variation and can be calculated simply and easily.

Conducting the one-tailed t-test will test whether the mean of the data is different from the overall data obtained. The values obtained from the t-test should then be used alongside confidence intervals, which will provide the limits to what data is acceptable and what is not. Confidence intervals could be provided in the standard. Tests of normality and t-tests can be calculated using spreadsheet software. This method considers the size of the data set and analyses with relevance to the scale of the data.

Another simpler proposed methodology would be to impose limitations on the number of decimal points used in the calculation. Limiting the data in the calculation to three decimal places would mitigate the effects of the variance calculation in materials such as plasterboard, which are non-combustible or produce very little volumes of smoke.

2.2.3.2.1 Plasterboard

The plasterboard was tested both as strips and in ground form, both with and without the external paper covering. When tested at 650 °C, no flaming occurred from the plasterboard but did on the paper when used. When tested with the paper finish, the paper burnt off at the start of the test. However, this did not provide a consistent flame throughout the test. The burning on the surface was continuous until all the paper had burnt. As the burning occurred on the material's surface and not the internal material, the test was deemed non-flaming. Further clarification in the standard may pose useful when testing non-combustible materials that have a combustible cover, as the internal material does not burn but the cover on the material does.

When the paper was removed from the board, no flaming occurred throughout the test. Rather than increasing the temperature in increments of 25 °C until flaming was achieved, the sample was tested at the maximum furnace temperature (900 °C). The paper finish of the material burnt off continuously, but no flaming of the material for the duration of the test was observed.

It is suggested that for materials where no flaming is expected (materials with an extremely low fuel content), a test should be conducted at 900 °C. If no consistent flaming occurs during the test at this temperature, this should be reported. A clause in the standard would be required to enable this result to be valid, as the standard currently deems a test invalid if a steady burning period for 5 minutes is not obtained. It could be related to the products Euroclass.

An additional clause will be needed to accommodate non-combustible materials with a combustible paint finish. While the material is non-combustible, the paint will produce a flame at sufficient temperatures. This means that the test would be classified as flaming, despite the flame not being from the material.

2.2.3.2.2 Plywood

Tests conducted on plywood (5 x 5 x 800 mm) showed sporadic flaming throughout, with difficulty obtaining a steady burning period in some tests. The most valid data were obtained at 825 °C under-ventilated conditions. CO data was also more valid under this condition, with six of the nine tests having validity. All tests showed very low short-term fluctuations during the steady period of burning.

There was difficulty in reaching a steady burning period early on in the test. To combat this, suggestions for sample preparation will be proposed. It is suggested to make the front end of the sample thinner than the end by cutting the end into a triangular point. This allowed a gradual increase in thickness to induce a steadier burn earlier in the test as a smaller mass would be present in the hot zone of the furnace allowing for faster ignition. As the strip begins to widen the fuel load gradually increases, resulting in a steadier ignition and steadier burn initially.

2.2.3.2.3 Data cables

Cables were cut to 800 mm, weighed and laid across the SSTF sample boat. The cable used was dissected and the individual components weighed to obtain the mass of copper in the cable. This allowed for the mass of combustible loading to be known so that the feed rate could be adjusted so that 1 g min⁻¹ of combustible components of the cable would enter the furnace per minute, rather than include the non-combustible copper.

The cables consistently proved difficult to achieve steady burning in well-ventilated conditions. Flaming was typically sporadic throughout. However, gas yields and equivalence ratios were consistent between identical tests. During under-ventilated conditions, steady periods of burning were achievable. However, equivalence ratios were consistently relatively low for under-ventilated conditions ($\phi = 1.06 \pm 0.01$). CO yields were also not representative of under-ventilated flaming. This could be resolved by requiring a calculation of the air flow before testing to get a higher equivalence ratio. As 3.2 L min⁻¹ is relatively low, it may be better to use more than one cable.

Although difficulties arose in achieving steady burning, the data was highly repeatable between tests. The validity of two of the three sets of data obtained at 650 °C, under-ventilated, were valid in regards to CO₂. All tests conducted at 825 °C under-ventilated were considered valid. Unfortunately, only one of three tests conducted at 650 °C, well-ventilated, were valid in terms of the validity calculations stipulated in the standard.

While the product produces steady-state flaming during under-ventilated conditions, achieving a high equivalence ratio is difficult. It is suggested that specific air flows are used depending on the test required rather than following the generic under-ventilated condition requirements in the standard. Further research would be required to identify more specific air flow guidance for the protocol.

While achieving correct equivalence ratios for well-ventilated conditions is easy, obtaining a steady burning period throughout the test is difficult. Burning was very sporadic throughout the test. Typically flaming is sporadic. This has been attributed to the multiple layers within the cable, with the most flammable on the inside. Further research would be required to determine the optimal testing protocol for cables.

2.2.3.2.4 Flexible Polyurethane:

Flexible polyurethane samples were prepared (800 mm sample of approximately 20 g) and tested in accordance with the current ISO 19700 standard.

Steady burning is typically reached after 10 minutes during an under-ventilated test, so minor adjustments to the feed rate will not affect the period of steady burning. Half-sized samples were tested at an increased feed rate to confirm no differences in steady burning were observed.

Under-ventilated testing at 650 °C appears to reach a steady burning period faster than the well-ventilated counterpart. No differences in the steady burning period were observed using half-mass samples with increased feed rates (10 g over 800 mm). In some cases, there was difficulty achieving steady burning.

In terms of CO₂, all tests conducted at 650 °C well-ventilated were considered valid. Two of the three tests conducted at 825 °C under-ventilated were considered valid. CO data was much less repeatable, with one in three tests being considered valid (at 650 °C well-ventilated and 650 °C under-ventilated). However, no test at 825 °C had valid CO data. This was expected and is acceptable when following the current standard.

Short-term fluctuations were valid for all tests conducted. For all tests conducted, CO yields did not reach steady concentrations. For under-ventilated tests, at both 650 °C and 825 °C, steady burning was achievable and was repeatable (shown between 3 tests).

Low-density materials will typically have a larger sample height. Due to potential difficulties in fitting such a bulky material into the tube, it is suggested that a smaller sample is used with the feed rate being adjusted so that it is consistently 1 g min⁻¹ to avoid difficulties when introducing the sample to the furnace. This would also be useful for PIR and phenolic foams as the materials typically swell upon heating, causing less dense samples to fill the quartz tube and impair airflow over the sample.

The areas of revision and improvement identified during this research can be expanded and implemented into the ISO/TS 19700 standard. These would provide the additional information required to enable the technical standard to become a full standard. These revisions will improve the test method's robustness and scope of use. The work has provided evidence that non-homogenous thermoplastics and non-combustible materials can be tested using the SSTF.

As one of the only test methods proven to measure smoke toxicity repeatably⁸⁸ and be representative of large-scale test data⁸⁹, the improvements to the standard will enable smoke toxicity regulations to be made with an existing and proven test method.

2.2.4 Formation of HCN as a function of time during an SSTF run

The SSTF is designed to sustain steady burning throughout the test. This is thought to create a reaction whereby the rate of decomposition of the fuel is equal to the rate of generation of gaseous species.

To ensure gas sampling was taken at the correct time (during steady combustion), HCN was sampled for several conditions throughout the duration of an SSTF test. Samples were taken in 4 minute intervals at a set flow rate of 1 L min⁻¹ from the start of the test (pre-ignition) until the end. The time intervals used are summarised in *Table 12*. Samples were collected and analysed in duplicate to assess the repeatability of HCN sampling measurements.

PA6.6 was chosen for the test material in the SSTF as it contains a significant proportion of nitrogen in its structure and would produce significant volumes of HCN during combustion. The PA6.6 was also tested at several different temperatures: 650 °C, 750 °C and 850 °C, to identify any potential differences resulting from temperature.

A series of dreschel bottles containing 0.1 M NaOH were set up and connected to an automated sampler (further described in 2.5). HCN was analysed using a spectrophotometric method, described in **Appendix 2**, in duplicate, with an average result being presented.

Table 12: Summary of the time intervals plotted with the time intervals used.

Time interval plotted	Time sampled /min
4	0-4
8	4-8
12	8-12
16	12-16
20	16-20

2.2.4.1 Results and discussion

The duplicate results of HCN data obtained were plotted against time to show the repeatability of the sampling. This is shown in *Figure 16*. The HCN data obtained showed high repeatability, with the samples showing very similar concentrations.

An average of the HCN data obtained was then plotted alongside the average CO concentrations measured throughout the tests. This is shown in *Figure 17*. The HCN was found to mirror the CO production throughout the test.

At approximately 12 mins into the test, HCN and CO measured began to level and be produced at a steady rate. This shows that the steady state tube furnace can generate fire effluent at a constant rate once steady burning is established, meaning sampling for toxicants, such as HCN, can be done in a repeatable way allowing for accurate determination of smoke toxicity.

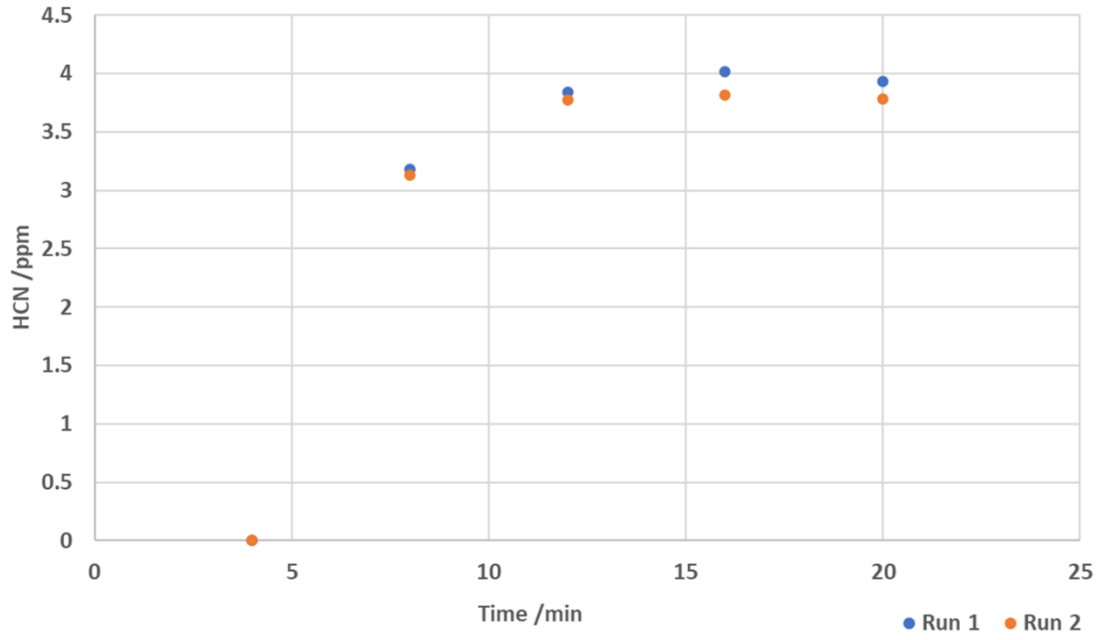


Figure 16: HCN concentrations generated over the duration of testing PA6.6 in the SSTF at 650 °C (under-ventilated flaming) ran in duplicate to test the repeatability of the methodology.

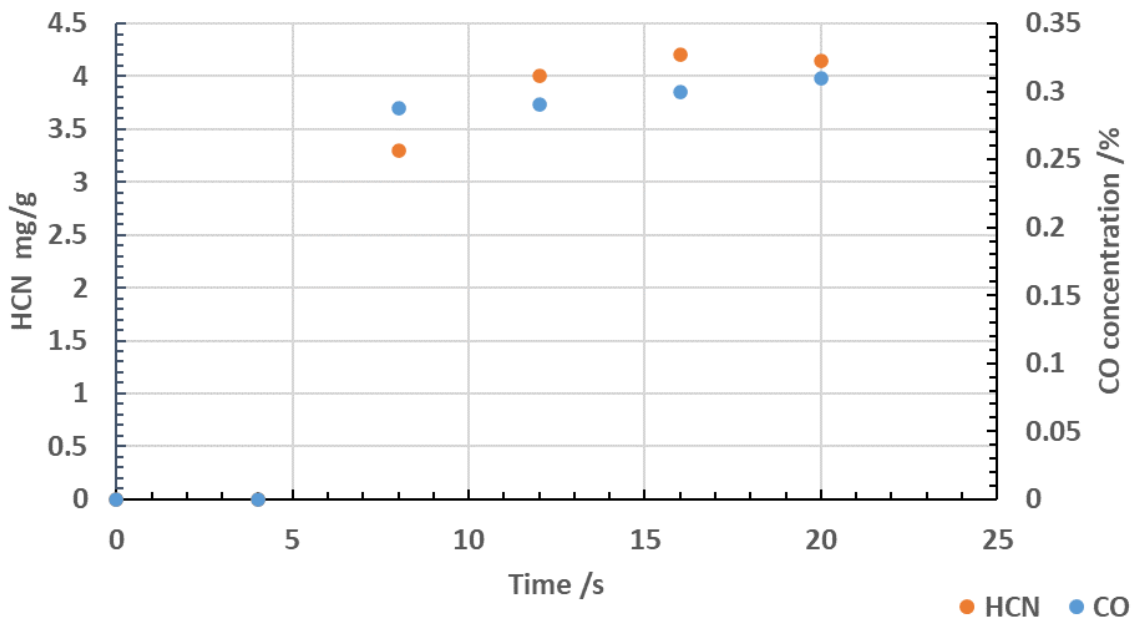


Figure 17: Average HCN concentrations measured over the duration of testing PA6.6 in the SSTF at 650 °C (under-ventilated flaming) VS CO concentration measured throughout the test.

2.2.5 The effects of using supplementary nitrogen to achieve low oxygen environments.

Although the SSTF is capable of recreating under-ventilated flaming conditions by reducing the primary air flow, there is no reported work of burning in extremely low oxygen environments (<10%). In fires, the same low-oxygen environments occur by replacing oxygen with CO₂ and water vapour.

The primary gas inlet of the SSTF was modified to introduce a mixture of air and nitrogen. The gases were pre-mixed in a gas-tight glass tube of steel wool before entering the primary air inlet of the tube furnace. Gas flows were controlled using mass flow controllers. In each test, the air volume remained at 2 L min⁻¹, and the volume of nitrogen was varied between tests altering the total volume of gas used in the primary gas inlet. The secondary gas flow was varied accordingly to make up a total volume of 50 L through the apparatus. Tests were conducted at 650 °C and, in some cases, repeated at 750 °C and 850 °C.

The materials used for this assessment were: strips of polymethylmethacrylate (PMMA), polyamide 6 (PA6) pellets and polyamide 6.6 (PA6.6) pellets.

The smoke toxicity of the material was assessed in each experiment, with CO, CO₂ and O₂ depletion being monitored constantly during each test using the box analysers. HCN was quantified using the method described in **Appendix 2**.

To ensure any observations were a result of the chemical reactions occurring in the combustion environment and not a direct result of changes in fluid flow through furnace, the Reynolds number for each air flow used was calculated based on the calibrated temperature profile of the furnace. If the effluent were to transition from laminar to turbulent, this would directly affect the mixing of the fire effluent, resulting in changes to the measured toxicity. The Reynolds number was calculated using Equation 8.

$$Re = \frac{\rho v d}{\mu} \quad \text{Equation 8}$$

Where ρ is the density of the gas, v is the velocity, d is diameter of the pipe, and μ is the viscosity of the gas. The calculated Reynolds number plotted as a function of temperature and distance from the centre of the furnace tube is shown in Figure 18. In all cases and conditions tested, the flow remained laminar.

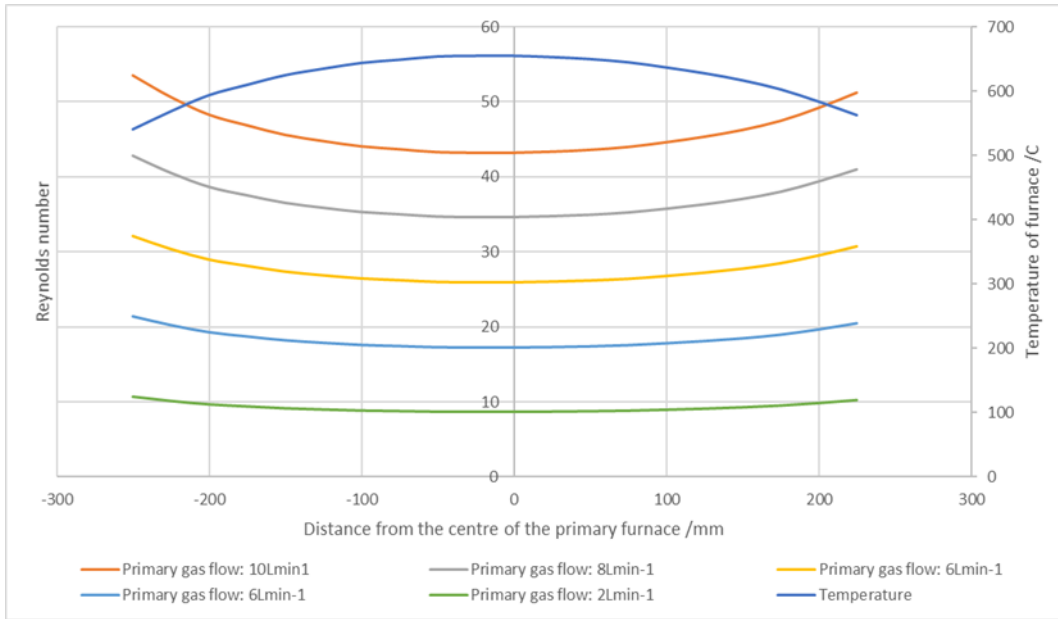


Figure 18: Reynolds number calculated at different air flows using the SSTF as a function of temperature and distance from the centre of the SSTF furnace.

2.2.5.1 N₂ in the SSTF

The calculated Reynolds number for each airflow based on the furnace temperature profile is shown in Figure 18. The fluidity of the gas is not entirely constant throughout the furnace due to the changes in gas density and viscosity based on the temperature gradient of the furnace. As the gas goes from 300 k to 900 k, its density will decrease by a factor of 3.

The flow through the tube furnace was consistently laminar at all gas flows used. From this, observations were deemed to be a result of chemical reactions instead of changes in effluent mixing.

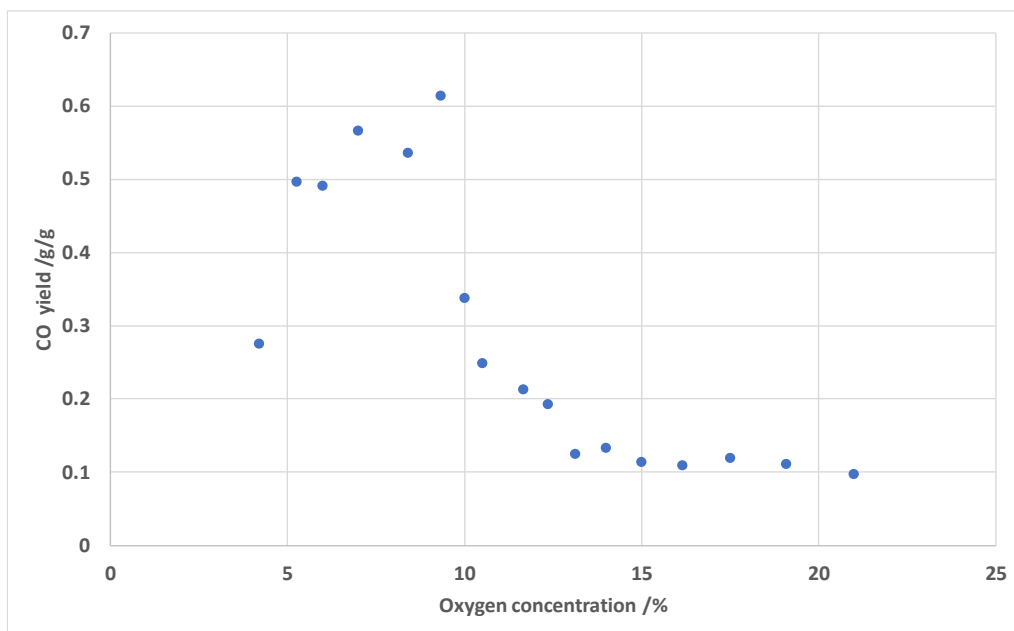


Figure 19: CO yields obtained at varying oxygen concentrations for tests conducted using PA6

Figure 19 shows CO yields obtained from tests conducted using PA6 at varying oxygen concentrations. The addition of nitrogen into the combustion environment had little effect on the CO yield at oxygen concentrations above 13%. Below this point, a sharp increase in CO yields was observed, with significant increases being observed between 10 and 8% O₂.

Figure 20 shows HCN yields obtained from tests conducted using PA6 at varying oxygen concentrations. As the oxygen concentration is reduced, there is an increase in the yield of HCN. This is particularly prominent below 15% O₂, with a sharp increase being seen between 10 and 8%, similar to the observations made with the CO yield.

At oxygen concentrations below 10.5%, the reaction zone within the flame appeared to distort to such an extent it reduced the flame's thickness. This was a visible effect that occurred in the tube furnace as the flame became smaller and wispy, coinciding with the point at which carbon monoxide yields significantly increased, suggesting that the free radical concentration has fallen below the critical value necessary to support flaming combustion, resulting in higher yields of products of incomplete combustion. However, the greater volume of nitrogen will also reduce the residence time in the furnace's hot zone, so the fuel vapours have a much shorter period to react. The shorter reaction time and flame quenching makes the combustion more incomplete, explaining the increase in products of incomplete combustion (CO and HCN) at this point. This explanation is supported by the CO₂ data obtained from these experiments, shown in Figure 21.

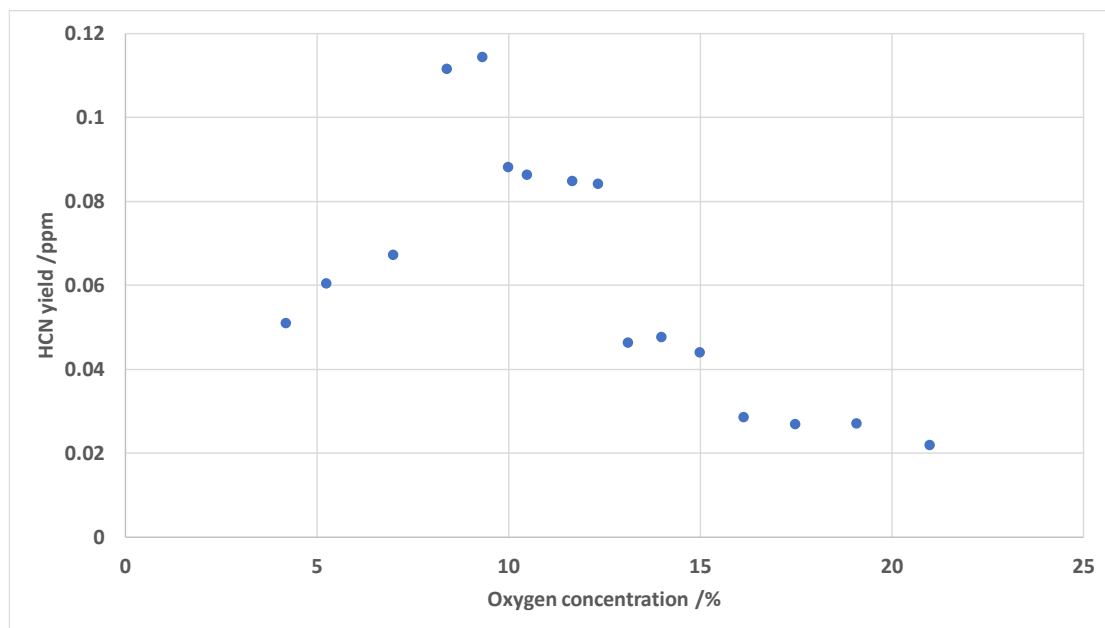


Figure 20: HCN yields obtained when conducting tests on PA.6 at varying oxygen concentrations

Similar to the trend observed in the CO yields, there is little change in the CO₂ yield in oxygen concentrations above 13%. Below this point, there is a significant decrease in CO₂ yield, with the sharpest decrease being observed between 10 and 8% O₂. A decrease in the yields of products of complete combustion suggests the burning behaviour becomes much less complete beyond this point.

Nitrogen's effects on CO formation were also studied at three different temperatures using PA6.6. This is shown in Figure 22 . Similar to tests conducted on PA6, the CO yields increase as the oxygen concentration decreases. A sharper increase in CO yield is observed at 850 °C than at lower temperatures, suggesting the effects are more prominent at higher temperatures. This is evident at

oxygen concentrations below 5% as at 850 °C, the yield of CO continued to rise, unlike the CO yield measured at 750 and 650 °C. At higher temperatures, the formation of more radical species in the gas phase would be expected to be greater than that at lower temperatures. With little oxygen being available for the radical species to form products of complete combustion (CO₂), there would be an increase in CO yield. At higher temperatures, there would be more radical species present, so it would be expected that more CO is formed than at lower temperatures resulting in the sharper increase observed.

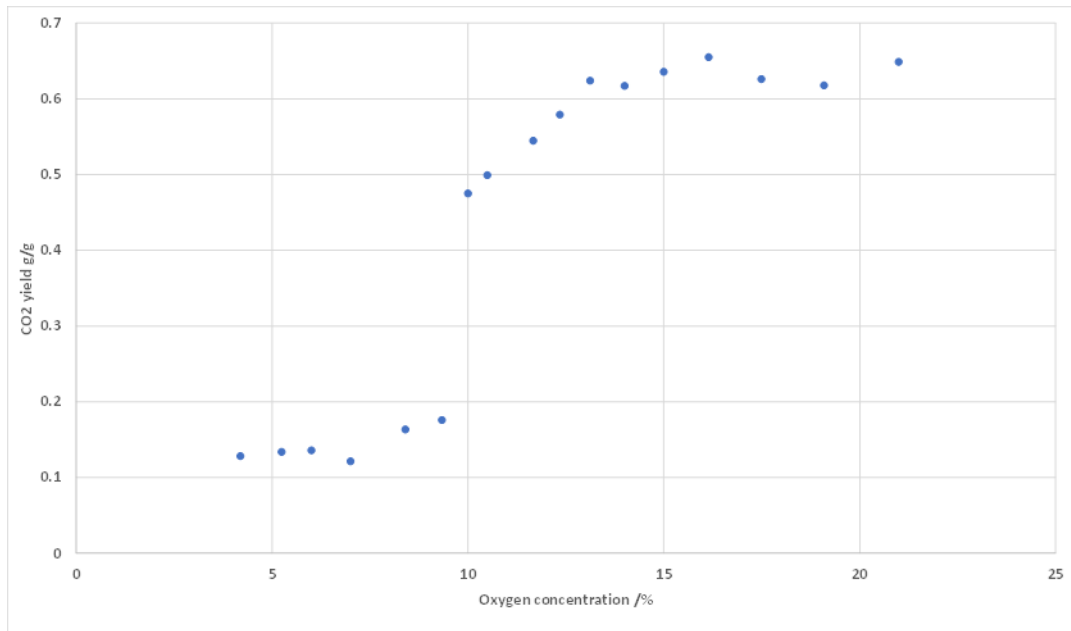


Figure 21: CO₂ yields obtained from tests conducted using PA6 at varying oxygen concentrations

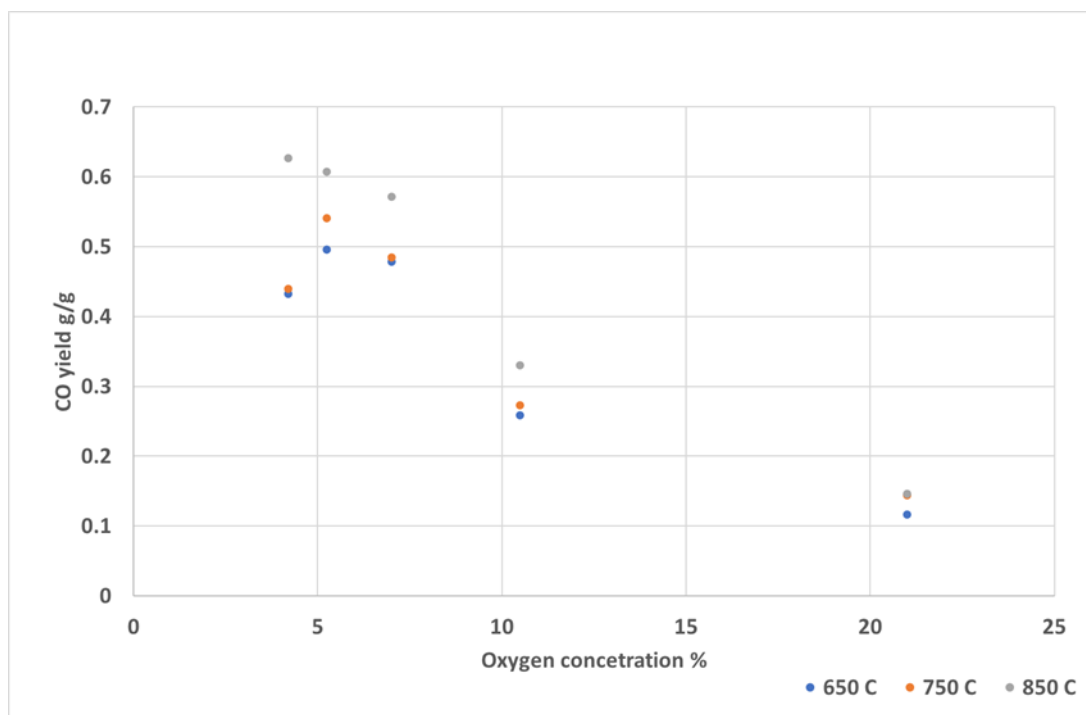


Figure 22: CO yields obtained at varying oxygen concentrations at 650, 750 and 850 °C, conducted using PA6.6

The effects of nitrogen on HCN formation studied at three different temperatures using PA 6.6 is shown in Figure 23. PA6.6 was used to produce more HCN (as a result of the additional nitrogen in its chemical structure) to allow the identification of trends to be easier seen. Its HCN yields varied with temperature, with higher temperatures yielding more HCN, similar to CO yields. The HCN yield was also found to vary with varying oxygen concentration, showing an increase in HCN as the oxygen concentration decreases. This is similar to the experiments conducted using PA6 and observations of CO yields.

To identify whether atmospheric nitrogen in the combustion environment impacted the yields of HCN, tests were conducted using strips of PMMA. PMMA was chosen as a validation material as it contains no nitrogen in its chemical structure, meaning any HCN formation and changes to HCN measurements would directly result from the nitrogen present in the combustion environment. All tests were conducted using the calculated primary air-flow required to produce an equivalence ratio of 1.5, which is representative of under-ventilated combustion. Tests were conducted at two different temperatures using four different oxygen concentrations, ranging from 21% to 9%.

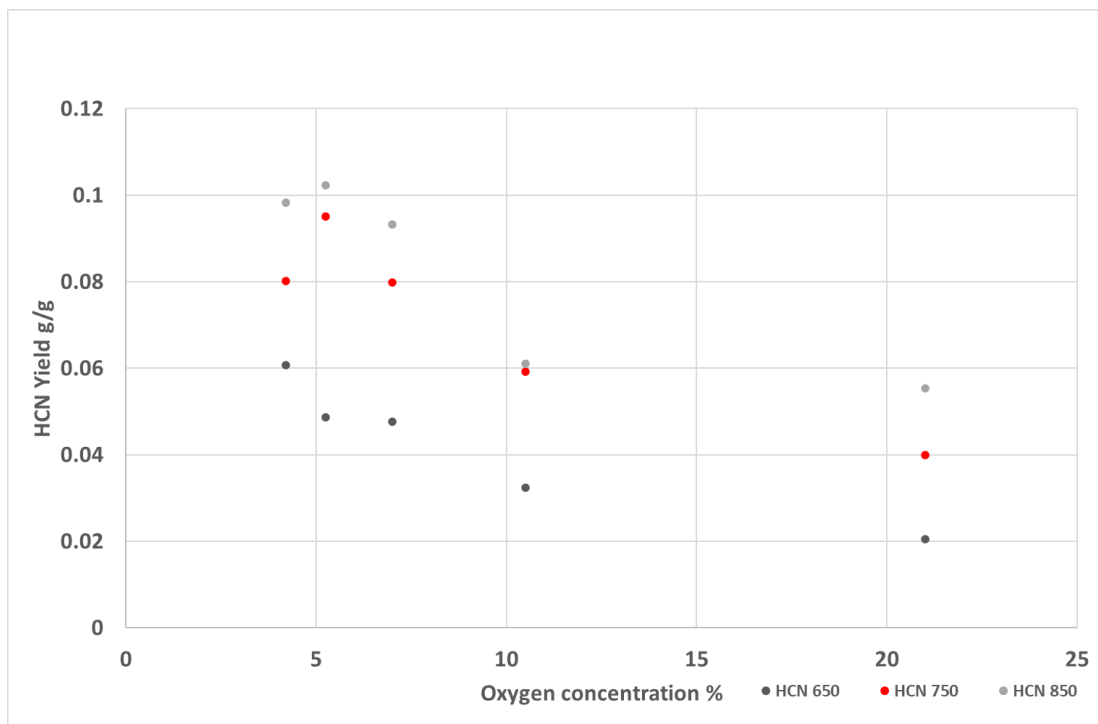


Figure 23: HCN yields quantified from testing PA6.6 in the SSTF under a range of oxygen concentrations using 3 different temperatures: 650, 750 and 850° C.

All HCN measurements on the tests conducted were below the limits of detection. This suggests that while the addition of nitrogen can impact the combustion conditions resulting in less complete combustion, the presence of nitrogen does not impact the chemistry of the effluent. As the addition of nitrogen did not result in measurable yields of HCN in non-nitrogen containing materials, the results observed in these experiments are deemed to be a result of the additional gas flow causing alterations to the time gaseous species spend in the reaction zone during combustion, resulting in less-complete combustion occurring.

2.2.5.2 Conclusions

The addition of nitrogen into the SSTF does not directly impact the chemistry of fire effluent during a test, making it a suitable addition to achieve low oxygen concentrations for replicating under-ventilated fire scenarios. A higher flow of nitrogen is required to achieve lower oxygen environments. When attempting to create oxygen environments below 10%, the primary air flow through the tube furnace is too strong and alters the size of the flame and hence the reaction zone. The thinning of the flame zone results in gaseous species spending less time in the reaction zone, resulting in less time for chemical reactions. This results in less complete combustion occurring, an increased yield of measured products of incomplete combustion (CO and HCN), and a decreased yield of products of complete combustion (CO₂).

Above 10% oxygen, there is little change in measured yields and within experimental variation limits. However, rather than altering the combustion environment, the addition of nitrogen seemed to have more effect on alterations to the flame zone rather than the actual burning conditions of the test. Additional future tests could be conducted where the total flow rate within the tube is kept constant and the ratio of oxygen and nitrogen are varied to study the effects of varying the concentration on the products of combustion in a similarly controlled way. As oxygen is a necessary component of fire, varying the concentration of oxygen within the environment with a total constant flow would have a much more significant impact on the study of low-ventilation conditions within the SSTF.

2.3 DEVELOPMENT OF THE PHI METER

A phi meter is a piece of equipment used to monitor the equivalence ratio during a fire¹⁰⁷. The core principle of a phi meter is to quantify any oxygen excess in the fire effluent and to convert any products of incomplete combustion present in the fire effluent to CO₂ and water (via supplementary O₂ and high temperatures). The equivalence ratio is calculated from the supplementary oxygen supply rate and the amount of oxygen in the effluent after all products have been converted to CO₂ and water (this can be found at the exhaust of the phi meter).

2.3.1 Understanding the phi meter.

2.3.1.1 Calculation of equivalence ratio using the phi meter

The phi meter calculations are based on a series of equations derived from the equivalence ratio. The equivalence ratio (ϕ) is the actual fuel-to-air ratio divided by the theoretical fuel-to-air ratio. This can be expressed in terms of the molar flow for well-ventilated flaming using Equation 9, where \dot{n}_f is the molar flow of fuel, $\dot{n}^0(O_2)$ is the molar flow of oxygen (under ambient conditions) and $\dot{n}_r(O_2)$ is the molar oxygen flow required for stoichiometric combustion.

$$\phi = \frac{\left(\frac{\dot{n}_f}{\dot{n}^0(O_2)}\right)}{\left(\frac{\dot{n}_f}{\dot{n}_r(O_2)}\right)} \quad \text{Equation 9}$$

The following part of the derivation addresses the conditions where $\phi < 1$. To calculate the molar flow of oxygen required for complete combustion (\dot{n}_r), the ambient molar flow of oxygen ($\dot{n}(O_2)$) can be subtracted from the actual molar flow of oxygen in the exhaust ($\dot{n}^0(O_2)$) Shown in Equation 10.

$$\dot{n}_r = \dot{n}^0(O_2) - \dot{n}(O_2) \quad \text{Equation 10}$$

Substituting Equation 10 into Equation 9 produces Equation 11. This equation allows the over-ventilated component of the equivalence ratio to be calculated by subtracting the actual molar flow of oxygen from the molar flow of oxygen under ambient conditions, then dividing by the actual flow of oxygen.

$$\phi = \frac{\dot{n}^0(O_2) - \dot{n}(O_2)}{\dot{n}^0(O_2)} \quad \text{Equation 11}$$

Nitrogen is present in the combustor environment but does not participate in the reactions. This means that the flow rate of nitrogen into the combustor is the same as the flow rate going out. By dividing the oxygen flow rates by the nitrogen flow rates, Equation 12 is produced.

$$\phi = \left(\frac{\dot{n}^0(O_2)}{\dot{n}^0(N_2)} - \frac{\dot{n}(O_2)}{\dot{n}(N_2)}\right) / \left(\frac{\dot{n}^0(O_2)}{\dot{n}^0(N_2)}\right) \quad \text{Equation 12}$$

The equivalence ratio can be expressed in terms of either molar flow or mole fractions. By substituting the molar flows with mole fractions X_{O_2} and X_{N_2} , Equation 13 is produced.

$$\phi = \left(\frac{X^0(O_2)}{X^0(N_2)} - \frac{X(O_2)}{X(N_2)}\right) / \left(\frac{X^0(O_2)}{X^0(N_2)}\right) \quad \text{Equation 13}$$

$X^0(O_2)$ is the ambient oxygen mole fraction and is therefore equal to 0.21. The mole fraction of oxygen and nitrogen can be said to equal 1, shown in Equation 14.

$$X(O_2) + X(N_2) = 1 \quad \text{Equation 14}$$

By substituting equation 13 into equation 14, equation 15 is produced.

$$\phi = 1 - \left[\frac{X_{O_2}^0}{X_{N_2}^0} \right] \frac{1 - X_{O_2}^0}{1 - X_{N_2}^0} \quad \text{Equation 15}$$

Equation 15 applies to the condition where $\phi < 1$. This is because if you take the extreme cases of equation [10]; $X(O_2) = X_{O_2}^0$ and $X(O_2) = 0$, the phi values calculated are $\phi = 0$ and $\phi = 1$.

In an under-ventilated system (conditions where $\phi > 1$) there is an excess of oxidisable fuel. The molar flow of supplemental oxygen is defined as $\dot{n}^a(O_2)$. This needs to be added to the molar flow of ambient oxygen as this takes into account the additional oxygen not used during the combustion, as shown in Equation 16.

$$\dot{n}_r = \dot{n}^a(O_2) + \dot{n}^0(O_2) - \dot{n}(O_2) \quad \text{Equation 16}$$

The molar flow of nitrogen can be added into equation 16 and expressed in terms of equivalence ratio. This produces equation 17.

$$\phi = \left(\frac{\dot{n}^a(O_2)}{\dot{n}(N_2)} + \frac{\dot{n}^0(O_2)}{\dot{n}^0(N_2)} - \frac{\dot{n}(O_2)}{\dot{n}(N_2)} \right) / \left(\frac{\dot{n}^0(O_2)}{\dot{n}^0(N_2)} \right) \quad \text{Equation 17}$$

Instead of using molar flows or mole fractions, the molar flow of nitrogen and the molar flow of supplemental oxygen can be expressed in terms of the volumetric flow of oxygen added to the combustor and the total volumetric flow of the combustor. To do this, the ideal gas law needs to be applied. By rearranging the ideal gas law to make $\dot{n}^a(O_2)$ (this replaces what would be n in the gas law) the subject, the molar flow of additional oxygen can be expressed in terms of the volumetric flow of oxygen added to the system, shown in equation 18.

$$\dot{n}^a(O_2) = \frac{P_a V_a}{RT_a} \quad \text{Equation 18}$$

The same can be done for the molar flow of nitrogen. However, as this is expressed in terms of the total flow to the analyser, Equation 14 needs to be rearranged to make $X(N_2)$ the subject. This produces equation 19.

$$X(N_2) = 1 - X(O_2) \quad \text{Equation 19}$$

By substituting the ideal gas law into Equation 19, Equation 20 is produced.

$$X(N_2) = \frac{PV(1-X_{O_2})}{RT} \quad \text{Equation 20}$$

Equation 20 shows the relationship between the molar flow of the ambient oxygen in the system and the mole fraction of nitrogen in the system. This is produced by substituting $X(N_2)$ for the relationship shown in Equation 21.

$$\frac{\dot{n}^0(O_2)}{\dot{n}^0(N_2)} = 1 - X(O_2) \quad \text{Equation 21}$$

By using equations 20 and 21, ϕ can be expressed using equation 22.

$$\phi = \frac{\dot{n}^a(O_2)}{\dot{n}(N_2)} / \frac{\dot{n}^0(O_2)}{\dot{n}^0(N_2)} = \frac{1 - (X_{O_2}^0) V_a P_a T}{X_{O_2}^0 (1 - X_{O_2}) V P T_a} \quad \text{Equation 22}$$

V_a/V Shown in Equation 22 describes the volumetric flow ratio and can be expressed as $X_{O_2}^i$ in terms of the volume fraction of ambient O_2 at the analyser and the volume fraction of O_2 at the inlet. $X_{O_2}^i$ needs to have a defined total volume of flow through the analyser allowing it to be linked to the flow

ratio (at a constant flow rate and volume of flow). The equations can be used to solve for V_a/V . Equation 22 can be separated and expanded to produce Equation 23.

$$X_{O_2}^i = \frac{1 - (X_{O_2}^0)V_a P_a T}{X_{O_2}^0 (1 - X_{O_2}) V P T_a}$$

$$X_{O_2}^i = \frac{V_a P_a T}{V P T_a} \cdot \frac{1 - (X_{O_2}^0)}{X_{O_2}^0 (1 - X_{O_2})}$$

$$X_{O_2}^i = \frac{V_a}{V} (1 - X_{O_2}^0) + X_{O_2}^0 \quad \text{Equation 23}$$

Equation 23 can be rearranged to produce Equation 24.

$$\frac{V_a}{V} = \frac{X_{O_2}^i - X_{O_2}^0}{(1 - X_{O_2}^0)} \quad \text{Equation 24}$$

Equation 23 can be substituted into Equation 24 to obtain the value of the equivalence ratio, producing Equation 25.

$$\Phi_1 = \frac{X_{O_2}^i - X_{O_2}^0}{X_{O_2}^0 (1 - X_{O_2}^0)} \quad \text{Equation 25}$$

To obtain a value for Φ , Equation 25 needs to be substituted into Equation 24 to produce Equation 26.

$$\Phi = 1 - \frac{X_{O_2} (1 - X_{O_2}^0)}{X_{O_2}^0 (1 - X_{O_2})} + \frac{X_{O_2}^i - X_{O_2}^0}{X_{O_2}^0 (1 - X_{O_2})} \quad \text{Equation 26}$$

Equation 26 can be expressed in terms of the volumetric flow rate. Equation 27 is produced by using Equation 12 and 26.

$$\Phi = 1 - \left[\frac{X_{O_2}}{X_{O_2}^0} \right] \frac{1 - X_{O_2}^0}{1 - X_{O_2}} + \frac{(1 - X_{O_2}^0)V_a}{X_{O_2}^0 (1 - X_{O_2})V} \quad \text{Equation 27}$$

Equation 27 can be simplified to produce Equation 28.

$$\Phi = 1 + \left(\frac{(1 - X_{O_2}^0)(V_a - V X_{O_2})}{X_{O_2}^0 (1 - X_{O_2})V} \right) \quad \text{Equation 28}$$

To calculate Φ using Equation 28, three parameters need to be measured under constant volumetric air flow: the oxygen concentration in the combustion environment (X_{O_2}), the baseline concentration of oxygen present at the oxygen inlet ($X_{O_2}^0$) and the baseline concentration of oxygen with no additional oxygen ($X_{O_2}^i$). A mass flow controller will adequately keep the volumetric flow constant through the system.

Using a phi-meter will allow for constant monitoring of the equivalence ratio throughout a test. This is particularly useful for identifying the fire stage during large-scale testing and allows for direct bench-to-large scale comparisons based on equivalence ratio to be made.

2.3.2 Chemical principles of the phi meter

The phi meter relies on two core chemical reactions: the water gas shift reaction and the Sabatier reaction. The main focus of the phi meter is the water-gas shift reaction, shown in Reaction 1.



This reaction is exothermic, releasing heat into the system. The equilibrium constant (K_p) for this reaction calculated using Equation 29. Equilibrium of this reaction occurs at approximately 1000 K. As the temperature of the reaction increases, K_p will decrease slowly, shifting the equilibrium leftwards, favouring the formation of CO. The reaction is therefore thermodynamically limited.

$$K_p = \exp((4577.7/T)-4.33) \quad \text{Equation 29}$$

The main objective of the phi meter is to convert CO to CO₂, and so this can cause limitations to the capabilities of the phi meter. To combat this, a catalyst is often used in the phi meter, most commonly Platinum gauze. Pt has been shown to be a poor reducing agent for CO₂, which is thought to help maintain a rightwards shifted equilibrium.

As the reaction is thermodynamically limited, it was thought that the conversion of CO to CO₂ and H₂O would occur without the presence of a catalyst providing sufficient temperatures were used. As no literature was available to check whether a catalyst was needed for the phi meter, several experimental studies were conducted to test this theory.

2.3.3 Background experimental research

2.3.3.1 Microscale Combustion Calorimetry

To find the optimal operational temperature of the phi meter, a series of experiments were conducted using microscale combustion calorimetry (MCC). The MCC was initially chosen as the furnace design used for the phi meter in this work is based on the design used in the MCC. The methodology used to conduct testing can be found in **Appendix 5**.

Polystyrene was used to calibrate the MCC. The oxidizer temperature of the MCC varied, ranging from 750 °C to 1000 °C. Higher temperatures were not viable to be conducted on the apparatus due to limitations of MCC design (the MCC furnace, unless modified, is incapable of sustaining temperatures over 1000 °C). An NDIR was connected to the exhaust line of the MCC to monitor CO and CO₂ yields at each oxidiser temperature.

The yields of CO₂ and CO obtained during testing have been presented as a function of temperature and are shown in Figure 24 and Figure 25.

At temperatures 800°C and above, CO concentrations became negligible, with little to no variations being observed. The lowest volumes of CO were produced at 1000 °C. The CO₂ was observed to be the highest when the furnace temperature was set to 960 °C. From this, the best operating temperature for the phi meter was 900 °C. This was chosen as a compromise between equipment design and cost and the best operating conditions for complete combustion. At 900 °C, all products in the effluent should have undergone complete combustion.

The difference in time delays in the data was not corrected as it resulted from the increased temperature increasing the volume, accounting for it flowing faster through the MCC.

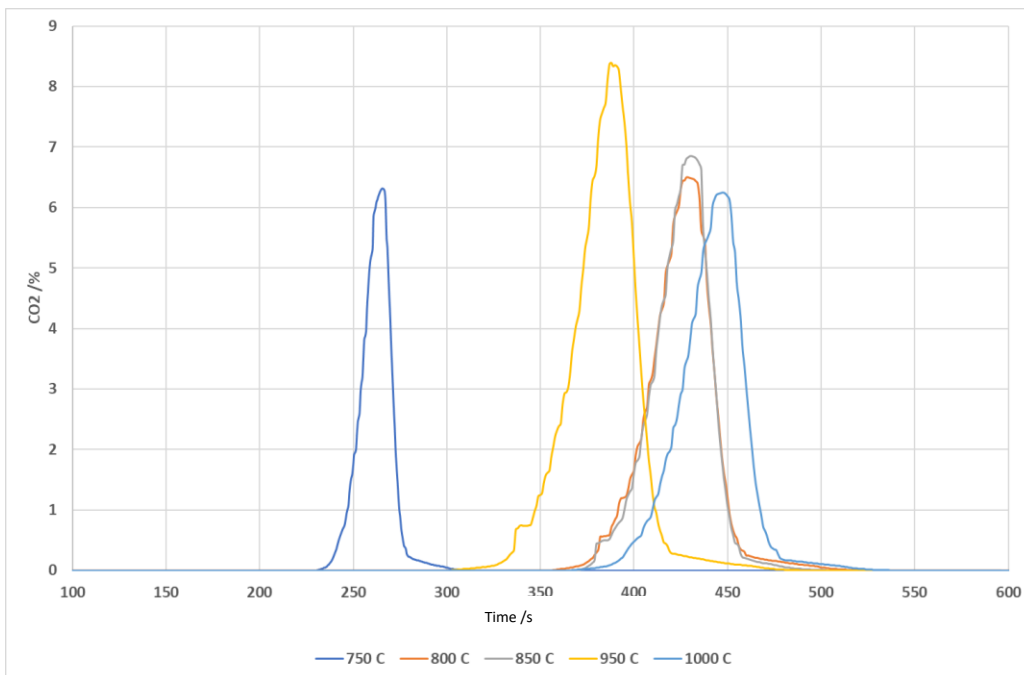


Figure 24: Yield of CO₂ produced from Microscale combustion calorimetry as a function of time, tested at a range of oxidiser temperatures

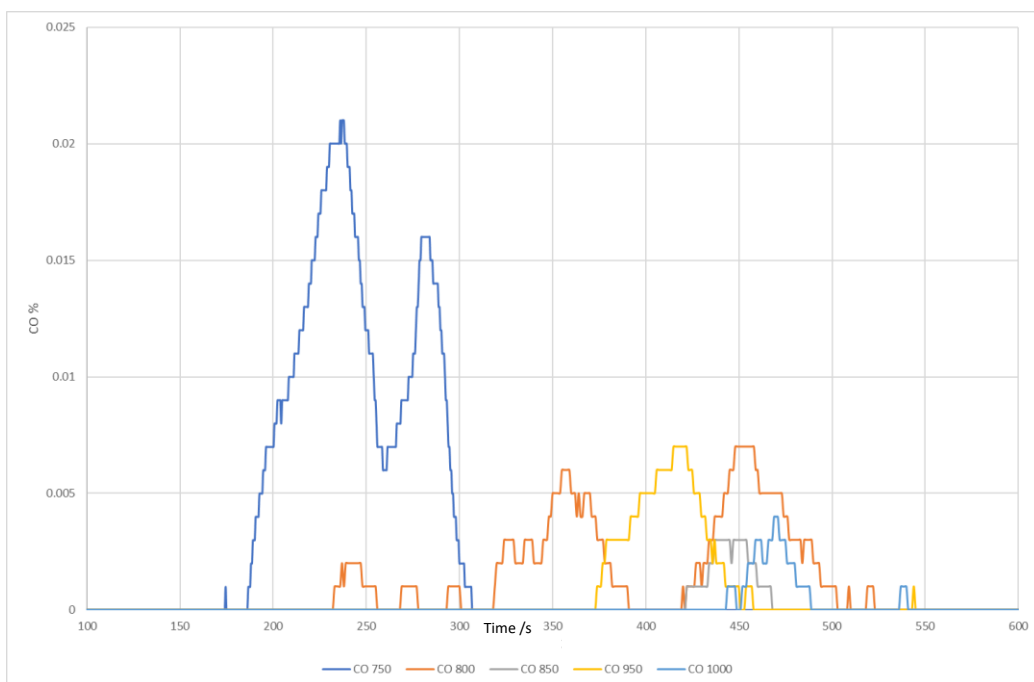


Figure 25: CO yields obtained from Polystyrene produced from Microscale Combustion calorimetry as a function of time, tested at a range of oxidiser temperatures.

2.3.3.2 Verification using the Steady State Tube Furnace

The steady state tube furnace used in this research had an additional secondary furnace. The furnace is typically set to 900 °C with quartz wool inside to act as a reactive surface to promote oxidation. This allowed for additional calculations and analysis to be conducted.

To aid the research conducted on the MCC, the secondary furnace temperature was varied from 750 °C to 900 °C with an NDIR placed on the exit of the furnace to monitor CO/CO₂ formation. The aim was to identify the temperatures necessary to convert all products of incomplete combustion to CO₂ and H₂O. This enabled the operating temperature range of the phi meter to be identified. This was also used to test whether a catalyst was necessary in the phi meter design for complete combustion to occur and whether furnace size was important.

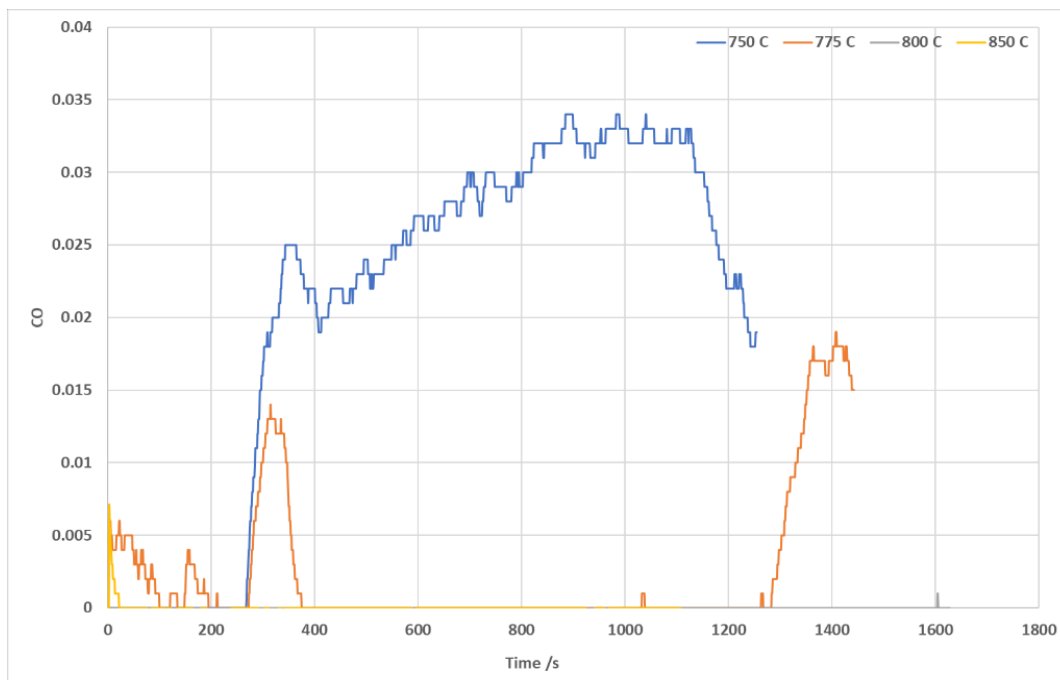


Figure 26: CO yields obtained from PMMA tested on the SSTF at an equivalence ratio of 1.5 using varying secondary furnace temperatures

A series of tests were conducted using PMMA at 650 °C. The air flows selected for the tests were calculated to give an equivalence ratio of 1.5. Yields of CO at varying secondary furnace temperatures are shown in Figure 26.

Similar to the data obtained using the MCC, conditions above 800 °C produced negligible amounts of CO, suggesting all products of incomplete combustion have fully combusted beyond this temperature.

The final operating temperature of the phi meter furnace was chosen to be 900 °C.

According to the chemical principles discussed previously, the Sabatier and water-gas shift reactions should be at mid-point in equilibrium at temperatures of 1000 °K (approximately 750 °C). During these experiments, the most CO₂ was produced at temperatures of 800 °C and above (1100 °K), suggesting the reactions are in equilibrium and all products of incomplete combustion are fully combusting under the test conditions.

No catalyst was used throughout the experiments. Due to optimal reaction conditions being obtainable without the use of a catalyst, the flow through the phi meter was sufficient to eliminate the need to include a catalyst.

2.3.4 Schematic designs

The schematic design for the original phi meter specified an 800 cm furnace, set to 1000 °C. The original design also incorporated a platinum-based catalyst in the furnace to ensure complete combustion occurred. Due to the impracticality of such a large furnace and the significant costs of a platinum catalyst, several modifications were made to the original design to create a phi meter more suited to the requirements of this research. The original phi meter design used additional oxygen. However, the phi meter used in this research used air. As the phi meter was planned to be used for large-scale testing, it was deemed safer to use clean air than a gas canister of oxygen near the test.

The decision to use air rather than oxygen was also based on the secondary oxidiser on the SSTF. The oxidiser is used in the same way as the phi meter is intended to be. The oxidiser drew fire effluent, pre-mixed with air. As no CO and soot have been observed when using the secondary oxidiser of the SSTF with air, adding pure oxygen was thought unnecessary.

As the purpose of the combustor is to convert all products of incomplete combustion to CO₂ and H₂O, it was determined that there was little need for a furnace of such size (as the original design uses an 800 mm furnace). The phi meter was also required to be easily portable to take to large-scale test facilities abroad, so portability was a concern.

As an alternative, a combustor similar to that used in the microscale combustion calorimeter (MCC) was used. The final schematic design used for the phi meter is shown in Figure 27.

As the phi meter created for this research was significantly smaller than the original design, much lower flow rates were required to be used. The MCC furnace operates at a maximum flow rate of 100 cm³ min⁻¹. Therefore, the phi meter was run with 50 cm³ fresh air and 50 cm³ fire effluent per minute. Due to the extremely low flow rates required, specialist mass flow controllers and pumps that could operate at such low flows were required.

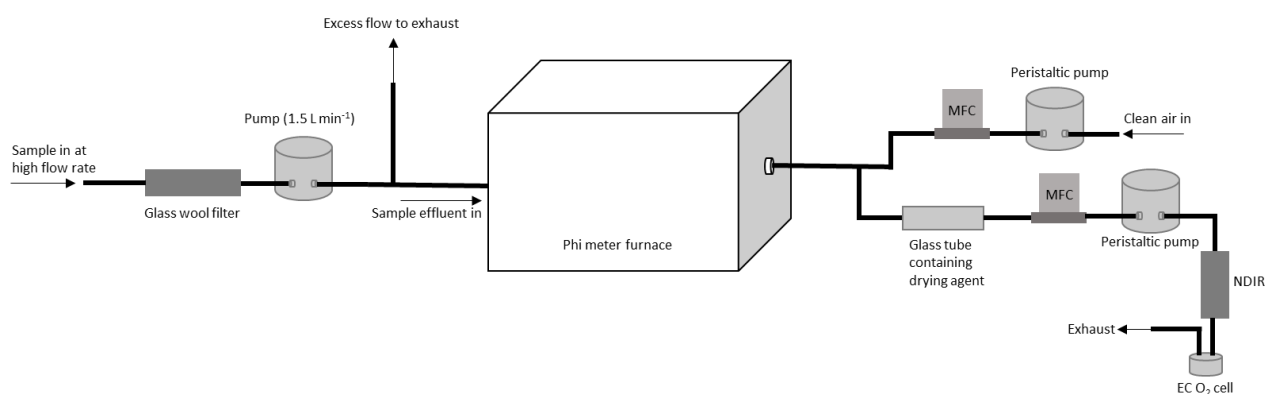


Figure 27: Final schematic design of phi meter created for this project, where MFC is a mass flow controller, NDIR is used for monitoring CO₂ and CO.

The furnace component of the phi meter was designed with engineers and constructed by Concept Equipment.

The gas analysis systems for the phi meter were placed in a 30 x 30 x 25 cm box, purchased from Farnell components, for portability. The effluent was drawn from the sampling location through a

stainless steel tube (with a 6 mm internal diameter) and a glass wool filter at 1.5 L min^{-1} by a standard pump. The effluent then passed through a glass splitter. One line went to the exhaust, the other drew $50 \text{ cm}^3 \text{ min}^{-1}$ through the phi meter furnace. The effluent was drawn through the system using a OMEGA mass flow controller connected to a peristaltic pump (Verdeflex peristaltic pump AUR 255 0120 RS1) purchased from RS components.

A simple schematic flow of the phi meter is also shown in *Figure 28*.

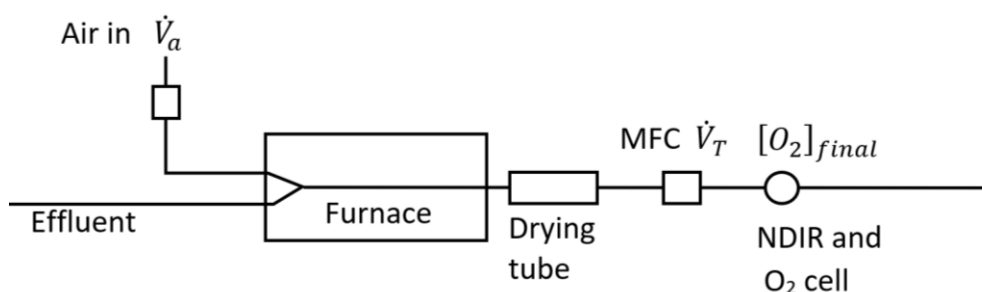


Figure 28: Simple, schematic flow diagram of the simplified phi meter designed for this thesis.

In practice, a ceramic tube was set up with two holes inside, as shown in *Figure 29*. The air inlet was mounted on the effluent exit side of the furnace, and the long ceramic tube with two holes pre-heated the air before mixing with the effluent. The hole was connected directly to the air inlet. Here, a gas line was set up, drawing open air at $50 \text{ cm}^3 \text{ min}^{-1}$ using a peristaltic pump and controlled using a mass flow controller. A photograph of the ceramic tube is shown in *Figure 29*. A labelled photograph of the ceramic tube and air inlets and sample mixture outlets is shown in *Figure 30*.

The fully oxidised gas mixture then leaves the ceramic tube and passes through a glass tube filled with Drierite with glass wool plugs at each end to act as filters. After passing through the mass flow controller and peristaltic pump, the effluent was drawn through an NDIR to monitor CO/CO_2 levels before passing through an electrochemical oxygen cell to the exhaust.



Figure 29: Picture of the ceramic tube used in the phi meter.



Figure 30: Labelled picture of the ceramic tube and air inlets and sample mixture outlets in the phi meter.

2.3.5 Validation of the phi meter

Before validating the phi meter, the system was leak checked, and the analytical components of the system were checked using nitrogen. The sampling line was connected to a Tedlar gas bag containing nitrogen. The mass flow controllers were set to varying gas ratios, and the oxygen was logged to test if the system was working correctly. The mass flow controllers were set to 4 different ratios: 100% air, 75% air with 25% N₂, 50% air with 50% N₂ and 25% air with 75% N₂. The oxygen percentage measured was logged against time. This is shown in Figure 31.

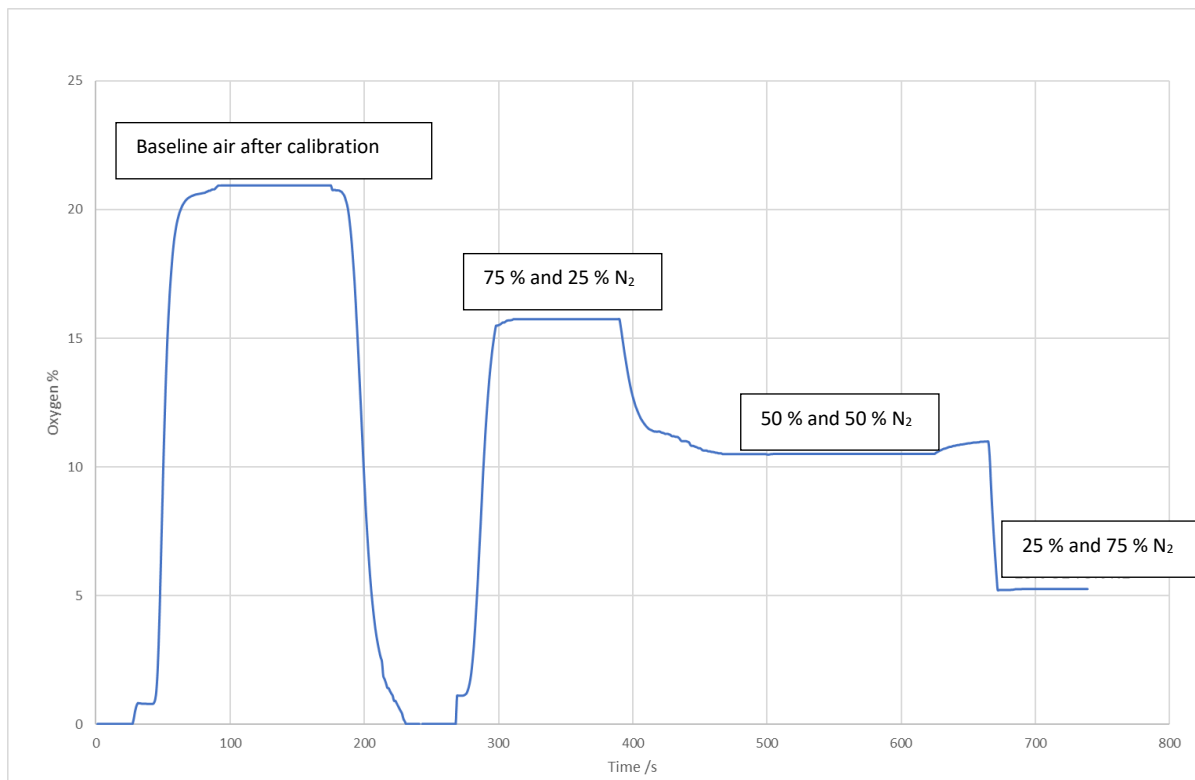


Figure 31: Oxygen percentage measured by the phi meter at varying ratios of oxygen and nitrogen

The phi meter was attached to the mixing chamber of the SSTF. PMMA sheet was cut into strips of 800 mm, weighing approximately 20 g. It was burned at 650 °C in the SSTF. Initially it was set up using a flow ratio of 50 mL min⁻¹ fire effluent with 50 mL min⁻¹ fresh air. Secondary testing was conducted using a flow ratio of 75 mL min⁻¹ effluent with 25 mL min⁻¹ fresh air. The data obtained is shown in *Table 13*. At equivalence ratios of 0.5, a 1:1 ratio of air to effluent produced data most similar to that obtained by the SSTF.

Table 13: A comparison of the data obtained from the SSTF ($\phi_{\text{sec-SSTF}}$) and phi meter ($\phi_{\text{phi-meter}}$) at varying flow ratios and equivalence ratios using PMMA.

		SSTF	Phi meter		
Material	Test number	$\phi_{\text{sec-SSTF}}$	Set flow rate		$\phi_{\text{phi-meter}}$
PMMA			Effluent flow mL min ⁻¹	Fresh air flow mL min ⁻¹	
	1	0.36	0.5	0.5	0.32
	2	0.24	0.5	0.5	0.25
	3	0.45	0.5	0.5	0.43
	4	0.50	0.5	0.5	0.52
	5	0.49	0.5	0.5	0.50
	6	0.35	0.75	0.25	0.20

Initial under-ventilated tests showed that the equivalence was greatly under-estimated when using a flow ratio of 3:1 air to effluent, presumably because there was not enough secondary air for complete oxidation in the furnace.

Tests conducted using a 1:1 ratio showed better agreement. Well-ventilated tests conducted at equivalence ratios below 0.5 showed poorer agreement than the higher equivalence ratios tests, but were still reflective of the data obtained by the SSTF. At equivalence ratios of 0.5, the phi meter showed good agreement, with the data being representative of the values measured using the SSTF.

A second set of experiments were conducted using PMMA, however the air flows used on the SSTF were set to create an equivalence ratio of 0.5 and 1.5 to check the response of the phi meter to under-ventilated flaming. Tests were run at 650 °C for both well-ventilated and under-ventilated flaming and ran in duplicate. The data obtained from the testing is shown in Table 14.

Table 14: Validation of the phi meter using the SSTF at set equivalence ratios set for well-ventilated and under-ventilated flaming at 650 °C and 850 °C using a 1:1 ratio of fire effluent to fresh air in the phi meter.

	Furnace temperature /°C	Equivalence ratio		
		ϕ_{preset}	$\phi_{\text{sec-SSTF}}$	$\phi_{\text{phi-meter}}$
PMMA	650	0.5	0.35	0.4
	650	1.5	1.40	1.45
	850	1.5	1.45	1.47

The phi meter measured equivalence ratios within ± 0.05 . The tests showed the phi meter produced valid data that correlated with the measured equivalence ratio using the SSTF.

An additional comparison used CO₂ yields obtained from the SSTF and the phi meter. The data are shown in *Figure 32*. The CO₂ yields obtained from the phi meter were representative of those measured in the secondary oxidizer, showing a linear relationship. The similarity of the CO₂ yields measured shows that the oxidation occurring in both the SSTF and phi meter was the same. This provided validation of the phi meter's chosen operating conditions.

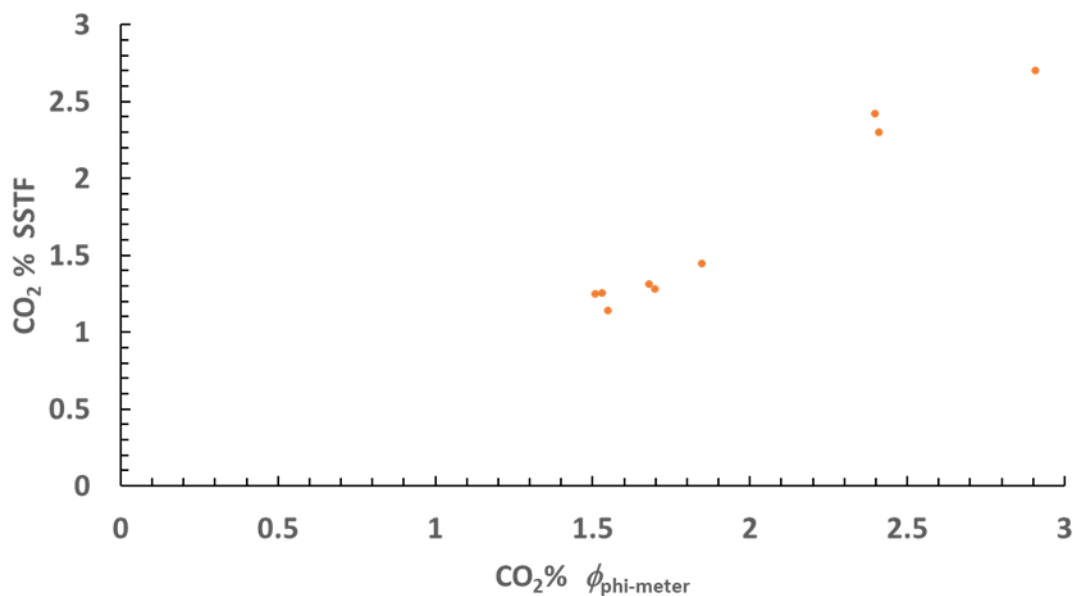


Figure 32: Comparison of the CO₂ yields measured using the phi meter and the SSTF at an equivalence ratio of 0.5 using PMMA.

The final air flows for operating the phi meter were chosen to be 50 mL min⁻¹ fire effluent with 50 mL min⁻¹ fresh air, producing equivalence ratios closest to those obtained in the SSTF. However, more under-ventilated fire effluents could have a greater oxygen requirement, potentially necessitating a 25 mL min⁻¹ effluent flow and a 75 mL min⁻¹ air flow. To validate this assessment, a further series of tests were conducted using PMMA to compare the equivalence ratio measured using the phi meter and the value measured using the SSTF when testing PMMA in the SSTF. This is shown in *Figure 33*. The additional experiments were run in duplicate, and the data shown is an average of the tests conducted.

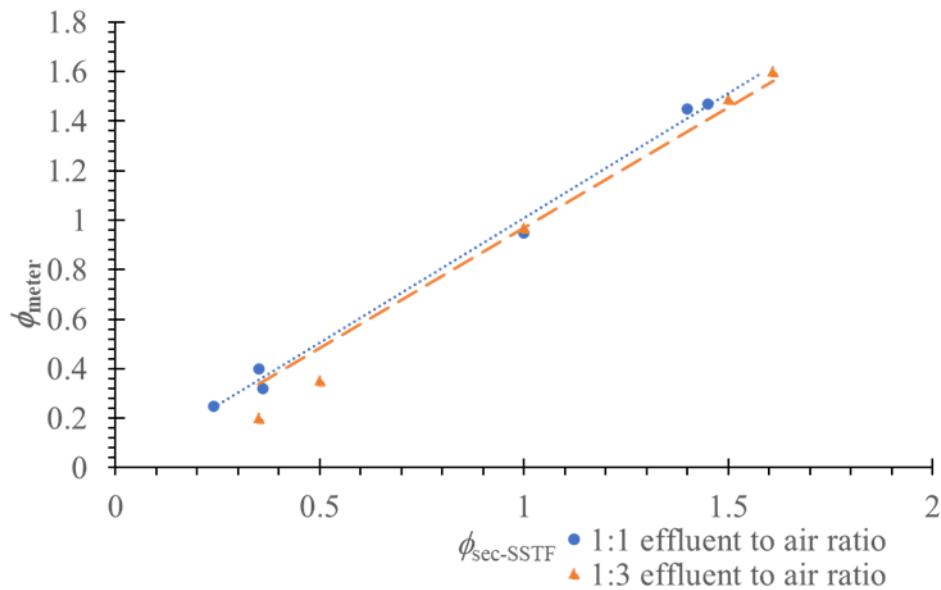


Figure 33: Comparison of the equivalence ratio measured using the phi meter and SSTF when testing PMMA at a range of equivalence ratios in the SSTF using different air to effluent ratios in the phi meter.

During tests conducted at equivalence ratios below 0.5 $\phi_{\text{phi-meter}}$ were more representative of the $\phi_{\text{sec-SSTF}}$ when using a flow ratio of 50 mL min⁻¹ air to 50 mL min⁻¹ effluent. When using the flow ratio of 25 mL min⁻¹ effluent to 75 mL min⁻¹ air mix, the phi meter typically under-predicted the equivalence ratio. This was likely due to the excess air in the system. At an equivalence ratio around 1.5, the 50 mL min⁻¹ air to 50 mL min⁻¹ effluent mix typically under-predicted the equivalence ratio, whereas the of 25 mL min⁻¹ effluent to 75 mL min⁻¹ mix was more representative of SSTF measured values. At equivalence ratios of 1.4 to 1.5, both the flow ratios were able to measure values reflective of those measured in the SSTF. This is probably due to the additional oxygen being almost completely consumed.

At higher equivalence ratios (> 1.5), the 25 mL min⁻¹ effluent to 75 mL min⁻¹ mix produced data that was representative of that measured in the SSTF, suggesting that when testing very under-ventilated fires the 1:3 effluent to air ratio should be used. The data shows that equivalence ratios of around 1.5 and below, both flow rates are suitable for measurement of equivalence ratio.

Typically, the phi meter would be 3 m away from the sampling point, connected using 8 mm stainless steel tube of wall thickness 0.6 mm. This gives a volume of 109 mL. Using the phi meter pump speed of 50 mL min⁻¹ this would give a 2 min delay. Using the 1.5 L min⁻¹ pump with a splitter decreases the delay to 4.5 s.

2.4 EQUIVALENCE RATIO INSIDE THE SSTF COMBUSTION TUBE.

There is some potential variation in the equivalence ratio inside the SSTF combustion tube. To enable sampling within the combustion tube of the SSTF, a Perspex sheet to replace the glass door on the mixing chamber was obtained. A small sampling port was created in the centre of the sheet, in alignment with the centre of the combustion tube. A stainless steel tube was then placed through the gas-tight seal in the Perspex sheet and pushed into the combustion tube at set distances, starting from sampling in the centre of the furnace. Subsequent tests were conducted by moving the sampling tube 20 cm from the centre of the tube. The distance measured was from the centre of the tube to the centre of the sampling port in the centre of the Perspex sheet covering the mixing chamber. The SSTF was operated using the standard methodology, except for the sampling procedure.

800 mm strips of PMMA were prepared for testing in the SSTF. The strips were tested at 650 °C, with the primary air flow set to create an equivalence ratio of 0.5 for well-ventilated and 1.5 for under-ventilated tests. Tests were run in duplicate.

2.4.1 Results and discussion

Figure 34 shows the variation in equivalence ratio throughout the combustion tube in the SSTF. While the variation is minimal, there is a slight downwards trend in the equivalence ratio as the sample line was moved further away from the centre of the furnace. The measured equivalence ratio was 1.4 in the centre of the furnace tube and lowered to 1.2 when sampling from the mixing chamber. Sampling did not take place in the flame zone of the test. This effect was much less prominent in well-ventilated conditions.

The equivalence ratios measured at set distances in the SSTF tube tested in well-ventilated conditions are shown in Figure 35. Unlike in the under-ventilated tests, the equivalence ratio was much more stable across the tube during testing.

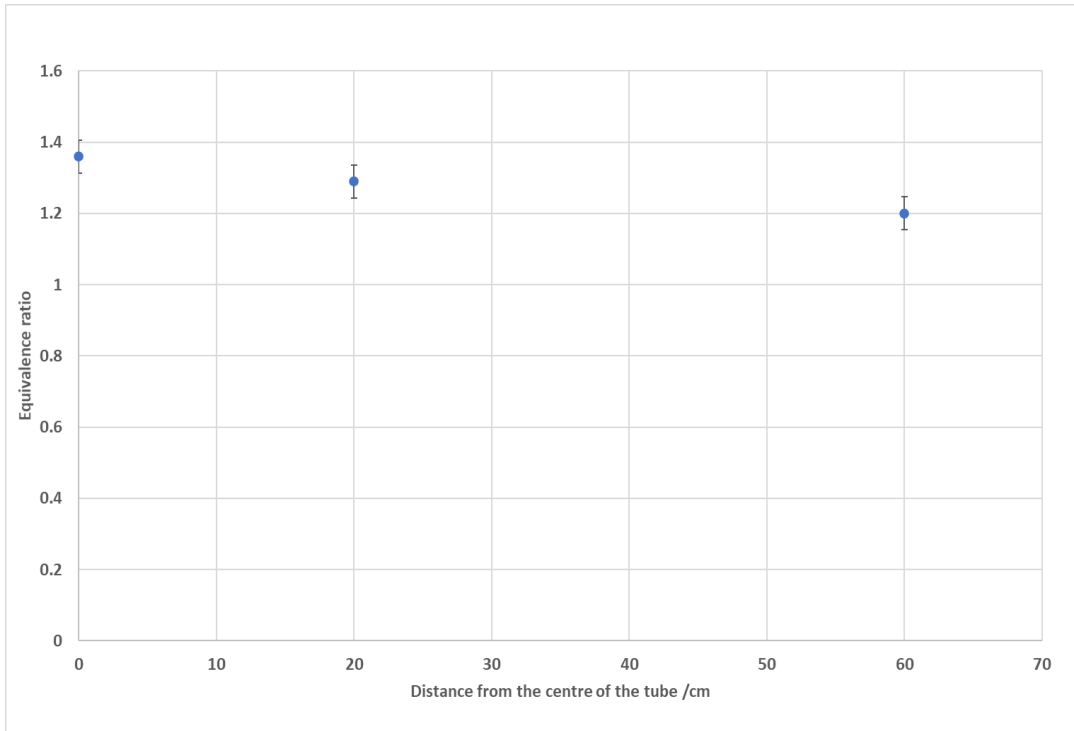


Figure 34: Equivalence ratio at varying distances in the SSTF tested in 650 °C under-ventilated flaming conditions.

In both experiments, the set equivalence ratio differs from the measured ratio. The lack of change in equivalence ratio across the mixing chamber and furnace tube is likely a result of the sampling tube remaining in the hot furnace tube. The heat of the furnace would allow for the effluent to undergo the same reactions as they would in the furnace tube, but within the sampling line. This resulted in no changes being observed in the measurements taken.

A better alternative would be to input sampling points within the quartz tube and sample at direct locations where the sampling tube was not in the hot furnace. As this would have required specialist equipment and major modifications to the quartz tube in the furnace, this additional research was not carried out.

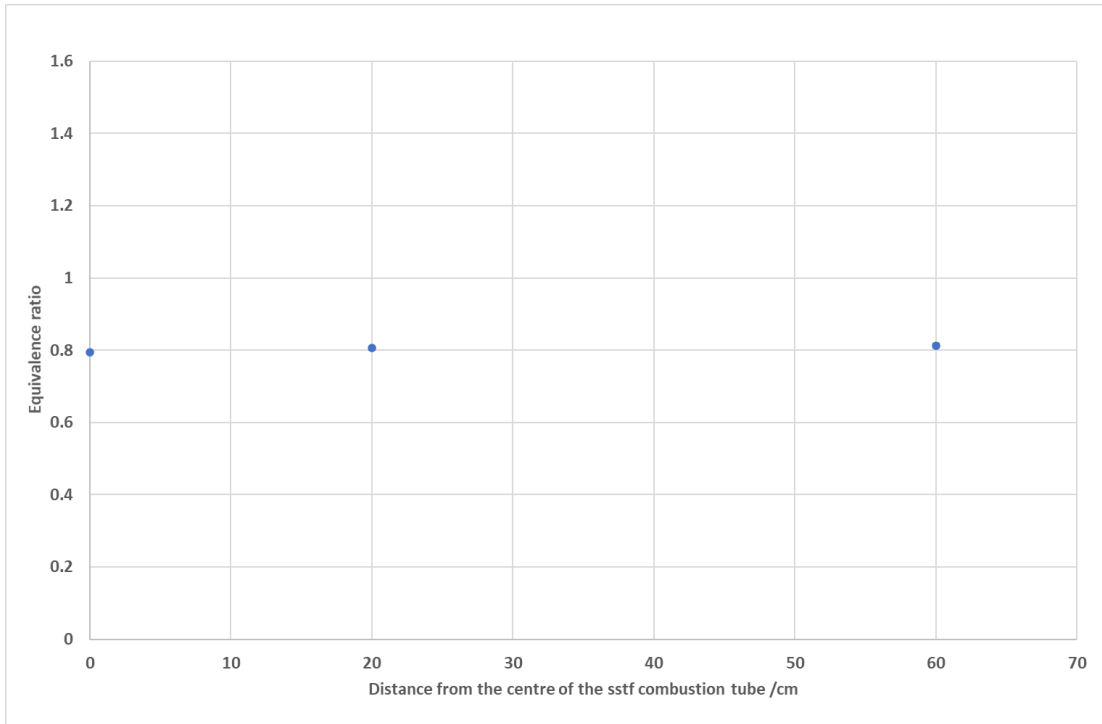


Figure 35: Equivalence ratio at varying distances in the SSTF tested in 650° C well-ventilated flaming conditions.

2.5 PORTABLE GAS ANALYSIS SYSTEM

2.5.1 Description of analysers

Portable analysis systems were designed and constructed for this project for fire effluent sampling for large-scale testing. The analysers were designed to be easy to use, portable and usable remotely to improve operator safety during large-scale fire tests.

The gas analysis system consisted of three specially made box analysers designed to continuously monitor: O₂, CO₂, and CO, and to sample for HCN and acid gases using pre-programmed switches automatically. Only two analysers were used for the large-scale testing.

2.5.2 Design and construction

Each analyser had three gas lines to connect to the sampling location. Two gas lines were connected to a specially designed glass manifold and split the gas into eight parallel gas lines. One gas line was designated for acid gas analysis, the other for HCN analysis. The third line was used to monitor CO, CO₂ and O₂.

The eight gas lines were connected to individual dreschel bottles containing either 0.1 M NaOH for trapping HCN or e-pure water for trapping acid gases. Specific details of the analytical methods used can be found in **Appendix 1** and **Appendix 2**. Each dreschel bottle was connected to an individual Geerte 2W-025-08 12 V normally closed solenoid valve (Tom Parker, UK). The solenoid valves were electronically controlled by a pre-programmed switch controlled by an Arduino Uno (Farnell components). Each gas line was controlled by its own Arduino-controlled switch. The solenoids were programmed to open in series for timed intervals. The program written for these switches can be found in **Appendix 9**.

After the solenoid valves, gas lines were reconnected using the same style glass manifold to reduce the eight individual lines back to one. The line was then connected to an Omega 3100 series 0-5 L min⁻¹ flow meter set to a regulated flow of 1 L min⁻¹, followed by a Charles Austen d5 SE air pump. The pump and MFC were protected by glass tubes filled with glass wool plugs and Drierite to remove moisture from the gas. The two separate gas lines are then connected to an exhaust line exiting the analyser. The third gas line drew effluent directly from the sampling line through two glass tubes, one containing glass wool to filter for soot and the other containing Drierite with glass wool plugs to remove moisture from the gas.

This was then connected to an Omega 3100 series 0-5 L min⁻¹ flow meter set to a regulated flow of 1 L min⁻¹, followed by a Charles Austen d5 SE air pump. This was followed by a 50 µm microporous (Hepavent) filter before connecting to an Andros 6500 NDIR and Lumisence electrochemical O₂ cell connected to a specialist holder to enable simple gas line connections to be made. The gas line was then connected to the analyser exhaust line, where the analysed effluent could leave the analyser.

All components were powered using a standard 12 V power supply (RS Components). The power supply was connected to a terminal block split into eight power lines connected to the individual components of the analyser. 12 V to 5 V step-down regulators were used to reduce the power supply to components requiring a lower voltage.

The NDIR was connected directly to a Raspberry Pi 3B+ (RS Components), which contained specialist software to log the data output of the NDIR. To enable viewing of the NDIR data output in real time, a screen was connected to the Raspberry Pi and placed into a slot cut out of the front face panel of the analyser. A USB hub was also connected to the Raspberry Pi and placed in a slot on the front face

of the analyser to enable easy access to USB ports to access data obtained from the analyser. The internal design of the analyser is shown in Figure 36.

The Raspberry Pi also contained software to remotely control the analyser via laptop or phone from a distance by linking to the IP address of the analyser. This was added to the analyser to improve the safety of operation, meaning the analyser could be operated remotely if required. The analyser could also be run from a laptop by connecting the NDIR to a laptop running the ANDROS 6500 NDIR software.

The components were placed inside a 50 x 50 x 25 cm blue box, constructed using extruded aluminium and blue aluminium composite panels for portability and durability. Internal components were connected using silicone tubing. Photographs of the final analysers made are shown in **Appendix 9**.

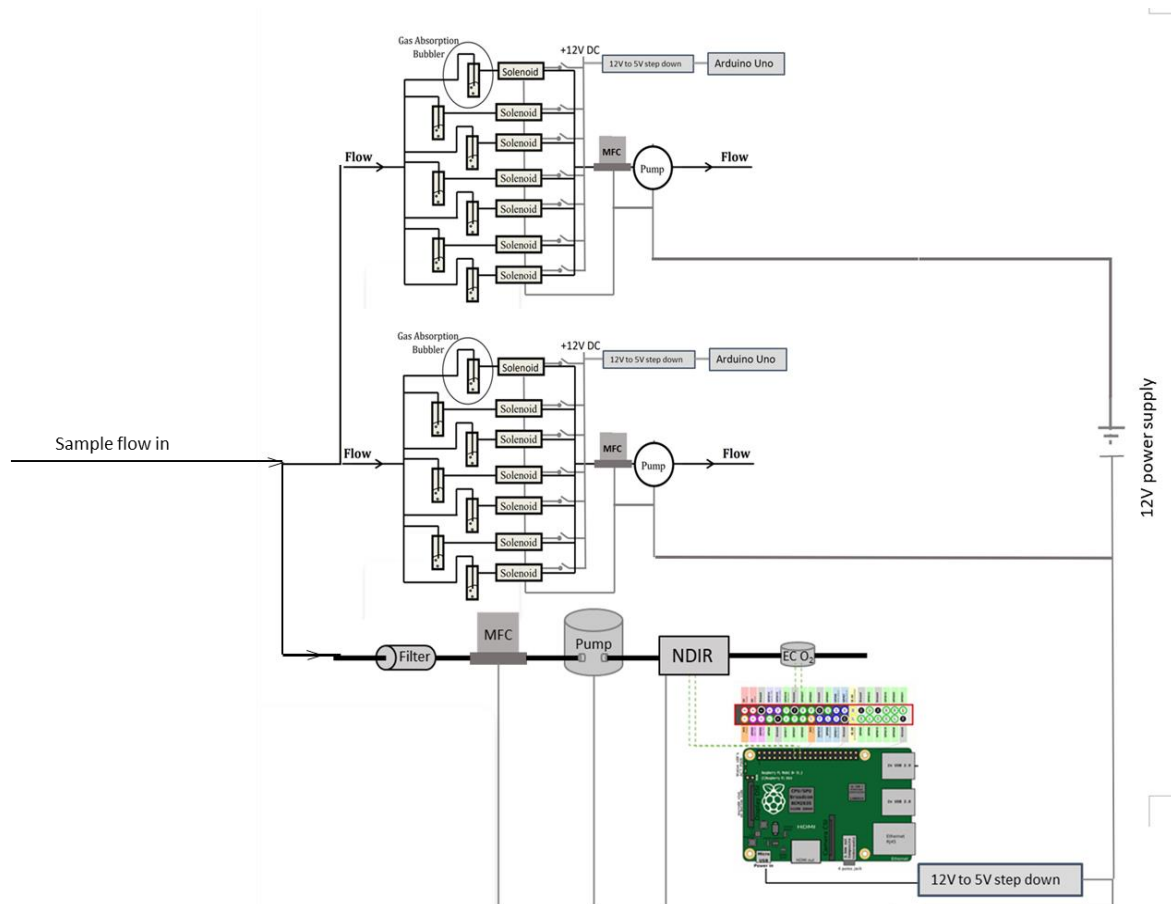


Figure 36: Schematic design of the portable box analysers designed and constructed for this research.

2.6 HCN ANALYSIS USING ION CHROMATOGRAPHY

ISO 19701⁸⁷ describes the methodologies for quantifying acute toxicants in fire effluent. It contains three methods for quantifying HCN: spectrophotometric analysis using chloramine-T/isonicotinic acid, spectrophotometrically using picric acid and ion chromatography.

HPIC is an established method for HCN quantification when studying soil, water and solutions containing low concentrations of HCN¹¹⁶. HPIC columns have been reported to be sensitive to fire effluent. However, they are prone to blockages and can age rapidly if fire effluent is routinely analysed⁸⁷. Samples were filtered to minimise the detrimental effects on the column¹¹⁷. Despite this, HPIC is characterised by its low limits of detection and high precision.

Analysis using spectrophotometry with chloramine-T/isonicotinic acid is the main methodology used throughout this research. Details and descriptions of the methodology can be found in **Appendix 2**. However, wet chemical analysis can be time consuming and has yet to be compared to alternative methods of analysis. For this reason, HCN samples were obtained and analysed using two techniques to provide a comparison.

The picric acid method was not chosen for comparison as it is more dependent on various analytical variables such as temperature and reaction time. This increases the potential for experimental variation¹¹⁸.

2.6.1 Generation of HCN samples

Samples of HCN were obtained from testing PA6 in the SSTF at three fire condition: 650 C well-ventilated representative of early well-ventilated flaming (650 WV), 650 C UV representative of pre-flashover conditions (650 UV) and 825 C under-ventilated representative of post-flashover conditions (825 UV).

The standard SSTF test procedure was followed. However, sampling took place at 5 minute intervals throughout the full duration of the test. The standard test procedure is described in **Appendix 3**.

Samples were taken throughout the test as low concentrations of HCN were expected at the start and expected to increase in concentration over the run linearly. Three fire conditions were chosen to generate samples containing lower levels of HCN to test the lower limits of detection of the methods and generate samples of significantly higher HCN concentration to test the upper limits of the methods. The samples obtained were poured into two separate air-tight containers and stored at room temperature.

2.6.2 Analysis of HCN in solution

The samples were tested using the chloramine-T/isonicotinic acid spectrophotometric method and using HPIC, described in **Appendix 2** to determine if the method of analysis affected the results obtained. All samples were run in duplicate, and an average concentration was used.

A Dionex™ Aquion™ Ion Chromatography (IC) System was used with a specific column for HCN analysis. Details of sample preparation and analytical procedures can be found in **Appendix 2**.

2.6.3 Results and comparison

The results obtained from HPIC and wet chemical analysis were plotted as a bar graph, shown in Figure 37. The data was plotted with 5 % error bars.

At 0 to 5 minutes into the test, very little HCN is produced. This results from ignition not occurring until 3 minutes into the test. The least HCN is produced at 650 °C well-ventilated flaming. This was expected as the fire had plenty of oxygen available, allowing for more complete combustion to occur. For this condition, 0.5 ppm HCN was detected by the spectrophotometric analysis, but HCN remained undetected by the HPIC. This was also the case for HCN samples obtained at 0-5 minutes when testing at 650 °C under-ventilated flaming. This suggests that, despite being characterised for its low limits of detection, the HPIC does not detect very low concentrations of HCN in samples where the spectrophotometric method could.

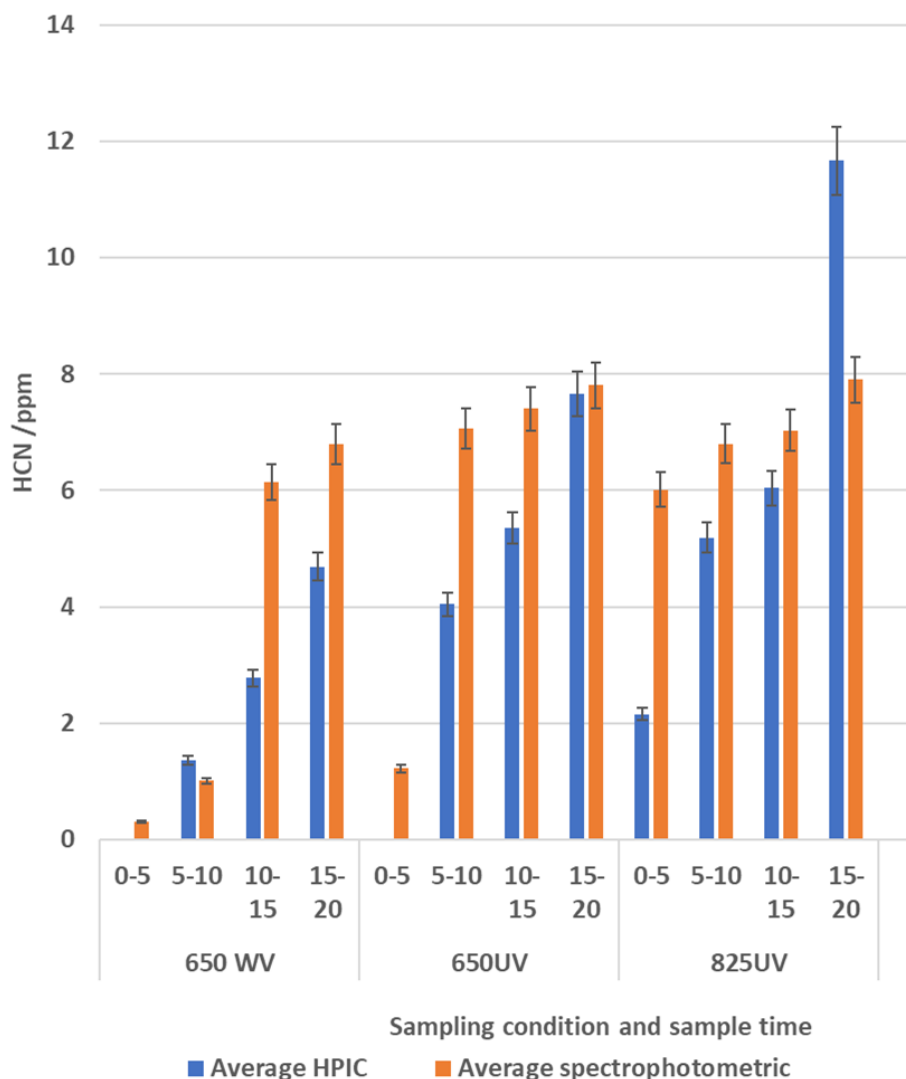


Figure 37: Comparison between HCN concentrations detected by HPIC and spectrophotometric analysis from samples obtained from testing PA6 in the SSTF

As the fire progresses during the tests, more HCN is produced. However, at 650 WV conditions, HCN was consistently under-predicted by the HPIC. This was also the case for samples obtained at 650 °C UV conditions. At 825 °C UV conditions, the most HCN was produced. While the HPIC measured HCN concentrations lower than those measured using spectrophotometry from most samples, it detected

much higher HCN concentrations than the spectrophotometric method when testing the highest concentration sample. A comparison between the duplicate tests and average HCN concentration measured using the HPIC is shown in Figure 38. The data obtained from repeat tests show a high degree of variation, particularly at lower concentrations. This suggests that, despite being a recommended method for HCN quantification, further work on optimising the analysis procedure is required before the HPIC can be regarded as a reliable means of HCN analysis.

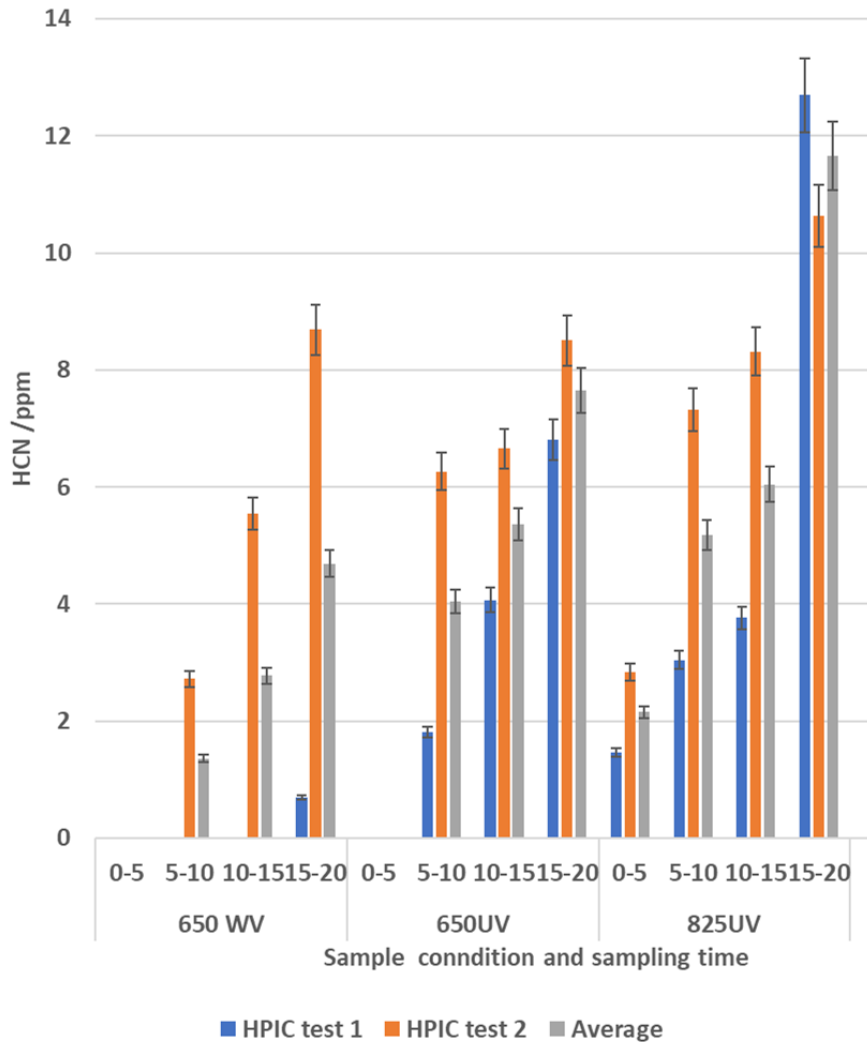


Figure 38: HCN concentrations detected by HPIC from samples obtained from testing PA6 in the SSTF

A comparison between the duplicate tests and average HCN concentration measured using spectrophotometry is shown in Figure 39. While the data shows variation between repeat tests, the variation is significantly less than that observed in the data obtained by using HPIC. The spectrophotometric method shows significantly less variation between tests at lower concentrations than the HPIC, suggesting this method produces much more reliable data. While a degree of variation is observed at higher concentrations, again, the variation is less than that observed in the HPIC data.

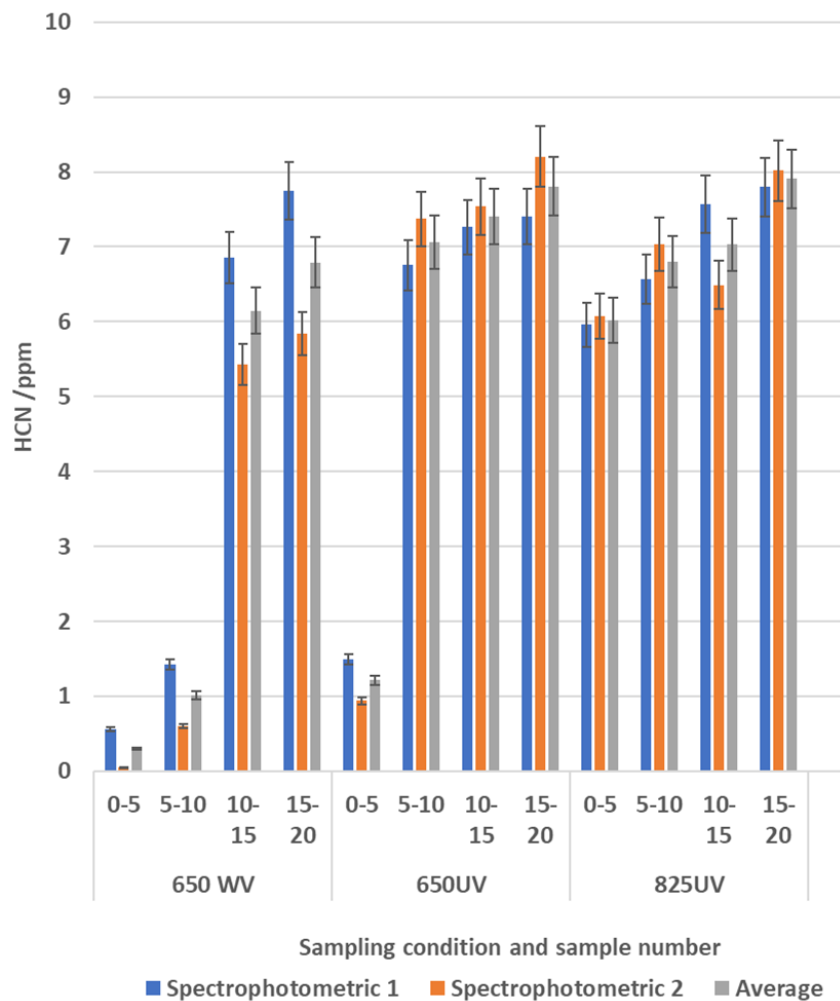


Figure 39: HCN concentrations detected by spectrophotometry from samples obtained from testing PA6 in the SSTF.

2.7 LARGE-SCALE TEST DESIGN

A series of ISO 9705 room corner tests were conducted at EIFC in Denmark. During each large-scale test, the fire conditions and smoke toxicity were monitored throughout from several locations. The equivalence ratio was also monitored throughout each test to determine the fire condition.

2.7.1 Description of the 9705 test.

The ISO 9705 test is a large-scale fire test scenario to replicate the behaviour of a fire, from ignition to flashover in a small, standardised room. It is the reference test scenario in Guidance document G used in the creation of the construction product regulations. The 9705 room is a 2.4 m x 2.4 m x 3.6 m lightweight concrete test room with a centrally located door opening of 2 m x 0.8 m on one of the shorter walls. The room contains a load cell in the centre to enable mass loss measurements to be made if the test design is modified. A diagram of the test is shown in Figure 40.

The ISO 9705 standard only requires gas measurements for O₂, CO₂, and CO to be taken in the exhaust duct to determine the heat release rate (HRR) and optical density of the smoke. A thermocouple tree is also commonly placed in the test room's doorway to help make air flow calculations.

The test method was designed to describe the fire behaviour of products in controlled conditions but is often modified to enable toxicity assessments. The ISO room corner test is typically conducted by lining the walls and ceiling of the test room with the test product and igniting using a standard propane burner in the corner of the room. The propane burner is set to 100 kW for 10 minutes, then 300 kW for 10 minutes (or until the room reaches flashover). The gas sampling system is located within the exhaust duct connected to the collection hood.

The 9705 room test has previously been modified to monitor the fire effluent toxicity during the test¹⁰⁸. This was used to design the experimental procedure for the large-scale test experiments for this work.

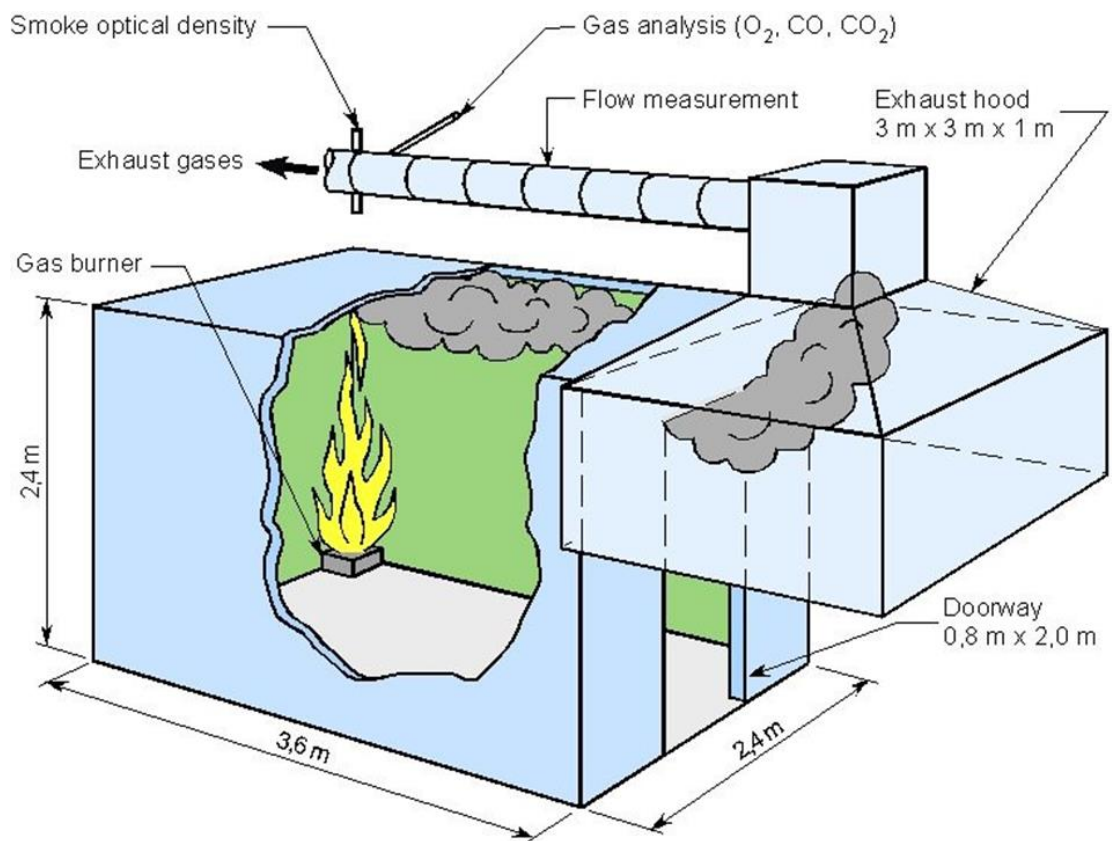


Figure 40: Diagram of the ISO 9705 room corner test⁹⁹.

2.7.2 Aims and objectives of the large-scale testing

The tests aimed to generate meaningful smoke toxicity data for well-ventilated and under-ventilated flaming of complex products that could then be compared to bench-scale test data. Standard test methods were used to make communication easier and the methodology more difficult to question.

Objectives:

1. To demonstrate the validity of bench-scale data by comparison with large-scale fires.
2. To determine the large-scale smoke toxicity of samples to be used for round robin tests
3. To measure during the tests:
 - a. Equivalence ratio (in doorway)
 - b. Mass loss
 - c. CO₂, O₂ (in doorway and inside the exhaust)
 - d. CO, HCN, acid gases (in doorway and inside the exhaust duct)
 - e. Smoke opacity (in the exhaust duct)
 - f. Thermocouples (in doorway).

3a, c and d were measured to enable characterisation the fire condition. 3b, e and f were measured to enable future quantification of the toxic product yields. 3g provided additional information on the air flow to the fire (height of neutral plane etc.).

2.7.3 Materials and testing

Table 15 shows a list of the materials and the aimed test condition that were conducted in the ISO room, with a planned nine tests in total. Unfortunately, due to supplier issues, high-pressure laminate could not be obtained. It was therefore excluded from the large-scale testing.

Extra material for each test was purchased to be later tested under the same fire condition in the steady state tube furnace and to run interlaboratory reproducibility assessments on the same material. Due to the time needed to organise and conduct these assessments, the interlaboratory reproducibility assessments were not conducted during this project.

Table 15: Summary of tests to conduct in the ISO 9705 room

Material	Large-scale test condition
Plasterboard	Well-ventilated
Flexible polyurethane foam	Well-ventilated Under-ventilated
Plywood	Well-ventilated Under-ventilated
Cables	Well-ventilated Under-ventilated

The preliminary order of the tests was as followed:

1. Plasterboard W-V
2. Plywood W-V
3. Plywood U-V
4. Cables W-V
5. Flexible PU W-V
6. Cables U-V
7. Flexible PU U-V

Materials were stored in a conditioning room at the EIFC prior to use.

2.7.4 Test layout and fuel load

Successful large-scale tests reported in the literature aimed to have an average heat release of 1000 kW during steady burning. Cone calorimetry tests have been conducted on the suggested test materials to provide guidance on the required fuel load of each material. These calculations were made based on the suggested test layout, as shown below.

During a typical 9705 room corner test, the material is mounted to the room's walls and ceiling, meaning mass loss measurements throughout the test are impossible as the material is not placed directly on the load cell. However, mass loss measurements were required for these experiments to allow for future calculation of toxic gas yields. For this reason, the test design was modified.

The Single Burning Item test (SBI) is a recognised intermediate scale test. This test would be easy to describe and reproduce. However, the fuel load may be too small. Therefore, it was decided that two SBI-style rigs were to be used (placed opposite one another, as shown in Figure 41). In addition, the SBI test propane burners could not be safely used in the ISO room.

Using two SBI tests facing each other inside the ISO room with a liquid fuel ignition source allowed the load cell in the ISO room to be used, have a well-known, standard geometry, and create high enough rates of burning to force under-ventilated flaming.

The two SBI rigs were set up in a rectangular configuration, with the wings being approximately 1m apart. The rigs were standard SBI rigs with a total exposed surface area of 1.5 m x 1.5 m per test rig. The individual rigs consisted of two parts: a surface of 1.5 x 1 m and a smaller wing of 1.5 m x 0.5 m put together to form a right-angle corner. The rigs were constructed of stainless steel at EIFC.

The final rig design is shown in Figure 41. A photograph of the final set up of the test rigs inside the room is shown in Figure 42. Two sets of test rigs were constructed to allow for a faster turnover time for testing.

The load cell in the room had a maximum capacity of 165 kg, including the mass of the rod and weighing pan and rig. For this reason, the rig and materials needed to be constructed to be as light as possible. The fuel loading was based on a combination of the available mass (total capacity- rig mass – rod and weighing pan) and an average heat release of 1000 kW. The details of the masses of each material used are summarised and sectioned with the results from each test and any modifications made during each test.

The rig sat on the load cell inside the room. The materials were slightly raised as in the SBI test to allow a gap between the materials and the burner. The materials could be glued directly to the calcium silicate boards of the SBI test rig or could have a 40 mm air gap between the material and the board. Plasterboard and plywood were mounted with a 40 mm air gap between the board and the material. As the PU foam was porous and expected to melt, the material was glued directly to the calcium silicate board and placed in a stainless steel tray to allow the material to burn as a pool fire once melted and reduce any damage to the test room.

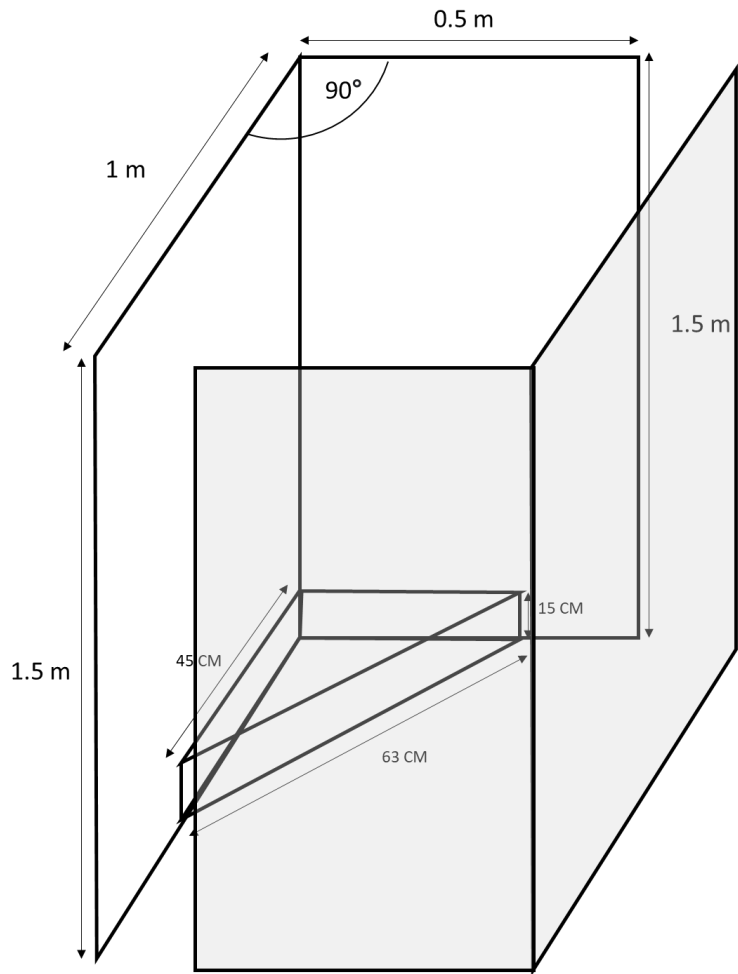


Figure 41: SBI rig design with triangular burner that was used in the large-scale testing.

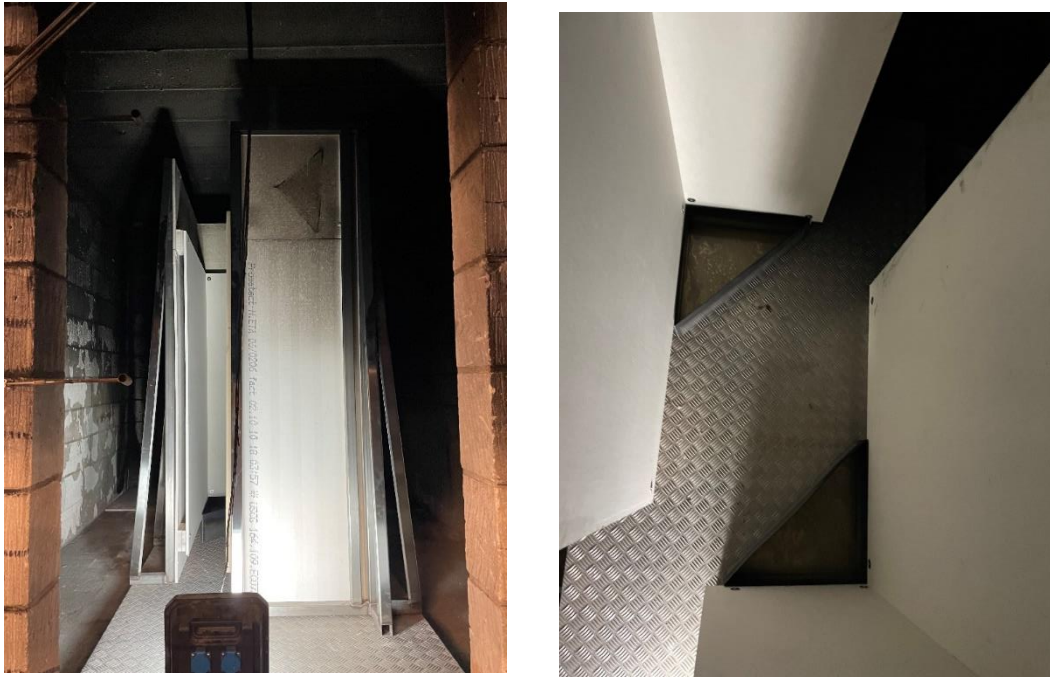


Figure 42: Picture of the final SBI rig set up inside the ISO 9705 test room

2.7.5 Cable test layout

Large-scale cable tests are often conducted to assess their fire resistance or reaction to fire. Like with other materials, their smoke toxicity is not assessed as construction products. External expertise was sought to determine the best method of testing cables in the ISO room. It was decided that the best method was to use cable baskets (baskets were chosen due to the weight limitations on the load cell). They are commonly used and readily available. The 4 m long baskets were placed diagonally in the room. Having them placed diagonally allowed the use of standard size cable ladders (as used in the cable reference scenario) on top of the load cell to allow for mass loss measurements. The choice of cable was RZ1-K (AS) (0.6/1 kV) cables. The cables were tied to the baskets using copper ties and were mounted to the specially designed holder. Details of the height and layout of the ladders is shown in Figure 43. Photographs of the final layout of the cable test layout is shown in Figure 44.

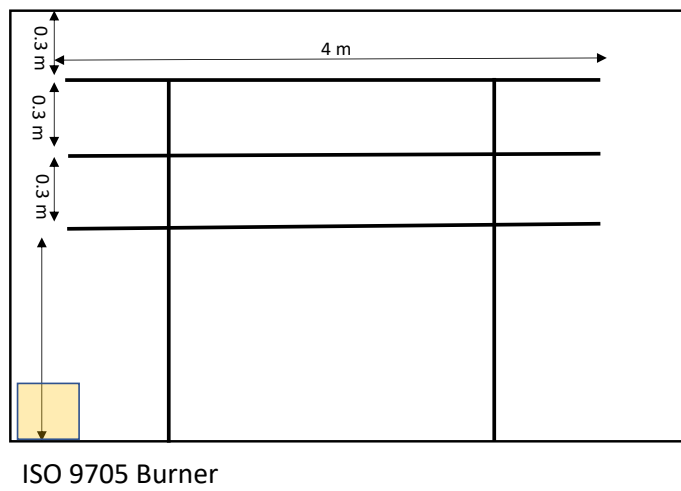
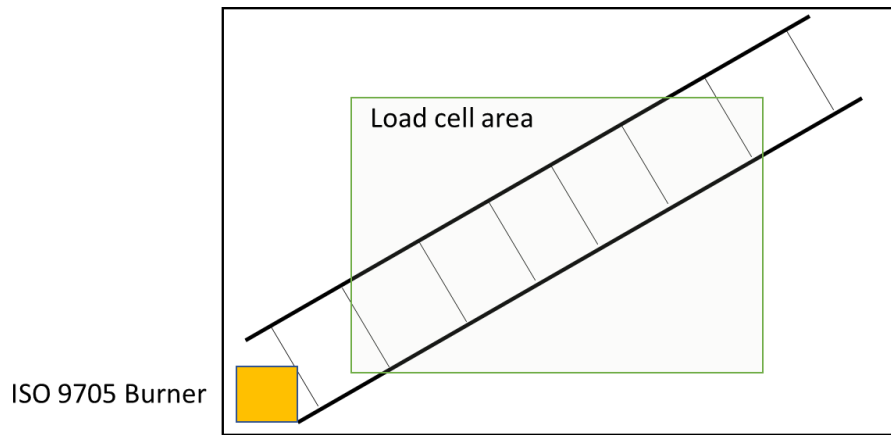


Figure 43: Frame position in room for the cable tests in the ISO 9705 room (Plan view – from above and side view).



Figure 44: Picture of the final cable test set up in the ISO 9705 room.

2.7.6 Controlling the ventilation of the test

A door of 1.3 m was fixed to the bottom of the doorway of the test room in an attempt to control the ventilation condition. The suggested door heights for specific equivalence ratios used in the TOXFire project are shown in Table 16. The door was used to block the bottom of the opening (as in the TOXFire project¹⁰⁸). This was also agreed to be more realistic than blocking the top of the doorway (simulating a window) in a room fire.

Table 17 shows the equivalence ratios obtained during the tests reported from the TOXFire project¹⁰⁸. Based on this information, the door was chosen to be 1.3 m (leaving an opening height of 0.7 m) to aim for an equivalence ratio between 1 and 1.5. As only two ventilation conditions were required (well-ventilated and under-ventilated), well-ventilated tests were conducted without a door, and under-ventilated tests were conducted using a door of 1.3 m. A diagram and photograph of the door set up are shown in Figure 45.

Table 16: Estimated height of opening for specific equivalence ratio ¹⁰⁸.

Expected equivalence ratio	Height of opening /m
0.5	1.41
1	0.89
1.5	0.68
2	0.56

Table 17: TOXFire project data: Actual equivalence ratios obtained from the door heights used¹⁰⁸.

Height of opening /m	Average equivalence ratio obtained during testing.
0.89	0.99
0.68	1.09
0.45	1.02

The door height used in this work was calculated based on the equation 30 as well as additional fuel loading measurements.

$$m_{in} \approx 0.5 \times A \times \sqrt{h} \quad \text{Equation 30}$$

Where m_{in} is the air inflow rate (in kg s^{-1}), A is the area of the opening (in m^2) and h is height of the opening (in m). This formula is used alongside an estimated 1000 kW HRR. Using the air inflow rate from preliminary tests in the room corner, just using the propane burner. The equation can be used to determine an estimated door height to be used in these tests.

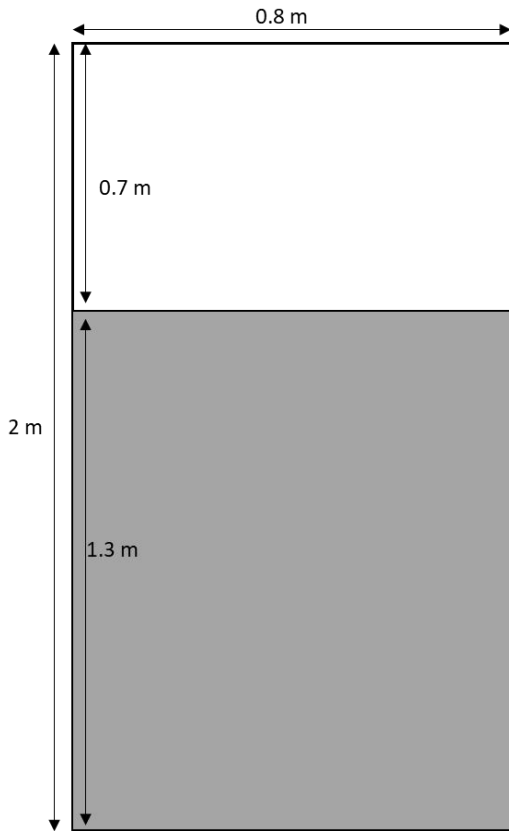


Figure 45: Diagram and picture of the door used to control the ventilation during under-ventilated tests.

2.7.7 Ignition source

Unlike the SBI test, which is used to discriminate between materials based on the degree of flame spread, products were aimed to be burnt completely. Therefore, the ignition source needed a greater heat release than the 30 kW of the SBI burner. Gas burners could not be used in this work for safety reasons, with the exception of the cable tests. In addition, they would be difficult to mount within the load cell or outside it. The SBI test uses a circular heptane burner for calibration with comparable HRR to the propane burner at 100 kW. To mimic the SBI test, two triangular burners were made with height and area equal to the SBI circular burners.

Heptane was chosen as the ignition source. Two triangular fuel pans of 58.5 cm x 35 cm x 25 cm were made to hold the heptane for ignition. A diagram of the burner is shown in Figure 46. The burner was placed in the corner of each SBI test rig and ignited at the start of the test.

As the cable tests used a different layout than the other tests, the 9705 propane burner was used as an ignition source. The propane burner was set to 100 kW for 10 minutes, then increased to 300 kW for 10 mins.

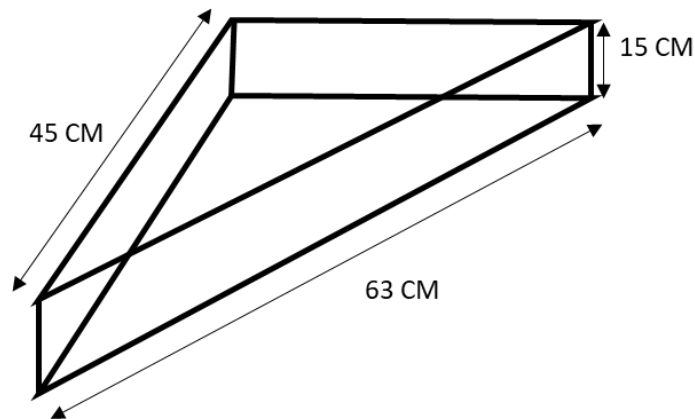


Figure 46: Diagram of the triangular fuel pan used to hold the ignition source during the ISO 9705 tests.

2.7.8 Predicted parameters

Due to the novel design of the experiment, two predictive models were made to obtain information about the potential burning behaviour of the materials during the large-scale tests. The predictive models have been separated as follows:

- Heat release predictions using cone calorimetry with cone tools
- Testing the layout of the tests in a miniature 9705 test room.

2.7.8.1 Prediction of large-scale test data using small-scale flashover box test

Flashover boxes used to re-create flashover in small-scale fire tests were used to provide models of the large-scale experimental set ups. The box dimensions are shown in Figure 47 and Figure 48 and are made from calcium silicate boards. The measurements were approximately 5x smaller than the large-scale 9705 room test, so the fuel loading and mass of the ignition source were scaled down accordingly. Due to the novelty of the large-scale test designs, the experiments were used to assess the overall layout of the test and to test if ignition is possible using the calculated ignition source.

Sheets of materials around $1/6^{\text{th}}$ of the thickness to be used in the large-scale tests were purchased from local building suppliers and cut into two segments of 100 x 200 mm and 300 x 200 mm. These dimensions were chosen to be representative of a reduced-scale SBI test. They were then tied to a steel basket and held with copper ties. On the opposite side of the basket, an identical set of materials were connected in the same way and placed inside the flashover box as shown in Figure 49.

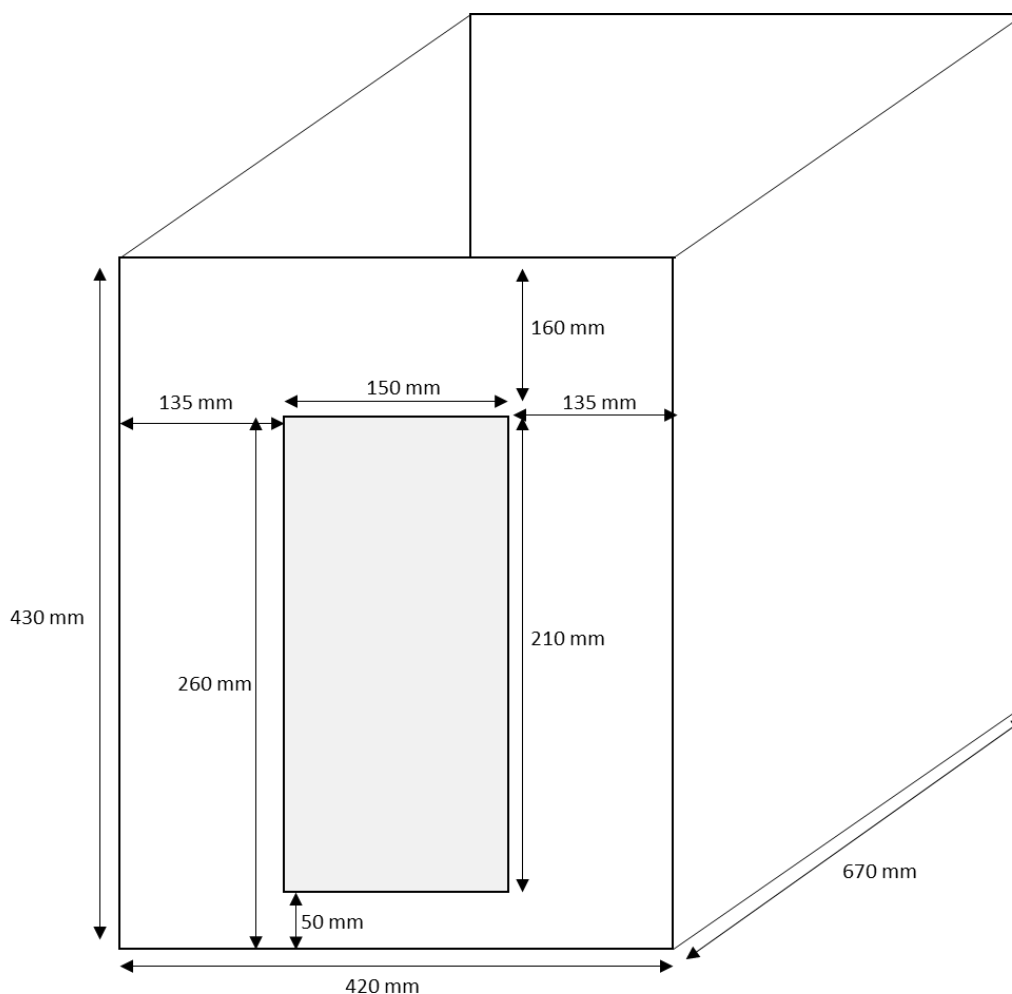


Figure 47: Dimensions of small-scale flashover box test

The fuel used was scaled down by a factor of 6^3 for volumetric proportionality so that the fuel loading was proportional to the size of the room and burner. For the cable tests, a series of small-scale cable ladders were constructed using wire mesh and data cables. The ladders were then placed at set distances on a vertical mesh sheet. The first cable tray was 50 mm from the ceiling, the second 100 mm below the ceiling and the third 150 mm from the ceiling. This was $1/6^{\text{th}}$ the measurements

used in the large-scale tests. A photograph of the final miniature cable test layout is shown in Figure 50.

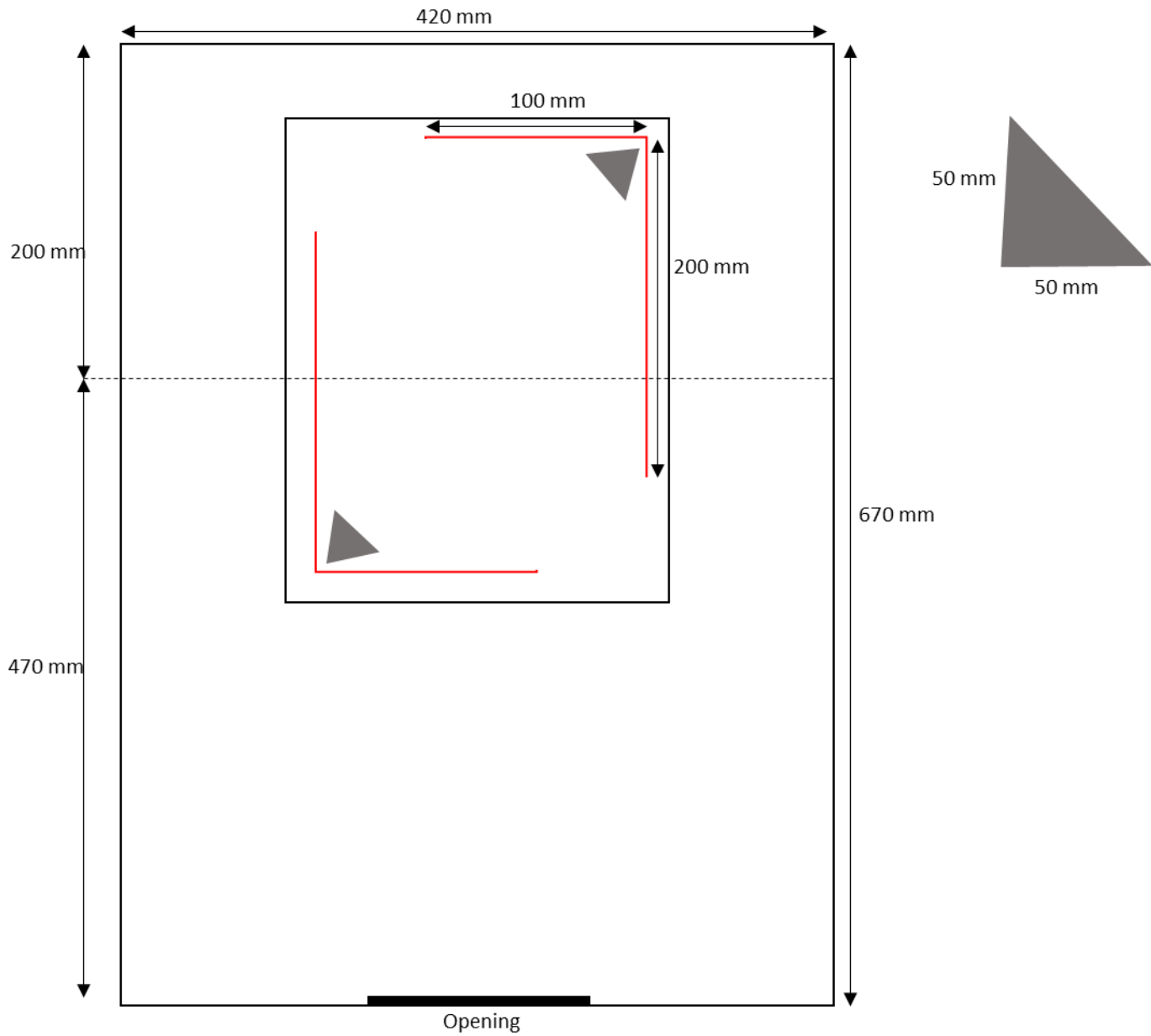


Figure 48: Dimensions of the internal layout of small-scale flashover box test



Figure 49: Picture of the reduced scale SBI rig set up in the flashover box.



Figure 50: Picture of the reduced scale cable set up used in the flashover box

2.7.8.1.1 Ignition source:

As in the large-scale tests, the ignition source used in the small-scale testing was a liquid fuel inside a small steel container. The large-scale tests use a heptane burner. For the small-scale tests, methanol was used as an ignition source. The volume of methanol was calculated prior to testing. The volume of fuel used was based on the fact that the heat of combustion of the burner fuel should be in the same ratio as the heat of combustion of the test sample, as it is for the large-scale tests. An example of the calculation for the fuel mass for ignition is as follows:

The SBI burner is 30 kW and runs for 20 mins. Plywood, as an example, has a heat of combustion of approximately 25 kJ g^{-1} , with a density of 0.6 g cm^3 . For 2.25 m^2 of plywood that is 12 mm thick:

$$22500 \times 1.2 \text{ cm}^3 = 27000 \text{ cm}^3.$$

The mass of plywood planned to be used for one test rig is 16.2 kg. Assuming all plywood burnt at a steady rate in 20 mins, the total heat release would equate to 405 MJ over 1200 seconds. The power output is, therefore:

$$405 \times 10^6 \text{ J} / (20 \times 60) = 337 \text{ kW}.$$

The burner is, therefore, $1/10^{\text{th}}$ the power output of the panels. For the small-scale tests, plywood of 2mm thickness is being used. For a single SBI rig:

$$30 \times 30 \times 0.2 \text{ cm}^3 = 180 \text{ cm}^3$$

The heat release is, therefore:

$$180 \times 0.6 \times 25 = 2700 \text{ kJ}.$$

If the burn time is 10 mins, the power output would be:

$$2700000 / (10 \times 60) = 4.5 \text{ kW}.$$

So the target for the heat release from each burner is approximately 0.5 kW.

The heat of combustion of methanol is 22.65 kJ g^{-1} . For a burn time of 10 mins, the power output would be:

$$(22.65 \times \text{mass of fuel}) / 600.$$

Therefore, 15 g of methanol would produce a power output of 566 W (20g = 750W).

For the ignition source to be proportional to the fuel loading of the test, 15g of methanol was required.

The fuel was put into a container and placed in the corner of the wire baskets at both corners of the rig.

2.7.8.1.2 Results of the reduced scale testing.

Unfortunately, gas measurements were extremely diluted as the fire box leaked significantly. The volume of smoke leaking from the walls and roof joints was excessive, so the measurements did not provide insight into the data obtained on a large scale. The tests provided insight and initial validation of the burning behaviour of the 2 L-shaped rig design.

Two sets of experiments were conducted, with each test being conducted in duplicate. A summary of the information collected on each test is shown in Table 18.

Table 18: Summary of the results obtained from the reduced scale ISO 9705 room tests.

Material	Heat release from ignition source/ kW	T _{ign} /s	Time period of sustained ignition? /s	Experimental notes
Plasterboard	0.5	9	45	Paper cover burnt.
Plywood	0.5	18	148	Successful ignition and burning
	1	15	160	Successful ignition and burning
Polyurethane	0.5	8	30	Sheet of PU was too thick and had a very small air gap. Flaming not visible, but excessive smoke.
	0.5	11	135	Higher density foam used to create bigger air gap.
Cables	0.5	-	-	Flame did not reach the bottom cable tray.
	1.0	-	-	Flame did not reach the bottom of cable tray.
	1.5	45	85	Flame reached all 3 trays.

The plasterboard and plywood tests were successful. The heat output from the fuel source was enough to ignite the paper surface of the material on all of the exposed surfaces on the SBI rig. The plywood burnt well, and flames spread across the SBI rig.

As the polyurethane used in these experiments was low density ($> 22 \text{ kg m}^{-3}$), a larger volume of foam was required to achieve a correctly scaled-down mass. This led to a very small air gap, and so ignition was not sustained. A more dense foam was selected, providing a bigger air gap. The foam burnt completely. A low-density foam was therefore selected for use in the large-scale testing.

As the cable tray was raised 180 mm from the base, the fuel was insufficient to produce a high flame to ignite the cables. This also occurred when doubling the initial heat release output from the ignition source. Using 3x the initial heat release output of fuel led to the ignition of all three cable trays. This suggested that a larger heat output may be needed to cause ignition when conducting large-scale testing. The comparison is difficult because the methanol/ethanol burning as a pool fire can not be compared to a propane burner.

2.8 LARGE-SCALE TEST MEASUREMENTS

Due to the scale of the tests conducted, details of the measurements taken have been sectioned by their location. The locations where measurements took place are as follows:

- **Measurements in the doorway**

This has been sectioned into gas analysis, monitoring the equivalence ratio and air flow and video recordings outside.

- **Measurements in the duct**

This has been sectioned into gas analysis and standard ISO room measurements.

- **Measurements in the room**

This has been sectioned into mass measurements, video recording and temperature monitoring within the room.

- **Overall measurement procedure**

This provides a brief description of the procedure used prior to starting the experiments.

2.8.1 Measurements at the doorway

2.8.1.1 Gas analysis and equivalence ratio

Three stainless steel tubes with an internal diameter of 6 mm were secured near the top of the doorway and used as a sampling line for the phi meter, and two sampling lines for the box analyser (containing the NDIR, O₂ electrochemical cells and gas bubblers). A diagram alongside a photograph of the sampling position is shown in Figure 51. The three tubes were placed approximately 0.1 m from the ceiling pointing upwards and were approximately 0.3 m across the doorway.

Silicone tubing was connected to the stainless steel tubing at the bottom. The stainless steel tubes were approximately 1 m in length. This allowed the effluent to cool slightly before using silicone tubing connections to the analysers and prevented the tubing from melting during testing. The silicone tubing was connected to a glass tube filled with glass wool to filter the soot from the sample gas to prevent blockages inside the analysers.

The analyser sampled O₂, CO and CO₂ continuously at a flow rate of 1 L min⁻¹. In addition, the analyser had a second gas line connected to another stainless steel tube using silicone tubing to sample for HCN and acid gases at pre-set 5 minute intervals. HCN was trapped in dreschel bottles containing 150 ml of 0.1 M NaOH, and acid gases were trapped in dreschel bottles containing 150 ml of e-pure water. The sample line was split between the two sets of dreschel bottles. The method and analysis of monitoring HCN and acid gasses are explained in more detail in **Appendix 1 and 2**.

The phi meter sampling line was connected to the third stainless steel tube in the doorway. Silicone tubing was attached to the stainless steel tube. A glass tube filled with glass wool to act as a filter was attached to the silicone tubing. The filter was attached to an Omega 3100 series 0-5 L min⁻¹ flow meter set to a regulated flow of 1.5 L min⁻¹, followed by a Charles Austen d5 SE air pump. The gas was then split into two lines using a glass T-piece. One line was connected directly to an exhaust, the other was connected to the sample inlet of the phi meter. This minimised sampling time delays due to the very low flow rates used in the phi meter for analysis.

Sampling for the phi meter and O₂, CO and CO₂ measurements were made continuously throughout the tests.

As silicone tubing was used, there is potential for losses to occur during sampling. Use of a heated line would have eliminated any potential losses, however heated lines were unavailable for this work. The main losses would be observed in acid gas sampling as the most significant losses would be seen in HCl sampling. As no material used for the testing was expected to have Cl present, the losses were not deemed a major issue in this work.

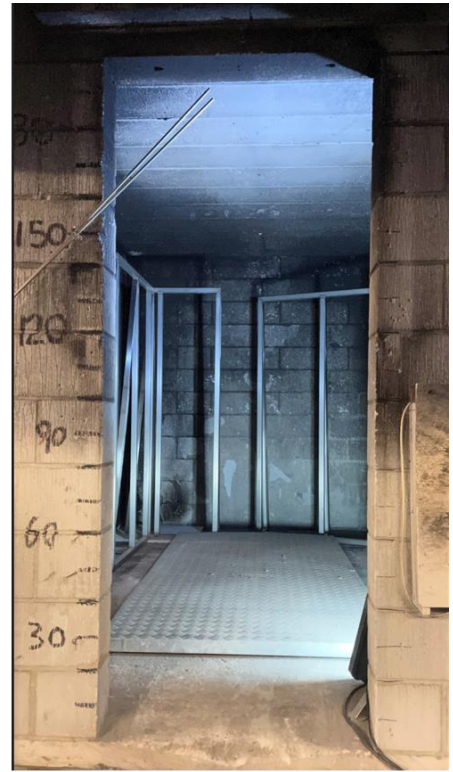
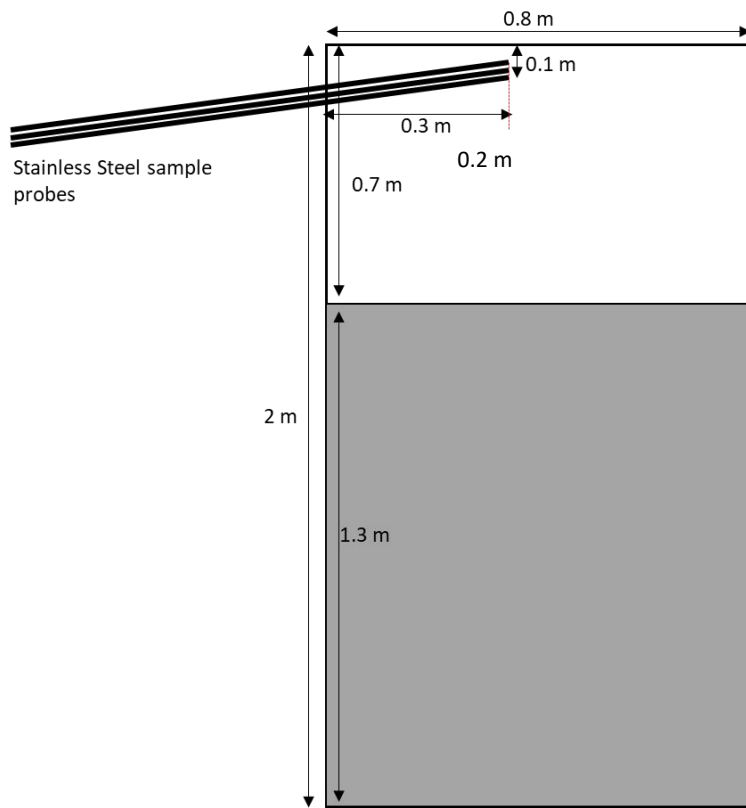


Figure 51: Layout of sampling set up for monitoring the equivalence ratio and gasses in the door during testing

2.8.1.2 Monitoring air flow and temperature

The airflow in the doorway was monitored to enable future calculation of the gas yields of reaction products produced during the test. Air velocity in and out of the door was monitored using bi-directional McCaffrey probes (McC)¹¹⁹ with a differential pressure transducer at the end. The pressure transducers were obtained from Farnell components. A Sensirion CMOSens SPD1000-LO25 pressure transducer was attached to the end of silicone tubing attached to the McCaffrey probe. This pressure transducer was used due to its low sensitivity (-5 to 125 Pa). The pressure transducer was connected to a 5 V power supply, and the signal wires were connected to a data logger to log the voltage output of the pressure transducer. The probes were placed in the doorway at set heights. The heights have been summarised in Table 19. The probes were placed approximately 0.2 m into the doorway for each test.

The gas velocity profile in the test doorway can be calculated by using the measurements obtained by the probes alongside the temperature profile data obtained from the thermocouple tree located in the centre of the doorway.

Table 19: Summary of the heights where the McCaffrey probes were placed during testing. The distance was measured from the ceiling.

Test condition	McCaffrey probe height from the ceiling /m		
	1	2	3
Well-ventilated	1.5	1	0.5
Under-ventilated	0.5	0.3	0.1

The McCaffrey probes were used alongside a thermocouple tree placed in the centre of the doorway. A diagram of the sampling set up, alongside a photo of the test set up, is shown in Figure 52. While the combined use of temperature and air velocity measurements is well documented for monitoring air flow during steady fires^{120,121}, there is little evidence to show the technique can produce meaningful data when the fire is transient¹²². When making air velocity measurements, three key factors are thought to be important¹⁰⁸:

1. The flow out of the door has a velocity component in both directions.
2. The velocity distribution is not uniform across the opening. Studies have shown that the velocity of the air will differ near the edges of the opening. In some cases, stagnant regions can occur in the centre of the doorway, with higher velocities being observed away from the central point¹²².
3. As a result of the low pressure difference when monitoring air flow using bi-directional probes, the data is often very noisy.

Taking these points into consideration, the probes were set up with the top two probes closest to the ceiling monitoring the flow out of the doorway. The bottom probe was turned in the other direction to monitor the flow going into the room. It was thought that the top probes would align with the hot smoke layer build-up and align with the point where the effluent would leave the doorway. The bottom probe was thought to be placed far away enough from the top of the door (during both under-ventilated and well-ventilated tests) to monitor the flow of air into the room.

The McCaffrey probes were placed approximately 0.2 m into the doorway to the left to avoid any stagnant zone measurements, should they occur. The pressure transducer chosen for monitoring the probes was selected for its ability to detect very low pressure changes to minimise any noise in the data.

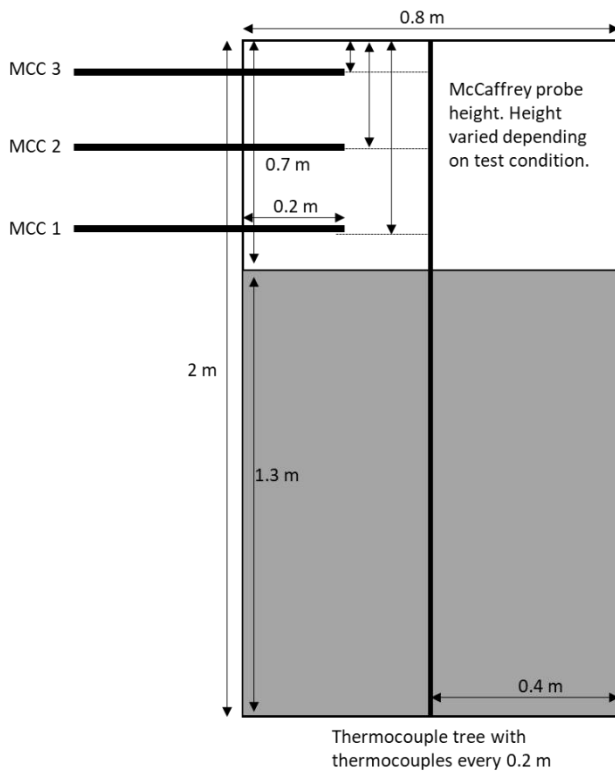


Figure 52: Diagram and picture of the placement of McCaffrey probes and thermocouple tree for air velocity and temperature measurements

2.8.2 Measurements in the duct

Two sets of measurements took place in the duct: standard ISO room measurements and additional gas analysis. The set up of the sampling taking place in the exhaust duct is shown in Figure 53.

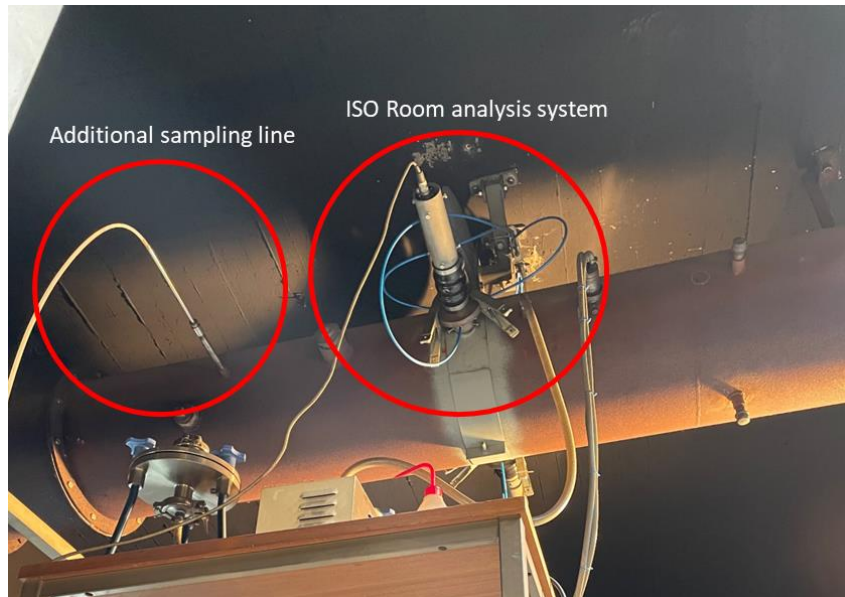


Figure 53: Picture of the sampling system and additional gas line set up to the ISO room corner exhaust duct.

2.8.2.1 Standard measurements

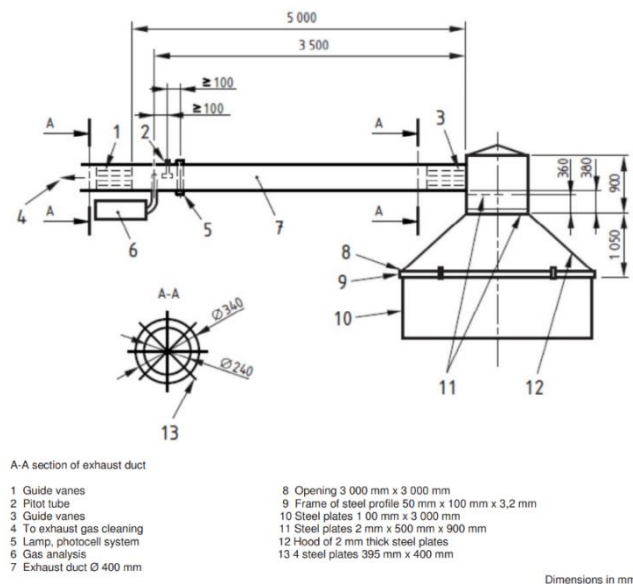


Figure 54: Standard gas analysis set up inside the ISO 9705 room corner exhaust duct⁹⁹.

All standard room corner measurements were taken throughout the experiments as described in ISO 9705. The standard set up for the analysis within the exhaust duct is shown in Figure 54, taken from ISO 9705⁹⁹.

Oxygen was monitored using a paramagnetic analyser, and CO/CO₂ was monitored using an infrared spectrophotometer within the analysis system. Additional measurements also included duct flow, temperature, smoke obscuration, air pressure, humidity and temperature. Systems were logged by a VeeCan DAQ system. The layout of the internal analysis system inside the duct of the ISO room corner test is shown in Figure 55.

All standard room corner measurements were logged every 3 seconds. The additional gas analysis systems used for the experiments were logged every 1 second. Consequentially, the two time scales were required to be matched afterwards.

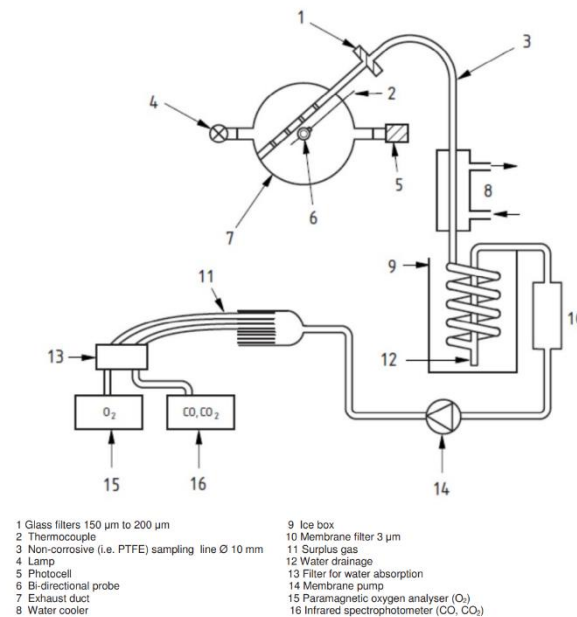


Figure 55: Layout of the gas analysis system sampling from the ISO room corner exhaust duct taken from ISO 9705⁹⁹.

2.8.2.2 Additional gas measurements

An additional sample line was connected to the exhaust duct of the ISO room, shown in Figure 53. A stainless steel tube (internal diameter 6 mm) was placed in the centre of the exhaust duct after the ISO room analysers. A long silicone tube (approximately 2.5 m) was attached to the stainless steel probe and fed to the ground to the gas analyser. The gas line was connected to a glass tube filled with glass wool to filter soot before connecting to a portable gas analyser used to monitor HCN and acid gasses in the duct.

2.8.3 Measurements in the room

2.8.3.1 Mass loss

The tests were designed to enable the collection of mass loss measurements throughout. The mass of the material was recorded before setting up the test rig. The test rigs were set up and placed on the load cell, and the mass loss was monitored for the entire test duration. In some cases, the test rig and material were too heavy and exceeded the scale's maximum capacity. This is discussed within the results section of each test.

2.8.3.2 Video recording

USB webcams were purchased from Amazon and used to record the test inside the room. The camera was placed on a small tripod in a box made of stone wool with a hole for the lens to look through. Stonewool was chosen as it is a non-flammable material. A sheet of heatproof glass covered the hole to protect the camera from the radiant heat. A small hole was drilled into the corner of the ISO room to feed the USB cable to an external laptop used to record the test. The camera was pointed to look directly at the test rig. In the cases where 2 x SBI rigs were to be used, the camera was aimed to look between the two rigs to capture footage of both test rigs. A photograph of the camera set up is shown in Figure 56.

Due to the heat damage each camera would sustain during testing, a new camera was used for each test, set up in the same way.



Figure 56: Picture of the camera set up to record the inside of the ISO room corner test protected by Rockwool and heat proof glass

2.8.4 Measurement procedure

Gas analysis equipment was calibrated daily using calibration gas at EIFC. Analysers were calibrated using 4% CO₂ and 9000 ppm CO.

The typical test procedure was as follows:

- The test rig was constructed and placed in the room.
- A camera was placed in the corner of the room and connected to a laptop to allow the test to be recorded. The camera was replaced for each test.
- Filters on the gas analysis lines and systems were cleaned and replaced after each test.
- Gas analysis systems were turned on, and sensors were leak-checked using N₂.
- The system was then calibrated using N₂, 4% CO₂ and 9000 ppm CO calibration gas.
- Calibrations were recorded and saved.
- The phi-meter was switched on and left to heat up, and the analysis system was turned on. The flow rate of the MFCs was set.
- The gas analysis system of the phi meter was then leak checked using N₂, and calibrated using N₂, 4% CO₂ and 9000 ppm CO.
- Power to McCaffrey probe sensors switched on and voltages checked.
- The room corner measurement system was set up.
- Water and hexane were then measured out and poured into the fuel pans set in the corners of the SBI rigs.
- All data logging systems were then set to record. Once ready, a 2 minute countdown was given.
- At 2 mins, the hexane was ignited, and the test began.
- If the fire had to be extinguished, all gas analysis systems were disconnected, and pumps turned off to avoid water entering the analysers.

2.8.4.1 Calculation of air flow through the opening

The velocity of the air flow can be found by using the McCaffrey probes and temperature measurements taken at the door. It is calculated by using Equation 31. An example calculation is given in **Appendix 6**.

$$v = \sqrt{\frac{2\Delta P}{\rho}} \quad \text{Equation 31}$$

Where v is air velocity in ms^{-1} , P is the pressure in Pa and ρ is the air density in kg m^{-3} .

2.8.4.2 Calculation of yields

To allow for better comparison for future use of the data obtained, gas yields (Y_i) can be calculated. Calculation of yields allows for direct comparisons between tests to be made, as well as comparing different material tests. Concentrations were converted to yields by dividing the mass of species produced (m_i) by the mass of fuel consumed (m_{fuel}), summarised in equation 32.

$$Y_i = m_i/m_{\text{fuel}} \quad \text{Equation 32}$$

Details of the full calculation can be found in **Appendix 7**.

2.8.4.3 Cone Calorimetry for large-scale fire predictions

Before conducting large-scale testing, cone calorimetry was used to test similar materials to provide an insight into their flammability and to enable loose predictions about the materials' burning behaviour during large-scale testing. The samples used for testing were: plasterboard, plywood, cables and flexible PU.

Samples were analysed using a Govmark model CC-2 cone calorimeter and tested following ISO 5660. Details of the methodology followed can be found in **Appendix 4**.

Plasterboard (PB), plywood (PW), high pressure laminate (HPL) and flexible polyurethane (PU) were cut to 100 mm x 100 mm and the bottom and sides of the materials wrapped in aluminium foil with the surface exposed and placed onto a lead sample holder with no case. Cables were cut into 10 cm strips and laid closely on the sample holder with the ends slightly exposed (approximately 0.5 mm). Plasterboard samples were tested with the paper still on. For each test, the sample was weighed, and relevant information was inputted into the cone calorimeter software. Samples were subjected to a heat of 50 kW and time to ignition, mass loss, rate of heat release and smoke production were measured.

The test was measured from time to ignition to when flaming ceased within the material. All samples were tested in duplicate. The heat release measurements and mass loss were inputted into cone tools to generate a prediction of the large-scale test behaviour. HPL was included as a potential test material, but was not used in the large-scale tests.

2.8.4.3.1 Heat release results

The data obtained from testing a series of materials in the cone calorimeter at 50 kW is shown in Figure 57. The plasterboard and plywood were approximately 4 mm thick. Flexible polyurethane was approximately 6 mm thick, and the cables were cut into 10 cm strips and laid out with minimal air gap.

The highest rate of heat release observed was from testing flexible polyurethane. This sample also had the fastest ignition time and one of the shortest test times. Plasterboard produced the lowest heat release. This test was the shortest duration as the tests were stopped once flaming ceased. As the only combustible component of the plasterboard was the paper cover on the sample's surface, only the paper burnt. Once the paper had burnt off, there was no longer any fuel for the fire, so flaming ceased and the test ended. The cables showed a lower heat release but burned for longer than other materials. HPL burnt with a relatively high heat release, over a long period of time.

The longest test durations were observed from HPL and PW. Although an initial spike from ignition occurred in both, they had a similar heat release to the cables but for a longer duration of the burn.

This suggests that the PW test on a large scale should be expected to be the longest in duration and potentially be one of the more aggressive fires. Tests conducted on PU indicate that the large-scale test can be expected to be ferocious initially, with rapid ignition occurring, but with a much shorter test duration than the other materials tested. Tests conducted on plasterboard indicate that the material may ignite initially on the paper surface but will not last due to the lack of combustible material.

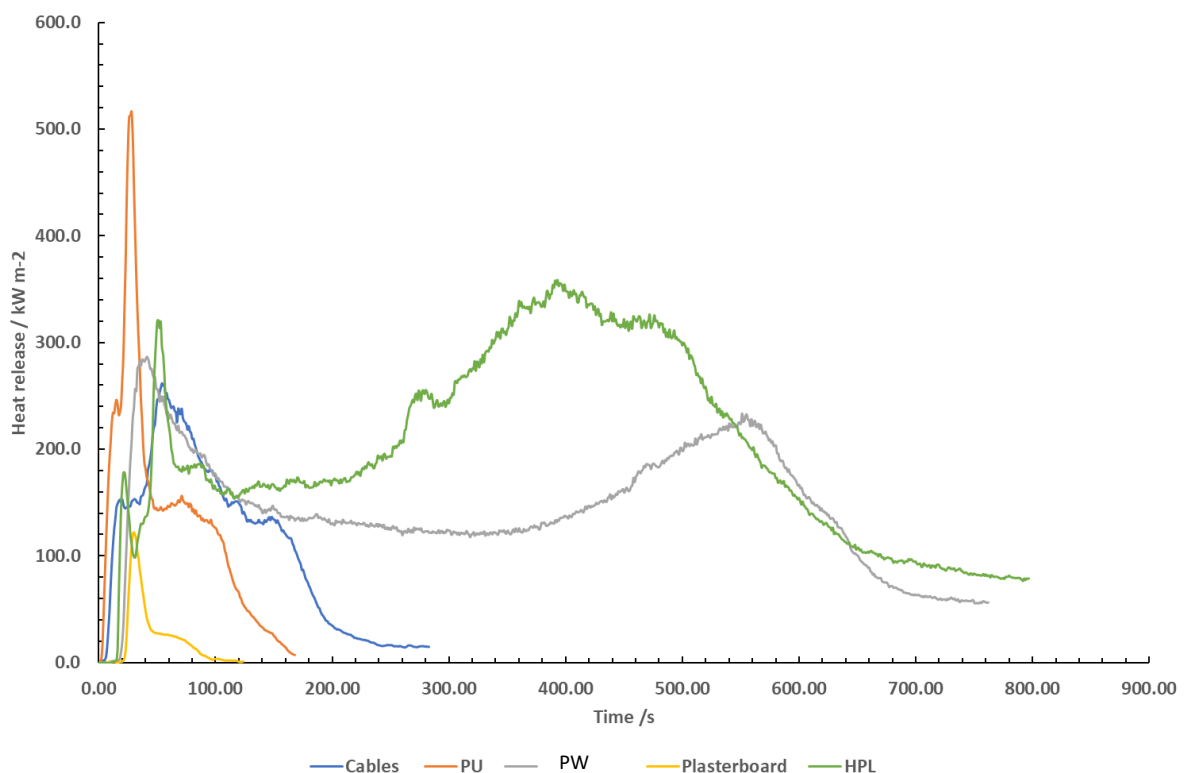


Figure 57: Heat Release rate data obtained from testing samples in the cone calorimeter at 50 kW.

2.8.4.3.2 Heat release predictions using cone tools

The test data obtained from the cone calorimetry tests was formatted and inputted into cone tools software to create predictive models of the large-scale test design to obtain an insight into the potential scale of the heat release that would be measured during the test. As the large-scale test was designed to use an SBI rig placed inside the test room, cone tools was used to predict the heat release by doubling the SBI test prediction produced from the software.

Table 20 shows total heat release predictions (for 2x SBI rigs) using a combination of calculations from raw cone data and cone tools. To determine the accuracy of the predictions, pre-existing test data⁸² from cone calorimetry was obtained and inputted into cone tools to produce a models to compare to its pre-existing, corresponding SBI data⁸². This is shown in Table 21. The materials that were used in this data comparison were two polyisocyanurate foams and one phenolic foam.

Table 20: Predicted parameters for 2 SBI rigs produced using cone tools and data obtained from cone calorimetry tests conducted at 50 kW.

Material	Total HR in cone / MJ m⁻²	Maximum total HR /MJ	Total HR from SBI test (cone tools) x2 (for 2x SBI rigs) / MJ
Plasterboard	2.7	12.15	0.32
Plywood	108.6	488.7	47.8
HPL	156.9	706.05	94.54
Cables	22.5	101.25	---
PU	30.5	137.25	12.06

Table 21: Comparison of predicted parameters and actual SBI data⁸².

Material	Total HR (obtained from cone calorimetry testing) / MJ	Actual total HR from SBI test /MJ
PIR 1	66.15	10.4
PIR 3	39.15	15.4
PF	43.75	16.4

The data in Table 21 shows that cone tools greatly overpredicts the total heat release compared to actual test data on a singular SBI rig. Although the comparison shows the predictions are incorrect, the tests in this project used 2 x SBI rigs facing each, so the radiant heat from the combined rigs may result in a higher total heat release during the test. The software is could have generated an over-prediction if the model does not take the exhaust into account, as well as heat losses that are a result of the calcium silicate board absorbing some heat from the test, as this is not an occurrence in a cone calorimetry test.

As cone tools only offered the option of predicting SBI test data or room corner data, rather than a combination of the two test methods, the predictions were made for an SBI test. It was expected that the predictions would under-predict the heat release value as the SBI is an open-faced test. The two rigs facing each other should produce a radiant heat effect, resulting in a higher measured heat release. As cone tools did not offer a predictive model for the large-scale set up used in this research, the predictive data obtained was not used for a direct comparison.

3 RESULTS AND DISCUSSION

The results from the large-scale tests conducted have been separated into materials. The individual tests have been separated into their target fire condition: well-ventilated and under-ventilated flaming. Each material has three main sections: Well-ventilated testing, under-ventilated testing and data summary and comparison. The two main test conditions are separated into four sub-sections: Internal room measurements, door measurements, duct measurements. A collective data summary and comparison between all tests conducted on the material is provided at the end of the materials section. The materials tested are described below.

The air flow was recorded for future use for calculating yields of toxic products. Due to the scale of the project, the concentration measurements were deemed to be of more use in terms of assessing the test design and measurement system. Additional air flow measurements were taken to allow for future calculations of toxic product yields for comparison between bench and large-scale test data. The tests results are shown as concentration measurements (for permanent gases).

- **Heptane and propane calibrations**

A summary of the fuel calibration tests can be found in this section. Heptane calibrations were carried out using three different burner set ups (circular burner, tall triangular burner, and medium triangular burner). The triangular burner was tested alone in the test room and when set up against a calcium silicate board set up as a blank test run with no material attached to the board. Propane burner calibrations for the cable tests can also be found in this section.

- **Plasterboard (PB)**

Details of the plasterboard test can be found in this section. The plasterboard was tested as a double SBI set up in well-ventilated conditions only.

- **Oriented strand board (OSB)**

Due to a translation error, it was thought that the material used in the tests would be plywood. The material actually used was oriented strand board (OSB). Details of the OSB tests can be found in this section. OSB was tested as 2 x SBI rigs with the door open (under-ventilated), 1 x SBI with the door fully open (well-ventilated) and as 1 x SBI with the door partly blocked (under-ventilated).

- **Horizontal cable trays (HCT)**

Details of the horizontal cable tray tests can be found in this section. Cable trays were tested without a door (fully open) (well-ventilated) and with a door (partly blocked) (under-ventilated).

- **Flexible polyurethane (PU)**

Details of the flexible polyurethane tests can be found in this section. PU was tested as 1 x SBI rig with the door fully open (well-ventilated) and as 2 x SBI rigs (also with the door fully open) (under-ventilated).

- **Summary of large-scale test results**

A summary table of the most important data and findings from all tests conducted is presented in this section, alongside a brief discussion of the overall findings from the entire set of tests conducted.

Changes to test procedures:

Due to a connection issue with the NDIR and electrochemical cell, the electrochemical cells used for logging oxygen were connected to an OMEGA- data logger where the raw voltage output was logged. The McCaffrey probes were also connected to the same data logger.

Any additional deviations from the test procedure have been noted in the additional test information of each section.

In addition, as several different instruments were used to log the data, the data was collected at different intervals. The data from the ISO room analysers was logged every 3 seconds and all other data was collected every 1 second. The time difference has been corrected.

Data logging:

All tests start logging from the 2 minute countdown. Test time 0 shown on the graphs includes a 2 minute period before the test starts (120 seconds).

Test data:

Due to the large volume of data generated during the ISO 9705 testing, only the HRR, mass loss, temperature, equivalence ratio and analysis of permanent gases have been included in the main body of the thesis. HCN data was most relevant for tests conducted using polyurethane, and so the data obtained is presented in the main body of the thesis. As there were no other significant HCN yields from the other tests conducted, the HCN data has been included in **Appendix 11**. Minimal concentrations of acid gases were also found, and provide less relevance in comparison to the measurement of permanent gases. They have therefore been placed in **Appendix 11**.

The data is shown with the inclusion of the heptane measurements.

3.1 HEPTANE AND PROPANE CALIBRATIONS

Four calibration tests were run to obtain calibration data for the ignition sources used. The tests were: heptane with calcium silicate boards with no door, heptane with calcium silicate boards with a door, and a burner with propane. All calibration data has been presented as a summarised table containing the relevant information used for data analysis.

3.1.1 Test layout and summary

Calcium silicate (CaSi) boards were set up on the SBI test rig and placed on the load cell. For the test requiring a door, a 1.3 m door blocker, made from calcium silicate, was screwed to the door of the ISO room.

The propane burner was calibrated following the ISO 9705 test procedure. For under-ventilated calibrations, the calibration was run in the same way but with the addition of a 1.3 m calcium silicate door.

3.1.2 Data summary

A summary of the information collected from the calibration tests conducted in the ISO 9705 room corner test is shown in Table 22. Unfortunately due to a data logging issue, the data for the CO₂ and CO in the doorways are unavailable for all calibration tests conducted. The heat release has been shown as a peak heat release value, and the average value taken during the steady period of burning during the calibration.

Table 22: Summary of the calibration data collected in the ISO 9705 room corner test.

Test ID	Door height /m	Peak heat release /kW	Average heat release during steady burning / kW	Lowest measured oxygen concentration / %		Peak CO ₂ concentration /%	Peak CO concentration %
				Door	Exhaust duct	Exhaust duct	Exhaust duct
Heptane with CaSi boards WV	No door used	151.2	97.25	17.52	20.65	0.23	0.020
Heptane with CaSi boards UV	1.3	136.1	93.65	20.70	15.96	0.21	0.026
Propane burner WV	No door used	150.76	(100 kW used) 101	-	20.471	0.23	0.020
Propane burner UV	1.3	227.9	(100 kW used) 101	-	20.473	0.32	0.026

Key: - indicates no result due to measurement error.

3.2 PLASTERBOARD

3.2.1 Test layout

Plasterboard was attached to two SBI rigs with a 4 mm air gap between the material and the calcium silicate boards. The board was approximately 12 mm thick and slightly raised above the burner as in the SBI test. One SBI rig was set up for the test. A total mass of 40.97 kg of plasterboard was used.

The SBI rig was placed on the load cell in the centre of the ISO room. Gas analysers were calibrated and set up for testing. Heptane was measured out and poured into the burner inside the room. The ISO room measurements were started alongside the gas analysers and phi meter 2 minutes before ignition. The heptane burner was ignited manually.

3.2.2 Description of test:

The heptane burner was ignited after a 2 minute count down. The paper cover of the plasterboard ignited rapidly. The fire spread rapidly across the board. At around 600 seconds, the front burner began to run out of fuel shown by the decline in HRR and temperature, but the rear burner continued until 800 s.

At the end of the test, the paper cover had all burnt off and only the board remained.

3.2.3 Heat release measurements:

The heat release data from the test is shown in Figure 58. The heat release rose rapidly upon ignition, reaching a peak heat release of 648 kW 360 seconds into the test. After reaching its peak heat release, the fire then entered a relatively steady period of burning from 360 to 540 seconds.

After 600 seconds, the heat release rapidly declines. This was the same time that the heptane burner used for ignition ran out of fuel, suggesting the rapid decline was a combination effect of the lack of combustible fuel to facilitate the fire, and the ignition sources running out of fuel. As the heat release did not surpass 1000 kW, flashover was not reached.

However, the heat release measurement is very large and steady for plasterboard. It is unexpected that the burning of the paper cover of plasterboard would achieve such a steady heat release output. This is most likely the heptane ignition source, with the additional heat release from the paper cover. However, the calibration of heptane (1 burner) produced an average heat release of 97.25 kW. The two burners used in this test would be an average heat release of 194.5 kW, meaning approximately 453.5 kW would have been produced from the plasterboard. While this could be a measurement issue in the ISO room, it could also be a result of the plasterboard retaining heat from the burners during the test, causing an increase in the heat release measured and the steady output seen in the data.

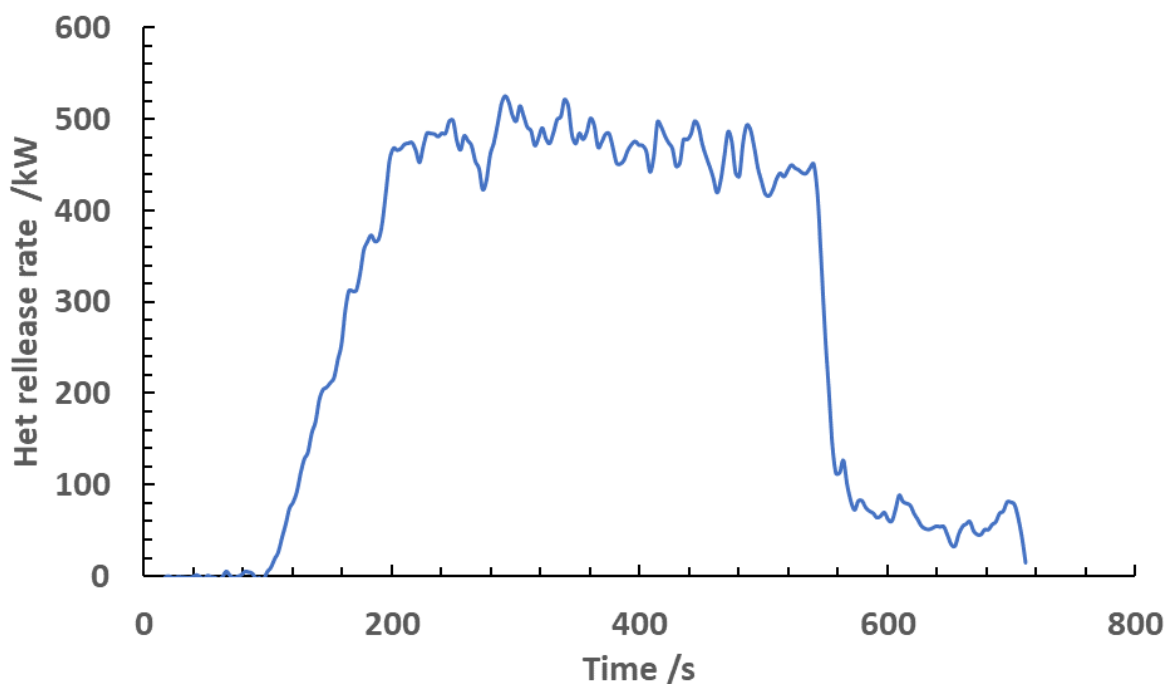


Figure 58: Heat release data measured in the ISO 9705 room corner when testing plasterboard.

3.2.4 Mass loss measurements:

The mass loss was monitored throughout the test using the scale inside the ISO room. Due to the excess mass of the material and test rigs, the total mass exceeded the maximum capacity of the scale. The data recorded on the scale is shown in *Figure 59*. The mass loss during the test was minimal as a result of the lack of available fuel during the test. Due to the test rigs exceeding the maximum measurement of the ISO room scale, the period between 400 and 700 seconds is likely to be the most representative of the test.

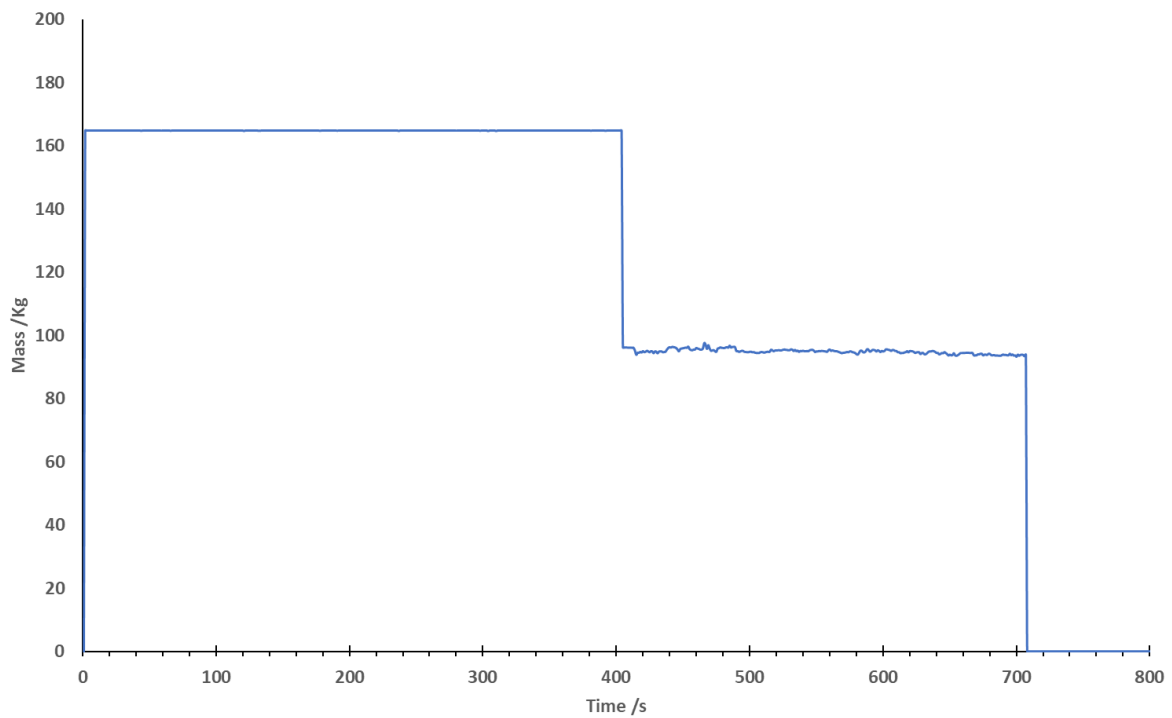


Figure 59: Mass loss measurements measured on the scale in the ISO 9705 room when testing plasterboard.

3.2.5 Temperature measurements

The temperature of the doorway was measured throughout the test. The thermocouple tree sat in the doorway and had thermocouples every 20 cm from the floor to the room's ceiling. The temperature measurements obtained throughout the test are shown in Figure 60.

The temperatures in the doorway gradually rose upon ignition, reaching a maximum temperature of 450 °C before slowly declining as the fire begins to decrease. The heat output measured in the doorway is relatively low for a fire, showing that despite the paper cover of the board burning, the temperatures in the doorway were not very high. They are indicative of early well-ventilated flaming.

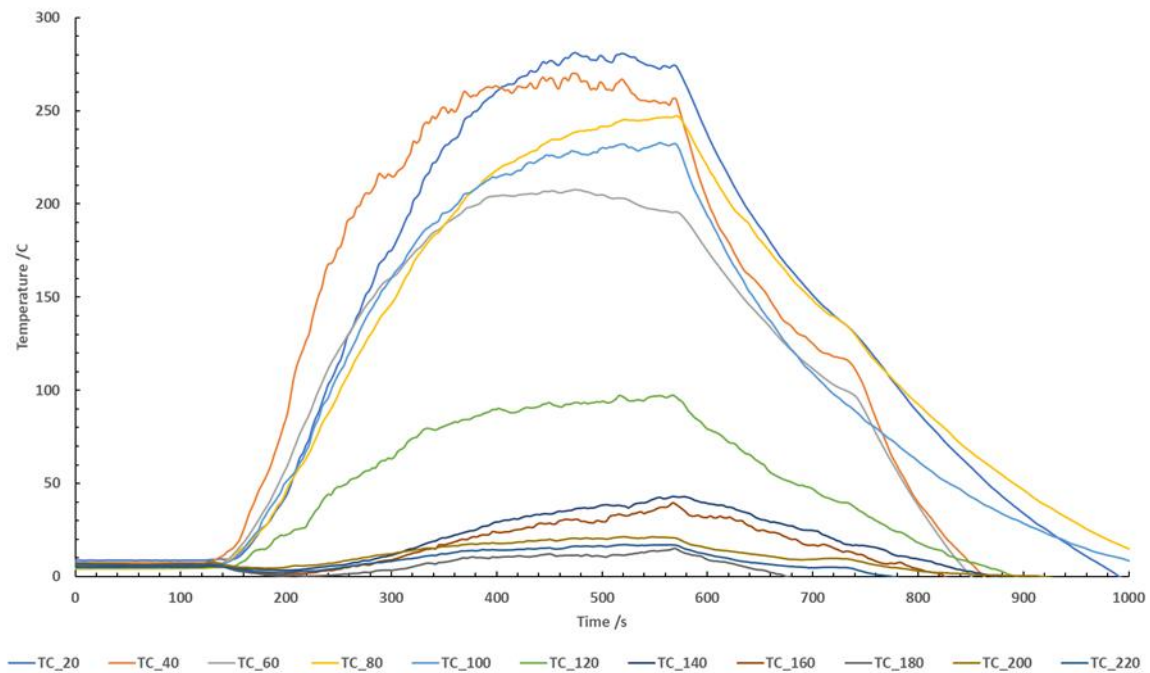


Figure 60: Temperature measurements taken in the doorway of the ISO room when testing plaster board (2 x SBI with no door). The measurements are taken from thermocouples labelled 'Thermo pile 1' with the final number indicating the distance from the ceiling in cm (e.g. Thermo pile 1 40, meaning thermocouple 1, 40 cm from the ceiling).

3.2.6 Fire condition

The fire condition of the test was found by monitoring the equivalence ratio using the phi meter. The equivalence ratio logged throughout the test is shown in *Figure 61*.

After ignition of the heptane burners, the equivalence ratio rises as the fire begins to develop. However, since plasterboard is a non-combustible material, with the exception of the paper covering the surface, there was little fuel to facilitate the fire. Ignition occurred on the surface of the plasterboard.

The maximum equivalence ratio reached during the test reached 0.33 approximately 220 seconds into the test. As plasterboard is non-combustible, this measured equivalence ratio was a combination of the burning of the paper cover and from combustion of the ignition source.

However, there is too little fuel available for flaming to be sustained. A small period of steady burning occurred from 250 seconds to 300 seconds before a decline in equivalence ratio is observed. This decline was likely a result of the fire running out of combustible fuel and the heptane running out in the ignition burner. A data acquisition problem occurred at 330 seconds, and so no equivalence ratio data is available for the remainder of the test.

As the equivalence ratio was declining at 250 to 300 seconds due to the lack of fuel in the test room (from the test material and ignition source), it is presumed that the equivalence ratio would not have risen any higher than 0.33 after the point where data was not recorded. The measured equivalence ratio was representative of early well-ventilated flaming.

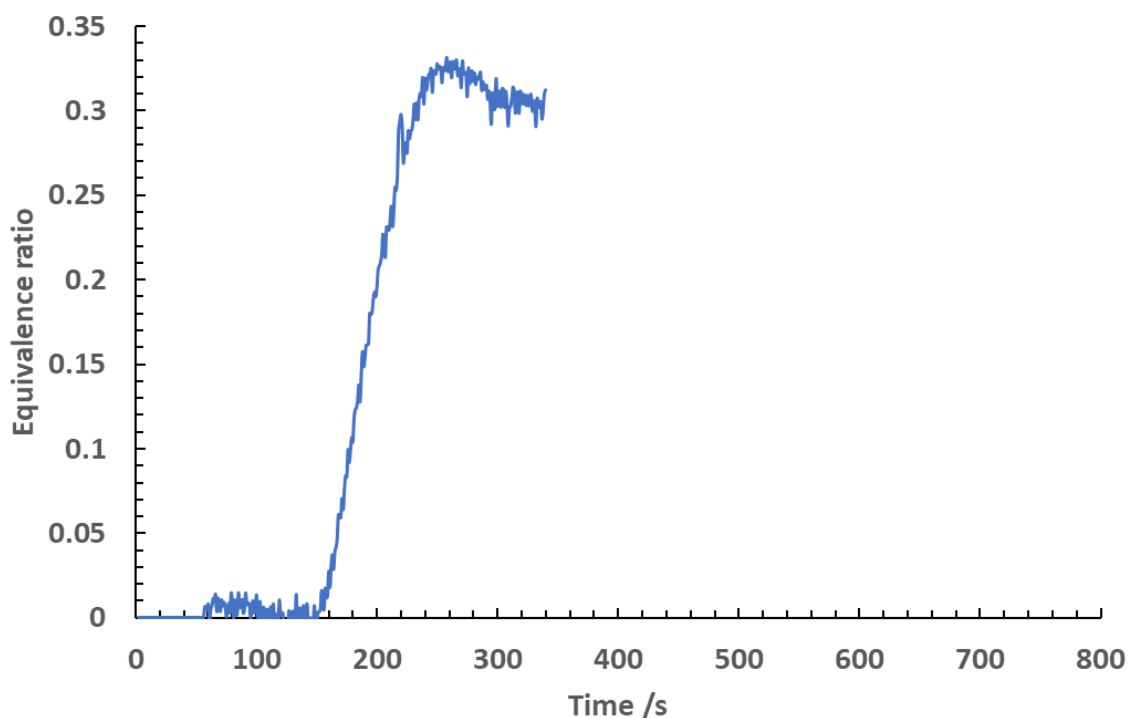


Figure 61: Equivalence ratio measured in the doorway of the ISO 9705 room when testing plasterboard.

3.2.7 O₂ measurements

The oxygen measured in the exhaust duct and the doorway throughout the test is shown in *Figure 62*. The oxygen measured in the exhaust duct did not show significant changes throughout the test.

The oxygen in the doorway decreases upon ignition, slowly declining until it settles around 14 %. The oxygen levels remained relatively steady from 200 seconds to 460 seconds. Data logging in the doorway stopped at 480 seconds due to an error in the equipment. Overall, the duct measurements were significantly more dilute than those taken in the doorway. The oxygen concentrations reached in the doorway are representative of early well-ventilated flaming.

If the oxygen data in the duct was measured at 19.5 % and 14 % in the doorway with no additional flaming outside of the test room, then the dilution factor from the doorway to the exhaust duct is approximately 4.6.

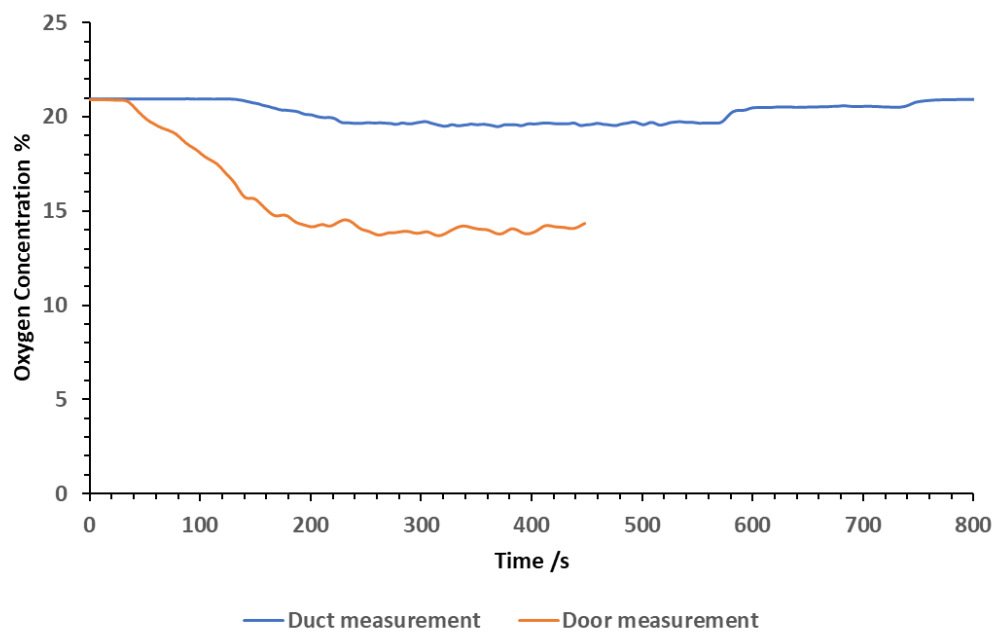


Figure 62: Oxygen concentrations measured in the doorway and exhaust duct of the ISO room when testing plasterboard.

3.2.8 CO₂ measurements

The CO₂ concentrations logged in the doorway and exhaust duct throughout the test are shown in *Figure 63*.

The CO₂ concentrations increased after ignition occurred, rising to a peak concentration of 4.4 % in the doorway, and a peak concentration of 1 % in the exhaust duct, suggesting the exhaust duct dilutes the concentrations in the doorway by around four times. The concentrations became relatively stable from 200 seconds to around 550 seconds, aligning with the steady equivalence ratio logged during the test. This short duration was likely the time when the paper cover of the plasterboard was burning, as well as the burning of the heptane ignition sources. The decline in CO₂ at 580 occurs rapidly, and concentrations decline to baseline values. The CO₂ concentrations reached in the doorway are representative of well-ventilated flaming. The measurements in the duct were significantly diluted due to the high flow rate of the exhaust (by approximately 4x).

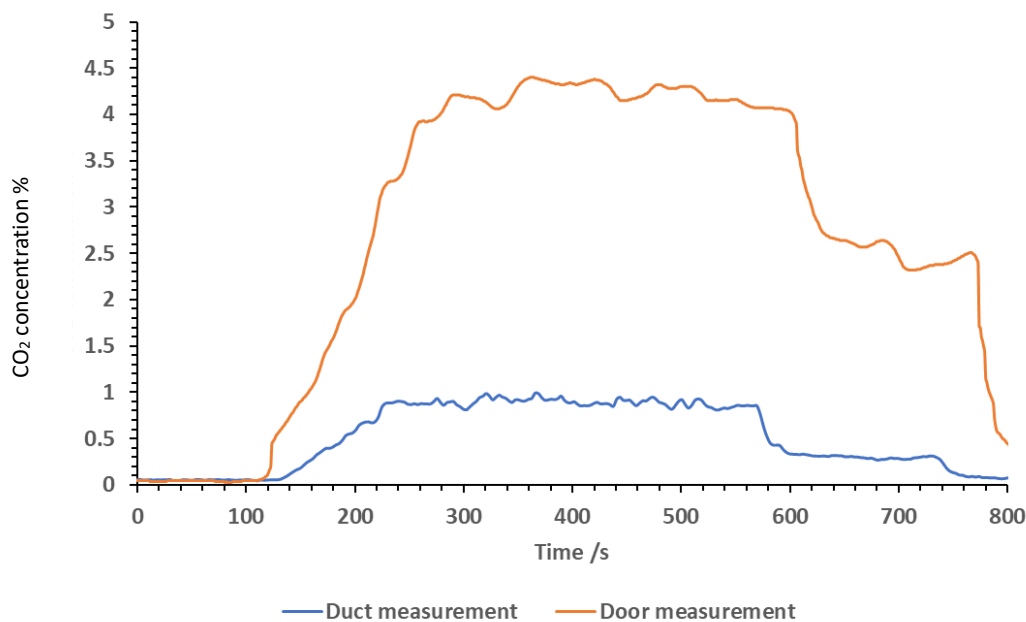


Figure 63: CO₂ concentrations measured in the doorway and exhaust duct of the ISO room when testing plasterboard.

3.2.9 CO measurements

The CO measurements taken in the exhaust duct and the door throughout the test are shown in *Figure 64*. The CO measured in the exhaust duct is largely sporadic and unsteady. This is likely due to the high flow rate in the exhaust duct in combination with the low volumes of CO being produced during the test. The highest CO concentration measured in the exhaust duct was 0.025 %.

CO measured in the door was significantly less sporadic than in the exhaust duct, with much higher concentrations measured. The peak CO concentration of 0.09 % was reached at 300 seconds into the test before declining rapidly. The measurements taken in the duct were around four times smaller than those in the room's doorway, similar to the difference in CO₂ concentrations measured.

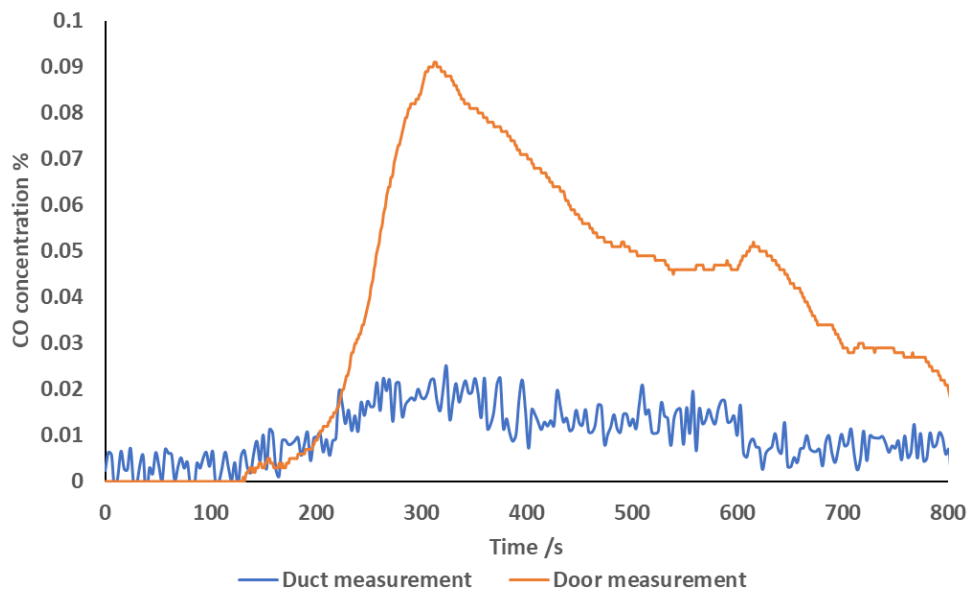


Figure 64: CO concentrations in the doorway and exhaust duct of the ISO room when testing plasterboard.

3.2.10 CO/CO₂ ratio

The CO/CO₂ ratio calculated in the exhaust duct and doorway throughout the test are shown in *Figure 65*. The ratio is largely sporadic in the exhaust duct, likely due to the highly variable and low CO concentrations measured in the duct. A maximum CO/CO₂ ratio of 0.13 was reached, however for most of the test, the ratio remained below 0.05, which is expected in a well-ventilated test.

The CO/CO₂ ratio in the doorway was much less sporadic, and similarly very low. For the majority of the test, the ratio remained between 0.01 and 0.04, which is typical for a well-ventilated fire.

Overall, there is good agreement between the two calculated ratios, particularly between 300 and 550 seconds. The high values from the duct (0 to 200 seconds and 500 to 800 seconds) result from the very low concentrations of CO₂.

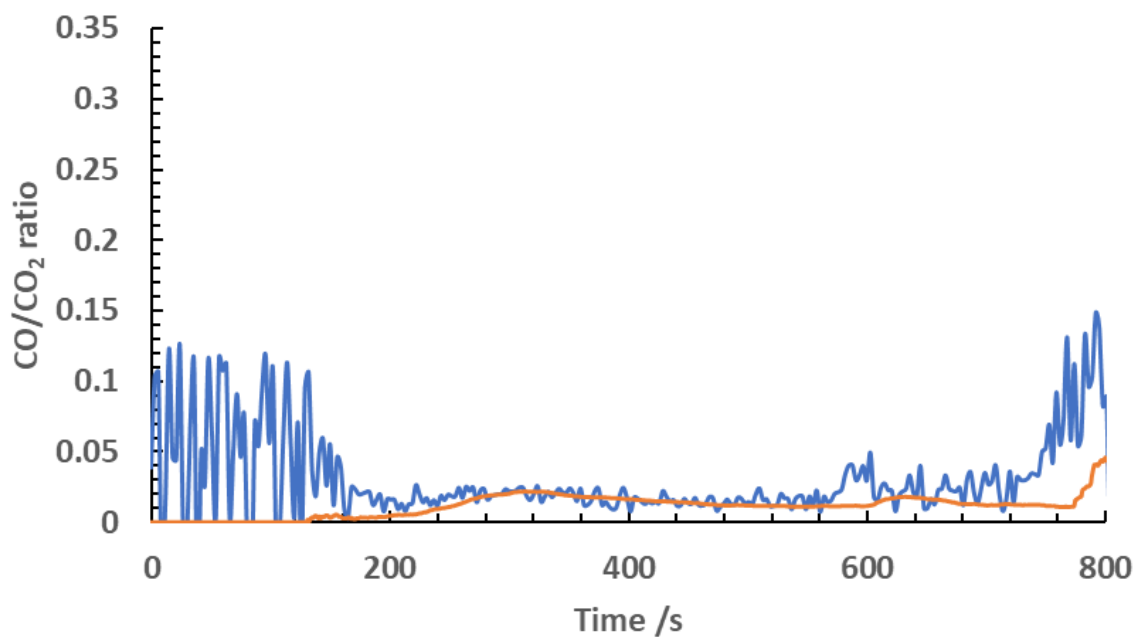


Figure 65: CO/CO₂ ratio calculated for the doorway and exhaust duct of the ISO room when testing plasterboard.

3.2.11 Summary of test data:

A summary of the test data is shown in *Table 23*. As only one test was conducted in the ISO room using plasterboard, no comparison can be made for this material. The test was aimed to be well-ventilated, and the data obtained was representative of an early well-ventilated fire. The test design was successful in achieving the aimed ventilation condition. The test also provided a useful benchmark for other tests.

Table 23: A summary of the test data obtained when testing plasterboard in the ISO room.

Test condition aim	Peak heat release / kW	Max equivalence ratio measured	Max CO concentration measured	
			Exhaust duct	Doorway
Well-ventilated	648	0.33	0.09	0.025

3.3 ORIENTED STRAND BOARD (OSB):

3.3.1 well-ventilated

3.3.1.1 *Test layout*

OSB sheets were attached to a singular SBI rig with a 4 mm air gap between the material and the calcium silicate boards. The board was approximately 12 mm thick and slightly raised above the burner, as in the SBI test. One SBI rig was set up for the test. A total mass of 14.72 kg of OSB was used.

The SBI rig was placed on the load cell in the centre of the ISO room. Gas analysers were calibrated and set up for testing. Heptane was measured out and poured into the burner(s) inside the room. The ISO room measurements were started alongside the gas analysers and phi meter 2 minutes before ignition. The heptane burner was ignited manually.

The airflow was monitored using McCaffrey probes throughout the test. In this test, the lower McCaffrey probe was altered so that the inlet to the probe was facing outwards so that the air flow could be monitored better.

3.3.1.2 Heat release

The heat release data from the test is shown in *Figure 66*. The heat release data is shown with the inclusion of the heat released from the ignition source. The heat release rose to 300 kW rapidly after ignition, which is likely a result of the heat release from the heptane burner and the ignition of the OSB sheet. From 250 to 450 seconds, the heat release was relatively steady. At 500 seconds, the heat release rose rapidly again, reaching its peak heat release of 990 kW at approximately 700 seconds into the test. At this point, the entire OSB sheet was burning. After reaching its peak, the heat release dropped rapidly. This was likely a result of the OSB becoming burnt through, meaning there was no fuel left to facilitate the fire. The time to flashover was calculated using the methodology described in the ISO 9705 standard. As the heat release did not surpass 1000 kW, flashover was not reached.

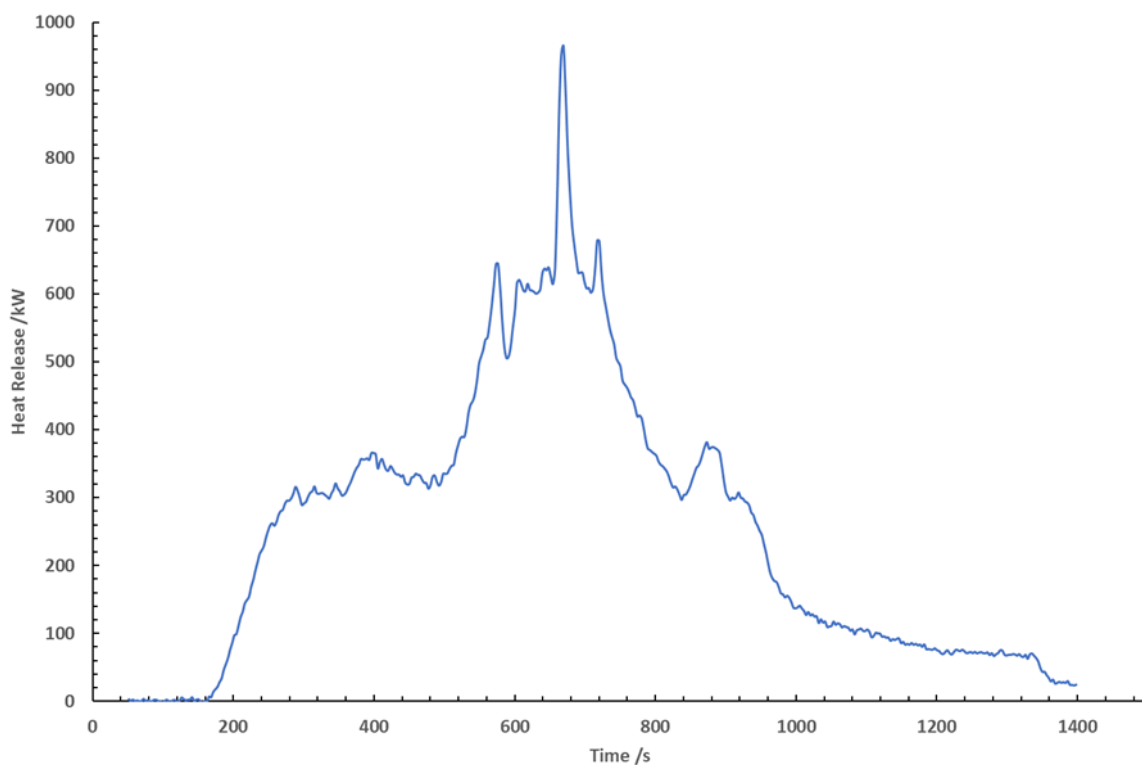


Figure 66: Heat release measurements taken when testing OSB (1x SBI rig with the door open) in the ISO 9705 room corner.

3.3.1.3 Mass loss

As the test only used one SBI rig, the test rig's total mass was within the range's limits. The mass loss measured using the scale in the test room is shown in Figure 67. The mass loss measurements showed a steady decline over the course of the entire test, with the mass reducing to approximately from 118 kg to 100 Kg by 800 seconds.

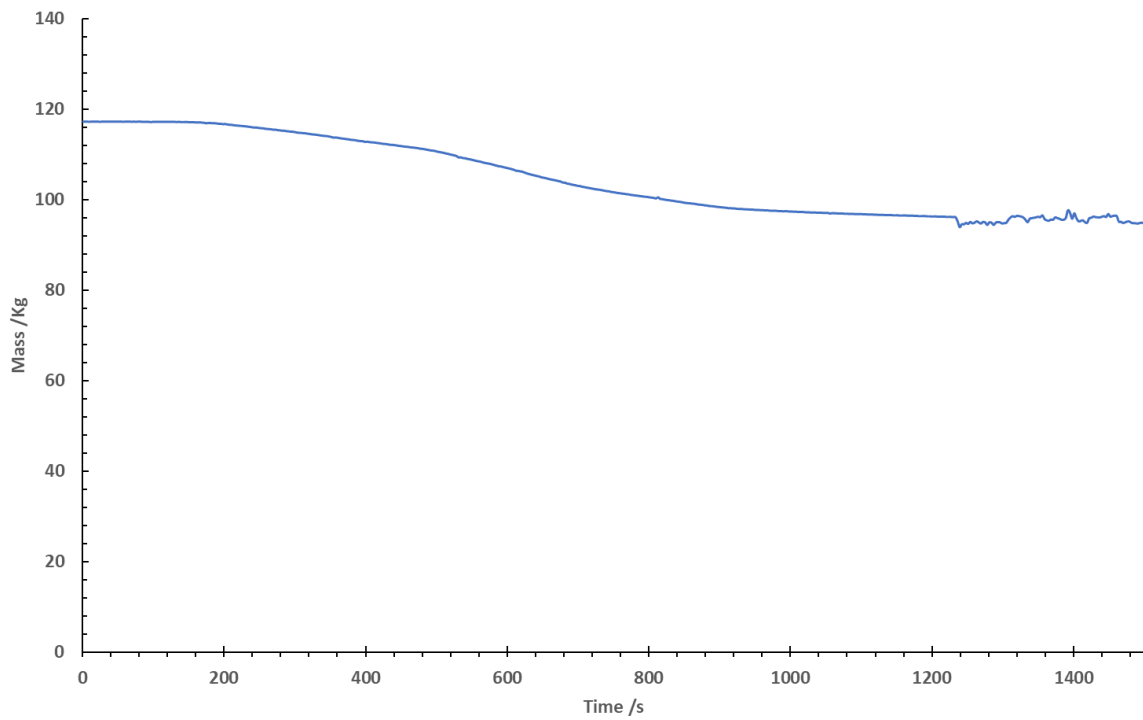


Figure 67: Mass loss measurements taken using the scale in the ISO room corner test, when testing OSB (1x SBI with the door open).

3.3.1.4 Temperature

Temperature measurements were taken in the doorway of the ISO room throughout the test. The temperature measurements obtained are shown in *Figure 68*.

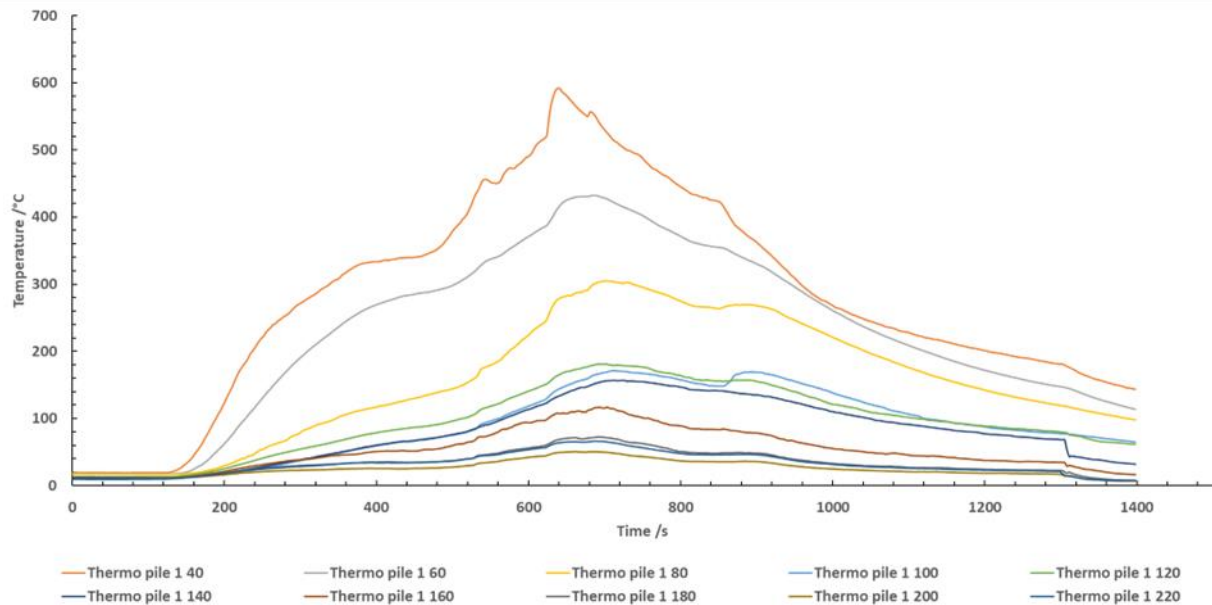


Figure 68: Temperature measurements taken in the doorway of the ISO room when testing OSB (1x SBI with no door). The measurements are taken from thermocouples labelled 'Thermo pile 1' with the final number indicating the distance from the ceiling in cm (e.g. Thermo pile 1 40, meaning thermocouple 1, 40 cm from the ceiling).

The temperatures show a rapid increase upon ignition, reaching a maximum temperature of 590 °C approximately 650 seconds into the test. After reaching its peak, the temperature began to slowly decline as the fire began to decrease. The peak temperature measured corresponds to the same point the peak heat release was measured during the test.

The temperature profile recorded can be used in the future to identify the neutral plane within the doorway to calculate air velocity in and out of the room with the addition of air velocity measurements. Within the temperature data, a clear distinction between the upper and lower plane in the doorway can be seen. The upper plane can be seen from 40 cm from the ceiling down to 80 cm from the ceiling. The lower plane is seen from 100 cm to the bottom of the room. The thermocouple at 80 cm sits in the middle of the two planes. This can be taken as the neutral plane point and used to calculate gas yields measured in the doorway for future work.

3.3.1.5 Fire condition

The equivalence ratio was logged throughout the test using a phi meter. This is shown in *Figure 69*. After ignition, the equivalence ratio grew steadily, reaching a peak value of 0.71 approximately 650 seconds into the test, corresponding to the same time the peak heat release was reached. The equivalence ratio remained below 1 throughout the test, showing that the fire remained well-ventilated for the test duration. For most of the test, the equivalence ratio remained between 0.3 and 0.7, which is representative of early well-ventilated flaming. This was likely a result of the open door, as fresh air could enter the fire allowing for more complete combustion to occur throughout. After 650 seconds, the equivalence ratio begins to decline as a result of the lack of fuel.

While the HRR data shows a sharp peak at 680 seconds, the phi meter peak is much softer. This is a result of the slower response time of the phi meter, resulting in a softer peak being measured.

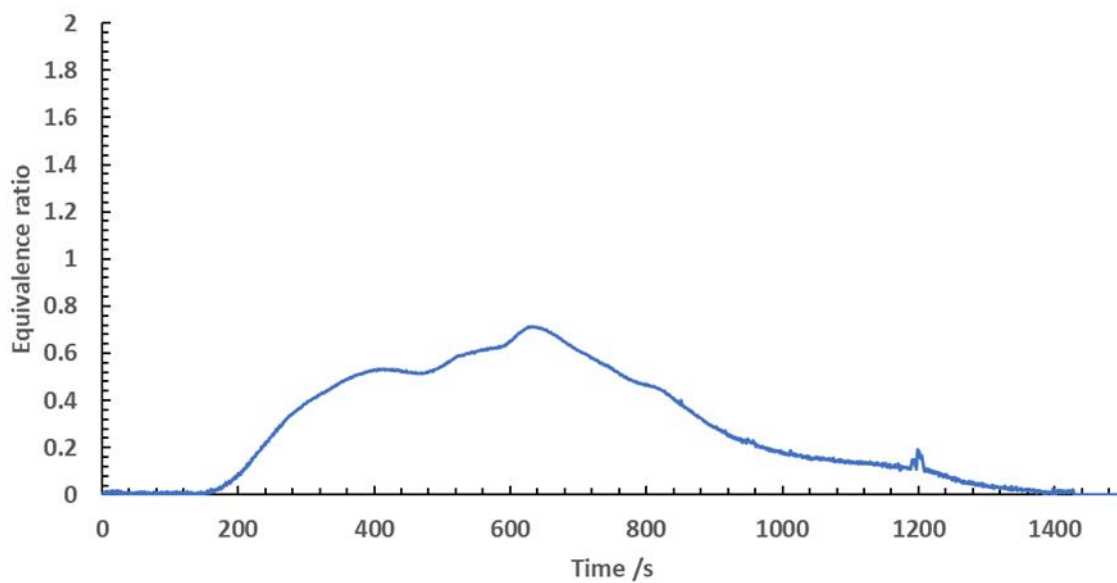


Figure 69: Equivalence ratio monitored using a phi meter when testing OSB (1x SBI no door) in the ISO room corner.

3.3.1.6 Oxygen measurements

The oxygen measured in the door and exhaust duct throughout the test is shown in *Figure 70*. After ignition, the oxygen levels in the door begin to decline rapidly before settling between 12 to 13 % for around 200 seconds. As the fire progressed, a significant drop in oxygen was observed, reaching 5.5 % in the door at 650 seconds. This corresponded with the time at which the equivalence ratio and the heat release was at its highest. The oxygen did not stay below 10 % for longer than 50 seconds. For the duration of the test, the oxygen predominantly settled between 10 to 15 %, indicating the fire was well-ventilated.

The oxygen concentration measured in the exhaust duct did not significantly change from its baseline value. This was likely due to the excess dilution occurring from the large flow rate used in the extraction hood causing significant dilution to the measurements taken.

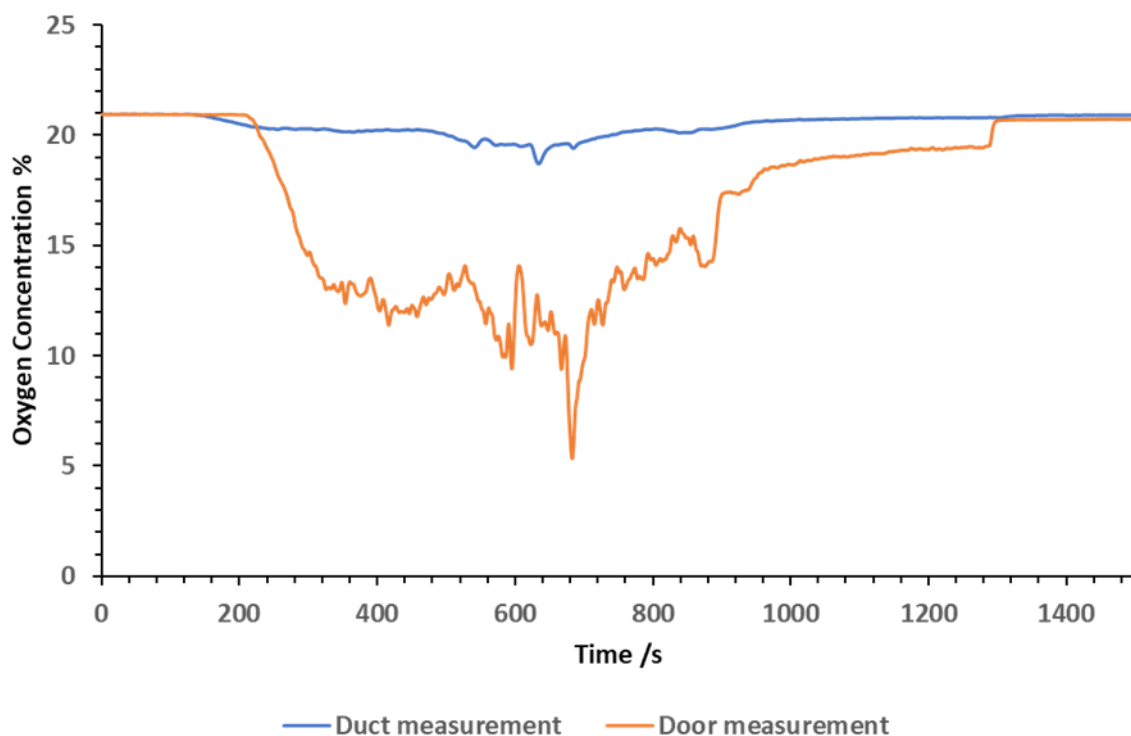


Figure 70: Oxygen measurements taken in both the door and duct of the ISO room corner when testing OSB (1x SBI no door).

3.3.1.7 CO₂ measurements

The CO₂ concentrations logged in the exhaust duct throughout the test is shown in Figure 71. The measurement of CO₂ in the doorway was not logged for this test due to an error in the test equipment, and so the CO₂ concentration in the doorway was calculated by multiplying the duct measurement by 4 (the approximate dilution factor).

The CO₂ increased after ignition occurred, rising to a predicted peak concentration of 7 % in the doorway, and a peak concentration of 1.7 % in the exhaust duct. The peak concentrations were reached approximately 650 seconds into the test. The dilution resulted in concentrations in the doorway being approximately 2.5 times more concentrated than those measured in the exhaust duct. The CO₂ concentrations reached in the doorway are representative of well-ventilated flaming.

The concentration measured became relatively stable from 400 seconds to around 700 seconds. The decline in CO₂ at 700 seconds occurs rapidly, and concentrations decline to baseline values. This was the point at which the fire began to slow down due to a lack of fuel.

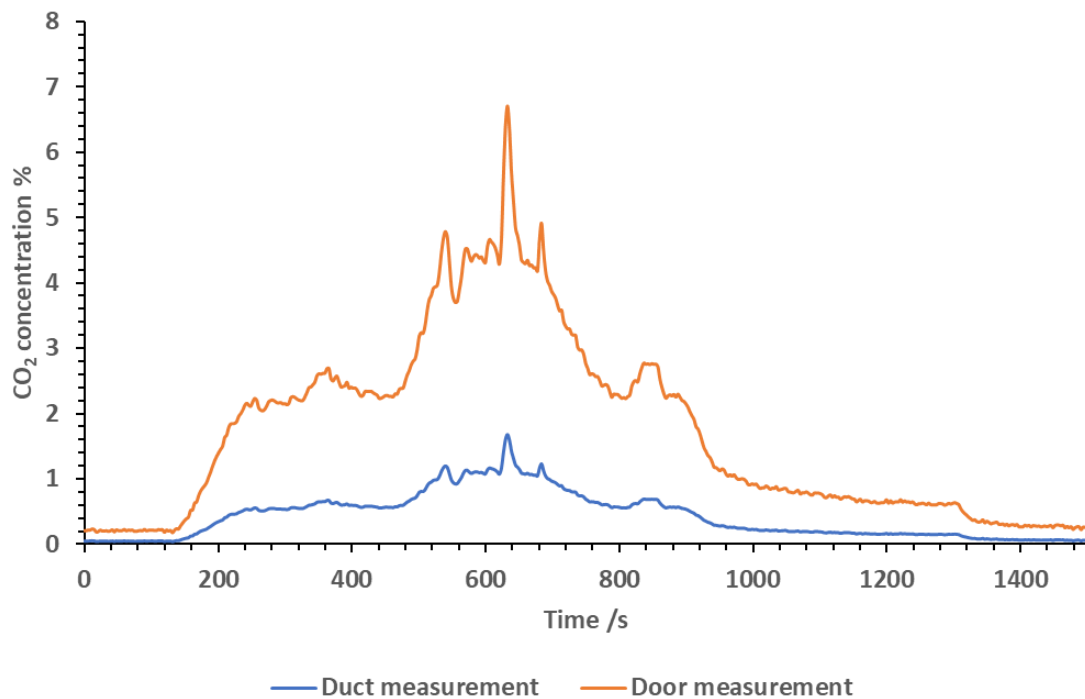


Figure 71: CO₂ measurements taken in duct of the ISO room corner when testing OSB (1x SBI no door) shown with a predicted CO₂ concentration of the doorway measurement.

3.3.1.8 CO measurements

The CO concentrations measured throughout the test are shown in Figure 72. Due to a measurement issue, the CO was not logged in the doorway during the test. The CO measurement of the doorway was calculated using the exhaust duct values multiplied by 4 (the approximate dilution factor).

Overall, the CO measured in the exhaust duct was substantially lower than that measured in the door. The CO concentrations remained low for the first 500 seconds of the test.

The CO concentration in both the doorway and exhaust duct peaked at 580 seconds, and again at 680 seconds. In the first initial peak, the CO concentrations reached 0.1 % in the exhaust duct, and 0.4 % in the doorway. In the second peak that occurred at 580 seconds, the CO reached 0.12 % in the exhaust duct, and 0.48 % in the doorway.

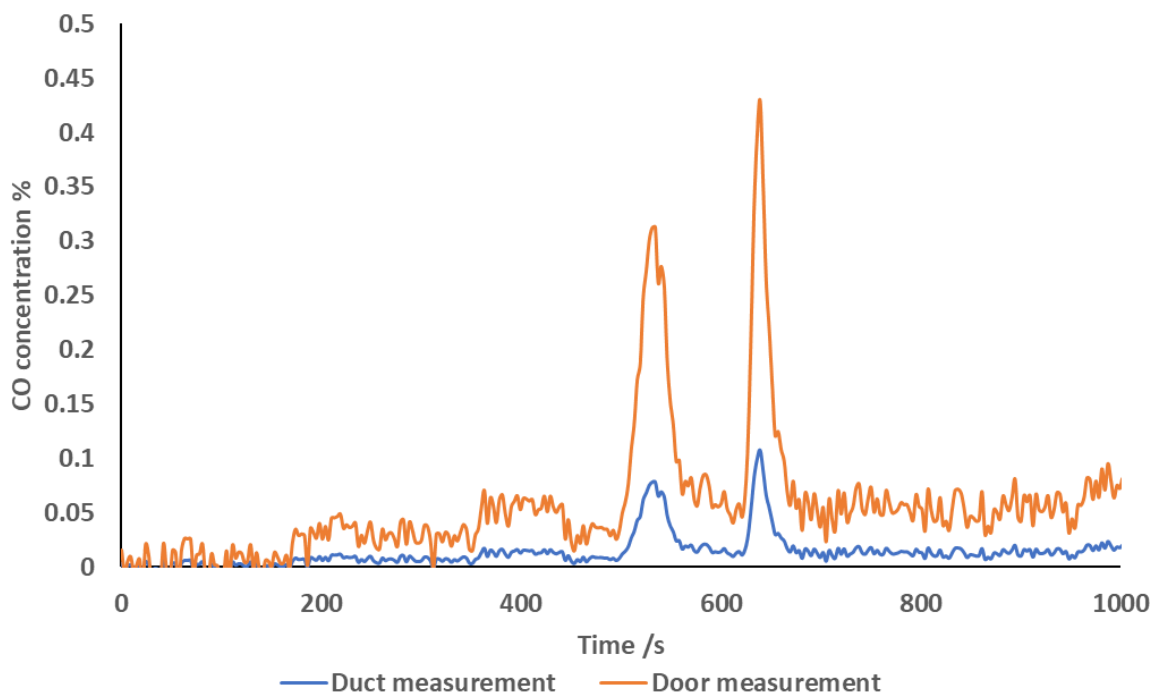


Figure 72: CO measurements taken in the exhaust duct of the ISO room when testing OSB (1x SBI no door), shown with a calculated doorway concentration found by using the duct measurement multiplied by the dilution factor (4x)

3.3.1.9 CO/CO₂ ratio

The CO/CO₂ ratio was calculated using the gas concentrations measured in the exhaust duct and the predicted door values throughout the test. This is shown in Figure 73.

The CO/CO₂ ratio was identical for both the doorway and exhaust duct, however this was expected as the doorway values were calculated using the exhaust duct measurements multiplied by a dilution factor of 4. The ratio is therefore identical.

The ratio calculations are very noisy at the start and end of the test as a result of the very low measurements of CO and CO₂. Therefore, the most representative data for the test can be seen from 200 seconds to 800 seconds. The ratio had 2 peaks, one at 580 seconds and another at 680 seconds, where the ratio reached approximately 0.1 both times. This is representative of well-ventilated flaming.

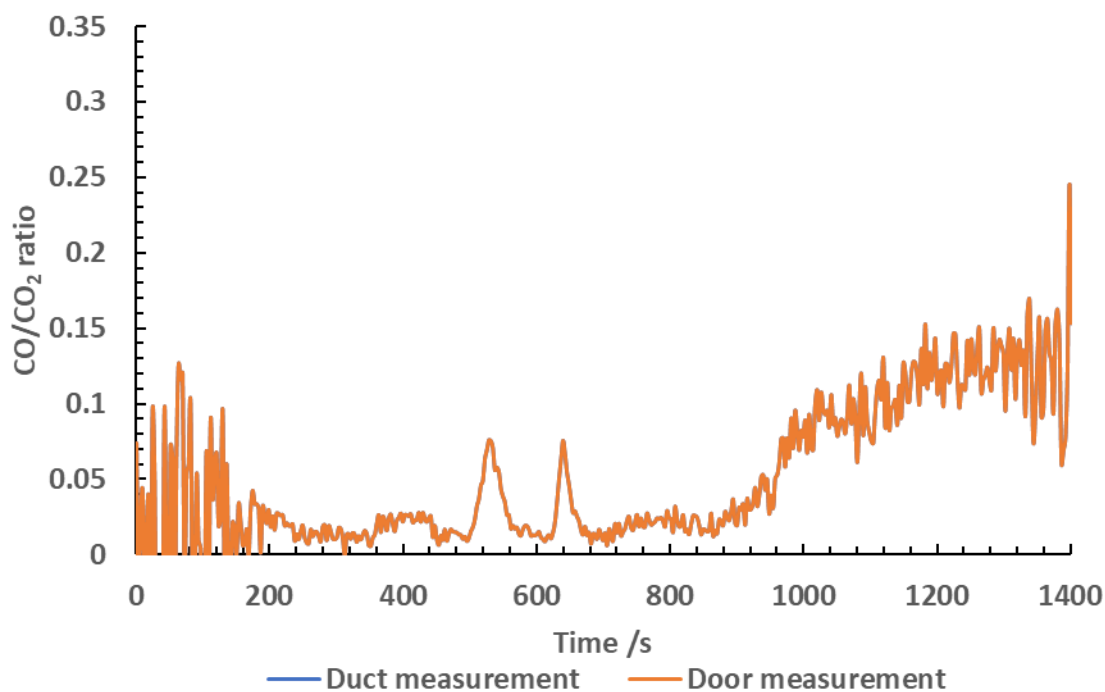


Figure 73: Calculated CO/CO₂ ratios in the exhaust duct and door when testing OSB in the ISO room (1x SBI no door).

3.3.1.10 Test observations and summary

After ignition, the fire effluent slowly rose to the ceiling and a smoke layer developed in the test room. As the fire progressed, the effluent became diluted with plenty of fresh air entering the room and mixed with the fire effluent. As the test continued, the hot smoke layer grew and was observed to leave the room in a plume 40 to 70 cm down from the ceiling. As the doorway was open and the fuel loading in the test was limited, the fire did not transition to under-ventilated flaming.

As the smoke was extracted from the room, the fire could continue growing until all the available fuel ran out due to the availability of oxygen from the open doorway. The smoke produced was relatively clean with only small amounts of sooty smoke being observed. Due to the availability of oxygen and fuel, the mixture of gasses and air in the smoke layer was able to burn efficiently.

The oxygen, CO and CO₂ data were all representative of well-ventilated flaming conditions, which were in agreement with the equivalence ratio measurements taken throughout the test. The test was deemed successful in achieving well-ventilated flaming.

3.3.2 Under-ventilated with door

3.3.2.1 Test layout and fuel loading

OSB was attached to an SBI rig with a 4 mm air gap between the material and the calcium silicate boards. The board was approximately 12 mm thick and slightly raised above the burner as in the SBI test. One SBI rig was set up for the test. A total mass of 14.59 kg of OSB was used. For this test, one SBI rig was used (denoted by 1 x SBI)

The SBI rig was placed on the load cell in the centre of the ISO room. Gas analysers were calibrated and set up for testing. Heptane was measured out and poured into the burners inside the room. The ISO room measurements were started alongside the gas analysers 2 minutes before ignition. The heptane burners were ignited manually. After ignition, a 1.3 m door was placed over the bottom part of the door of the ISO room to restrict the ventilation into the room.

The airflow was monitored using McCaffrey probes throughout the test. In this test, the lower McCaffrey probe was altered so that the inlet to the probe was facing outwards. The data was recorded for future use for calculations of the volume flow of gas in the doorway to be used for yield calculations.

3.3.2.2 Heat release measurements

The heat release measured throughout the test is shown in *Figure 74*. The heat release data is shown with the inclusion of the heat released from the ignition source. The heat release rose rapidly after ignition and reached the peak heat release of 670 kW at 720 seconds into the test. At 725 seconds, the heat release dropped rapidly before gradually declining as the fuel began to run out.

The time to flashover was calculated using the methodology described in the ISO 9705 standard. As the heat release did not surpass 1000 kW, flashover was not reached.

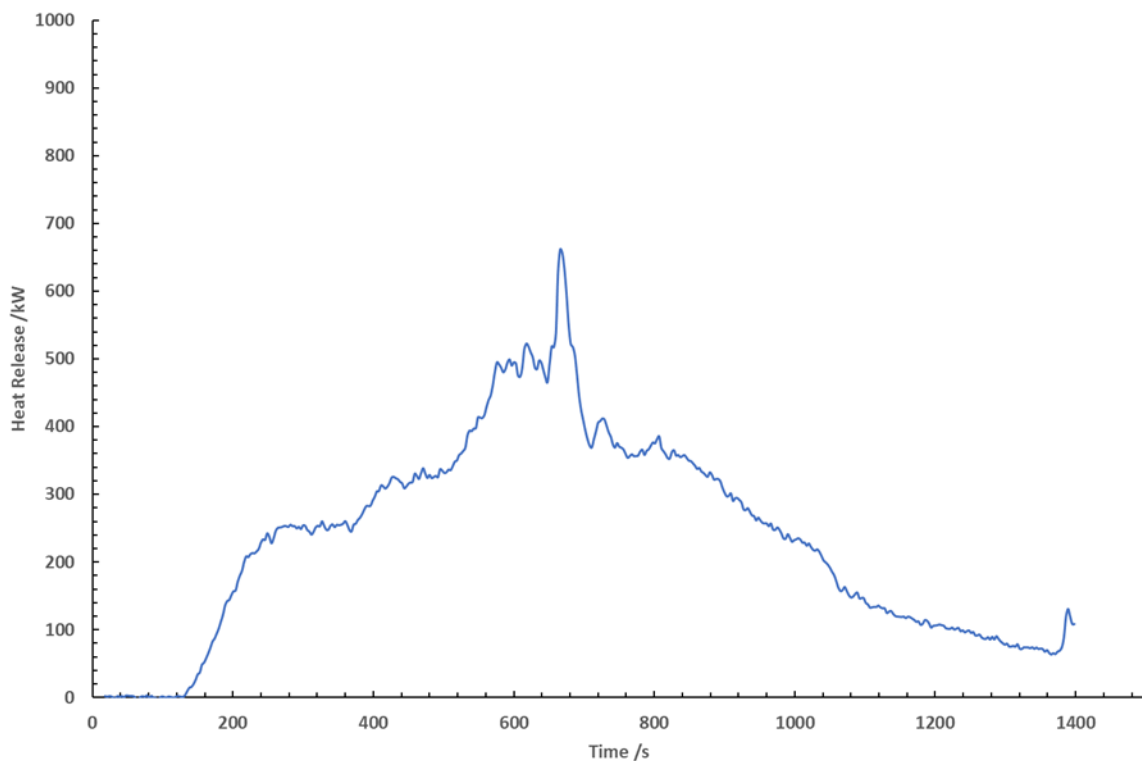


Figure 74: Heat release measurements taken in the ISO room when testing OSB (1x SBI with door)

3.3.2.3 Mass loss

The mass loss measured using the scale in the ISO room throughout the test is shown in *Figure 75*. While the data has been presented, it is thought that the scale did not appear to provide an accurate mass loss measurement as the mass appears to only change by approximately 15 Kg. An additional graph was made using a reduced scale to show the mass loss in more detail. This is shown in *Figure 76*. This more accurately shows the mass loss from OSB that occurred, as the majority of the weight was from the steel frame. The mass was seen to steadily decline over the course of the test.

The mass of the residue at the end of the test was unfortunately not recorded.

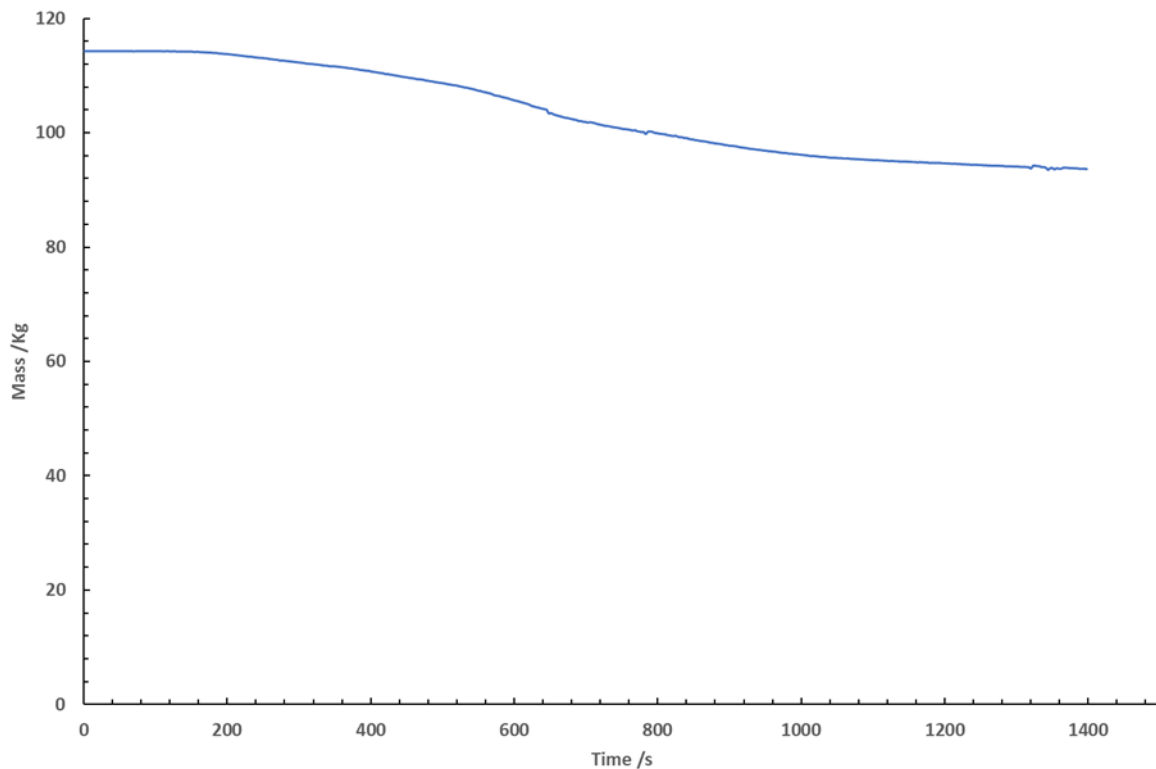


Figure 75: Mass loss measured using the scale in the ISO room when testing OSB (1x SBI with door).

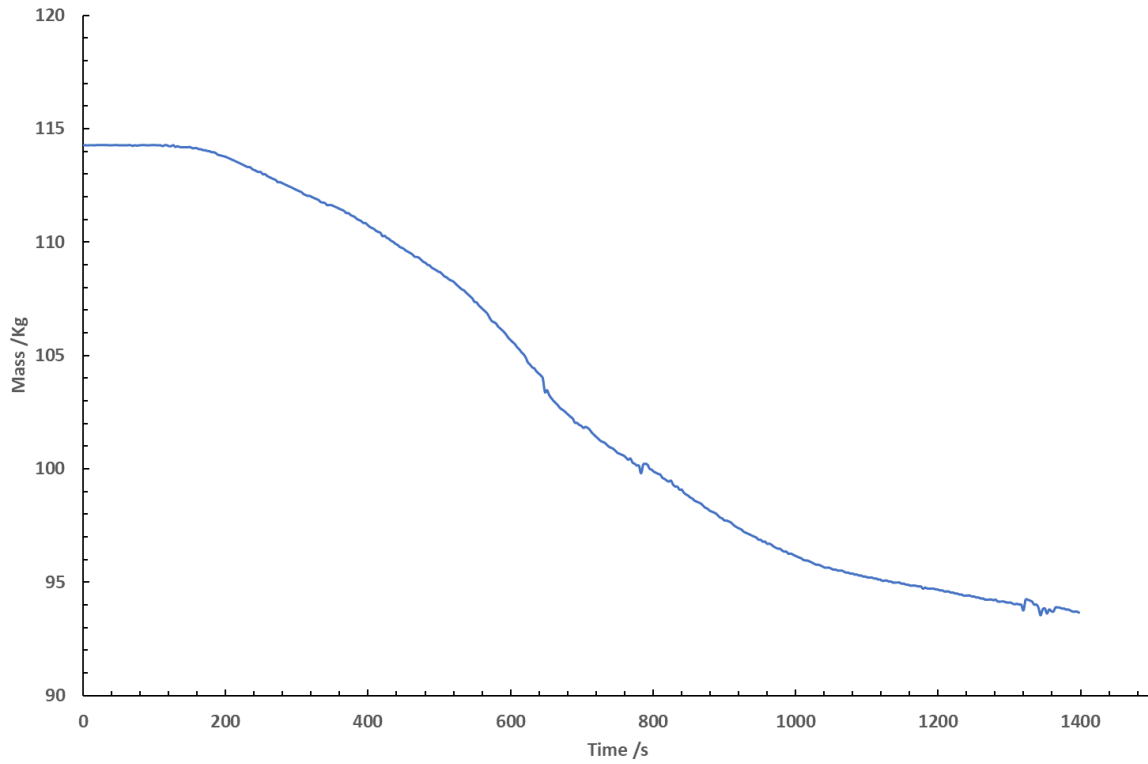


Figure 76: Mass loss measured by the ISO room scale when testing OSB (1 x SBI with door), with a reduced scale axis.

3.3.2.4 Temperature

The temperature measurements taken in the doorway of the ISO room throughout the test are shown in *Figure 77*. The temperatures show a rapid increase upon ignition, reaching a maximum temperature of 580 °C before slowly declining as the fire begins to decrease.

The temperature profile was used to identify the neutral plane to calculate air velocity in and out of the room. As the door covered the bottom third of the door, the measurements taken more than 80 cm from the ceiling are negligible. It should be noted that the temperatures below the door-block are closely grouped as this was entirely static air. It is interesting to note the similarity of the peak temperature compared to *Figure 68*, despite the additional door block.

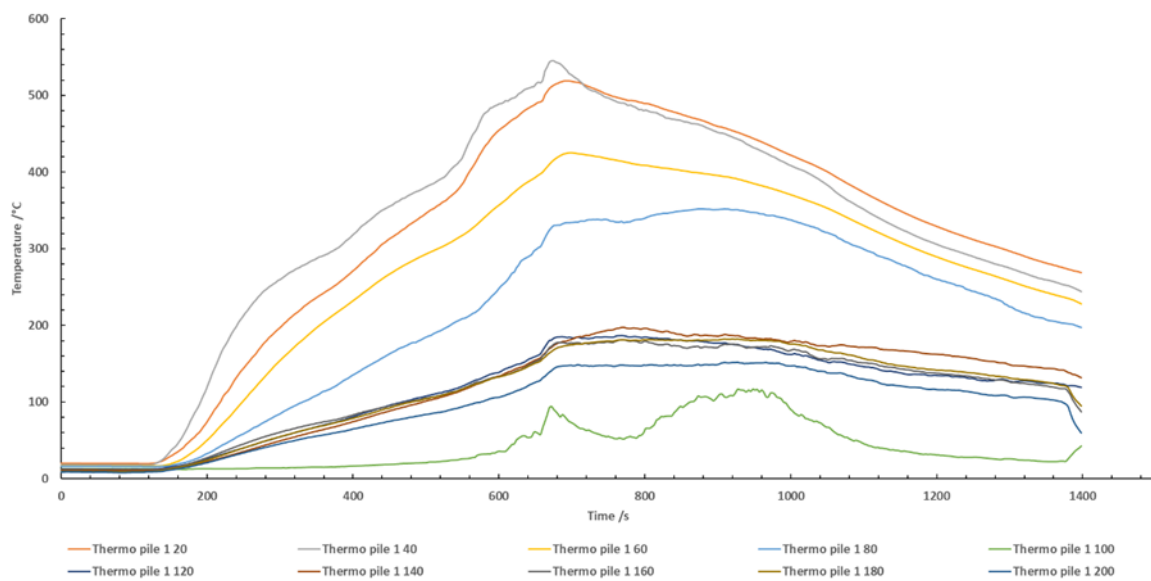


Figure 77: Temperature measurements taken in the doorway of the ISO room when testing OSB (1x SBI with door). The measurements are taken from thermocouples labelled 'Thermo pile 1' with the final number indicating the distance from the ceiling in cm (e.g. Thermo pile 1 40, meaning thermocouple 1, 40 cm from the ceiling).

3.3.2.5 Fire condition

The fire condition was monitored using a phi meter throughout the test. The equivalence ratio was calculated and is shown in *Figure 78*. The peak equivalence ratio of 0.95 was reached 610 seconds into the test.

The equivalence ratio rose steadily upon ignition, however the fire did not transition into under-ventilated flaming despite the door restricting the ventilation of the test room.

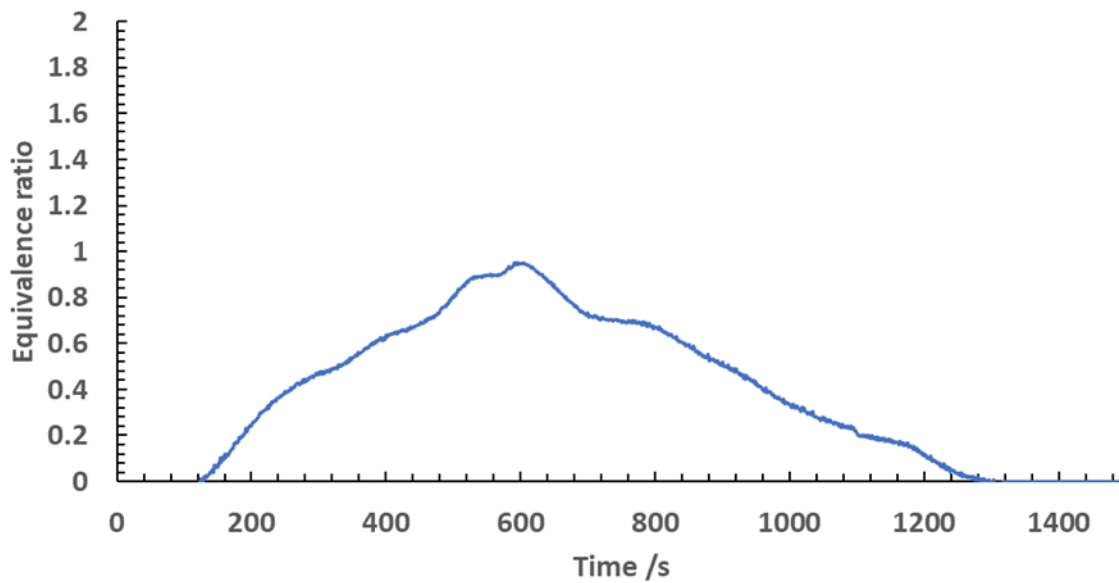


Figure 78: Equivalence ratio measured when testing OSB (1x SBI with door) in the ISO room.

3.3.2.6 Oxygen measurements

The oxygen concentrations logged throughout the test are shown in *Figure 79*. The oxygen concentrations measured in the door dropped rapidly upon ignition, gradually lowering to 2.5 % at 620 seconds. The oxygen concentrations remained below 15 % throughout the middle of the test. In the duct, the oxygen concentration did not deviate significantly from baseline values. This is likely a result of the excess flow used in the exhaust duct.

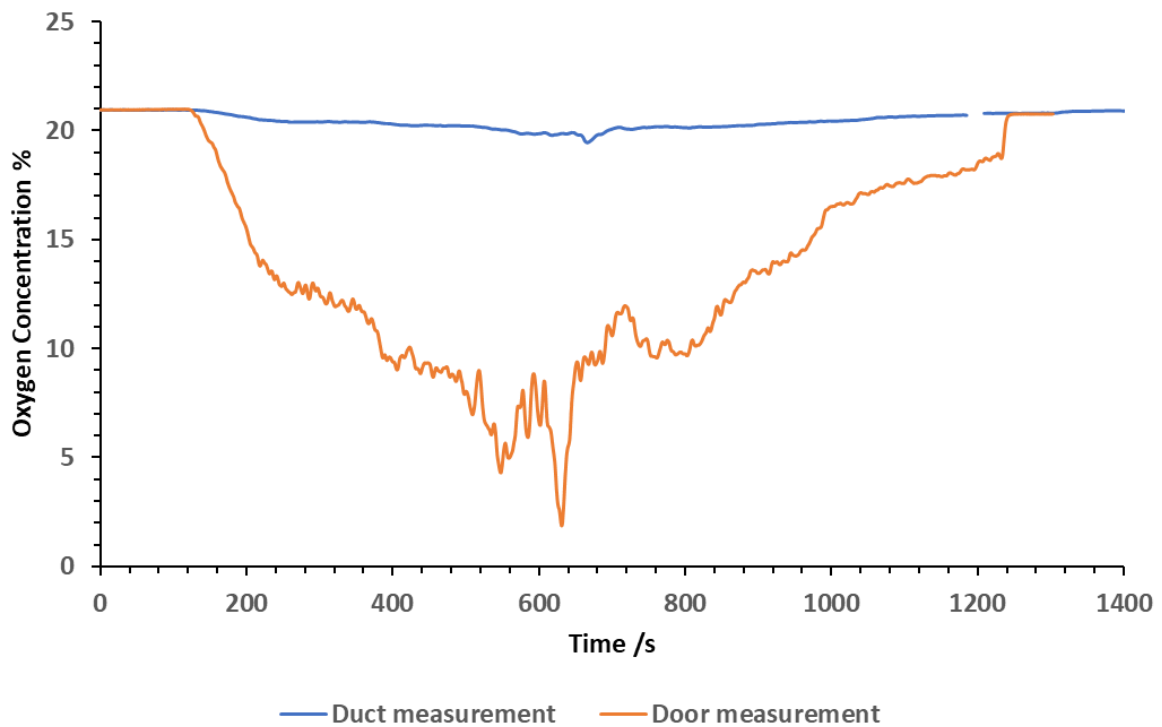


Figure 79: Oxygen measurements taken in the doorway and duct of the ISO room when testing OSB (1x SBI with door).

3.3.2.7 CO₂ measurements

The CO₂ concentrations measured in the door and exhaust duct throughout the test are shown in Figure 80. Due to a measurement issue in the doorway, the CO₂ concentrations were not logged. The doorway measurement was calculated using the exhaust duct data multiplied by the dilution factor (4).

The CO₂ measured in the exhaust duct remained relatively low, reaching its peak concentration of 1.2 % at approximately 620 seconds into the test. Overall, the CO₂ measured was relatively stable and steady. The CO₂ measured in the door reached a calculated peak concentration of 4.45 % 620 seconds into the test.

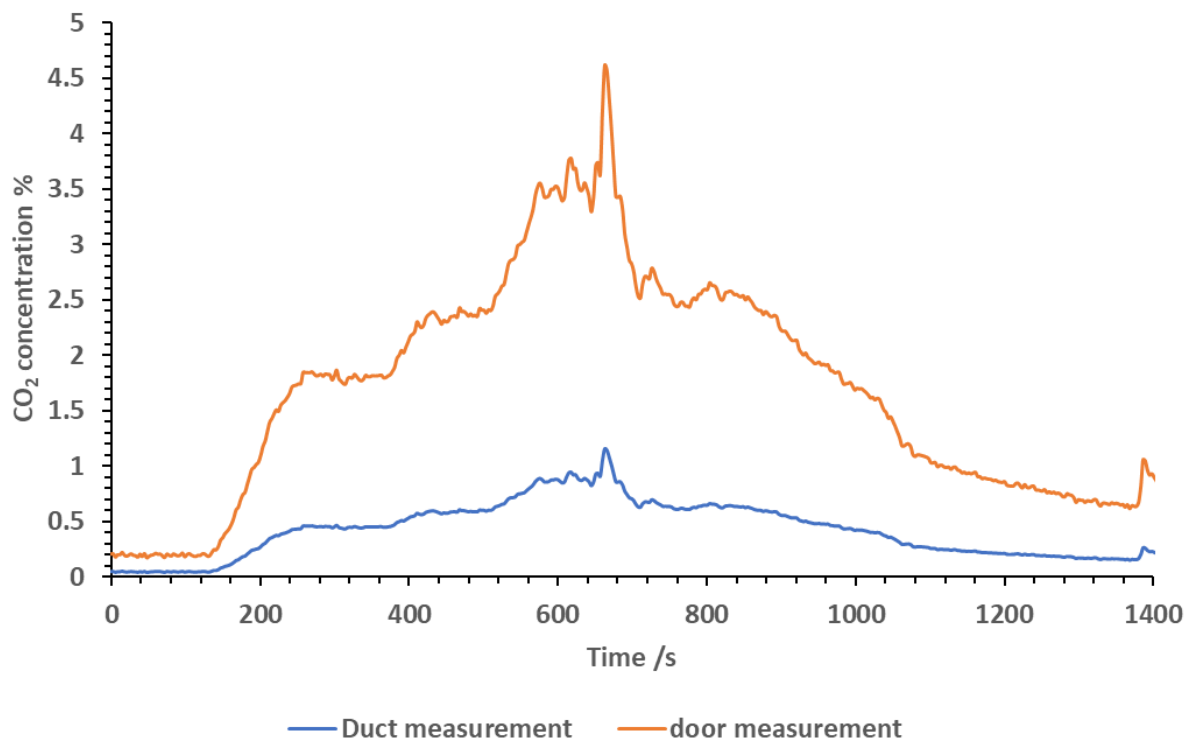


Figure 80: CO₂ measurements taken in the door and exhaust duct of the ISO room when testing OSB (1x SBI with door using a calculated doorway measurement value).

3.3.2.8 CO measurements

The CO measurements taken throughout the test in the door and exhaust duct are shown in Figure 81. Due to a measurement issue in the doorway, the concentrations of CO were not logged. The CO presented is a calculated value using the exhaust duct data multiplied by the dilution factor of 4. The CO in the exhaust duct was similar to the concentrations measured in the door. The door measured slightly higher concentrations of CO, with a peak concentration of 0.09 % at 600 seconds into the test, shortly after ignition. At this point it was calculated that the concentration in the doorway was 0.36 %. A peak concentration of 0.075% was reached in the exhaust duct at 700 seconds into the test, and 0.3 % in the doorway.

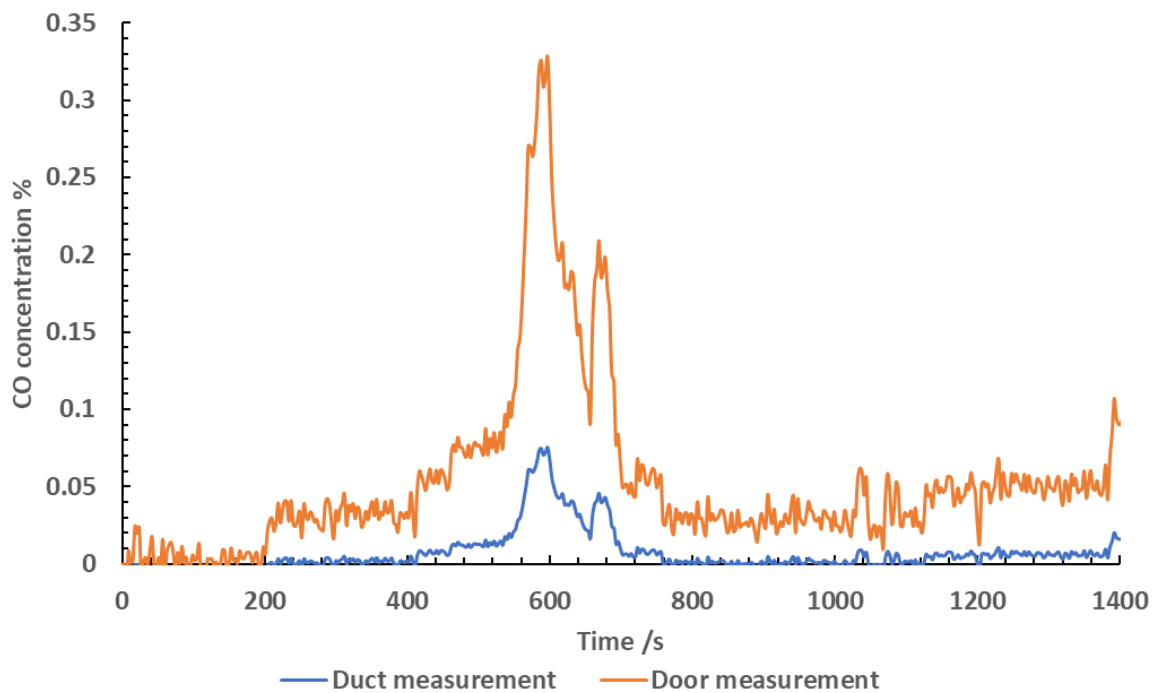


Figure 81: CO measurements taken in the door and exhaust duct of the ISO room when testing OSB (1x SBI with door).

3.3.2.9 CO/CO₂ ratio

The calculated CO/CO₂ ratio in the exhaust duct and door is shown in Figure 82. As the doorway values were calculated using the exhaust duct data, only the calculated ratio for the duct is shown. This is because the ratio would be identical for both places.

The first 200 seconds of the test are very noisy as a result of very low measurements of CO and CO₂ in the exhaust duct. As this was during ignition, it is not representative of the actual test. The most representative part of the data is from 400 to 800 seconds. During this time, there is a peak ratio of 0.13. This is within the realms of well-ventilated flaming. Towards the end of the test (post 800 seconds) the data becomes very noisy again, and begins to increase. As flaming had ceased by this point in the test, the data beyond 800 seconds is not meaningful.

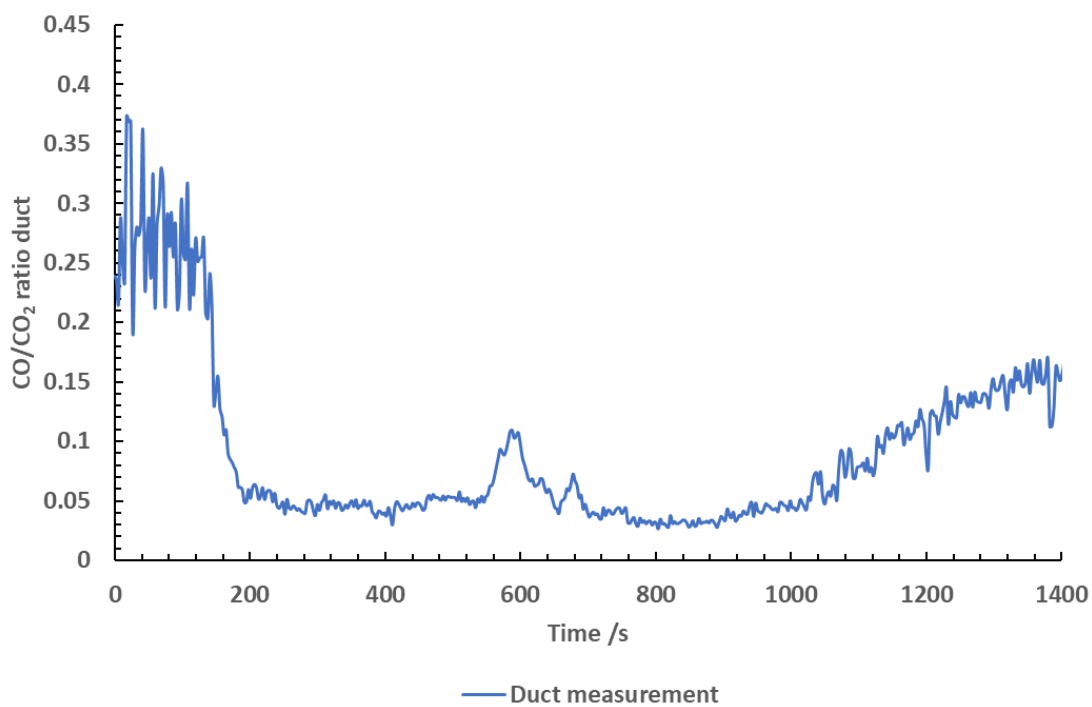


Figure 82: CO/CO₂ ratio calculated when testing OSB (1x SBI with door) in the ISO room.

3.3.3 Under-ventilated (using 2x fuel load)

3.3.3.1 *Test layout*

OSB was attached to an SBI rig with a 4 mm air gap between the material and the calcium silicate boards. The board was approximately 12 mm thick and slightly raised above the burner as in the SBI test. Two SBI rigs were set up for the test. A total mass of 30.65 kg of OSB was used.

The SBI rigs were placed on the load cell in the centre of the ISO room. Gas analysers were calibrated and set up for testing. Heptane was measured out and poured into the burners inside the room. The ISO room measurements were started alongside the gas analysers 2 minutes before ignition. The heptane burners were ignited manually.

3.3.3.2 Heat release measurements

The heat release measured throughout the test is shown in *Figure 83*, with the inclusion of the heat released from the ignition source. The peak heat release of 4500 kW was reached at 420 seconds into the test. Prior to reaching its peak heat release, the fire plateaued at around 2000 kW from 200 seconds to 400. The sharp rise could be a radiant effect from the two SBI rigs facing each other after both were fully flaming, or could be a result of both sides of the OSB flaming at once. After the peak heat release was reached, the heat release began to decline rapidly. The time to flashover was calculated using the methodology described in the ISO 9705 standard. The Time to flashover was calculated as 180 seconds.

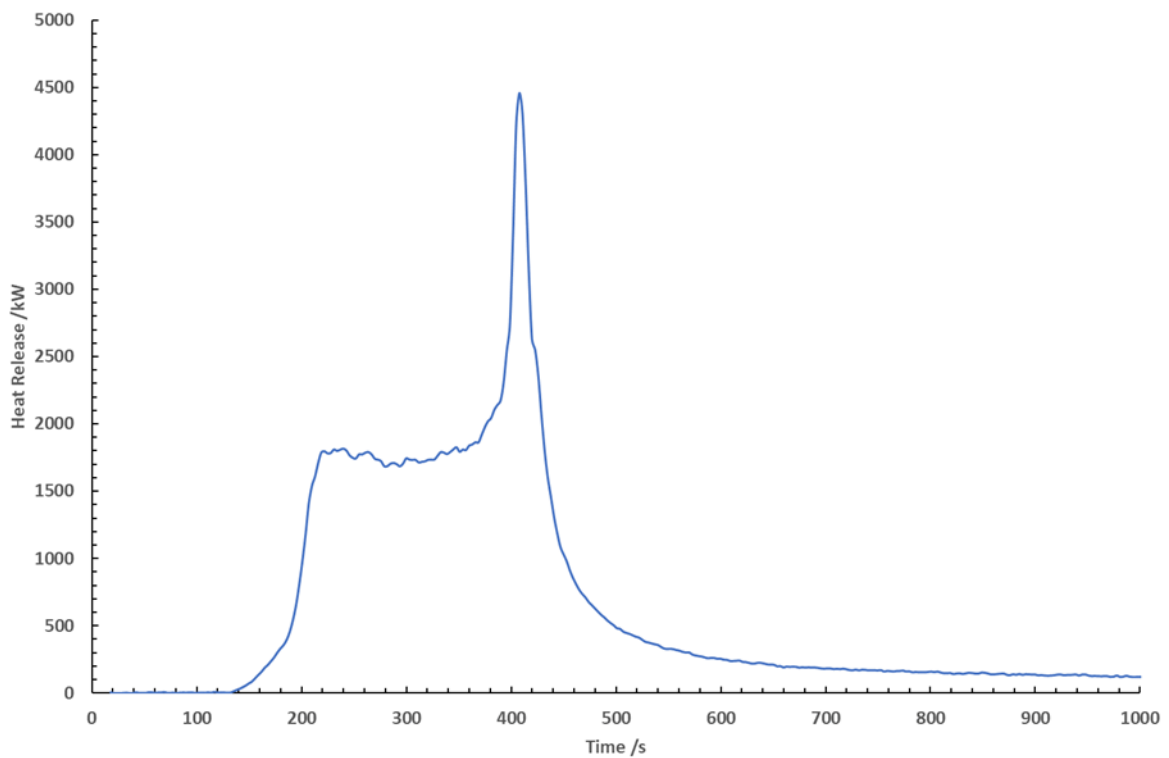


Figure 83: Heat release measurements taken in the ISO room when testing OSB (2x SBI no door).

3.3.3.3 Mass loss

The mass loss measured throughout the test is shown in Figure 84. The initial measurement was not recorded due to the test rig exceeding the maximum measurement of the scale (165 kg). The mass had reduced enough by 420 seconds to measure the actual mass loss occurring in the test rig. The largest mass loss was observed at 320 seconds to 420 seconds. The plateau observed from 400 onwards is a result of a slow smouldering fire occurring after the test had finished.

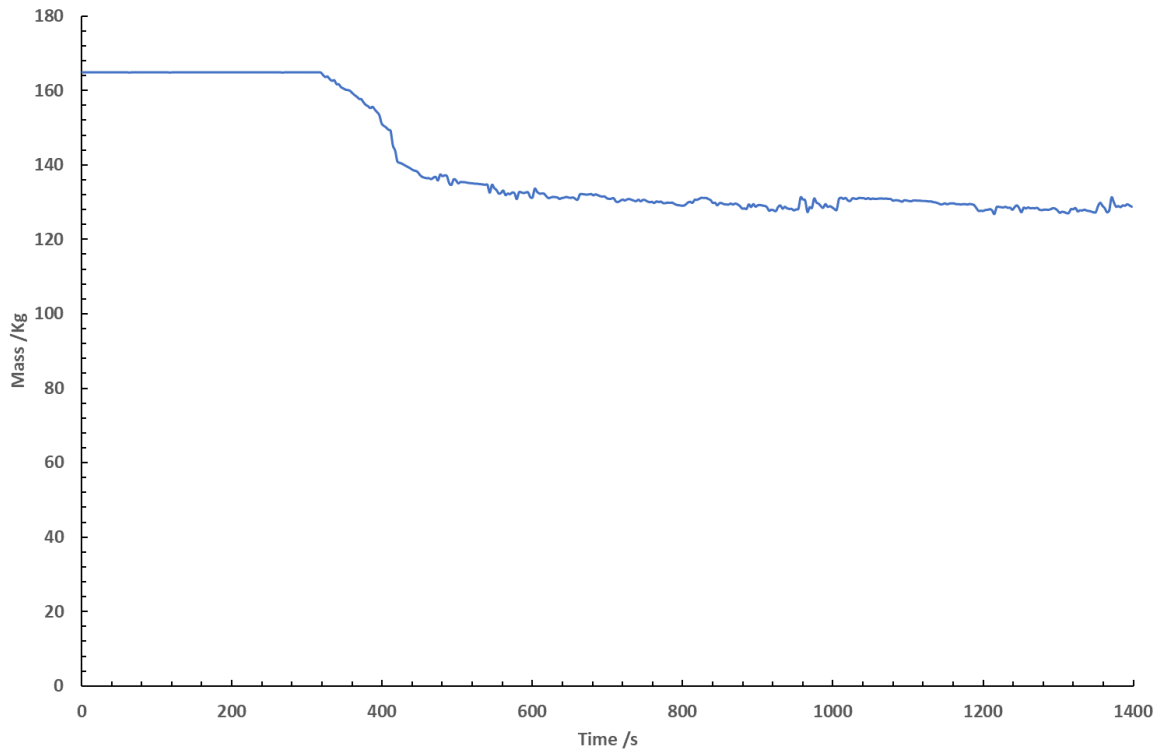


Figure 84: Mass loss measured using the scale in the ISO room when testing OSB (2x SBI no door).

3.3.3.4 Fire condition

The fire condition was monitored throughout the test using a phi meter. The data is shown in *Figure 85*. Upon ignition, the equivalence ratio grew rapidly, reaching its peak value of 1.50 at 400 seconds into the test. The fire was able to transition fully into under-ventilated flaming due to the significant amount of fuel present in the test room and the high heat release. Under-ventilated flaming was sustained between 300 to 420 seconds. After this point, the fuel became limited, and the fire began to decrease in size, seen by a decrease in equivalence ratio.

When the maximum equivalence ratio was reached, flaming combustion occurred in the doorway, and so the stainless steel sampling lines were sampling from the flame zone within the doorway. This means that while the fire was clearly under-ventilated, the measurements taken may not be truly representative of the actual burning conditions occurring inside of the room. It would have been useful to know the equivalence ratio in the exhaust duct and compare the data in an attempt to understand the test condition better.

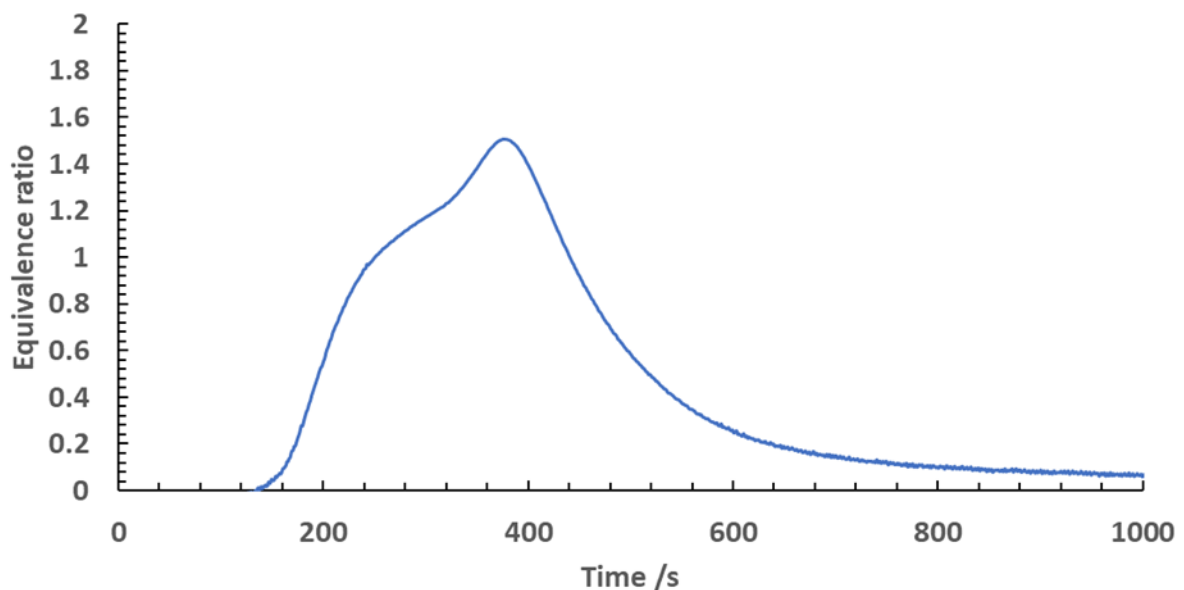


Figure 85: Equivalence ratio monitored in the ISO room when testing OSB (2x SBI no door).

3.3.3.5 Temperature measurements

The temperature measurements are shown in *Figure 86*. The peak temperature reached was 900 °C, 40 cm below the ceiling. The excess heat produced from the fire is likely a result of radiant effects occurring as the two burning test rigs faced each other, causing an increase in the overall heat measured inside the room.

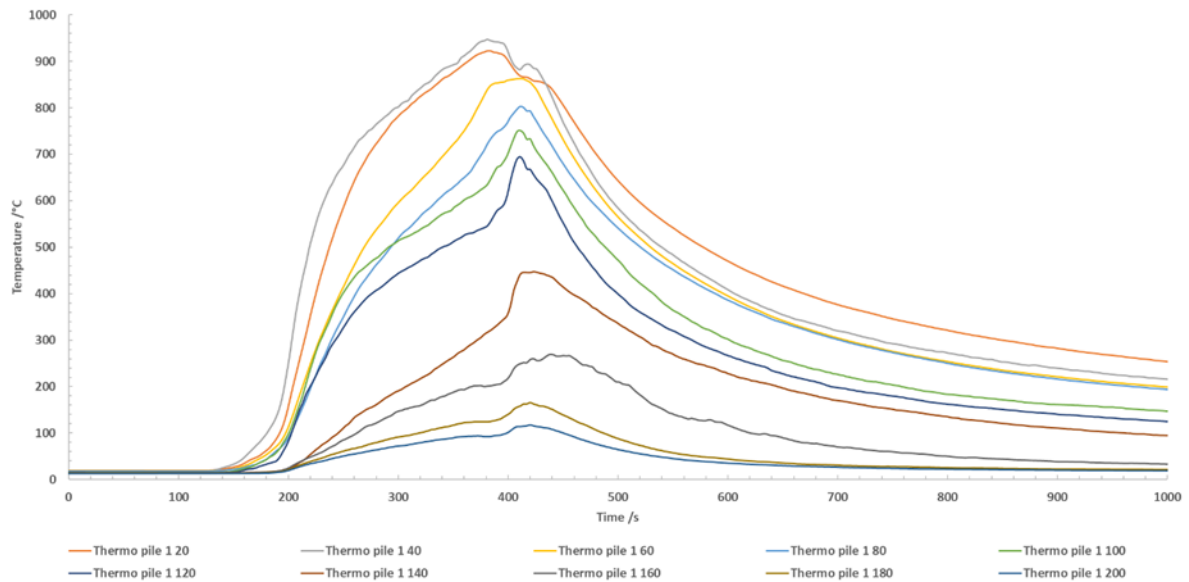


Figure 86: Temperature measurements taken in the doorway of the ISO room when testing OSB (2x SBI no door). The measurements are taken from thermocouples labelled 'Thermo pile 1' with the final number indicating the distance from the ceiling in cm (e.g. Thermo pile 1 40, meaning thermocouple 1, 40 cm from the ceiling).

3.3.3.6 Oxygen measurements

The oxygen measured in the door and exhaust duct throughout the test is shown in *Figure 87*. After ignition, the oxygen levels in the door begin to decline rapidly. The oxygen in the exhaust duct dropped to 16.5 % approximately 200 seconds into the test, with the door measurements dropping to 2% comparatively. At 350 seconds into the test, the oxygen measurements in the doorway dropped to 0%, and remaining that low for 200 seconds. The sampling at this point was occurring within the flame zone as the flames from the fire were seen to be exiting the doorway during this time. The oxygen concentrations in the exhaust duct fell to 5% at approximately 400 seconds into the test. The concentration was higher than that measured in the door from a combination of the excess air flow being drawn into the exhaust duct, as well as the sampling not occurring within the flame zone. The concentrations measured in the exhaust duct and the doorway were representative of under-ventilated flaming. After 400 seconds, the fire began to run out of fuel, resulting in less flaming combustion occurring. This allowed more oxygen to enter the room and the oxygen concentrations were observed to rise gradually until baseline values were reached.

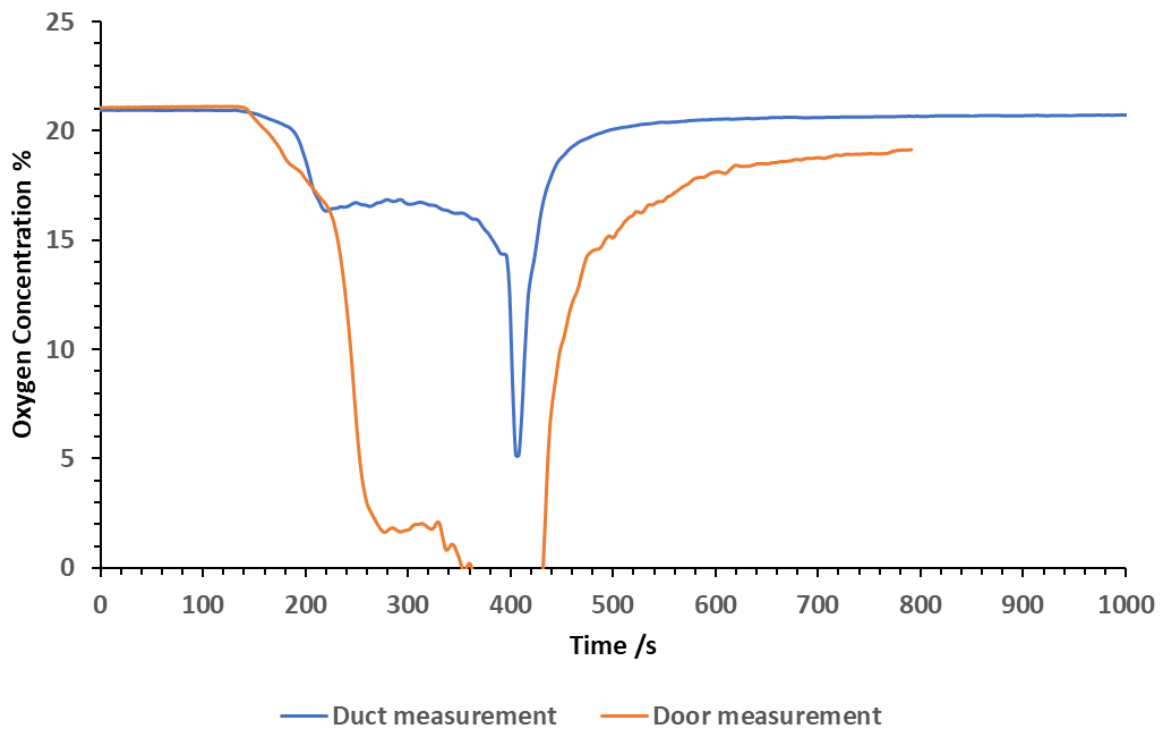


Figure 87: Oxygen measurements taken in the door and exhaust duct of the ISO room when testing OSB (2x SBI no door).

3.3.3.7 CO₂ measurements

The CO₂ concentrations logged throughout the test are shown in Figure 88. The CO₂ concentrations measured in the exhaust rose rapidly upon ignition, reaching a concentration of 5.8 % in the exhaust duct at 200 seconds. The concentration plateaued, until another sharp rise in concentration was observed at 400 seconds, reaching 14 %. Similarly, the CO₂ in the doorway rose rapidly upon ignition, reaching a concentration of 14.8 % and plateauing for approximately 40 seconds before rising again, recording a peak concentration of 16.8%. This is towards the upper limit of the measurable range of the NDIR. However, it is also indicative of more CO₂ being formed after it passed the doorway.

The CO₂ concentration declined rapidly after reaching the peak concentration as a result of the fire running out of fuel. The CO₂ concentrations measured in the door were indicative of under-ventilated flaming occurring. The point at which the CO₂ concentrations were at their highest coincides with the point at which the equivalence ratio was at its highest, and the oxygen concentration was at its lowest.

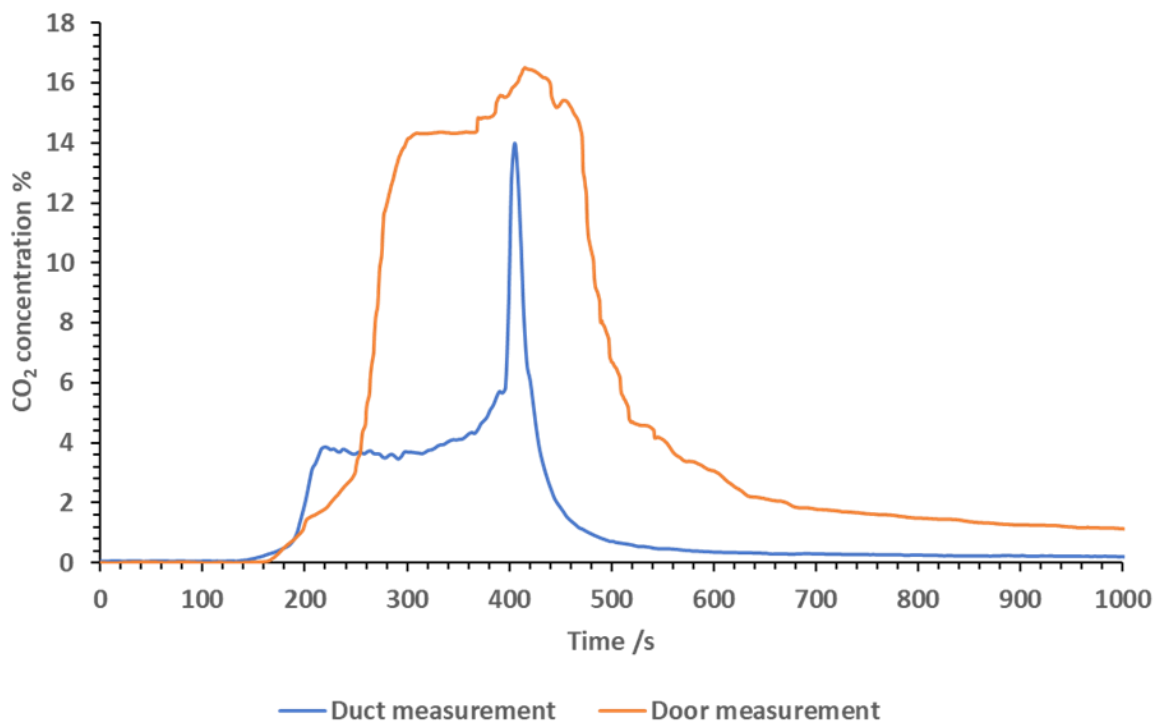


Figure 88: CO₂ measurements taken in the door and exhaust duct of the ISO room when testing OSB (2x SBI no door)

3.3.3.8 CO measurements

The CO measurements taken in the exhaust duct and door throughout the test are shown in *Figure 89*. The CO concentration rose rapidly upon ignition, with the measurements in the exhaust reaching a peak of 0.9 % and a peak of 5.1 % in the door. The CO concentrations measured in the exhaust duct were relatively stable and remained below 1% throughout the duration of the test, suggesting that the effluent in the duct was either very diluted, or undergoing further chemistry between the doorway and duct, or inside the duct. This is supported by the difference in shape seen in the graph. It shows that CO is leaving the room, and becoming CO₂ by the time it reaches the duct.

The CO measurements taken in the doorway were significantly higher, however for part of the test that the flames were exiting the room door, resulting in the sampling taking place within the flame zone. While the measurements taken are representative of under-ventilated flaming, there are limitations in the conclusions that can be made from the data as the sampling was not in the smoke plume but rather the flaming zone.

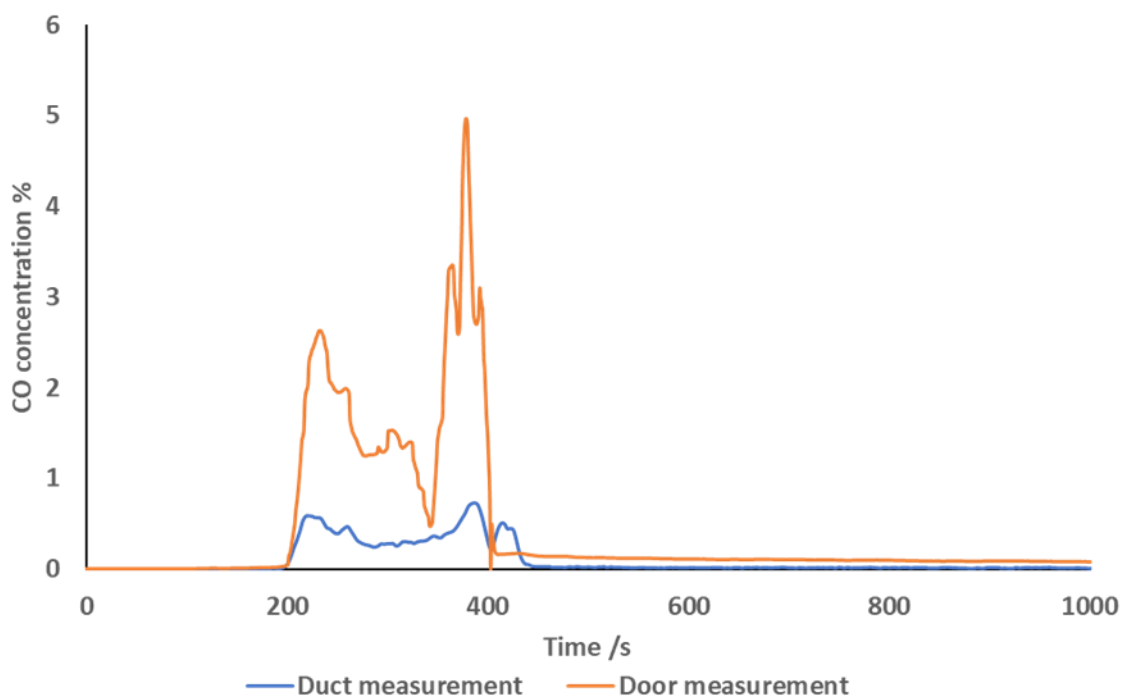


Figure 89: CO measurements taken in the door and exhaust duct of the ISO room when testing OSB (2x SBI no door).

3.3.3.9 CO/CO₂

The CO/CO₂ ratio calculated throughout the test in the exhaust duct and doorway is shown in *Figure 90*. The CO/CO₂ ratio showed the same initial peak at the beginning of the test as in the CO data. Upon sample ignition, the CO/CO₂ ratio increased gradually throughout the test. A peak ratio of 1.2 was calculated from the measurements taken in the doorway, however due to the flames engulfing the sampling tubes throughout the test, the measurements were therefore taken in the flame zone and not the smoke plume, meaning the ratio is not directly indicative of the actual burning conditions in the room. The CO/CO₂ ratio calculated in the exhaust duct was much lower, reaching a peak value of 0.2. The difference between the two ratios is a good indicator of the extent of the oxidation occurring outside of the ISO room. The ratios are indicative of under-ventilated conditions.

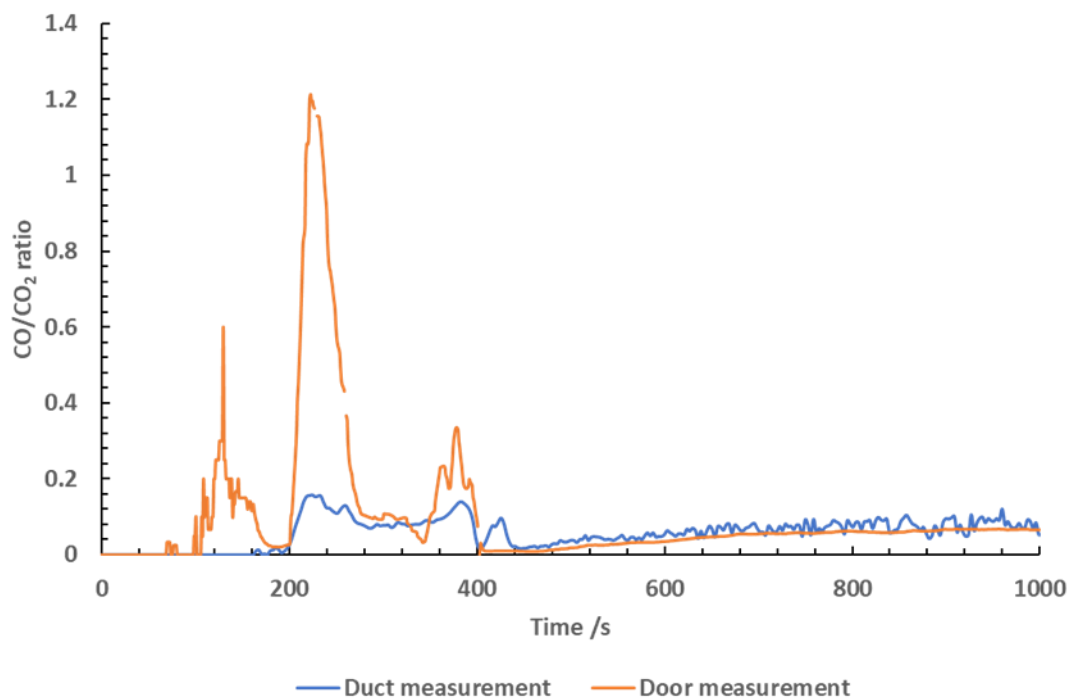


Figure 90: CO/CO₂ ratio calculated from the measurements taken in the doorway and exhaust duct of the ISO room when testing OSB (2x SBI no door).

3.3.3.10 Summary description of test:

The fire started off well-ventilated. As the fire continued to grow, the upper smoke layer grew and descended in the room. As the fire progressed, the smoke layer started to pour out of the doorway. As the equivalence ratio surpasses 1, the fire visibly transitioned to under-ventilated flaming where the flames were seen to reach the room's ceiling. The concentration of air entering the fire began to decrease. This continued as the equivalence ratio increased.

During the test, the flames descended below the smoke layer. This is typical in fires where the size of the room is the limiting factor. At this point, the smoke layer began to descend until it reached a steady burning period. During this point, oxygen concentrations in the door dropped below 1%, reaching 0% at their lowest. At this point of the test, the flames were pouring out of the door, passing over the stainless steel sampling lines. The measurements were taken in the flame zone, so it is likely that the effluent sampled underwent further chemistry later in the exhaust duct.

The peak equivalence ratio reached was 1.5. The peak aligns with the point at which CO concentrations measured at the door are at their highest, and where the oxygen concentration in the door dropped to its lowest.

3.3.4 OSB: Data comparison

The heat release, equivalence ratio and CO concentrations were compared between the three tests in the following sub-sections. The data is summarised in *Table 24*.

Table 24: A comparison of the data obtained from testing OSB in the ISO room using several different test configurations for different fire conditions.

Material	Test set up	Aimed test condition	Max equivalence ratio measured	Peak heat release measured /kW	Max CO concentration %	
					Door	Exhaust duct
OSB	1x SBI with no door	Well-ventilated	0.70	990	0.48	0.12*
	1x SBI with door	Under-ventilated	0.95	760	0.36	0.09*
	2x SBI with no door	Under-ventilated	1.50	4500	5.1	0.9

*indicates calculated value using exhaust duct data.

Using 3 different test configurations allowed for different experimental set-ups to be assessed to identify what is needed to achieve specific burning conditions in the ISO room corner test. The use of 1x SBI rig with no door meant that the fire had enough ventilation and fuel to burn well-ventilated. This was evidenced by the equivalence ratio of 0.7. The heat release from the test was relatively high, with a peak heat release of 990 kW being measured. The CO yield obtained were representative of well-ventilated flaming. The measurements taken in the exhaust duct were very dilute. This was the case for most of the gas measurements taken in the duct when compared to the door measurements.

The HRR curves for 1 x SBI where the doorway was fully open and shut off show remarkable similarity, including a similar peak occurring at 640 seconds. This was presumably when both sides of the OSB were burning at the same time. However, the peak HR for the partially blocked doorway is around 660 kW, rather than 990 kW for the open doorway. This demonstrates the effect of partially blocking the door to the ISO room is slowing the rate of burning, rather than forcing under-ventilated flaming.

Comparatively, the addition of a door to the test room did not force the fire to transition to under-ventilated flaming. Despite the restriction on the ventilation, the maximum equivalence ratio reached was only 0.95. The peak heat release measured decreased with the addition of the door on the test room. This was likely a result of the calcium silicate board used as the door absorbing a portion of the heat from the fire, resulting in a lower heat measurement.

When using 2x SBI rigs with no door, there was sufficient fuel for the fire to transition to under-ventilated flaming. The equivalence ratio was measured to be 1.5 at its peak, which is representative of under-ventilated conditions. However, the sampling did take place inside of the flame as the fire became so vigorous that the flames poured out of the test room for a significant portion of the test. This means that the equivalence ratio was 1.5 within the flame zone, and is less indicative of the actual fire condition in the room.

Conducting three different test scenarios on the same material has allowed for the identification of test conditions to be made in regards to controlling the ventilation of the test. In large-scale testing, particularly when using the ISO room, fuel loading and test geometry has more significant impact on the fire condition than restricting the ventilation. While imposing restrictions on the test rooms ventilation did increase the equivalence ratio, it was not sufficient enough to force the transition into under-ventilated flaming.

This research has provided the experimental methodologies to assess smoke toxicity at a range of ventilation conditions in an ISO 9705 test room. The equivalence ratios obtained were representative of well-ventilated and under-ventilated flaming and the transition point between the ventilation conditions ($\phi = 0.95$).

3.4 CABLES

Two tests were conducted using cables. The aimed conditions were: well-ventilated (by use of no door) and under-ventilated (by using a door).

3.4.1 Test layout

RZ1-L (AS) (0.6/1 kV) low smoke, zero halogen energy cables (from Eland cables Ltd) were purchased and attached to steel cable baskets using copper ties. The cables were laid out with a minimal air gap. Three individual 4 m long cable baskets were set up on a stainless steel holder. The cable tray set up was placed diagonally inside the test room to allow the scale to be used during the test. The cables were set up with the top tray 0.3 m from the ceiling. The second and third trays were set up 0.6 and 0.9 m from the ceiling. Photographs of the final set up of the cable tests is shown in *Figure 91*.

The test used a standard ISO room propane burner and followed standard procedure for ignition. For the well-ventilated test, the test room door was left uncovered. A 1.3 m door blocker was placed on the test room with the attempt of restricting the ventilation and forcing under-ventilated conditions to occur. McCaffrey probes for air flow measurements and gas sampling were set up in the same locations as aforementioned.



Figure 91: Picture of the cable trays set up on a stainless steel holder for testing in the ISO 9705 room corner. The ISO 9705 propane burner, while not visible, is below the end of the cable trays in the corner.

3.4.2 Well-ventilated

This test was conducted as described above and did not use a door to restrict ventilation. The test was aimed to be well-ventilated.

3.4.2.1 Heat release

The heat release measured throughout the test, after exclusion of the propane burner, is shown in *Figure 92*. The heat release rises rapidly upon ignition, but remained relatively sporadic from 250 to 800 seconds. The peak heat release of 720 kW was reached at 900 seconds into the test. After this, the heat release rate declined rapidly over the course of 500 seconds. The time to flashover was calculated using the methodology described in the ISO 9705 standard. As the heat release did not surpass 1000 kW, flashover was not reached.

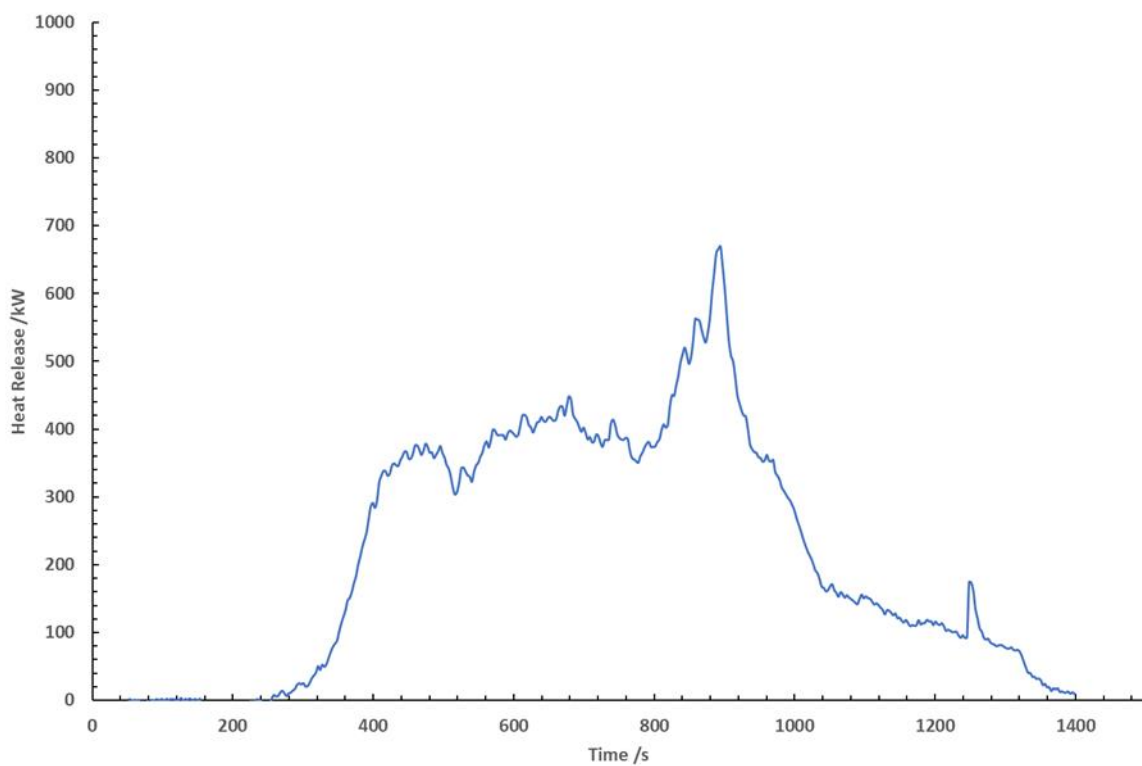


Figure 92: Heat release measurements taken when testing cables in the ISO room with no door.

3.4.2.2 Mass loss

The total mass of the test rig exceeded the capacity of the scale. The data was recorded and shown in Figure 93. As the change in mass was difficult to see in the graph due to the weight of the cable tray and stand, a reduced scale, zoomed in graph has been provided to show the mass loss more clearly. This is shown in Figure 94. The mass loss is very unsteady, showing increases in mass measurements during the test. This could be due to a measurement issue with the scale as it is very unlikely that the cables increased in mass during the test.

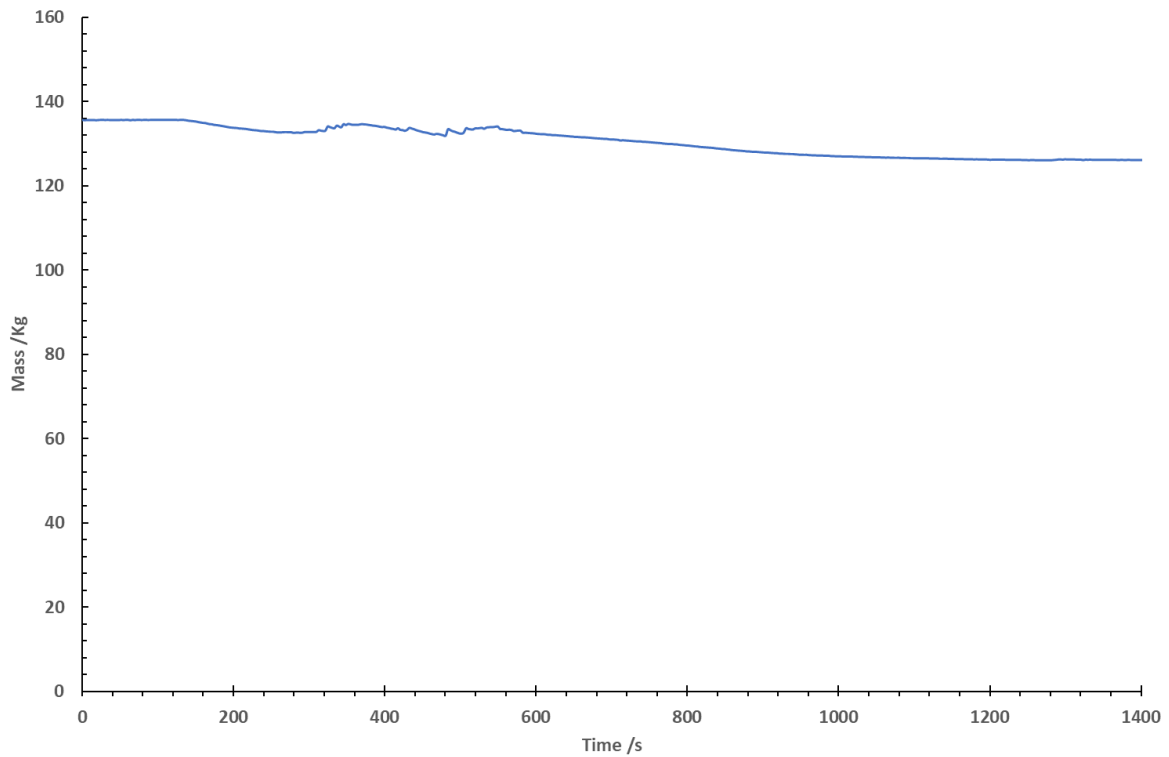


Figure 93: Mass loss measurements taken by the scale in the ISO room when testing cables with no door.

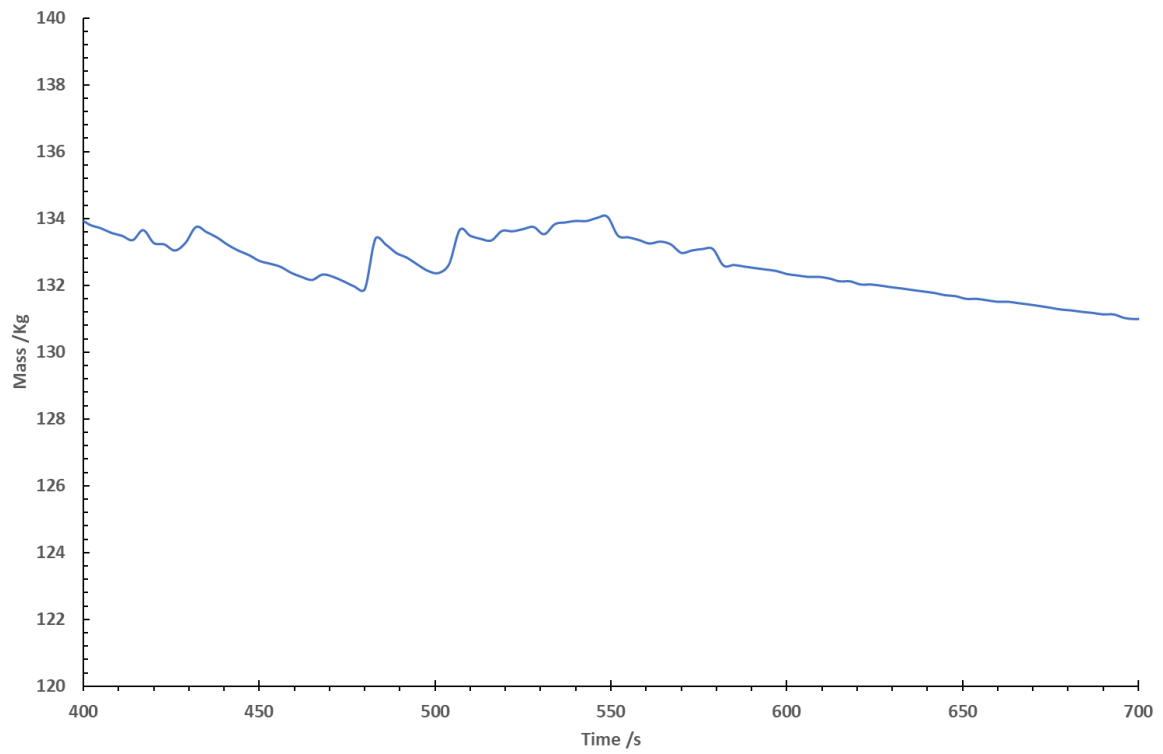


Figure 94: Mass loss measured in the ISO room when testing cables (no door), with a reduced, zoomed in scale.

3.4.2.3 Temperature

The temperature measured were logged in the doorway and are shown in *Figure 95*. The maximum temperature of 825 °C was reached around 900 seconds into the test. The temperature grew steadily over the first 800 seconds of the test, only showing a sharp increase after 800 seconds, despite the cyclic burning behaviour observed throughout the test.

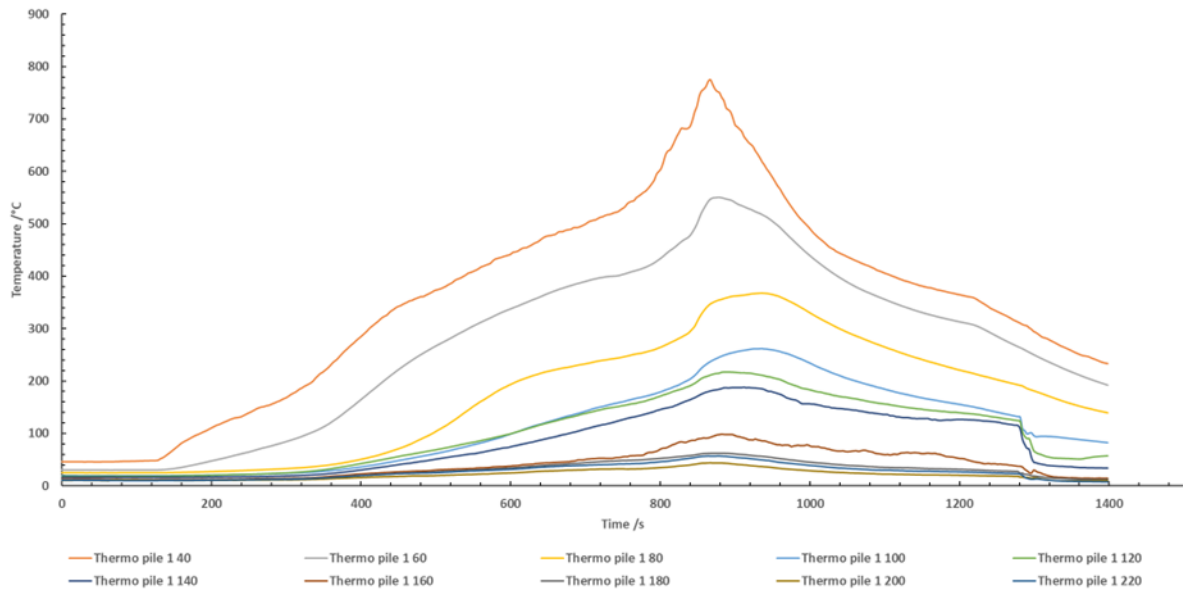


Figure 95: Temperature measurements taken in the doorway of the ISO room when testing Cables with no door. The measurements are taken from thermocouples labelled 'Thermo pile 1' with the final number indicating the distance from the ceiling in cm (e.g. Thermo pile 1 40, meaning thermocouple 1, 40 cm from the ceiling).

3.4.2.4 Fire condition

The fire condition of the test was determined by monitoring the equivalence ratio throughout the test using the phi meter and is shown in *Figure 96*. The equivalence ratio was not logged for the first 200 seconds of the test due to a logging issue with the equipment. The equivalence ratio had reached 0.6 at 200 seconds into the test, which is representative of well-ventilated flaming.

From 200 to 600 seconds in the test, the burning of the cables was somewhat cyclic as fire spread from tray to tray, indicated by the inconsistent equivalence ratio measured. The equivalence ratio stayed between 0.6 and 0.8 throughout. The peak equivalence ratio of 0.76 was reached at 720 seconds and declined gradually shortly after.

While cyclic, the equivalence ratio remained below 1 throughout the test, meaning the fire was well-ventilated.

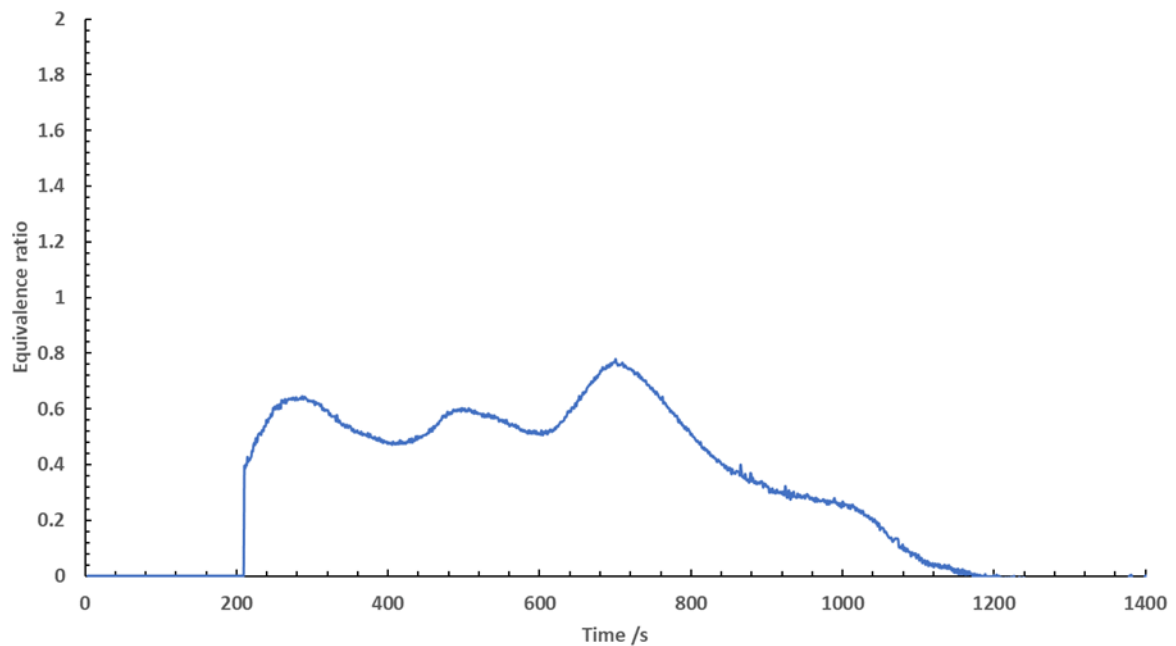


Figure 96: Equivalence ratio measured when testing cables with no door in the ISO room.

3.4.2.5 Oxygen measurements

The oxygen concentrations measured in the exhaust duct and door throughout the test are shown in *Figure 97*. The oxygen concentrations in the exhaust did not deviate significantly from the baseline values. This is likely a result of the dilution from the excess flow in the exhaust.

The oxygen in the doorway dropped rapidly upon ignition, reaching 6 % at 500 seconds. The oxygen concentration then rose rapidly and continued to rise and fall as the cables burned. The lowest concentration of oxygen reached during this test was 5.2 % which occurred at approximately 900 seconds into the test. This sporadic burning of linear cables was similar to the observations made when testing cables on a bench-scale.

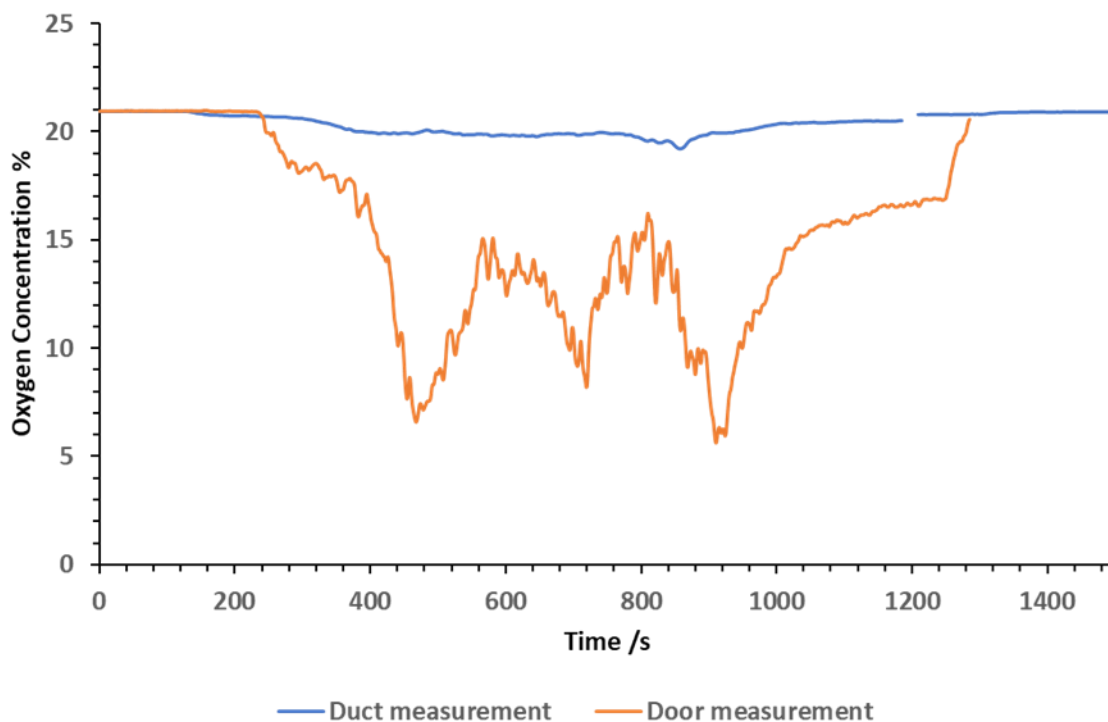


Figure 97: Oxygen concentrations measured in the door and exhaust duct of the ISO room when testing cables with no door.

3.4.2.6 CO₂ measurements

Due to an issue with the data logging in the doorway, only the measurements in the exhaust duct are available. The CO₂ measurements taken in the exhaust duct throughout the test are shown in *Figure 98*. Similar to the oxygen measurements, the CO₂ did not remain steady throughout the test showing somewhat cyclic burning. The CO₂ rose rapidly upon ignition and settled at a concentration range between 0.6 to 0.8%. The CO₂ concentration peaked at approximately 900 seconds at 1.19%.

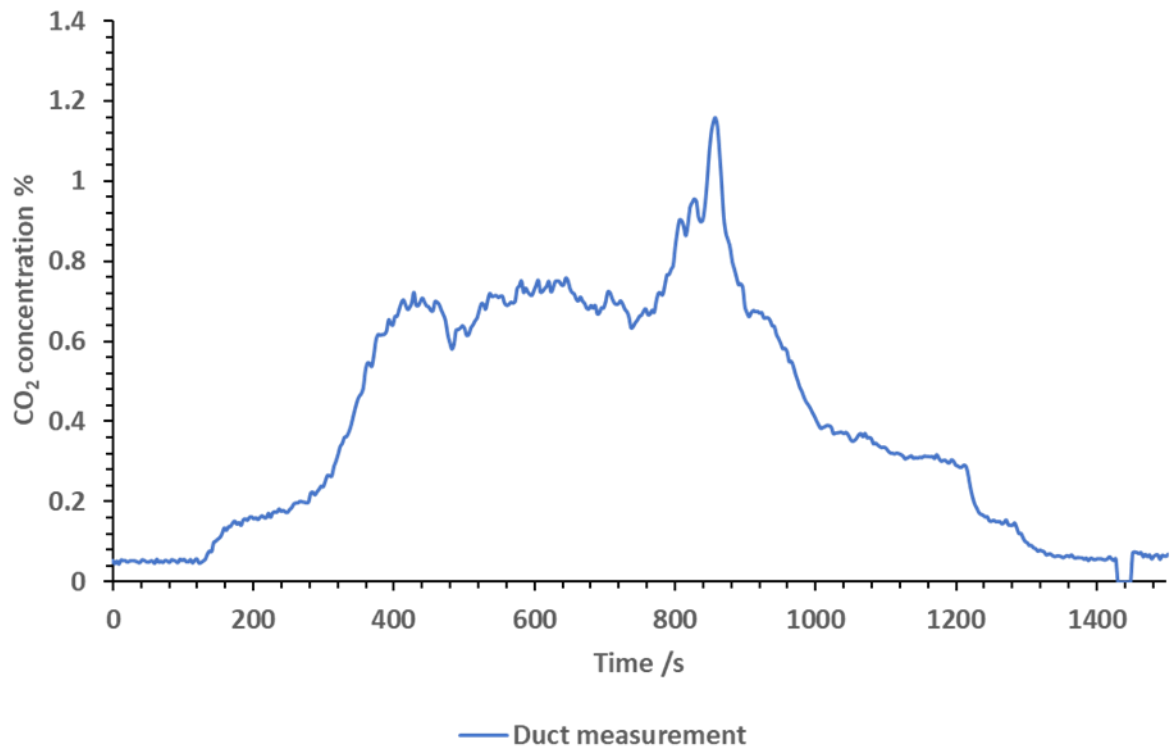


Figure 98: CO₂ concentrations logged in the exhaust duct of the ISO room when testing cables with no door.

3.4.2.7 CO measurements

Due to an issue with the data logging in the doorway, only the measurements in the exhaust duct are available. The CO measurements taken in the exhaust duct throughout the test are shown in Figure 99.

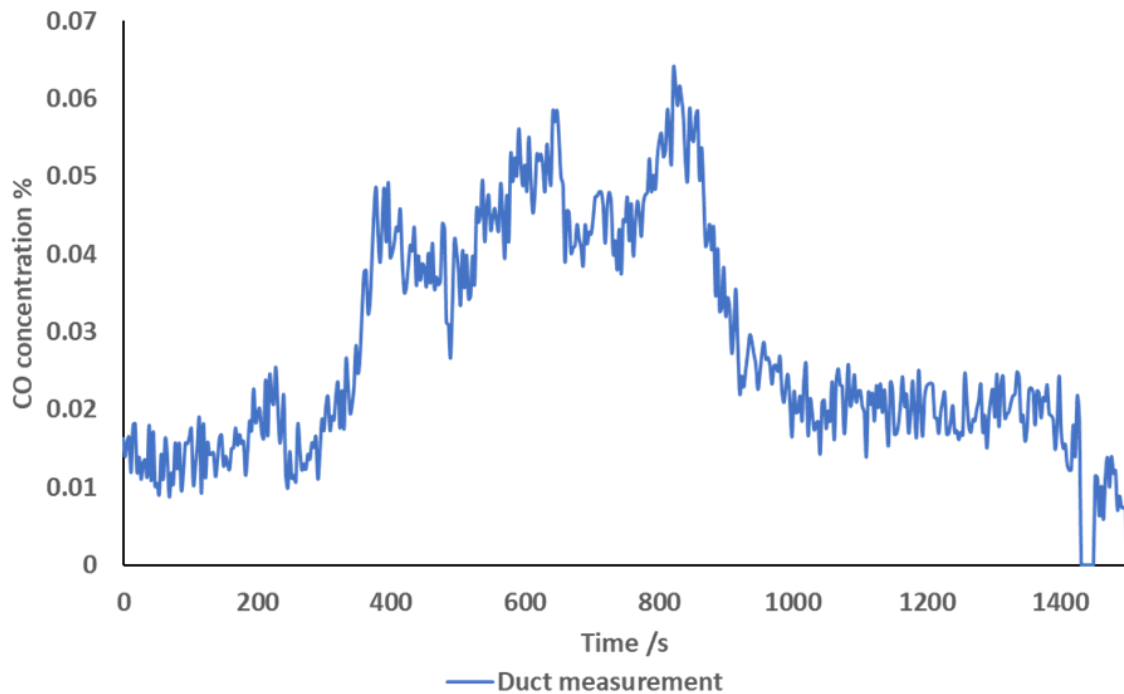


Figure 99: CO concentration measured in the exhaust duct of the ISO room when testing cables with no door.

The CO concentrations in the exhaust duct were very low, however this is expected when the fire is well-ventilated. The peak concentration of 0.064 % was reached at 820 seconds into the test. The data obtained was very noisy, likely as a result of a high exhaust flow being used in combination with very low CO measurements. Throughout the majority of the test, the concentration of CO kept within a range of 0.02 to 0.06 %.

3.4.2.8 CO/CO₂ ratio

The calculated CO/CO₂ ratio in the exhaust duct of the test is shown in *Figure 100*. Due to the aforementioned data logging issues experienced with the CO₂ and CO data in the door, the CO/CO₂ ratio for the door is therefore unavailable.

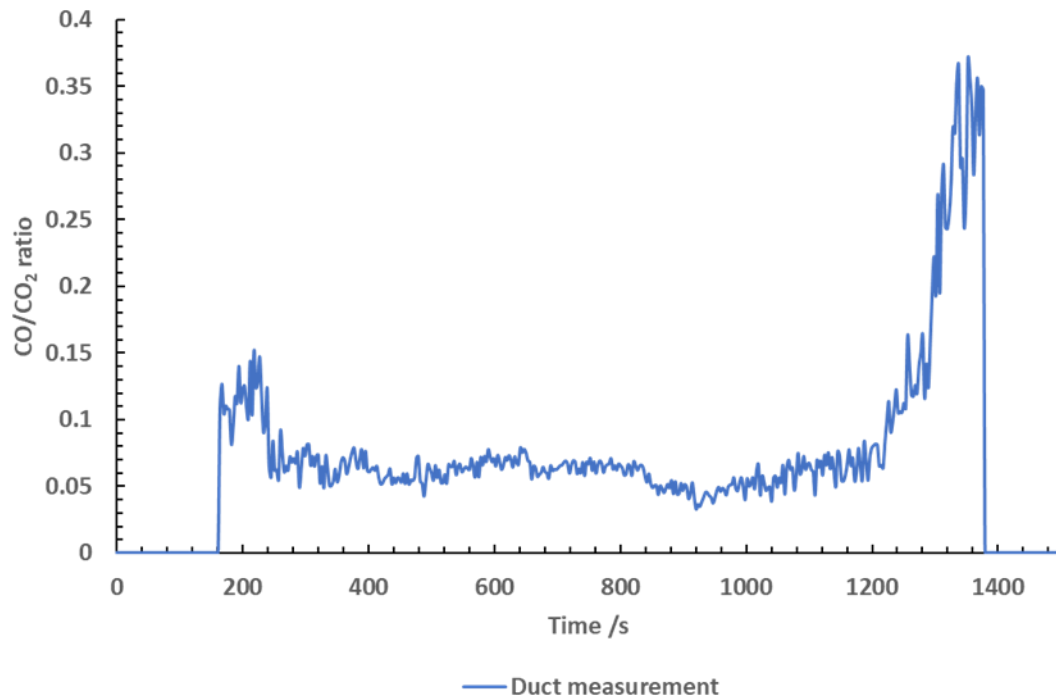


Figure 100: Calculated CO/CO₂ ratio in the exhaust duct of the ISO room when testing cables with no door.

The CO/CO₂ ratio showed spikes at the start and end of the test, with the ratio reaching 0.37 1400 seconds into the test. However, as this was towards the end of the test, this value arose as CO₂ concentrations became negligibly small. The CO/CO₂ ratio taken from 300 seconds into the test is more representative of the test condition. The peak here was calculated to be 0.15, which is more representative of under-ventilated flaming conditions. For the majority of the test, the ratio fluctuated between 0.04 to 0.08. On average, as the ratio is slightly above and below 0.05, the test condition can be deemed to be fairly well-ventilated on average.

3.4.3 Under-ventilated

3.4.3.1 Test layout

The test was set up as described in section 3.4.1. A 1.3 m calcium silicate door panel was placed in the front of the test room to limit the ventilation into the room during the test in an attempt to force under-ventilated flaming conditions.

3.4.3.2 Heat release

The heat release measured throughout the test, including the ignition source, is shown in *Figure 101*. The heat release gradually rose after ignition, before briefly settling at around 400 kW. The heat release throughout the test was very sporadic due to the inconsistent burning of the cables throughout the test.

The peak heat release of 480 kW was not reached until 800 seconds into the test. The low heat release rate measured is likely due to a large amount of copper inside the cables, as the copper would absorb some heat produced during the fire, resulting in a lower heat release rate. However, the oxygen depletion calorimetry would not be affected by the copper, and thus the total heat release, or area under the curve, would be independent of the presence of copper.

The time to flashover was calculated using the methodology described in the ISO 9705 standard. As the heat release did not surpass 1000 kW, flashover was not reached.

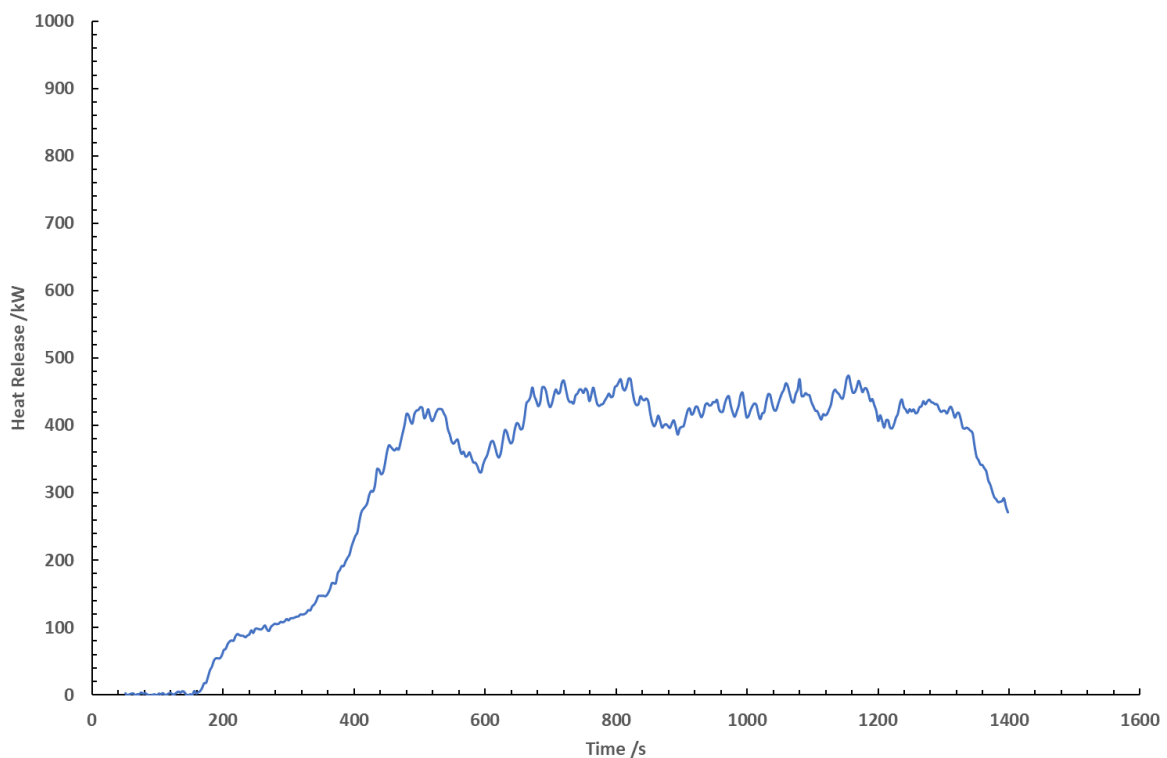


Figure 101: Heat release measurements taken in the ISO room when testing Cables with a door.

3.4.3.3 Mass loss

The mass loss measured throughout the test is shown in Figure 102. The mass loss was very small overall, only reducing by approximately 10 kg. Similar to the well-ventilated test prior, there are instances of increases in mass during the test, most noticeable at 580 seconds.

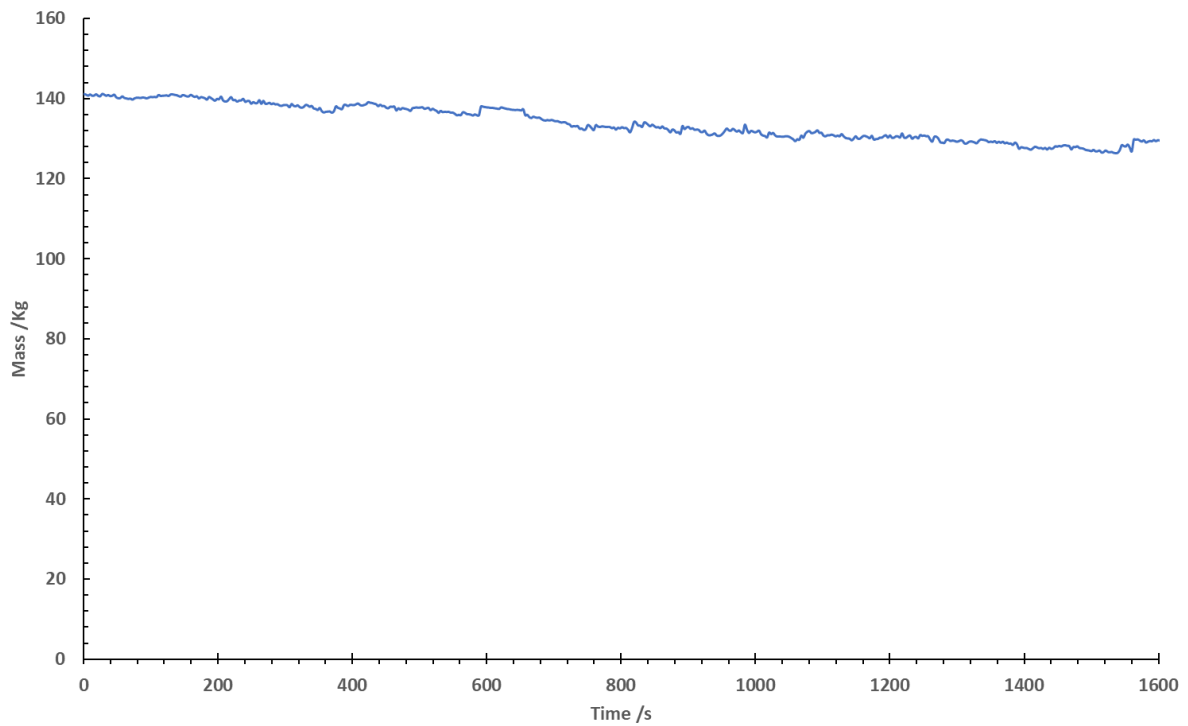


Figure 102: Mass loss measured using the scale in the ISO room when testing cables with a door.

3.4.3.4 Temperature

The temperature measurements taken throughout the test are shown in *Figure 103*.

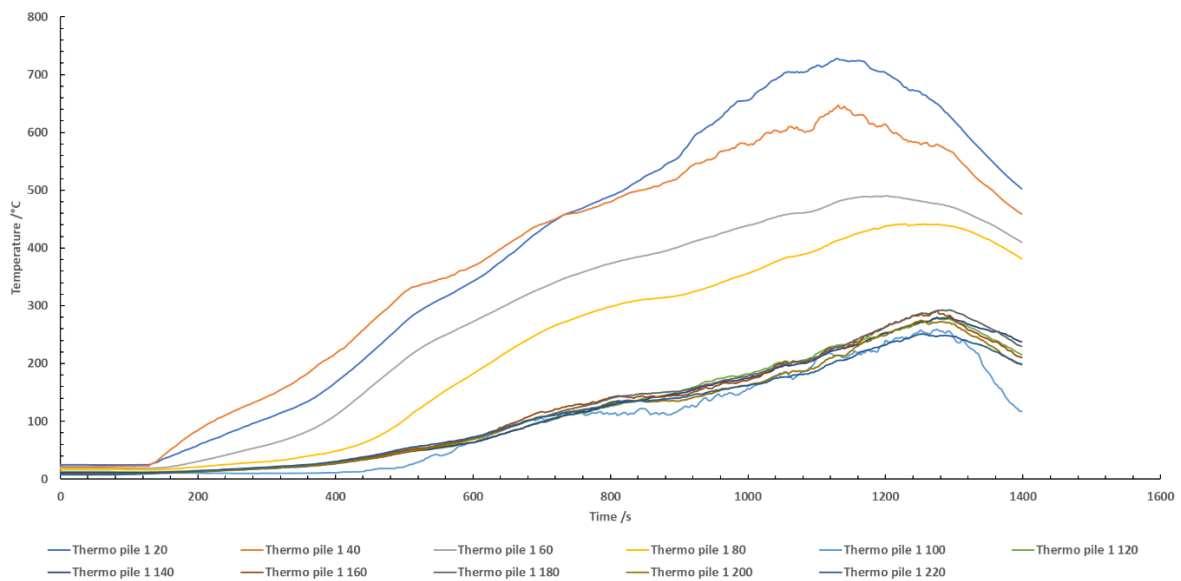


Figure 103: Temperature measurements taken in the doorway of the ISO room when testing Cables with a door. The measurements are taken from thermocouples labelled 'Thermo pile 1' with the final number indicating the distance from the ceiling in cm (e.g. Thermo pile 1 40, meaning thermocouple 1, 40 cm from the ceiling).

The temperature measured in the doorway rose gradually, reaching a peak temperature of 750 °C approximately 1100 seconds into the test. The measurements taken 100 cm from the ceiling and below are very similar, lower values due to the door covering the thermocouples. The temperature measurements were steady. The decreased heat measurements are likely a result of the copper present in the cables absorbing heat from the fire.

3.4.3.5 Fire condition

The fire condition of the test was found by monitoring the equivalence ratio throughout the test using the phi meter. The data is shown in *Figure 104*.

Due to a data logging issue, the first 180 seconds of the test were not logged. Once the data logging issue was resolved at 180 seconds, the equivalence ratio had reached 0.65 which is representative of well-ventilated flaming. This was followed by an oscillation in equivalence ratio as the burning behaviour of the cables was relatively cyclic. This is shown by the fluctuating equivalence ratio 200 to 600 seconds of the test. At 600 seconds, the equivalence ratio began to rise again. At this point, all three trays were on fire and the flame spread across the ceiling and along the top cable tray. The equivalence ratio continued to rise, peaking at 0.71 at 1000 seconds into the test. As the fire began to run out of fuel, the equivalence ratio gradually declined.

The equivalence ratio remained between 0.4 and 0.7 for most of the test. This is reflective of well-ventilated flaming, suggesting that despite the restriction of ventilation placed on the doorway there was insufficient heat release (or excess air flow) to force under-ventilated flaming.

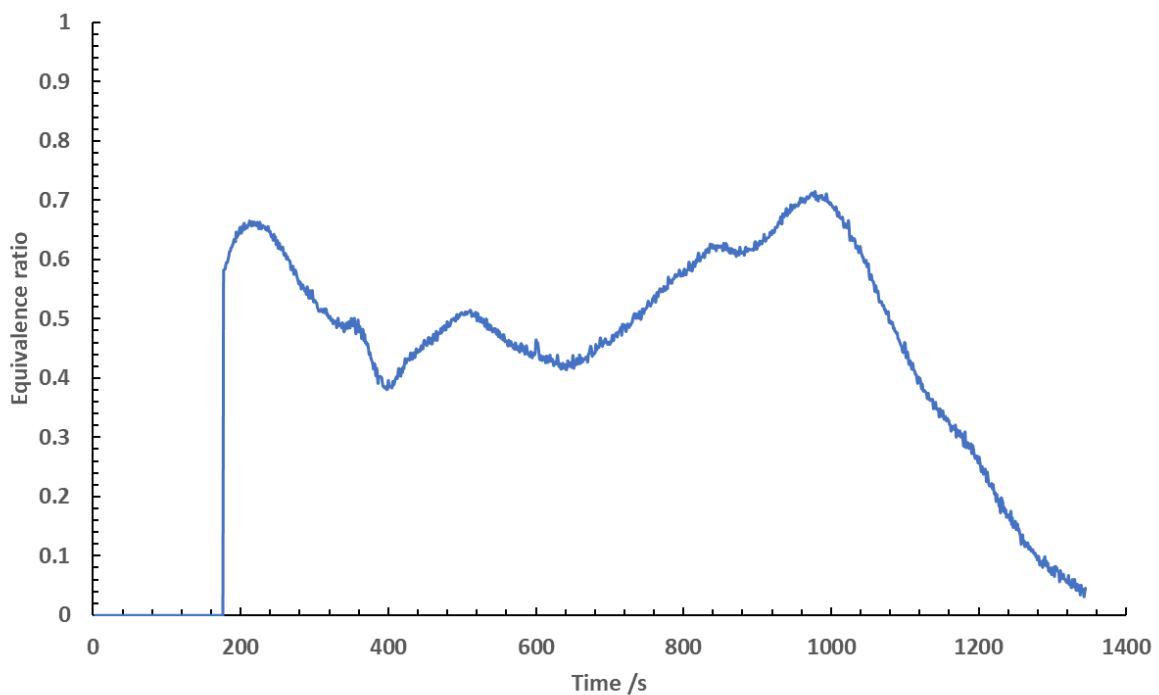


Figure 104: Equivalence ratio measured in the ISO room when testing cables with a door.

3.4.3.6 Oxygen measurements

The oxygen concentrations measured in the door and exhaust throughout the test are shown in *Figure 105*. The oxygen measured in the exhaust duct did not deviate significantly from the baseline values due to the dilution that occurs in the exhaust duct. Comparatively, the oxygen measured in the door was less inconsistent. The oxygen dropped rapidly upon ignition, dropping to 6 % at 420 seconds. The oxygen then rose sharply afterwards and remained sporadic until 1100 seconds before dropping again to 7 %, corresponding with the time at which all three cable trays had ignited. The measurements taken show the inconsistencies in burning behaviour observed throughout the test.

The peak observed at 680 seconds in the doorway is a result of swapping from the original sampling line in the doorway to a spare sampling line due to a blockage occurring.

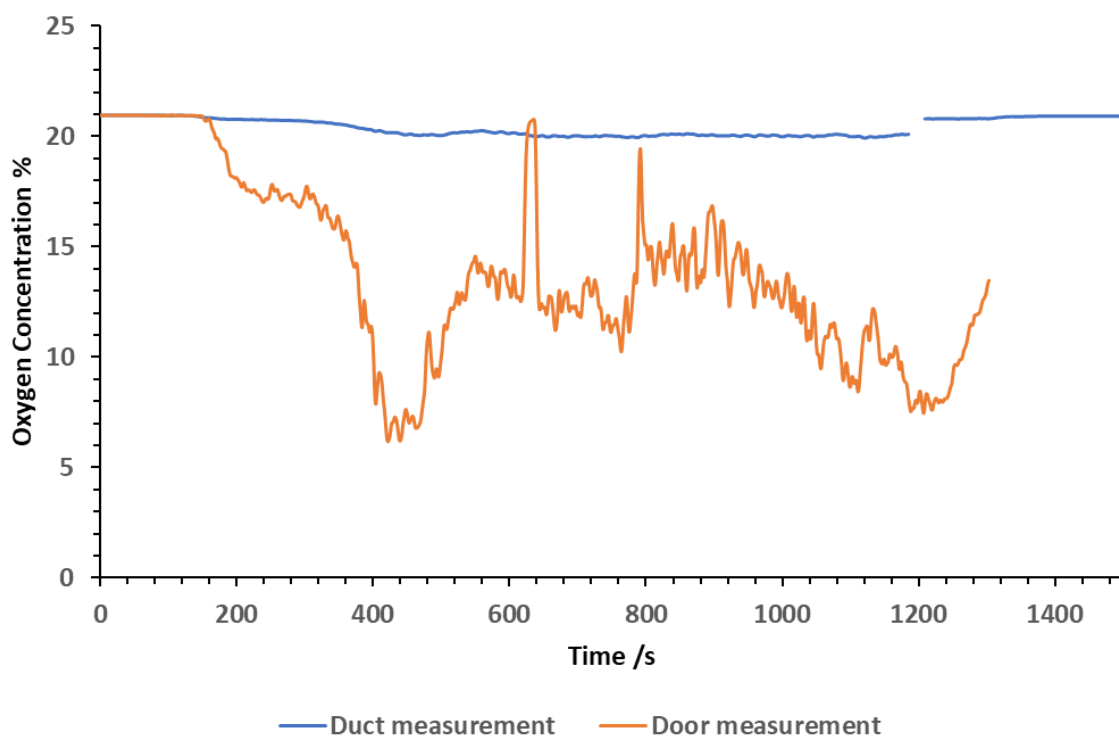


Figure 105: Oxygen measurements taken in the door and exhaust duct of the ISO room when testing cables with a door.

3.4.3.7 CO₂ measurements

Due to an issue with the data logging in the doorway, only the measurements in the exhaust duct are available. The CO₂ measurements taken in the exhaust duct throughout the test are shown in *Figure 106*. The CO₂ rose gradually upon ignition and reached its peak value of 0.68 % at 790 seconds into the test. Unlike the oxygen measurements, the CO₂ remained relatively steady from 600 to 1200 seconds, with concentrations ranging between 0.5 and 0.7 %. The concentrations measured are within range of expected values of well-ventilated flaming, however they are likely diluted as the measurements were taken in the exhaust duct.

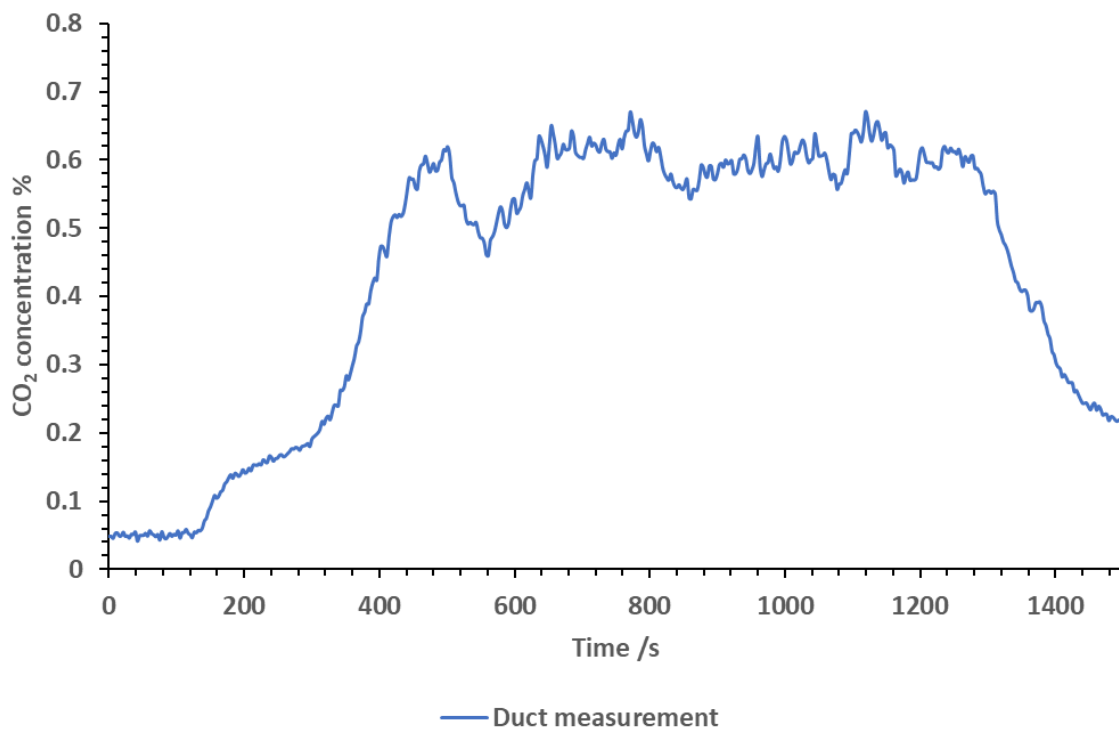


Figure 106: CO₂ measurements taken in the exhaust duct of the ISO room when testing cables with a door.

3.4.3.8 CO/CO₂ ratio

The CO/CO₂ ratio was calculated from the measurements taken in the exhaust duct, shown in *Figure 107*. The CO/CO₂ ratio showed a sharp peak at the start of the test, however as this was pre-ignition, it is therefore a result of the very low concentrations of CO and CO₂ in the duct. The ratio shown between 200 and 1200 seconds is therefore representative of the actual test conditions. For the majority of the test, the ratio remained between 0.05 and 0.1, meaning a significant proportion of the test was well-ventilated. This is in agreement with the equivalence ratio measured and the gas concentrations measured. The calculated ratio is slightly inconsistent as a result of the unsteady burning observed throughout the test.

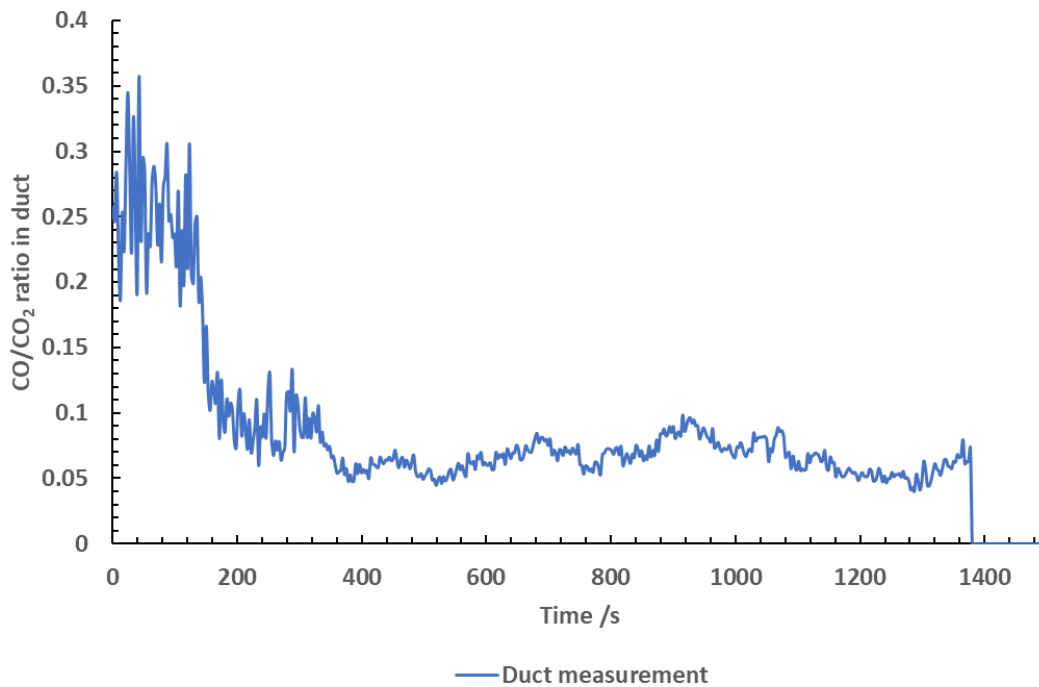


Figure 107: CO/CO₂ ratio calculated from measurements taken in the exhaust duct of the ISO room when testing cables with a door.

3.4.4 Comparison

A comparison of the test data from the tests conducted on cables is shown in *Table 25*.

Table 25: A comparison of the data obtained from testing cables two different ways in the ISO room.

Aimed test condition	Peak heat release /kW	Max equivalence ratio	Max CO concentration measured in exhaust duct %
Well-ventilated (with no door)	750	0.60	0.065
Under-ventilated (with door)	480	0.71	0.061

The peak heat release was much lower when a door was placed across the test room doorway to restrict the ventilation. The calcium silicate board used reduced ventilation, reducing the heat release rate. As this was the only difference in the test set up, this is the most likely reason for the difference in measurement. The reduction in heat resulted in a fire of less severity in terms of burning temperatures.

The addition of the door blocker to restrict ventilation did not seem to have a significant impact on the equivalence ratio throughout the test, with the equivalence ratio being 0.60 with no door present, only increasing to 0.71 when a door was added to the set up. This suggests that although an increase in equivalence ratio was observed, restriction to the ventilation of the room is not significant enough to force the fire to transition to under-ventilated burning. Increasing the fuel loading may have increased the equivalence ratio more. For example, 2 cable trays could have been used in the first test, and 4 in the second test.

These conclusions are further reinforced by a comparison of the CO concentrations measured in the test. The concentrations are very low, indicative of well-ventilated burning conditions.

As the test set up and material was so very different from the previous tests conducted using the SBI style set up, it was uncertain that the dilution factor would remain similar to that observed previously. Additionally, the burning of the cables was cyclic, and so presented difficulty in obtaining an accurate dilution factor from the oxygen measured in the doorway and duct, particularly as there was very little change in measurement in the duct. A prediction was therefore not made for the measurements in the doorway as in previous tests where it was needed.

3.5 POLYURETHANE

3.5.1 Test layout

Sheets of non-fire retarded flexible polyurethane foam made for furniture, (200 mm thick of nominal density 35 Kg m^{-3}) was glued directly to calcium silicate boards used for the SBI test rig. The board was slightly raised above the burner as in the SBI test. The test rig was then placed in a steel tray as it was expected that the polyurethane would drip and continue to burn as a pool fire during the test. The polyurethane was tested in two different ways with the aim of altering the ventilation condition of the tests. Test one was conducted using 1 x SBI test rig with an open door aiming for well-ventilated flaming, and test two was conducted using 2 x SBI rigs (doubling the fuel loading) with an open door aiming for under-ventilated flaming.

3.5.2 Well-ventilated

3.5.2.1 *Test layout and summary*

One SBI rig was set up for the test. A total mass of 15.02 kg of foam was used in this test.

The SBI rig was placed on the load cell in the centre of the ISO room. Gas analysers were calibrated and set up for testing. Heptane was measured out and poured into the burner inside the room. The ISO room measurements were started alongside the gas analysers and phi meter 2 minutes before ignition. The heptane burner was ignited manually.

3.5.2.2 Heat release measurements:

The heat release measured throughout the test, including the ignition source, is shown in *Figure 108*.

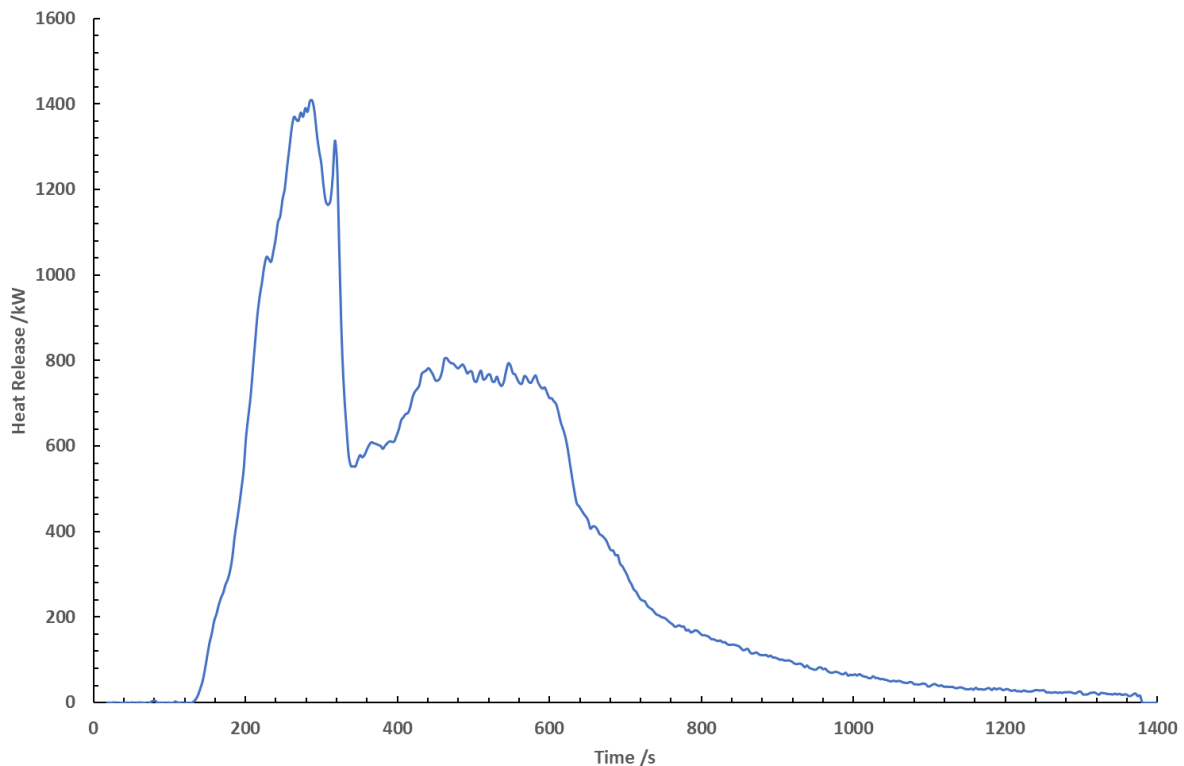


Figure 108: Heat release measured in the ISO room when testing polyurethane (1 x SBI).

The heat release rose rapidly upon ignition, reaching a peak heat release of 1410 kW. The drop in heat release at 380 seconds may be the result of the calcium silicate boards collapsing during the test. However, when the flexible polyurethane is burnt in laboratory scale tests, it shows a classic two peak heat release as the volatile isocyanates (predominantly toluene di-isocyanate) burn first, followed by the less volatile polyols. This is similar to the heat release shown here.

After this point, the test reached a steady period of burning as the polyurethane burnt as a pool fire. At this point the heat release remained around 800 kW before declining as the fire ran out of fuel. The time to flashover was calculated using the methodology described in the ISO 9705 standard. The Time to flashover was calculated as 185 seconds.

3.5.2.3 Mass loss measurements

The mass loss was monitored throughout the test using the scale inside the ISO room. The data recorded on the scale is shown in *Figure 109*. The initial mass was seen to steadily decline upon ignition. However, due to damage that occurred to the scale during testing, the mass loss measurements stopped recording at 640 seconds into the test. Before that, the mass declined steadily, falling below 100 kg at 309 seconds. The drop in mass at 380 seconds is a result of the calcium silicate boards collapsing before the test began to burn as a pool fire.

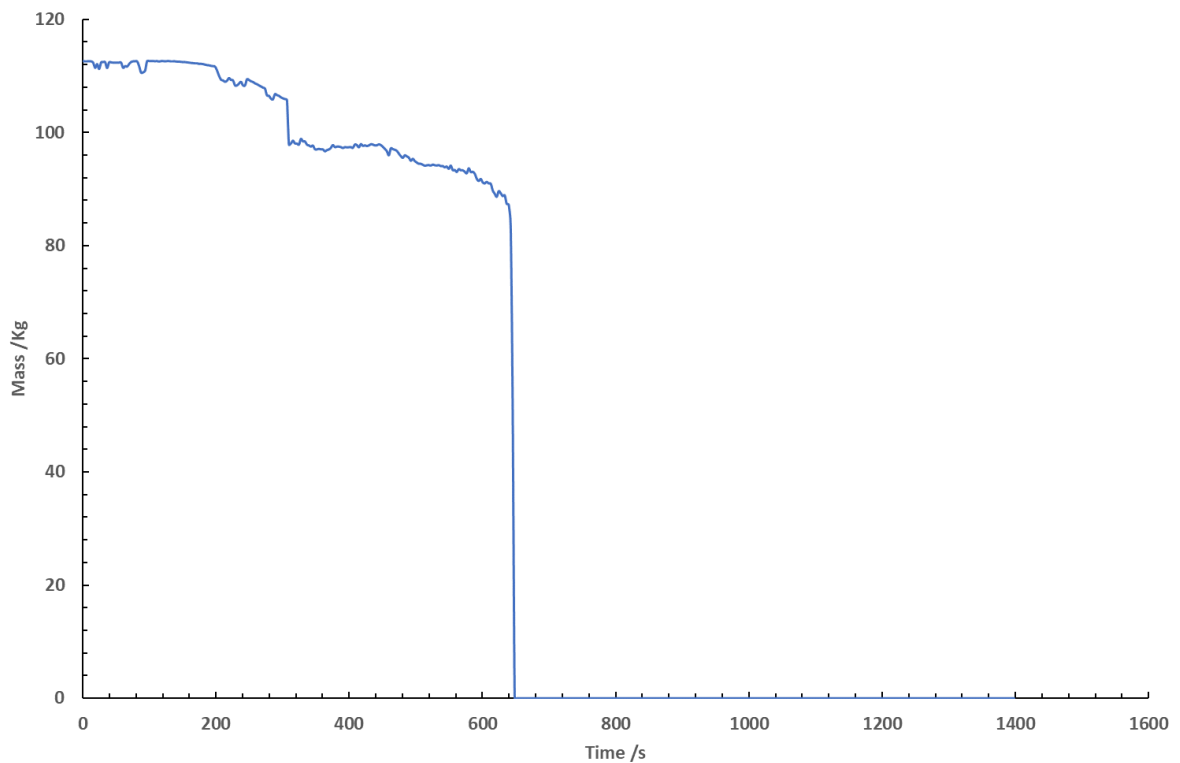


Figure 109: Mass loss measured by the scale in the ISO room when testing polyurethane (1x SBI).

3.5.2.4 Temperature measurements

The temperature of the doorway was measured throughout the test by a thermocouple tree sat in the doorway. The tree had thermocouples every 20 cm from the floor to the room's ceiling. The temperature measurements obtained throughout the test are shown in *Figure 110*. The data containing heat from the ignition source was used for calculating the air flow due to its influence on the behaviour of the fire effluent produced.

The temperatures show a rapid increase upon ignition, reaching a maximum temperature of 580 °C around 220 seconds into the test. A decline in temperature is then observed before plateauing between 400 and 500 °C in the thermocouples higher up (in thermocouples 20 to 60 cm from the ceiling). At 380 seconds, a drop followed by a steady increase in temperature is observed. This corresponds to the point of the test where the test rig collapsed. After 700 seconds, the temperature gradually begins to decrease as the fire begins to cease due to a lack of fuel left in the test room.

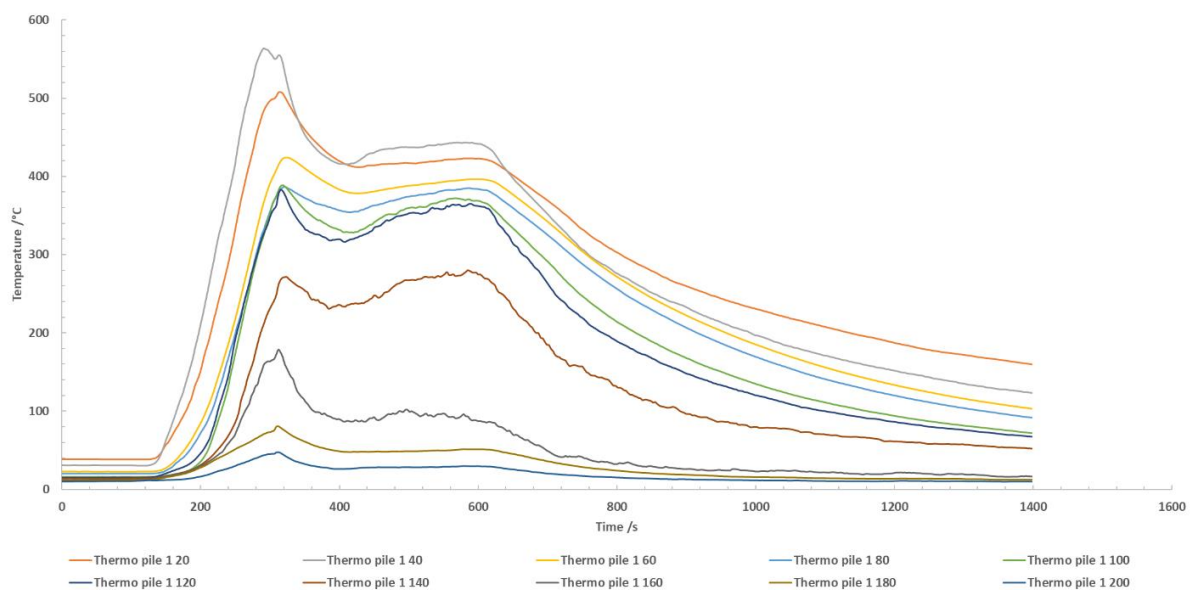


Figure 110: Temperature measurements taken in the doorway of the ISO room when testing polyurethane (1x SBI) with no door. The measurements are taken from thermocouples labelled 'Thermo pile 1' with the final number indicating the distance from the ceiling in cm (e.g. Thermo pile 1 40, meaning thermocouple 1, 40 cm from the ceiling).

3.5.2.5 Fire condition

The fire condition of the test was found by monitoring the equivalence ratio using a phi meter. The equivalence ratio logged throughout the test is shown in *Figure 111*.

After ignition of the heptane burners, the equivalence ratio rises rapidly, reaching a peak ratio of 0.52 approximately 100 seconds into the test. This is shortly followed by a rapid decline in the equivalence ratio, before plateauing between 0.3 to 0.35 from 220 to 400 seconds. Surprisingly, there was no rapid change in equivalence ratio at 380 seconds when the test rig collapsed.

Throughout the test, the measured equivalence ratio was representative of early well-ventilated flaming.

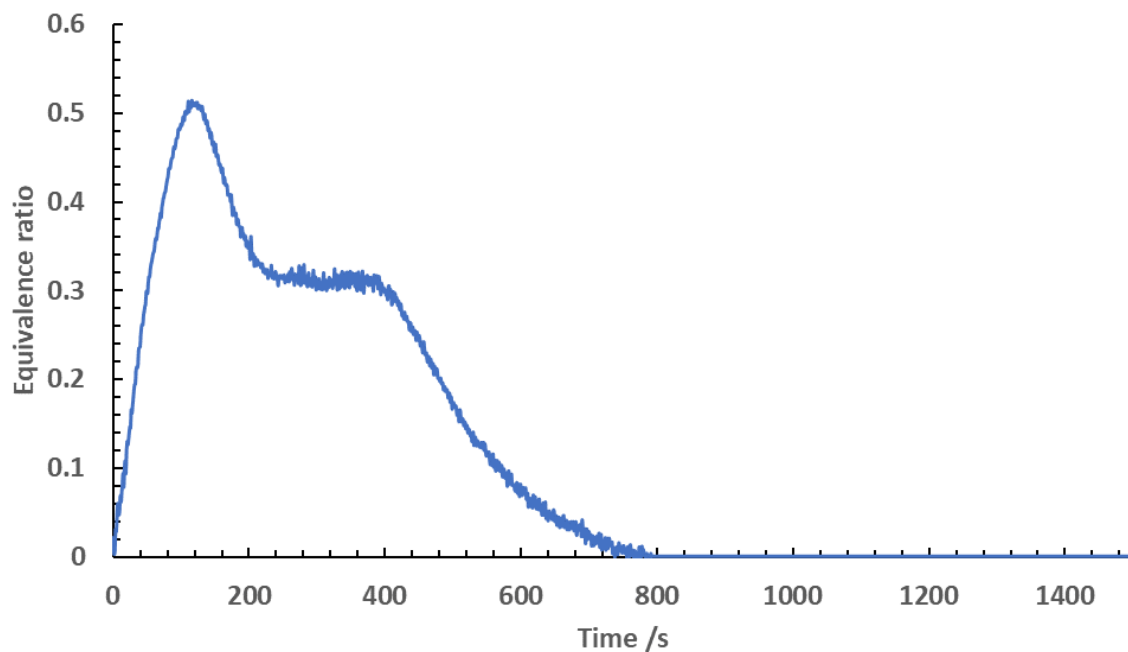


Figure 111: Equivalence ratio when testing polyurethane (1x SBI) in the ISO room.

3.5.2.6 O₂ measurements

The oxygen concentration measured in the exhaust duct and the doorway throughout the test are shown in *Figure 112*.

The oxygen measured in the exhaust duct showed significant deviation from baseline early in the test, and the changes observed in concentration mirrored those measured in the door. The oxygen in the exhaust duct dropped to 19% upon ignition, with a slight increase to 20% at 380 seconds, which was when the test rig collapsed. The oxygen remained around 20% for the rest of the test, before returning to baseline values at approximately 650 seconds.

The oxygen in the doorway decreases upon ignition, significantly more so than in the duct. At 200 seconds the oxygen had decreased to 5.2%, approximately 4x lower than that measured in the exhaust. The oxygen concentration was not stable, showing significant fluctuations from 200 to 400 seconds, but remained below 10%. At 380 seconds, the test rig collapsed and a sharp increase in oxygen concentration is observed. The oxygen reached 15%, before declining and settling around 14% until the fuel began to run out, and the measurements returned to baseline values. The oxygen levels reached in the doorway are significantly lower than those of early well-ventilated flaming.

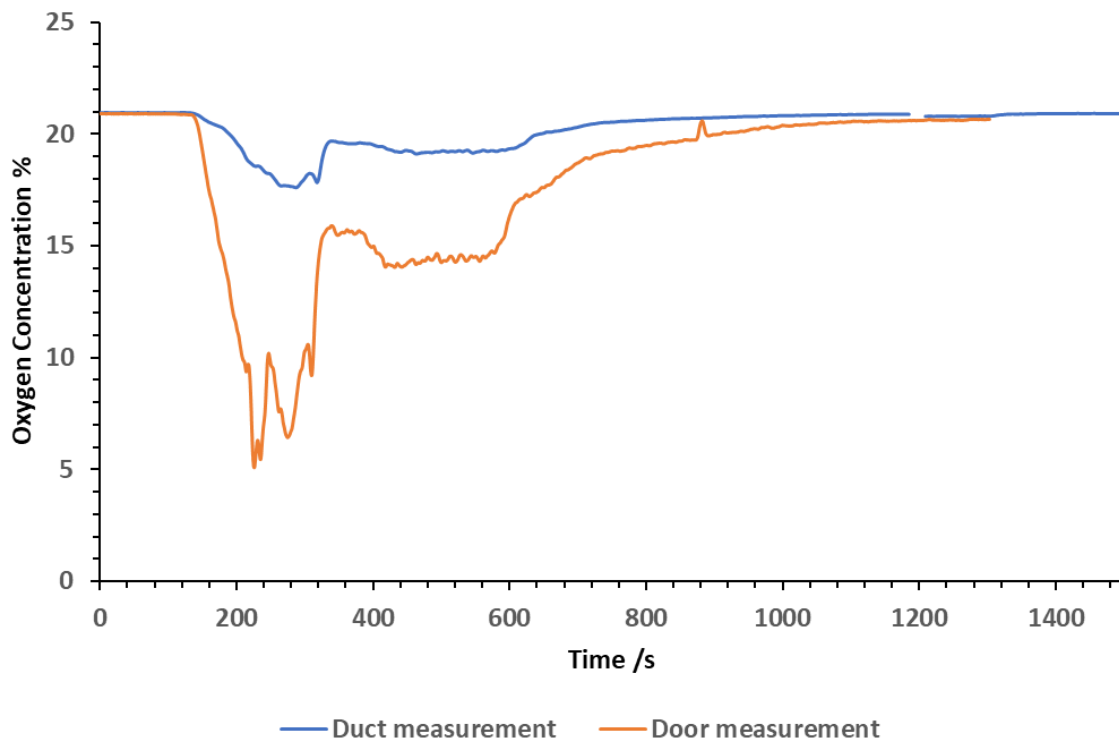


Figure 112: Oxygen measurements taken in the door and exhaust duct of the ISO room when testing polyurethane with no door.

3.5.2.7 CO₂ measurements

The CO₂ concentrations measured in the doorway and exhaust duct throughout the test are shown in Figure 113.

The CO₂ concentrations increased rapidly after ignition occurred, rising to a peak concentration of 2.6 % in the exhaust duct. The CO₂ in the doorway increased much higher upon ignition, reaching a concentration of 5.5 %. At around 380 seconds into the test, the test rig collapsed causing an increase in CO₂ concentration. The peak CO₂ concentration of 5.65 % was reached in the doorway at this point. An observed peak in the concentrations measured in the exhaust duct was also observed. Upon the test rig collapsing, the concentration rapidly declined, before slowly increasing to a plateau of approximately 1.3 % in the duct and approximately 3 % in the doorway. For this test, the dilution factor has fallen to around 2x, rather than the 4x in the tests conducted using OSB.

The CO₂ concentrations measured in the doorway are representative of well-ventilated flaming. The measurements in the duct were significantly diluted due to the high flow rate of the exhaust, but were still representative of well-ventilated flaming.

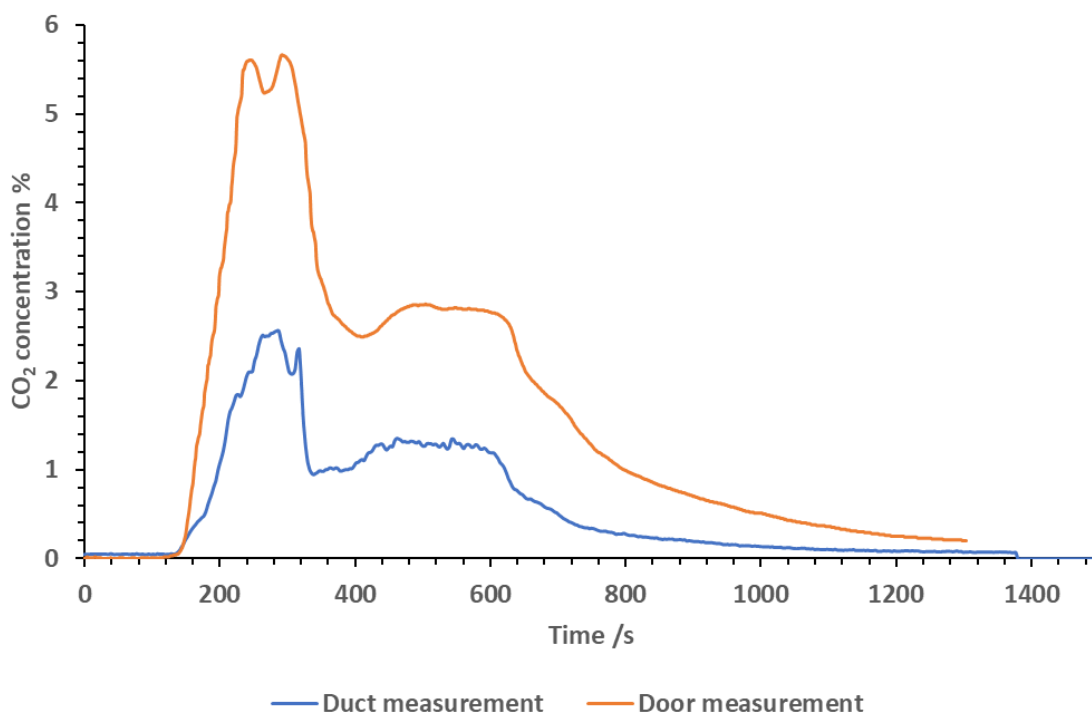


Figure 113: CO₂ concentrations measured in the doorway and exhaust duct of the ISO room when testing polyurethane (1x SBI no door)

3.5.2.8 CO measurements

The CO measurements taken in the exhaust duct and the door throughout the test are shown in Figure 114. The CO measurements in the exhaust duct were quite low, reaching a peak concentration of 0.02 % at 380 seconds. The concentration measured in the doorway were significantly higher than those measured in the duct. Similarly to the exhaust duct, there was a sharp peak in concentration in the doorway at 380 seconds where a peak concentration of 0.1 % was recorded. These peaks correspond to the time where the test rig collapsed.

The low CO concentrations measured are representative of well-ventilated flaming.

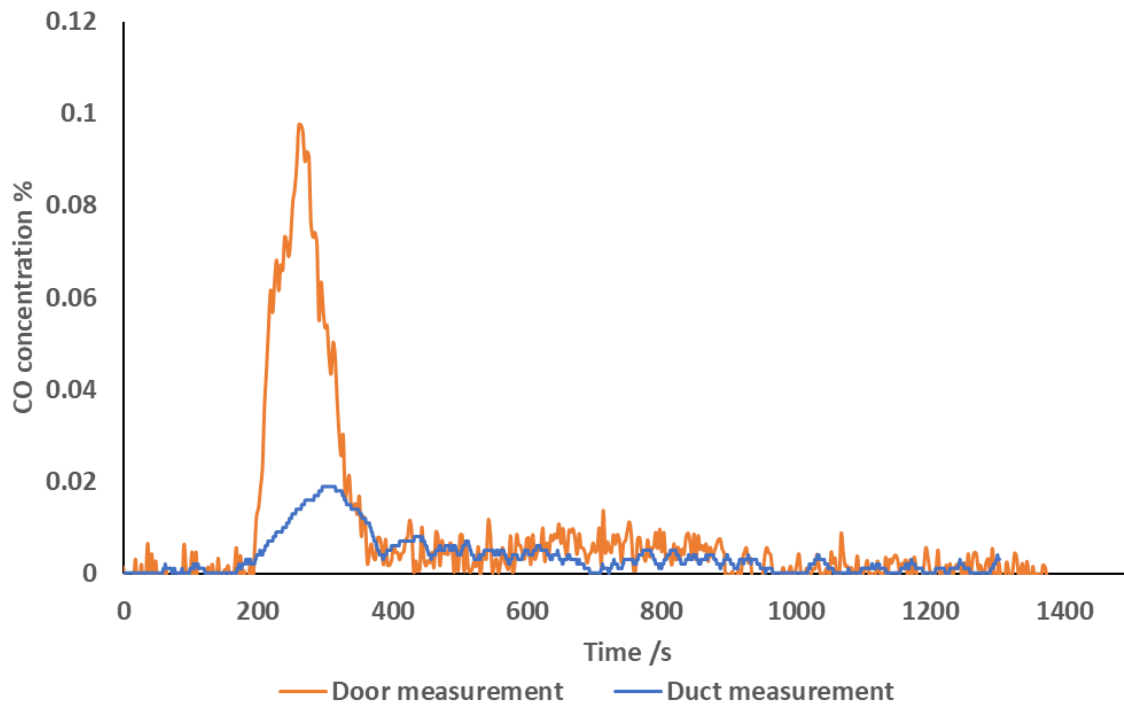


Figure 114: CO concentration measured in the exhaust duct and doorway of the ISO room when testing polyurethane (1x SBI no door).

3.5.2.9 CO/CO₂ ratio

The CO/CO₂ ratio in the exhaust duct and doorway was calculated for the duration of the test. This is shown in Figure 115.

Both ratios show strong peaks at the beginning of the tests, however as this occurs before ignition occurs these peaks are negligible and not representative of the actual test condition. In the door, the ratio is extremely low, with the ratio remaining below 0.005 for the majority of the test. This ratio is within the expected range of a well-ventilated test, however it is likely a result of the very low concentrations of CO being divided by a much higher concentration of CO₂. The ratio calculated throughout the test does not give a very good indication as to what the test condition was.

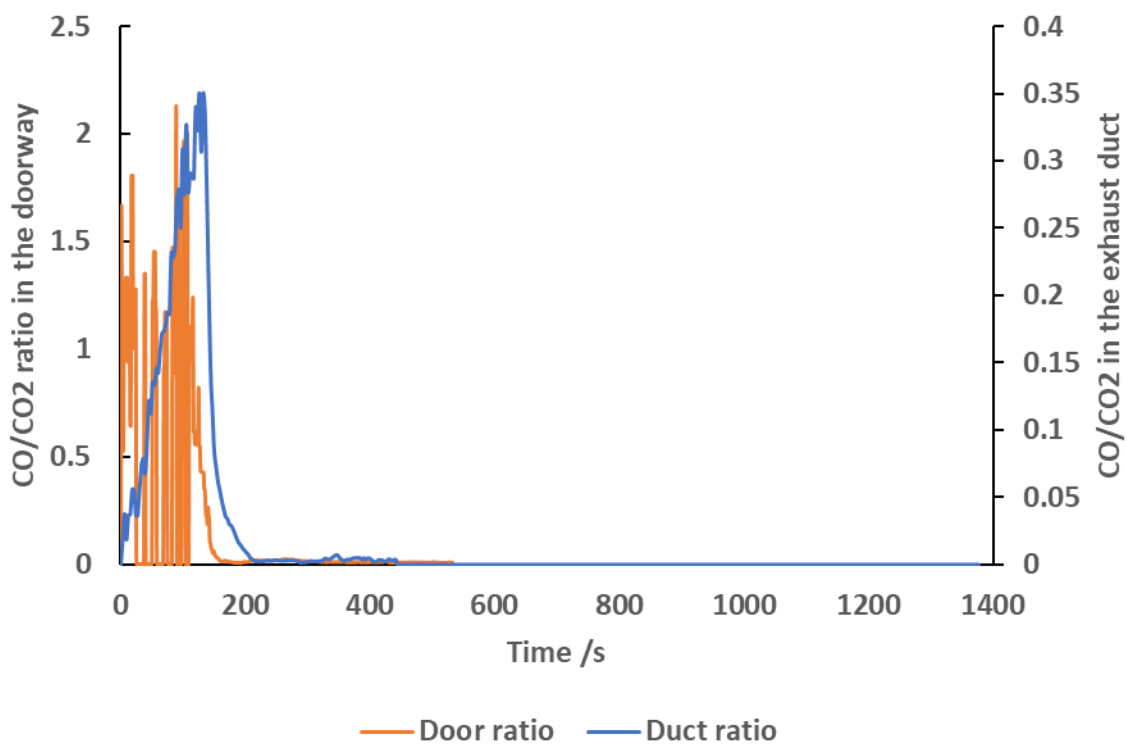


Figure 115: CO/CO₂ ratio calculated for the doorway and exhaust duct in the ISO room when testing polyurethane (1x SBI no door).

3.5.3 Under-ventilated

3.5.3.1 Test layout

Two SBI rigs were set up for the test. A total mass of 30.65 kg of polyurethane was used.

The SBI rigs were placed in a steel tray on the load cell in the centre of the ISO room. Gas analysers were calibrated and set up for testing. Heptane was measured out and poured into the burners inside the room. The ISO room measurements were started alongside the gas analysers and phi meter 2 minutes before ignition. The heptane burners were ignited manually.

3.5.3.2 Heat release measurements

The heat release measurements taken in the ISO room throughout the test are shown in Figure 116. The heat release rose rapidly upon ignition, rising to 3100 kW 280 seconds into the test. After this point, the polyurethane had melted and was burning as a pool fire. As the fuel load began to diminish and the heat release dropped steadily. The time to flashover was calculated using the methodology described in the ISO 9705 standard. The Time to flashover was calculated as 160 seconds.

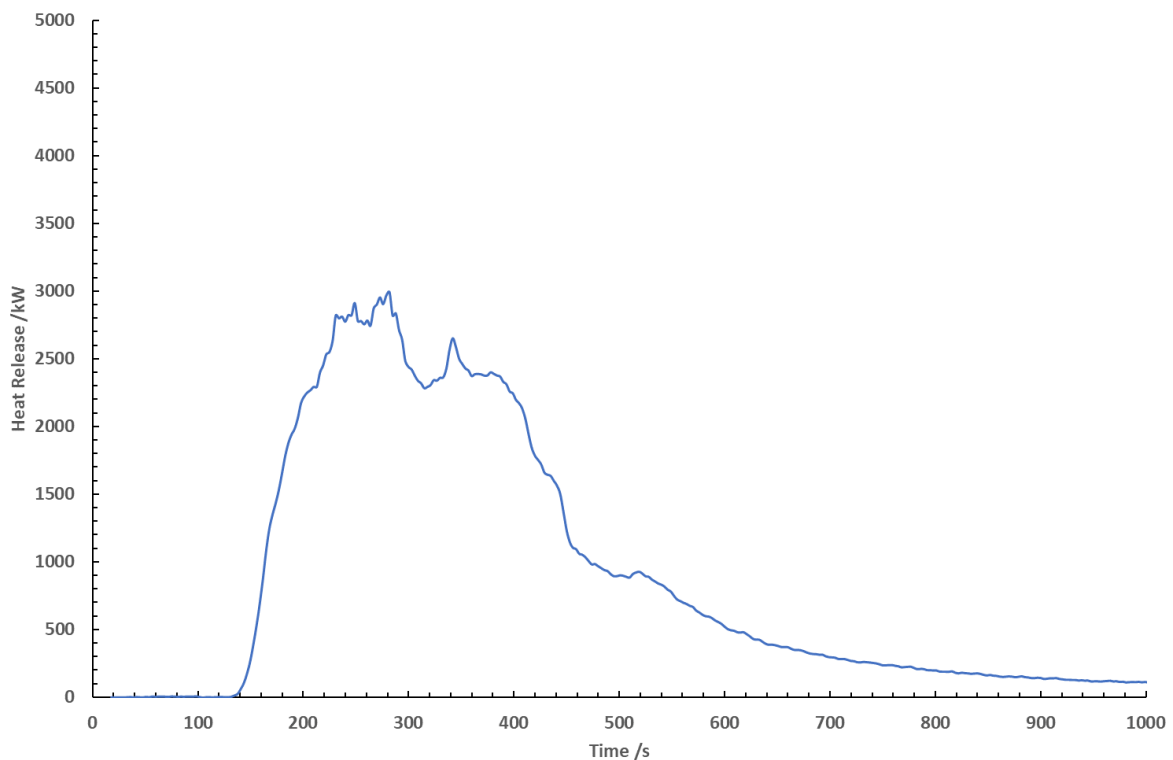


Figure 116: Heat release rate measured in the ISO room when testing polyurethane (2x SBI).

3.5.3.3 Mass loss measurements

Due to the damage sustained to the ISO 9705 scale from previous testing, the mass loss measurements were unable to be logged for this test.

3.5.3.4 Temperature measurements

The temperature measurements taken in the doorway of the ISO room are shown in Figure 117. The temperature across the doorway rose rapidly on ignition. The measurements taken in the top of the room 40 cm from the ceiling reached a maximum temperature of 900 °C approximately 250 seconds into the test. There was a noticeable difference in the temperature measurements in the top 140 cm of the doorway. It should be noted that the test conditions throughout were so severe that the flames were exiting the doorway by this point. Evidence of the severity of the flaming in the doorway is shown in *Figure 118*.

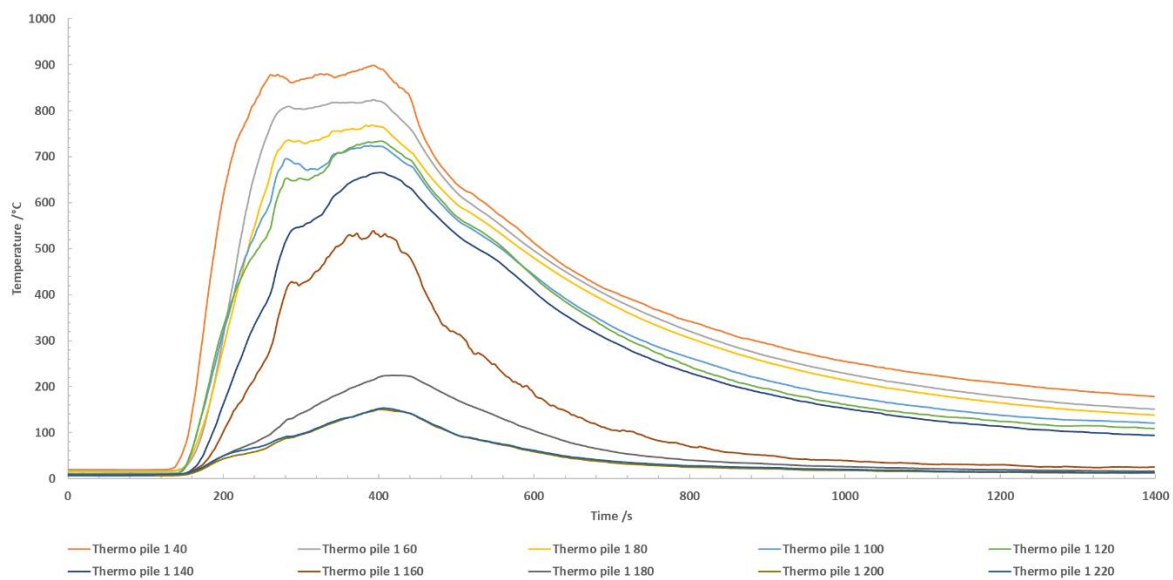


Figure 117: Temperature measurements taken in the doorway of the ISO room when testing polyurethane (2x SBI) with no door. The measurements are taken from thermocouples labelled 'Thermo pile 1' with the final number indicating the distance from the ceiling in cm (e.g. Thermo pile 1 40, meaning thermocouple 1, 40 cm from the ceiling).



Figure 118: Picture taken approximately 300 seconds into the polyurethane (2x SBI) ISO 9705 room test.

3.5.3.5 Fire condition

The fire condition was determined by use of a phi meter, which logged the equivalence ratio throughout the test. The measured equivalence ratio is shown in Figure 119. The equivalence ratio rose rapidly on ignition, reaching a peak equivalence ratio of 1.48 at 300 seconds into the test, corresponding with the time at which flaming was most severe.

During this time, as the flames were pouring out of the doorway, the sampling took place within fire zone and not the smoke plume. The measurements should therefore be treated more as an indication of the fire condition as opposed to the actual equivalence ratio in the test room. It would have posed useful to measure the equivalence ratio for this test in the exhaust duct to identify the equivalence ratio in the smoke plume as opposed to within the flaming zone. The equivalence ratio measured showed that the fire condition had reached under-ventilated conditions.

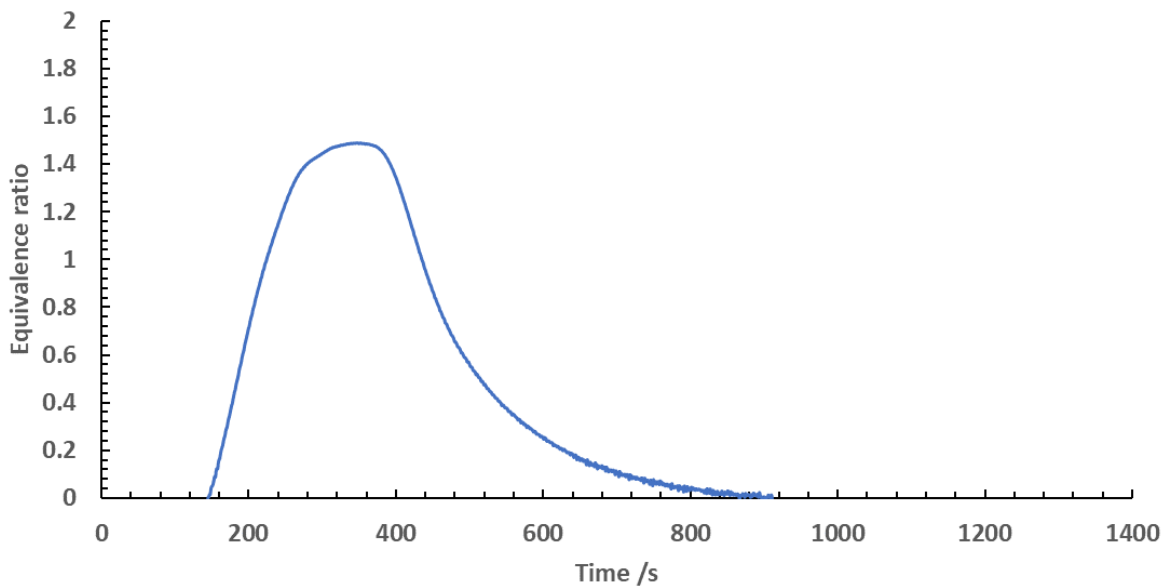


Figure 119: Equivalence ratio measured in the doorway of the ISO room when testing polyurethane (2x SBI)

3.5.3.6 Oxygen concentration

The oxygen concentrations measured in the exhaust duct and doorway of the test room are shown in Figure 120. Upon ignition, the oxygen concentration in both the exhaust and doorway dropped rapidly. By 180 seconds, the oxygen in the doorway had fallen to 0 % and 16.5 % in the exhaust duct. This is representative of severely under-ventilated conditions.

The oxygen measured in the doorway remained at 0 % until 380 seconds. The exhaust duct concentrations remained below 15 % during this time period. While this is characteristic of severely under-ventilated flaming, at this point the test condition was so severe that the flames were exiting the doorway, engulfing the sampling lines. As the sampling was taking place in the flame zone, it is therefore unsurprising to have measured 0 % oxygen.

Taking into consideration the dilution that occurs in the exhaust duct, the oxygen concentration in the smoke plume, while not definitively known, would be representative of under-ventilated flaming when comparing the measurements taken from the two locations.

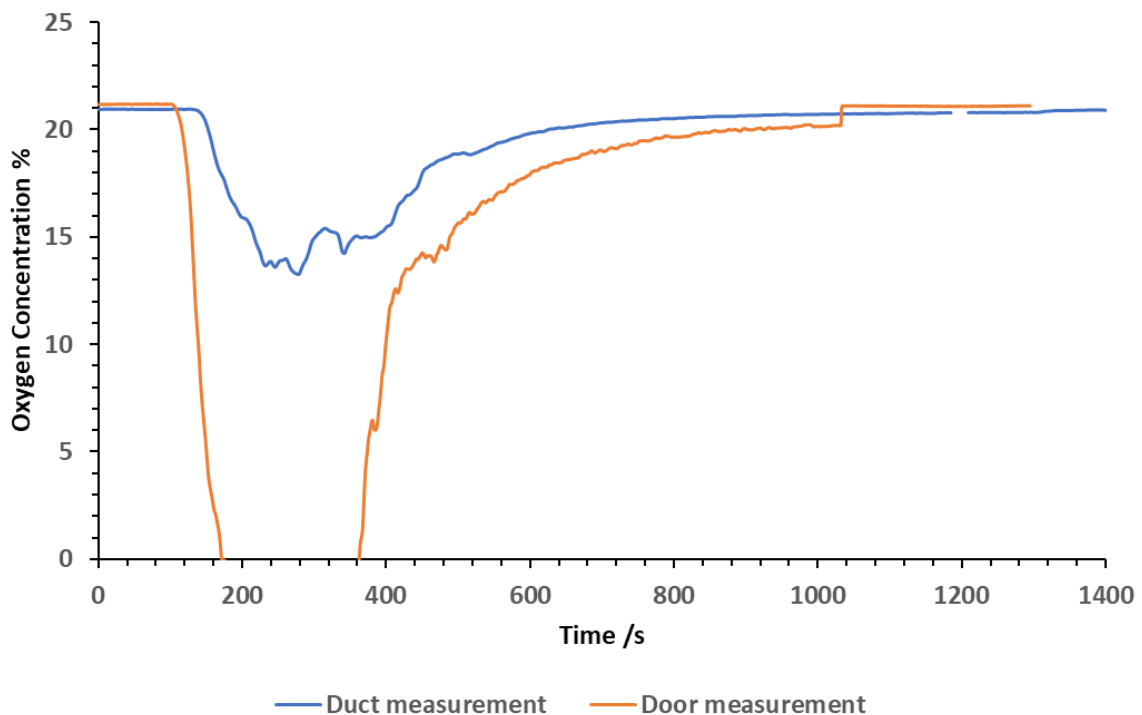


Figure 120: Oxygen measurements taken when testing polyurethane (2x SBI) in the ISO room.

3.5.3.7 CO₂ measurements

The CO₂ concentrations measured in the door and exhaust duct throughout the test are shown in Figure 121. The CO₂ measured in the doorway was overall, much higher than in the exhaust duct. The CO₂ in the exhaust duct rose rapidly on ignition, and by 200 seconds had reached 4 %. The concentration rose, reaching a peak concentration of 6 % by 250 seconds. From 200 to 400 seconds, the concentration remained between 4 and 6 %.

The CO₂ in the doorway sharply rose upon ignition, reaching 15 % at 200 seconds into the test. This was near the limits of the NDIRs measuring capabilities. Unlike in the exhaust duct measurements, there was no significant increase in concentration at 400 seconds. Instead, the increase was slight, with the concentration remaining between 14 and 16 % from 200 to 400 seconds.

However, the sampling in the doorway did take place in the fire zone as flames were observed to be exiting the doorway. In tests where sampling takes place within the flame zone, it can be difficult to determine what the actual CO₂ concentration would have been in the test room. Additionally, as the flames were exiting the doorway into the top of the exhaust duct, the fire effluent could have undergone further chemistry in the duct. The actual CO₂ concentration during the test is therefore likely a value in the range between the two measurements, as opposed to one of the two specific measurements.

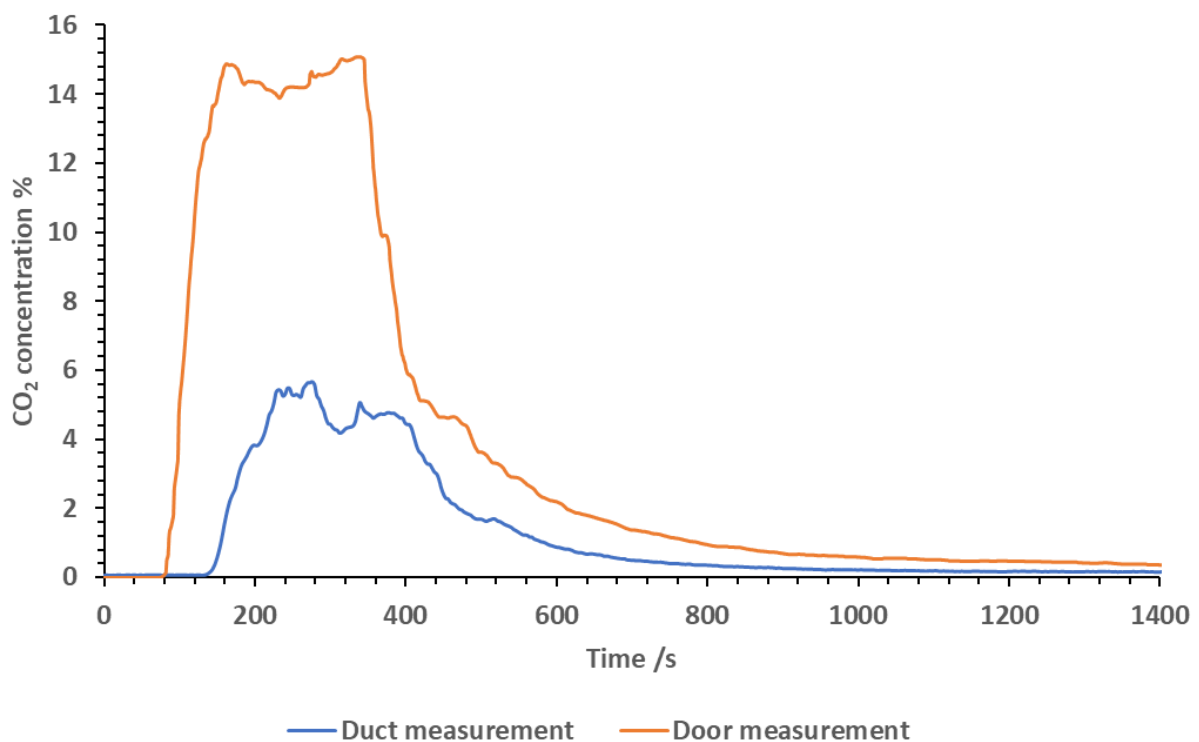


Figure 121: CO₂ concentrations measured in the exhaust duct and doorway of the ISO room when testing polyurethane (2x SBI).

3.5.3.8 CO measurements

The CO measurements taken in the exhaust duct and doorway throughout the test are shown in Figure 122.

The CO concentrations in the doorway are significantly higher than in the duct. However, as flames exited the doorway for a significant proportion of the test, the sampling probe in the doorway was engulfed in flames and was therefore sampling within the flame zone.

The CO concentrations in the doorway rose rapidly upon ignition, with the CO concentration reaching 2.6 % by 250 seconds. The measurements in the doorway sharply declined when the test rig collapsed, dropping to 0.7 %. This was also mirrored in the exhaust duct measurements, but much less dramatically. The exhaust duct reached a peak concentration of 0.52 %, but remained very low for the majority of the test.

The low concentrations of CO alongside the high CO₂ concentrations measured in both the exhaust duct and door suggest that the fire effluent was undergoing further chemistry in the exhaust duct as the flames extending out of the test room and into the front of the exhaust duct.

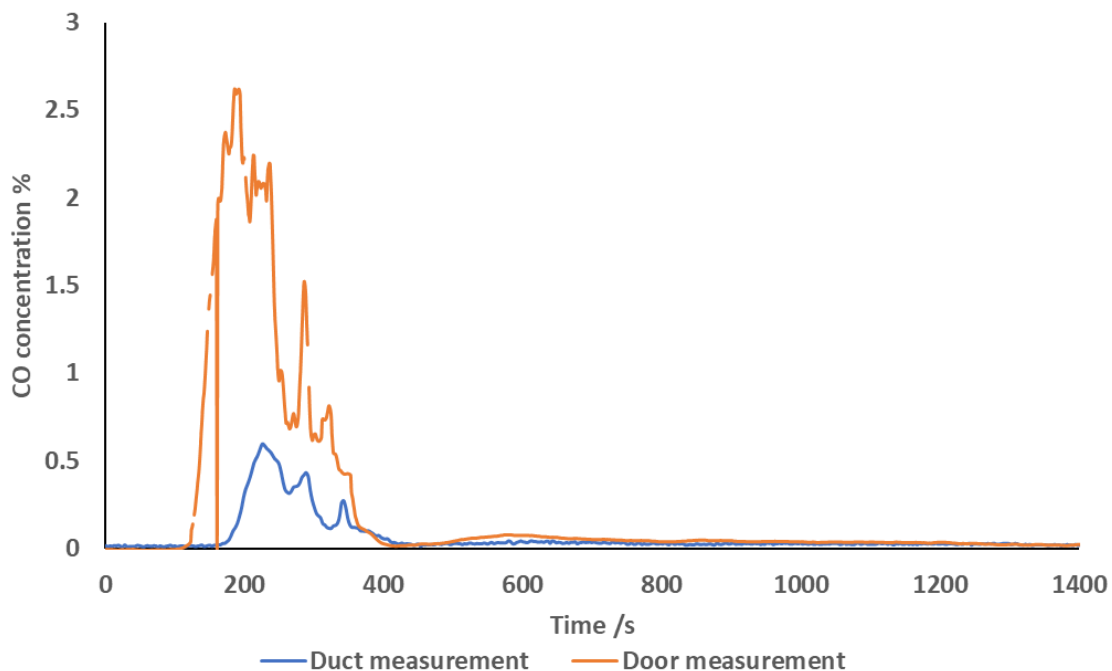


Figure 122: CO concentrations measured in the doorway and exhaust duct of the ISO room when testing polyurethane (2x SBI)

3.5.3.9 CO/CO₂ ratio

The CO/CO₂ ratio was calculated using the CO and CO₂ concentrations measured in the doorway and exhaust duct throughout the test. This is shown in Figure 123. The CO/CO₂ ratio was higher in the doorway than the exhaust duct, with the peak ratio reaching 0.17 in the door, and 0.12 in the exhaust duct. However, as there was flaming in the doorway throughout the test, it was not expected for the ratios to be the same. The CO/CO₂ ratio calculated for the doorway is not representative of the actual ratio for this reason. As the sampling was within the flame, the concentrations measured would not be the same as they would in the smoke plume due to changes that would occur to the chemistry of the smoke as it cools down (as the products of decomposition migrate away from the heat source).

The exhaust duct ratio is representative of under-ventilated flaming, particularly stage 3a of the ISO fire stages (ISO stage 3a: low-ventilation room fire). The measurements in the doorway is also representative of under-ventilated flaming.

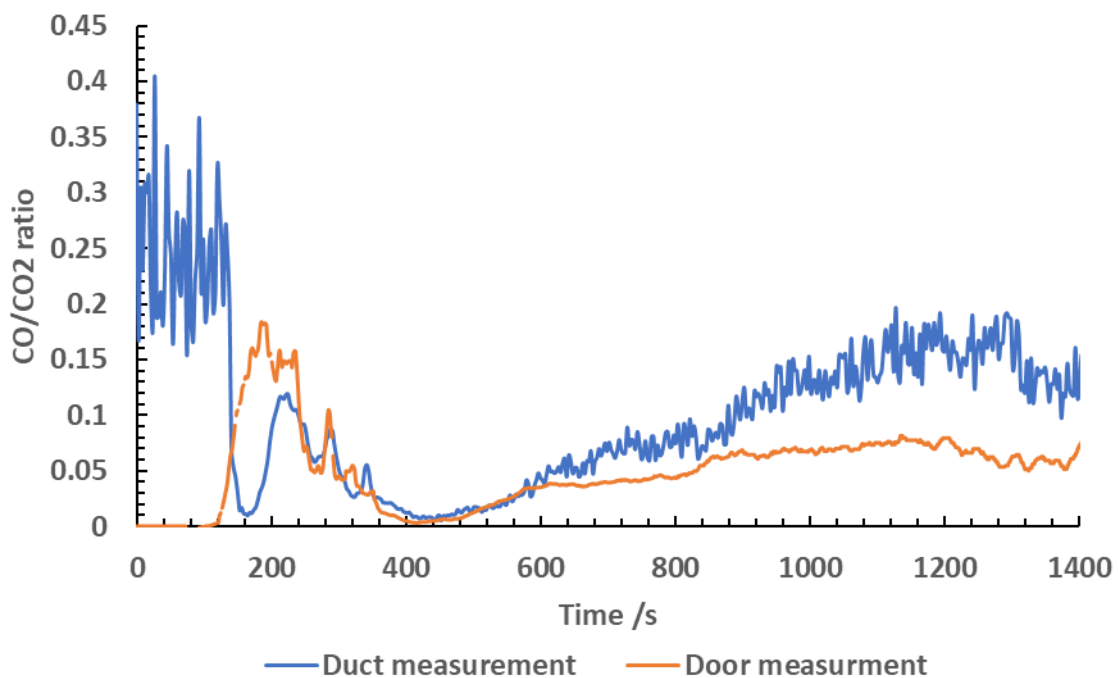


Figure 123: CO/CO₂ ratio calculated for the doorway and exhaust duct of the ISO room when testing polyurethane (2x SBI).

3.5.4 Comparison of data

A summary table comparing some of the data obtained when testing polyurethane in the ISO room has been shown in *Table 26*.

Table 26: Summary of the test data obtained when testing Polyurethane in the ISO room in two different test conditions.

Aimed test condition	Peak heat release /kW	Max equivalence ratio	Max CO concentration measured %	
			Exhaust duct	Doorway
Well-ventilated (1x SBI)	1410	0.52	0.02	0.10
Under-ventilated (2x SBI)	3100	1.55	0.52	2.60

The two different configurations used were successful in achieving both well-ventilated flaming and under-ventilated flaming, shown by the measured equivalence ratios. By doubling the fuel loading within the test room, the equivalence ratio was able to surpass 1 and develop into under-ventilated flaming. This is evidenced by the test using 1 x SBI achieving an equivalence ratio of 0.52, and the 2 x SBI test rig set up achieving a ratio of 1.45. The CO concentrations measured were also significantly higher when using two SBI rigs in the test room.

The use of the two test rigs facing each other caused a significant increase in the heat release measured, as the radiant heat from the opposing test rigs would increase the heat each test rig was being exposed to, resulting in faster flame spread and a higher heat release.

3.6 SUMMARY OF TESTS

The key information obtained from each test has been summarised in 3 tables: time to flashover, equivalence ratio and heat release.

3.6.1 Time to flashover:

Time to flashover is defined in the ISO 9705 standard as the point at which the heat release (from the material and ignition source) reaches 1000 kW. This was calculated for all tests conducted. A summary of the time to flashover calculated for each test using the actual test data, combined with the mass of fuel used and the desired test condition is shown in Table 27.

Table 27: A summary table of test conditions, time to flashover, the mass of fuel and comments on each test conducted in the ISO 9705 room corner.

Material	Test condition	Time to flashover /s	Mass of material / Kg	Comments
Plasterboard	Well-ventilated	-	40.97	Flaming combustion of paper surface occurred. Once the paper on the surface had run out, the fire stopped.
OSB	Well-ventilated	-	14.72	
	Under-ventilated (using door)	-	14.59	Test looked similar to when testing without the door. No flames exited the ISO room.
	Under-ventilated (2x fuel load)	180	30.65	Flames poured out of the test door resulting in sampling lines being inside flames.
Cables	Well-ventilated	-	*	Cables ignited using 100 kW for 10 minutes. The propane burner was not used for the additional 10 minutes at 300 kW.
	Under-ventilated (using door)	-	*	Cables ignited using 100 kW for 10 minutes. The propane burner was not used for the additional 10 minutes at 300 kW.
PU	Well-ventilated	185	15.02	
	Under-ventilated	160	30.65	Flames poured out of the test door resulting in sampling lines being inside flames.

Key: * Indicates no data available, - indicates flashover was not reached

3.6.2 Equivalence ratio:

The maximum equivalence ratio reached during each test has been summarised in Table 28.

Table 28: Summary of the maximum equivalence ratio reached for each test conducted in the ISO 9705 room corner.

Material	Test condition	Max Equivalence ratio
Plasterboard	Well-ventilated	0.33
OSB	Well-ventilated	0.70
	Under-ventilated (using door)	0.95
	Under-ventilated (2x fuel load)	1.55
Cables	Well-ventilated	0.76
	Under-ventilated (using door)	0.70
PU	Well-ventilated	0.51
	Under-ventilated	1.48

In the case of most tests, the target ventilation condition of the test was met. The exceptions to this are OSB where the test aimed to be under-ventilated by use of restricted ventilation (using a door), and Cables where the test aimed for under-ventilated burning by again using the restricted ventilation (addition of a door blocker). In these cases, while the use of the door blocker did increase the maximum equivalence ratio reached, the restriction was insufficient enough to cause the fire to transition to under-ventilated burning. The results show that the use of restricted ventilation is not enough to force a fire to transition to under-ventilated conditions.

For each well-ventilated test conducted, the desired test condition was achieved showing that the open test door and moderate fuel loading (1 x SBI test rig) was enough for a well-ventilated fire to occur.

In the cases where the fuel load was doubled (2 x SBI), the equivalence ratio reached around 1.5 each time which is representative of under-ventilated conditions. The tests conducted using the 2 x fuel loading did not have any restriction on the ventilation of the test room. The results have shown that to achieve under-ventilated conditions, the fuel loading of the test should be doubled to force under-ventilation to occur.

3.6.3 Heat release

A summary of the peak heat release recorded in each test conducted in the ISO 9705 room corner is shown in Table 29.

Table 29: Summary of the peak heat release in each test conducted in the ISO 9705 room corner.

Material	Test condition	Peak heat release / kW
Plasterboard	Well-ventilated	648
OSB	Well-ventilated	990
	Under-ventilated (using door)	760
	Under-ventilated (2x fuel load)	4500
Cables	Well-ventilated	750
	Under-ventilated (using door)	480
PU	Well-ventilated	1410
	Under-ventilated	3100

The comparison of the peak heat release reached in tests where a calcium silicate door was used to restrict ventilation shows a reduction in the heat release output measured during the test compared to the test conducted without. This could be a result of the ratio of the heat release to the heat release capacity of the fire room. As ISO room lined with CaSi boards will absorb a lot of heat and inhibit flashover for smaller fires. the geometry and larger fuel load of the 2 x SBI in the 9705 room configuration is excellent for forcing flashover to occur.

In the cases where 2x fuel loading was used, the fires transitioned to under-ventilated flaming. The peak heat release measured in the 2 x OSB test reached, and potentially exceeded, the maximum capacity of heat release measurement (4500 kW). When using 2 x SBI for polyurethane, the heat release increased by approximately 2x.

3.7 SUMMARY OF FIRE EFFLUENT TOXICITY MEASUREMENT

The smoke toxicity was measured throughout each test in both the doorway and exhaust duct. The complete data set obtained for HCN and acid gas sampling can be located in the **Appendix 11**.

A sample of the HCN data obtained from the doorway measurements when testing polyurethane (well-ventilated and under-ventilated) has been shown in Table 30.

Table 30: Summary of the average HCN data obtained in the doorway of the ISO room when testing polyurethane, where the sample number is indicative of sample duration (where 1: 0 to 5 min, 2: 5 to 10 min, 3: 10 to 15 min, 4: 15 to 20 min, 5: 20 to 25 min and 6: 25 to 30 min)

Material	Test condition	Location	Sample number	HCN ppm
Polyurethane	Under-ventilated (2x SBI)	Doorway	1	527.2
			2	97.6
			3	9.9
			4	0
	Well-ventilated (1x SBI no door)	Doorway	1	269.4
			2	25.4
			3	2.3
			4	1.9

The HCN data obtained in the doorway is relatively sporadic, however the lower measurements taken mid-way through the test are likely a result of blockages that occurred in the sampling lines as a result of very sooty testing. The box analysers were successful in sampling using dreschel bottles for wet chemical analysis, but did potentially suffer losses as a result of possible blockages and losses from the use of silicone tubing rather than a heated line. Blockages were not immediately detected as operators were remote from the test room the 9705 room corner was running in.

Minimal losses were expected for permanent unreactive gases (O₂, CO₂ and CO) and so minimal losses were expected by using silicone tubing to connect the stainless steel sampling tube to the box analysers and phi meter. As most of the materials selected for testing were not thought to contain halogenated or phosphorus fire retardants, acid gas concentrations were expected to be very low. Unfortunately, acid gases are reactive, and so without the use of a heated line, gases such as HCl, will dissolve in any condensation that forms in the sample line. As minimal acid gases were expected, this loss was deemed acceptable. Access to, and use of a heated line would have minimised losses, however because of the known sample composition (halogen and phosphorous free) this option was not considered necessary for these tests.

4 CONCLUSIONS AND FUTURE WORK

4.1 STEADY STATE TUBE FURNACE

The developments made to the SSTF have provided the background work and methodology required to enable the standard to begin the process of reaching full specification. The additional methodologies aim to provide the solutions needed to reduce the limitations of the equipment. The methodology for testing non-homogenous thermoplastics and non-combustible materials has been established. Data is now valid, and there are working methodologies for materials previously not covered by the standard.

The SSTF has also been proven to steadily generate toxic species during a test, enabling accurate and repeatable measurements.

With the suggested revisions to the standard, alongside the use of the new methodologies, the SSTF can test a wide range of materials proven by the successful bench-scale testing. Two potential methodologies to calculate the validity of test data have been proposed. The first methodology proposed is based on a Shapiro-wilk test, which would enable the size of the data set to be considered and analysed with relevance to the scale of the data. This would eliminate the problem of very low concentration data sets (such as those obtained from testing non-combustible materials) being rendered invalid due to the variation calculated in the current methodology within the ISO/TS 19700 standard. The second alternative methodology proposed is to impose limitations on the number of decimal points used in the calculation. Limiting the data in the calculation to three decimal places would mitigate the effects of the variance calculation in materials such as plasterboard, which are non-combustible or produce very little volumes of smoke.

The suggested revisions also include methodologies relevant to the materials tested for this project. For non-combustible materials, further clarification should be included in the methodology, particularly for non-combustible materials that have a combustible cover. In tests where no flaming is expected (materials with extremely low fuel contents) the test is to be conducted at 900 °C.

An additional clause would be useful to accommodate non-combustible materials with a combustible paint finish. While the material is non-combustible, the paint will produce a flame at sufficient temperatures. This means that the test would be classified as flaming, despite the flame not being from the material.

Specific suggestions for sample preparation in the standard would also aid testing procedures, as this would allow operators to obtain periods of steady burning during testing and assist in the measurement of a materials smoke toxicity.

A significant amount of bench-scale future work could be conducted based on the findings of this work. Attempting to monitor the equivalence ratio inside the SSTF gave an insight into how the fire conditions located at varying points in an apparatus could be measured. Further improvements to this research could be made by modifying the SSTF combustion tube to allow for direct sampling from the tube, rather than the use of a stainless steel probe sampling through the apparatus. The research conducted in this project aimed to study the fire condition at varying points inside the SSTF, however as the stainless steel sampling line was heated by being placed inside the furnace, the effluent would have undergone the same chemistry as in the combustion tube, resulting in the measurement not working as initially intended. This is why the data reported showed little variation. By placing sample ports into the combustor tube, the equivalence ratio and effluent toxicity could be

monitored at different stages of the experiments conducted in the SSTF. This would provide useful insights into the actual chemistry of the fire effluent taking place as it leaves the flame zone and travels into the cooler, more dilute mixing chamber of the SSTF.

It would also prove interesting to conduct similar experiments using other available bench-scale fire testing apparatus. This would allow for a deeper understanding of the fire conditions achieved in different tests. The phi meter could also be used to monitor the equivalence ratio where gas sampling would occur to provide an insight into the ventilation condition for tests adapted to assess smoke toxicity.

There is also further work that could be conducted using additional nitrogen in the SSTF. While the initial intention of the research was to study the possibilities of creating low oxygen environments to study under-ventilated combustion, the results showed that above a specific flow rate in the apparatus, the flow was too strong compared to the flame, so the flame zone was distorted. The distortion of the flame zone resulted in an alteration in residence time in the flame, making combustion much more inefficient—this increased CO and HCN. Additional research could be conducted to study the effects the alteration in residence time has on smoke toxicity.

Furthermore, additional research using a fixed flow rate and altering the flow ratios of nitrogen and air would also provide a much better insight into creating very low oxygen environments within the SSTF. This would be a better approach of testing lower oxygen environments in the apparatus as there is less chance of flame zone distortions occurring as a result of excess primary air flow in the SSTF.

4.2 PHI METER

The phi meter designed and created for this project successfully monitored the equivalence ratio in large-scale testing. In each test, the equivalence ratio was monitored successfully.

The additional research and design process created a more compact and portable phi meter. The original designs for the phi meter¹⁰⁹ used a significantly bigger furnace with a platinum catalyst and a series of gas and water traps. The original designs also required using oxygen to mix with the fire effluent.

Additional research was conducted to streamline the original designs. Operating conditions were identified through a series of microscale and bench-scale experiments designed using the theoretical background of the concept. The additional research led to a smaller furnace size being used. By using a smaller furnace with low flow rates, the system did not become blocked easily. Additional control over the effluent to air ratio was also obtained using peristaltic pumps with high precision low flow rate mass flow controllers. To minimise the time delay from the use of low flow rates within the furnace, an additional 1.5 L min⁻¹ pump was connected to the sampling line, which was then split between an exhaust line and the sampling line to the phi meter. This also mitigated the time delay from using such low flow rates in the analysis.

The phi meter made and used in this research did not require a catalyst. The furnace design was based on the existing MCC furnace. The preliminary tests were conducted to study the effects of varying furnace temperatures on combustion efficiency. It was found that at temperatures above 800 °C, no CO was formed, and more CO₂ was formed. The temperature of the furnace was chosen to be 900 °C. The phi meter was then fully constructed, calibrated and then tested alongside the SSTF. The SSTF was chosen as it was the only test method available that could quantify the

equivalence ratio. As the data was in agreement with the data obtained on the SSTF without a catalyst, no catalyst was added to the apparatus.

The system was also streamlined by using one drying agent. The final design used a singular tube of Drierite with two glass wool plugs at each end. This was to dry the effluent/air mixture.

The additional research allowed for a more streamlined, cheaper apparatus. The optimal operating conditions and set up procedures have been identified, making it simpler and easier to monitor the equivalence ratio of fires.

The phi meter has been proven to work successfully on both bench and large-scale, and shown to correlate well to the equivalence ratio measured using the validated SSTF methodology on a bench-scale.

In future use, it would pose useful to measure the unburnt hydrocarbons in the doorway. This would allow for an easier comparative calculation to be made between bench and large-scale data. Additionally, the use of 2 phi meters, one in the doorway and one in the exhaust duct, would pose useful to understand the extent of the dilution that occurs in the exhaust duct. It would also be useful for tests where flaming occurs in the doorway.

Additional research could be done on the use of the phi meter for equivalence ratios above 2. The background research focussed on the set up for measuring equivalence ratios of 1.5 and below as it was not expected that the equivalence ratio would reach values above this. Further research into the different flow ratios (where a 1:3 effluent to air ratio is used) would also give an insight into the limitations of the phi meter.

4.3 BOX ANALYSERS

After their construction, the box analysers were used alongside the SSTF to analyse HCN at set intervals over the duration of a test. The electronic circuits functioned as designed, and the timers programmed into the switches were successful in each use throughout this project. As the data collected by the box analysers was in agreement with the data collected using the SSTF, the box analysers were proved to be successful for use in bench-scale assessments.

The box analysers working automatically proved useful in large-scale testing, particularly when the near vicinity of the ISO test room became unsafe from excess smoke release during testing. This was the case when using 2x SBI rigs in the test. When testing OSB and polyurethane with 2x SBI, the smoke poured out of the doorway resulting in the sample lines drawing effluent from the flame zone.

The box analysers were used to monitor the smoke toxicity in the door and exhaust duct during the test. In most tests, the analyser was shown to be proficient at measuring permanent gases (CO, CO₂ and O₂) in the doorway of the test room. The addition of pre-programmed switches meant that operators could remain a safe distance from the test room when a test was conducted.

In some experiments, the filters on the sampling line became blocked easily. Additional research into the design to mitigate the blockages occurring would also pose useful if the analysers were to be used in the future.

As none of the materials contained halogenated species, most ions were below the detection limits. HCN was only within the limits of detection for tests conducted using polyurethane.

In this work, a heated line was not available for use for gas sampling. In the future, it would be ideal to conduct similar testing but with the addition of the heated line. This would mitigate the sample losses that would have occurred (particularly in the case of HCl).

4.4 LARGE-SCALE TEST DESIGN

The large-scale test design provided a significant amount of information surrounding smoke toxicity analysis on a large scale.

One of the most significant findings of this study was how to achieve under-ventilated flaming in the ISO 9705 test successfully. Previous tests conducted in the ISO 9705 room used a door to control the ventilation of the fire in an attempt to achieve under-ventilated flaming¹⁰⁸.

When the fuel loading of the test was doubled (with no door controlling the ventilation), the equivalence ratio surpassed 1.2 and transitioned into under-ventilated flaming. This was proved when testing OSB in 3 different ways in the test room. Using a low fuel loading with a fully open door, allowing for fresh air to enter the room, produced a well-ventilated fire test. For the transition to under-ventilated flaming, a higher fuel loading in relation to the test room should be used.

The ventilation restriction increases the equivalence ratio, but does not have as much of a significant impact on the equivalence ratio than increasing the fuel loading does. To conduct a test in under-ventilated conditions, a high fuel loading should be used with no restriction to the air flow. The high fuel load in a small enclosure results in under-ventilated flaming.

In all tests conducted using a double fuel loading to force under-ventilated flaming, the maximum equivalence ratio reached was 1.55. This is characteristic of an early under-ventilated fire. If a high fuel loading was used, it is thought that the equivalence ratio would surpass 2 and enter post-flashover conditions. This test was not conducted due to safety concerns and time constraints.

The findings of the research suggest that, particularly for enclosed spaces, fuel loading has a much more significant impact on the fire condition than the size of the door opening of a test room that provides ventilation.

Although the large-scale tests were successful, additional tests would provide a significantly deeper insight into the findings of this research. It would prove interesting to study this methodology with other materials and test if this observation is limited to specific materials.

4.5 LARGE-SCALE TESTING: FUTURE WORK

Excess materials were purchased when organising the large-scale testing. This was to enable future bench-scale toxicity assessments to be made using a variety of bench-scale fire tests to test each tests ability to correlate to large-scale toxicity tests using a range of non-combustible and non-homogenous materials. The additional air flow measurements taken in the doorway could be used to calculate the yields of toxicants produced to be used for comparison to bench-scale data collected on the same materials.

The bench-scale assessment comparisons would provide a robust study to identify the test methodology most relatable to large-scale fire behaviour. The bench-scale assessments could be conducted using the same analytical equipment and measurement principles as used in large-scale fire testing.

The selected methodology would then progress onto an inter-laboratory reproducibility assessment where its reproducibility could be assessed. If the test was deemed both repeatable and correlated to large-scale toxicity measurements, then a robust methodology could be proposed to assess the smoke toxicity of construction products.

If it were possible, further large-scale testing using larger fuel loading would be insightful. From the data obtained in this research, it could be possible to use a larger fuel loading (3x) and test if equivalence ratios above 2 could be reached. This would provide data representative of very under-ventilated flaming and be useful for bench-scale data comparisons as well as assessing materials toxicity under a wider variety of fire conditions.

4.6 SUMMARY OF CONCLUSIONS

For smoke toxicity to be regulated as a part of the Construction Product Regulations (CPR), a robust methodology for assessing smoke toxicity for bench-scale and large-scale fires was required. The thesis began by providing a critical review of smoke toxicity studies, focusing on bench-scale apparatus and large-scale testing. The review of bench-scale apparatuses allowed for the selection of a bench-scale test that could be further developed for smoke toxicity analysis. The ISO/TS 19700 SSTF was chosen as a result of it being proven as a repeatable test method for smoke toxicity analysis, and its correlations with large-scale smoke toxicity measurements. The in-depth review of large-scale tests allowed for the methodology for smoke toxicity analysis on a large scale to be defined.

This research studied four materials comprising non-homogenous and non-flammable materials, chosen with the aid of a critical review of the surrounding literature. The materials were studied on a bench-scale using the ISO/TS 19700 SSTF. The current ISO/TS 19700 standard contained several gaps in literature, preventing it from becoming a full standard. This research has provided the specific methodologies for assessing materials currently not covered by the scope of the technical standard. This research has also critically reviewed the information regarding calculations of validity, offering improvements to the methodology.

The relevant background research, method developments and revisions to enable the ISO/TS 19700 to reach full standard have been provided. Initial practical assessments were used alongside a critical review to identify the additional protocols and revisions required. The revisions and practical assessments aimed to assist the development of specific bench-scale methodologies for smoke toxicity assessment.

It is hoped that bench-scale toxicity assessments can be made in the future for direct comparisons using the methodologies and data provided. The SSTF could undergo an inter-laboratory reproducibility assessment after completion of this project to demonstrate the methodology's reproducibility when testing non-homogenous and non-combustible materials, to test its suitability as a test method for use in the construction product regulations.

In addition, this research has provided supportive research behind the ISO/TS 19700 smoke toxicity methodology. The SSTF was used to monitor the formation of HCN and CO over the duration of a test to identify if steady the measurement of CO was indicative of other toxicants being generated steadily, and to ensure gas sampling times suggested in the standard were correct. The formation of HCN mirrored the formation of CO. HCN and CO formation was found to be steady and relatively consistent approximately 5 to 7 mins after sample ignition, and remained steady throughout the test. While this was only observed in simple polymers, it is likely the case with other materials where

a steady concentration of CO is observed. This research confirms the suggested sampling times used in the standard.

Furthering this, the equivalence ratio was also monitored at several locations within the SSTF to identify any changes in equivalence ratio throughout the apparatus and to identify correct sampling positions within the apparatus. The research found that there were no significant deviations in the equivalence ratio throughout the combustion tube or sampling from the mixing chamber, however this was a result of the effluent undergoing the same chemistry as it would in the SSTF tube but inside the stainless steel sampling line as a result of the tube being inside of the SSTF furnace. To further this research, additional modifications could be made to the SSTF to sample from specific locations throughout the tube and draw samples directly, as opposed to through the tube to the analysers. This would allow for the actual measurement of the constituents of smoke at specific points to be measured.

This research also developed methodologies to test smoke toxicity at low oxygen concentrations (< 10%) with the use of additional nitrogen. Supplementary nitrogen was added to the primary gas inlet of the SSTF and used in set volumes to create low oxygen environments when testing simple polymers (PMMA, PA6 and PA6.6). The effects this had on the measured smoke toxicity was also studied. To achieve very low oxygen environments, higher volumes of nitrogen were required. At higher flow rates, the gas flow distorted the flame zone to such an extent that the gas molecules could not remain in the reaction zone long enough to combust fully, resulting in higher yields of products of incomplete combustion occurring (observed and quantified for both HCN and CO). When testing at oxygen concentrations 10 % and above, no significant deviations to the smoke toxicity measured was observed. The method developed is therefore useful to reduce the oxygen environment to 10 % reliably, and much less reliably for concentrations <10 %). To mitigate the effects of this, a set flow rate could be used, and the ratio of nitrogen to air could be altered using mass flow controllers. This would allow for the low oxygen environment measurements to be made, but with no interference from changes in the size of the reaction zone within the flame as a result of a high flow rate.

As all large-scale methods for construction products focus on flammability only, methodologies were required to be modified and developed. In addition, the equipment and methodologies for assessing smoke toxicity on a large scale required design and development.

To measure the smoke toxicity on a large-scale, portable gas analysers were required. As no such analyser was available, portable analysers were designed and created. The analysers were designed to continuously monitor CO, CO₂ and O₂, and specific sampling of HCN and acid gases produced during a fire test. The specific sampling was controlled by program-controlled switches created for the analyser. To ensure the analyser functioned as designed, it was used alongside the SSTF when conducting additional research into HCN formation using standard materials. The analysers were successful in most tests when monitoring the permanent gases evolved during the large-scale testing, as well as proving their success when used on a bench-scale.

The portable gas systems will allow for future toxicity assessments to be made on a large-scale as a cheaper alternative to online FTIR measurements, which require a skilled operator, or manual gas sampling. As the analysers were pre-programmed, they could be set up and left to operate during a test, allowing for analysis to continue if operators must leave due to safety concerns. The addition of online connections to operate and view the data in real-time also adds additional benefits to the system, as the smoke toxicity can be monitored by the operator at a distance.

To identify the fire condition of the large-scale tests, a phi meter was designed and created for this research, based on the original designs of the phi meter. The phi meter designed in this research was much smaller and more streamlined than the original designs to increase portability and improve the original designs. The final apparatus was tested and calibrated using bench-scale methodologies where the equivalence ratio is controllable and known.

This was also used to identify the correct flow of fresh air to fire effluent for determining the equivalence ratio. The research concluded that the best ratio is a 1:1 mix. The phi meter was then used to successfully identify the equivalence ratio throughout the large-scale fire tests. The phi meter was much smaller and portable than the original designs. In addition, the analysis system created had the ability to connect online to other devices, allowing the fire condition to be monitored by the operator at a safe distance. As the controller for the gas flows in the system were controlled by the raspberry pi unit, used to control the phi meter, the flow rates could be adjusted during tests if necessary. The final phi meter created for this work offers a smaller, cheaper design for monitoring the equivalence ratio during fires on a large-scale and bench-scale. If the phi meter were to be used on several pieces of bench-scale apparatus for smoke toxicity quantification, the yields obtained from each methodology could be directly compared by their equivalence ratios. This apparatus allows for the equivalence ratio to be monitored in bench-scale apparatus that do not offer such measurements.

The ISO 9705 room corner test was modified to assess smoke toxicity. The novel methodology used 1 to 2 SBI rig(s) placed on the central load cell within the ISO test room. Standard measurements were taken throughout the tests and fire effluent was additionally studied in the exhaust duct and the doorway of the test room. The tests aimed to represent a range of fire conditions, from well-ventilated to under-ventilated flaming. The fire condition was controlled in several ways, including limiting the ventilation and increasing fuel loading. To enable gas yield calculations for the measurements taken in the doorway, McCaffrey probes were used alongside pressure transducers to for future yield calculations to be made if a bench to large-scale data comparison was required.

Under-ventilated flaming was reached in both tests conducted using double fuel loading (2x SBI rigs). Under-ventilated flaming was not achieved when restricting the ventilation. The experiments showed that restriction of the ventilation does not have a significant enough impact to force the fire to transition into under-ventilated flaming during large-scale assessments made in the ISO room. While the equivalence ratio was raised as a result of the addition of a door, the fuel loading was insufficient and so the equivalence ratio never surpassed 1 when using a door, resulting in the tests being representative of either well-ventilated flaming, or the transitional point between well-ventilated and under-ventilated flaming.

The fire behaviour of the materials was predicted before testing using Cone Tools fire modelling. Cone calorimetry tests were conducted and the mass loss and heat release measurements taken by the cone calorimeter were imputed into the cone tools software.

As cone tools did not allow for the prediction of the specific test layout used (due to its novelty), the data was used to create heat release predictions for an SBI test and an ISO room test conducted using the standard wall lining. Data taken from literature was also used to test the comparison between the cone tools prediction from the data in the literature to actual SBI data obtained on the same material (all taken data was taken from literature). It was found that cone tools greatly overestimated the heat release predictions compared to actual SBI test data (obtained from literature).

This research has provided the information and methodologies required to aid the regulation of smoke toxicity within the CPR. It has provided the revised methodologies required to allow the ISO/TS 19700 to become a full standard and provided robust research to reinforce existing methodologies. The method of testing smoke toxicity on a large scale has also been provided, including details of specific equipment required to assess specific parameters during a large-scale test.

APPENDICES

Appendix 1: Sampling and analysis of acid gases in fire effluent

This appendix contains information regarding the procedures used for acid gas sampling in fire effluent, and analysis of the samples collected. The analysis contains the methodologies for making standard solutions for calibration and the set up of the equipment used for analysis.

Method of sampling:

Acid gases present in fire effluent were trapped by bubbling fire effluent through a known volume of e-pure water in a dreschel bottle at a set flow rate of 1 L min^{-1} . All samples obtained from bench and large-scale testing used 100 mL of e-pure water to collect the samples in. Bench-scale tests conducted on the SSTF used a secondary dreschel bottle containing 100 mL e-pure water to trap any residual acid gases that were not trapped in the first dreschel bottle. The acid gases in both solutions were quantified using ion chromatography and combined to give a total measured quantity.

Preparation of standards:

All chemicals used for the preparation of the anion standards were purchased from Sigma-Aldrich.

A 100 ppm stock solution containing the following salts was prepared: sodium chloride, sodium bromide, sodium nitrite, sodium nitrate and sodium dihydrogen phosphate. The appropriate mass of salt required to make a 100 ppm solution were weighed and dissolved into e-pure water. The stock solution was then used to prepare standard solutions ranging from 1 to 25 ppm via serial dilution.

Preparation of samples for analysis:

Samples collected from experiments were transferred to airtight 150 mL plastic bottles and stored at room temperature. Once ready for analysis, a $0.1 \mu\text{L}$ micro Hepavent filter attached to a 5 mL syringe and the sample was drawn through the filter and into the syringe. The filter was then removed, and the sample was ejected into a 2 mL HPIC vial. The lid was placed onto the vial and loaded into the autosampler, alongside standard solutions containing known quantities of the ions being looked for. Samples were loaded with a blank (water) every 5 samples, and a standard every 10 samples to ensure the HPIC was functioning correctly. 0.1 mL of filtrate was injected into the HPIC for analysis.

Sample information was inputted into the software and set to run. The concentration of the ions in the samples were quantified against the standard concentration curves using Chromelion Software used to run the HPIC. Samples that were out of range were diluted $1/10^{\text{th}}$ and re-analysed.

The concentration of the individual acid gases were quantified using the known flow rate used when sampling, and the duration of the sampling.

Method of analysis

Acid gas samples were analysed using Dionex ICS-2000 High Pressure Ion Chromatography (HPIC) with an IonPak AS11 heated column (set and maintained at $30 \text{ }^{\circ}\text{C}$). Separation of

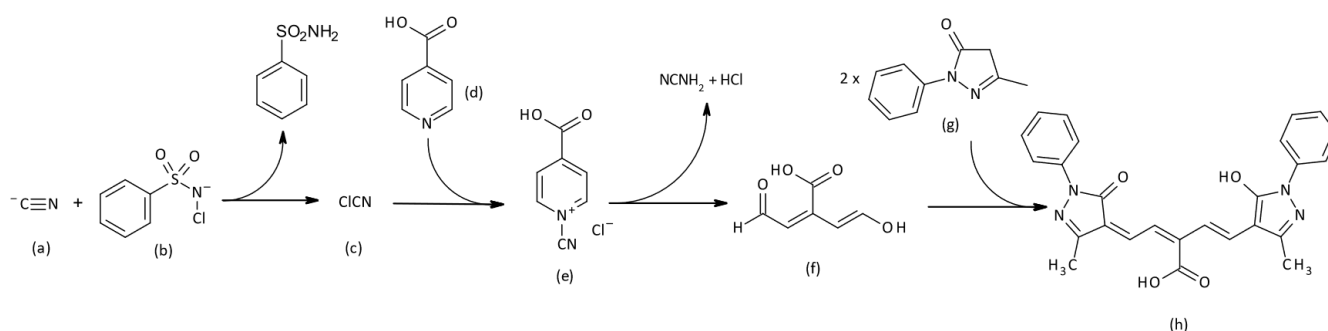
anions was achieved by using a KOH mobile phase of increasing concentration, starting at 1 nmol mL⁻¹ for 15 minutes and linearly increasing to 10 nmol mL⁻¹ at 20 minutes. Samples were quantified against standard concentration curves. Concentrations of acid gases in the samples were calculated by using the sampling flow rate, duration of sampling period and known volume of solution used for sampling.

Appendix 2: Sampling and analysis of Hydrogen cyanide

This appendix contains information regarding the chemical theory behind wet chemical analysis of HCN, details of sampling methodologies and information on how to calculate the concentration of HCN in solution. It also details ion chromatography methodologies for sample analysis.

Chemical theory behind the wet chemical analysis of HCN

HCN was trapped in a solution of weak sodium hydroxide (0.1 M) and quantified by derivatising the solution using chloramine T. The chloramine T reacts with cyanide present in samples producing cyanogen chloride. This then goes on to react with the reagents 1-phenyl-3-methylpyrazole-5-one and isonicotinic acid yielding a blue solution. The cyanogen chloride breaks the aromatic ring present in isonicotinic acid producing carboxy-glutaconic aldehyde, which can then react with 1-phenyl-3-methylpyrazole present in the reagents to produce the polymethine dye. Hydrochloric acid and cyanamide are also produced as by-products. This can be shown in reaction scheme 1. The intensity of the solution will increase with increasing cyanide concentration which can be measured colourimetrically as the dye follows Beer-Lambert law whereby the concentration of cyanide ions in solution is directly proportional to absorbance. This method is described in ISO 19701⁸⁷.



Scheme 1 a) Cyanide ions b) Chloramine-T c) Cyanogen Chloride d) Isonicotinic Acid e) 1-cyano-4-carboxy-pyridinium chloride f) Carboxy-glutaconic aldehyde product g) 1-phenyl-3-methyl-5-pyrazolone h) Polymethine dye product

Sampling for HCN in fire effluent:

All reagents used for analysis were purchased from Sigma Aldridge.

Effluent was bubbled into 150 ml 0.1M NaOH at a constant flow of 1 L min^{-1} . While the time sampled for individual experiments varied, sampling generally took place for a minimum of 5 minutes.

A solution containing 1 mg mL^{-1} Chloramine-T in deionised water was prepared and labelled reagent 1. A second reagent was prepared by combining 7.5 mg mL^{-1} isonicotinic acid, 1.5 mg mL^{-1} 1-phenyl-3-methyl-5-pyrazolone and 10% v/v dimethyl formamide (DMF) in deionised water. A phosphate buffer solution at pH 7.2 was also prepared using a combination of sodium hydrogen phosphate and potassium dihydrogen phosphate.

A series of CN^- standards were prepared, ranging from 0.2 ppm CN^- to 8.0 ppm CN^- . 1 mL of each standard was placed in individual test tubes, followed by 1 mL of each sample collected

during testing. To each test tube, the following was added: 9 mL deionised water, 4.5 mL phosphate buffer solution and 2 mL of reagent 1. As the analysis was conducted sequentially, 4.5 mL of reagent 1 was added to the solutions (1 minute apart). At 5 minutes, 4.5 mL of reagent 2 was added to the first test tube. 35 mins after the addition of reagent 1, the sample was placed in a 1 cm and 4 cm cuvette and analysed using a ultra-violet-visible spectrophotometer (UV-Vis) set to $\lambda=638$ nm. The absorbance was recorded and later compared to the calibration standards to calculate the concentration of HCN in solution. Solutions where the absorbance exceeded the limits of detection of the UV-Vis (> 2.5) were diluted $1/10^{\text{th}}$ and analysed again.

Calculation of HCN concentration

The HCN concentration in solution was calculated from the absorbance data by using the following method.

The absorbance values obtained from the standard solutions were plotted against their concentration and used to input values into Equation 1. The calculated values from equation 1 were used to calculate the concentration of cyanide ions in solution in mg L^{-1} by using equation 2. Using equation 3, the total mass of HCN sampled in milligrams was calculated. To calculate the concentration of HCN in the effluent in mg L^{-1} equation 4 was used, and in ppm equation 5 was used.

$$y = ax^2 + bx + c \quad \text{Equation 1}$$

$$\text{mg L}^{-1} \text{CN}^- \text{ in solution} = ((a \times \text{absorbance}^2) + (b \times \text{absorbance}) + c) \times \text{dilution factor} \quad \text{Equation 2}$$

$$\text{mg of HCN sampled} = \text{mg/L CN}^- \times \text{volume} \times (27/26) \quad \text{Equation 3}$$

$$\text{mg L}^{-1} \text{ in atmosphere} = \text{HCN mg} / \text{volume of air sampled} \quad \text{Equation 4}$$

$$\text{ppm} = \text{HCN mg} \times 888 / \text{volume of air sampled} \quad \text{Equation 5}$$

Ion chromatography for HCN analysis:

Potassium cyanide was purchased from Sigma-Aldrich and used to make a series of KCN⁻ standard solutions ranging from 1 ppm to 8 ppm. Standard solutions were used to create graphs used for calibration and for quantifying HCN concentration of samples by creating a standard curve.

Samples were analysed using a Dionex ICS-2000. It contained an IonPak AS11 heated column set to a constant temperature of 30 °C.

Samples collected from experiments were transferred to airtight plastic bottles and stored at room temperature. Once ready for analysis, a 5 mL syringe was connected to a 10 µm microporous Hepavent filter. The sample was then drawn through the filter and into the syringe. The filter was then removed, and the sample was ejected into a HPIC vial. The lid was placed onto the vial and loaded into the autosampler, alongside standard solutions containing known quantities of the ions being looked for. Samples were loaded with a blank (0.1 M NaOH) every 5 samples, and a low concentration (1 – 5 ppm) standard every 10 samples to ensure the HPIC was functioning correctly. 0.1 mL of filtrate was injected into the HPIC for analysis.

Sample information was inputted into the software and set to run. The concentration of HCN in the samples were quantified against the standard concentration curves using Chromelion Software used to run the HPIC. Samples that were out of range were diluted 1/10th and re-analysed.

The concentration of the individual acid gases were quantified using the known flow rate used when sampling and the duration of the sampling.

Appendix 3: ISO/TS 19700 Steady State Tube Furnace Standard methodology

This appendix contains information regarding the set up of the SSTF and details regarding sample preparation. It also contains instructions on how to calculate the equivalence ratio for a test, information regarding the calibration of the apparatus as well as information pertaining to equipment maintenance and test modifications.

Set up and sample preparation for the SSTF

The fire toxicity of materials tested using the ISO/TS 19700 Steady State Tube Furnace under standard conditions using standard methodology followed the following procedures.

Materials were tested in three fire conditions as defined in ISO 19706. A summary of the fire conditions and the corresponding apparatus air flow settings are shown Table 1

Table 1: Air flow settings used in the ISO/TS 19700 SSTF for different fire conditions.

Fire stage	SSTF Primary air flow setting / L min ⁻¹	SSTF Secondary air flow setting / L min ⁻¹	Total flow of gas through the SSTF / L min ⁻¹
Stage 2 well-ventilated flaming	10	40	50
Stage 3a small under-ventilated flaming	3.2 (or calculated from the well-ventilated test data if possible)	46.8	50
Stage 3b large under-ventilated flaming	3.2 (or calculated from the well-ventilated test data if possible)	46.8	50

Samples were prepared by cutting materials into strips of 800 mm weighing approximately 20 g. In the case of pellets, 20 g of sample material was weighed out and evenly distributed across the sample boat.

Once samples were prepared and placed on the sample boat, and the air flows were set to produce the desired test condition. Air flows were regulated to specific flow rates using Brooks Instruments 0254 mass flow transmitter with Brooks Instruments GF Series Thermal Mass flow controllers to keep the air flow consistent during testing. The sample feed rate was calculated and inputted to achieve a sample input rate of 1 g min⁻¹.

Oxygen concentrations were monitored using paramagnetic oxygen analysers and electrochemical cells. CO₂ was monitored using non-dispersive infrared (NDIR), and CO was monitored using an electrochemical cell with a range of up to 20,000 ppm. Each analyser was connected to an OMEGA 5600 personal DAQ data logger connected to a computer to measure the raw voltage output. All analysers were protected from soot deposits and moisture by using a combination of 50 µm microporous (Hepavent) filters obtained from Fisher Scientific, glass wool traps and drying agents (a combination of silicone-gel drying agent and Drierite was used). Effluent was drawn through the analysers at 1 L min⁻¹ and regulated by Brooks Instruments GF series thermal Mass flow controllers.

Sampling for HCN and acid gasses was achieved by connecting a silicone tube for each analyte (one for HCN, one for acid gasses) to the mixing chamber of the SSTF and drawing effluent through a Dreschel bottle containing 150 mL 0.1 M NaOH and 150 mL deionised water respectively at 1 L min⁻¹ during steady burning for approximately 5 mins. A second Dreschel bottle containing the same solutions was placed in series to prevent any losses of analytes occurring.

Calculation of equivalence ratio

A significant reason for using the SSTF for smoke toxicity measurement is its ability to identify the equivalence ratio during testing. Fire effluent is drawn from the mixing chamber through to the secondary furnace at a constant flow rate of 1 L min⁻¹. The furnace is pre-set to 900 °C and contains a quartz wool filter. As the effluent is drawn through the furnace, the high temperatures forces products of incomplete combustion in the effluent to fully combust to CO₂ and H₂O. The effluent then passes through an NDIR used to measure CO₂ and a paramagnetic O₂ analyser. The CO₂ measurement can then be used for a carbon balance calculation. The O₂ measurement is then used to calculate the equivalence ratio, and hence fire condition, of the test.

Equivalence ratio has been calculated based on oxygen depletion as shown in equation [6].

The calculation of equivalence ratio was carried out using a derived equation based on the available parameters measured in the ISO 19700 SSTF. The derivation can be Shown in equations [6] through [13]

$$\Phi = \text{stoichiometric fuel - to - air ratio} / \text{actual fuel - to - air ratio} \quad \text{Equation 6}$$

$$[O_2] \text{ in tube} = VO_{2\text{Primary}} - VO_{2\text{Secondary}} \quad \text{Equation 7}$$

By taking equations [6] and [7] into consideration, equation [8] and [9] are formed.

$$VO_{2\text{Primary}} = ([O_2]_{\text{Primary}}/100) X V_{\text{total}} \quad \text{Equation 8}$$

$$VO_{2\text{Secondary}} = ([O_2]_{\text{Secondary}}/100) X V_{\text{Secondary}} \quad \text{Equation 9}$$

By adding equations [8] and [9] and simplifying, equation [10] is formed.

$$[O_2] \text{ in tube} = \left(\frac{[O_2]_{\text{Primary}}}{100} X V_{\text{total}} \right) - \left(V_{\text{SEC}} X \frac{[O_2]_{\text{Secondary}}}{100} \right) / V_{\text{PM}} \quad \text{Equation 10}$$

In the case of an over-ventilated fire, the [O₂] in the tube can be calculated using equation [11].

$$\Phi = [O_2]_{\text{air}} - [O_2]_{\text{tube}} / [O_2]_{\text{air}} \quad \text{Equation 11}$$

This equation then expands to produce equation [12]

$$\Phi = \frac{20.95}{20.95} - \left(\frac{([O_2]_{\text{primary}} \times V_{\text{tot}}) - ([O_2]_{\text{air}} \times V_{\text{secondary}})}{(V_{\text{primary}} \times [O_2]_{\text{air}})} \right) \quad \text{Equation 12}$$

Equation [12] can then be simplified to produce [13].

$$\Phi = 1 - \left(\frac{([O_2]_{air} \times V_{secondary}) - ([O_2]_{primary} \times V_{secondary})}{(V_{primary} \times [O_2]_{air})} \right) \quad \text{Equation 13}$$

Where:

$V_{O_2 \text{ Primary}}$ is the volume of O_2 used for the primary air inlet in $L \text{ min}^{-1}$.

$V_{O_2 \text{ Secondary}}$ is the volume of O_2 used for the secondary air inlet in $L \text{ min}^{-1}$.

$[O_2]_{\text{primary}}$ is the % of oxygen measured in the mixing chamber.

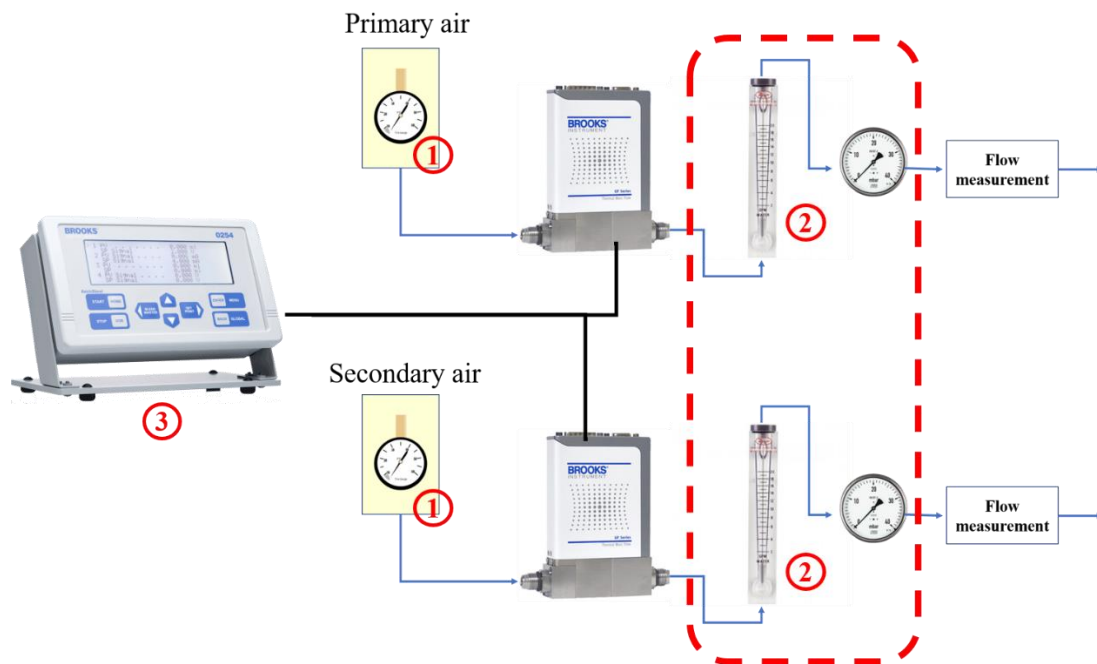
$[O_2]_{\text{secondary}}$ is the % of oxygen measured after complete combustion has occurred.

V_{tot} is the total volume of gas passing through the system in $L \text{ min}^{-1}$.

V_{pm} is total volume of primary air used.

V_{sec} is the total volume of secondary air used.

Calibration of SSTF: Flow meter controllers



- ① Pressure of primary and secondary wall air supply are set at 2.5 bars. The pressure of secondary air supply must be greater than 2 bars.
- ② The rotameters and their pressure gauges are useless, they have no effect on the airflow rate. The mass flow meters perform well for the airflow control.
- ③ Mass flow secondary electronics settings

Select CHANNEL 1 (or 2) by press the Enter/Menu key

Select Instrument configuration by press the Enter/Menu key

Input the following parameters

Table 2: Channel input settings for the SSTF used in this research

CHANNEL 1: primary air control	Measure Unit	sl	<i>fixed</i>
	Time Base	min	<i>fixed</i>
	Decimal Point	x.xx	<i>fixed</i>
	Gas factor	1.000	<i>fixed</i>
	Log Type	Off	<i>fixed</i>
	PV Signal Type	4-20mA	<i>fixed</i>
	PV Full Scale	55 sl/m	<i>fixed</i>
	SP Signal Type	4-20mA	<i>fixed</i>
	SP Full Scale	55 sl/m	<i>fixed</i>
	SP Function	Rate	<i>fixed</i>
	SP rate	10 sl/m	<i>(can be vary from 2 to 12 sl/m)</i>
	SP VOR	Normal	<i>fixed</i>
	SP Batch	0.00	<i>fixed</i>
	SP Blend	0%	<i>fixed</i>
SP Source	Keypad	<i>fixed</i>	

CHANNEL 2: secondary air control	Measure Unit	sl	<i>fixed</i>
	Time Base	min	<i>fixed</i>
	Decimal Point	x.xx	<i>fixed</i>
	Gas factor	1.000	<i>fixed</i>
	Log Type	Off	<i>fixed</i>
	PV Signal Type	4-20mA	<i>fixed</i>
	PV Full Scale	48 sl/m	<i>fixed</i>
	SP Signal Type	4-20mA	<i>fixed</i>
	SP Full Scale	48 sl/m	<i>fixed</i>
	SP Function	Rate	<i>fixed</i>
	SP rate	40 sl/m	<i>(can be vary from 38 to 48 sl/m)</i>
	SP VOR	Normal	<i>fixed</i>
	SP Batch	0.00	<i>fixed</i>
	SP Blend	0%	<i>fixed</i>
SP Source	Keypad	<i>fixed</i>	

Table 3: Primary air supply (PV-SP signal type 4-20mA, PV-SP full scale 50 sl/m)

Flow rate (sl/m) \ Pressure (bar)	2	4	8	12
1	2.2	4.3	8.3	12.3
2	2.2	4.3	8.3	12.3
3	2.2	4.3	8.3	12.3
4	2.2	4.3	8.3	12.3
5	2.2	4.3	8.3	12.4

Table 4: Primary air supply (PV-SP signal type 4-20mA, PV-SP full scale 55 sl/m)

Flow rate (sl/m) \ Pressure (bar)	2	4	8	12
1	2.0	4.0	8.0	12.0
2	2.0	4.0	8.0	12.0
3	2.0	4.0	8.0	12.0
4	2.0	4.0	8.0	12.0
5	2.0	4.0	8.0	12.0

Table 5: Primary air supply (PV-SP signal type 0-20mA, PV-SP full scale 50 sl/m)

Flow rate (sl/m) \ Pressure (bar)	2	4	8	12
1	2.2	4.3	8.3	12.3
2	2.2	4.3	8.3	12.2
3	2.2	4.3	8.3	12.2
4	2.2	4.3	8.3	12.2
5	2.2	4.3	8.3	12.4

Table 6: Primary air supply (PV-SP signal type 4-20mA, pressure 2.5 bar)

Flow rate (sl/m) \ Primary full scale	2	4	8	12
50	2.2	4.3	8.3	12.3
55	2.0	4.0	8.0	12.1
60	1.5	3.5	7.3	11.4

Table 7: Secondary air supply (PV-SP signal type **0-20mA**, PV-SP full scale **50 sl/m**)

Flow rate (sl/m) \ Pressure (bar)	38	40	48
1	30.2	-	-
2	34.6	36.4	44.6
3	34.6	36.4	44.6
4	34.6	36.4	44.6
5	34.6	36.4	44.6

Table 8: Secondary air supply (PV-SP signal type **4-20mA**, pressure **2.5 bar**)

Flow rate (sl/m) \ Primary full scale	38	40	48
40	51.2	54.0	62.5
45	42.2	45.1	53.0
48	38.1	40.0	48.0
50	36.6	38.4	46.8

Temperature calibration

The SSTF furnace was calibrated by following the procedure outlines in sections 7.2 and 7.2 in the ISO/TS 19700 standard.

The temperature calibration for the equipment is shown in Figure 1 and Table 9.

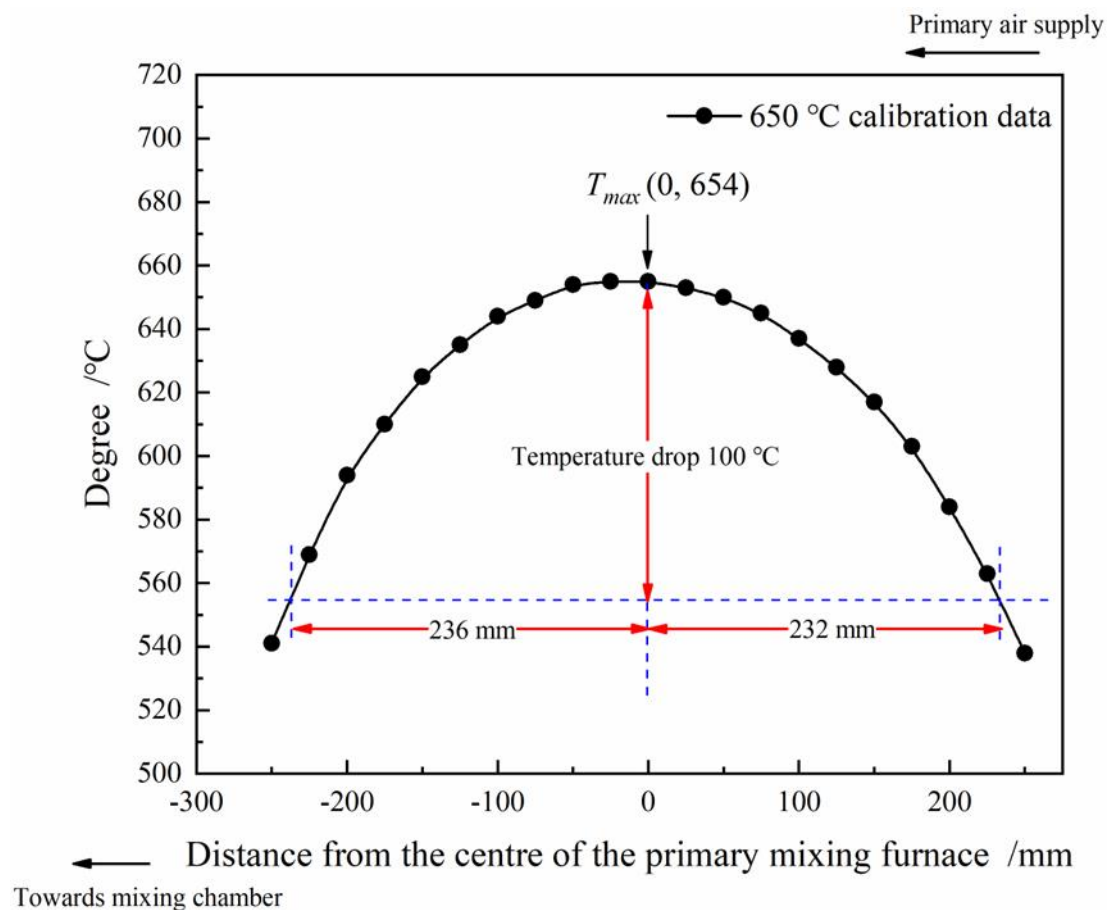


Figure 1: Temperature profile obtained from calibrating the SSTF furnace at 650 °C well-ventilated conditions .

Table 9: Desired and set temperatures under different air flow conditions in the SSTF used in this project.

Desired T_{Run} °C	Air flow condition (sl/m)	2	5	10
	Set Temperature °C			
350		350	355	375
650		650	652	670
825		830	840	865
900		920	924	935

SSTF Maintenance and modifications

The initial state of the SSTF used for experimental procedure often leaked and was in a state of decline. The SSTF was dismantled and refurbished and set up in accordance with the standard.

An additional 4 sampling ports were added to the SSTF mixing chamber to allow for additional sampling to take place. The mixing chamber was then stripped and relined with Teflon sheets. All quartz tubes and boats were cleaned by passing them through a furnace set to 1000 °C. All gas lines connecting the equipment were replaced with new PTFE tubing. The laser system was replaced and recalibrated using optical filters.

The SSTF primary and secondary gas inlets were upgraded and a new gas sampling system was added to the equipment. All outdated gas flow systems were removed and replaced with direct connections from the gas supply to the mass flow controllers. The correct operating pressure for the gas supply was set and remains constant. O₂ and CO electrochemical cells were also replaced.

The gas lines were connected to individual sampling lines. The sampling lines were connected to Hepa vent filters, stainless steel Swagelok filters purchased from Tom Parker, UK. These were connected to mass flow meters before connecting 24 V Charles-Austin LTD pumps. The pump then connected to an exhaust line. A final schematic diagram is shown in Figure 2, and a photograph of the final set up is shown in Figure 3.

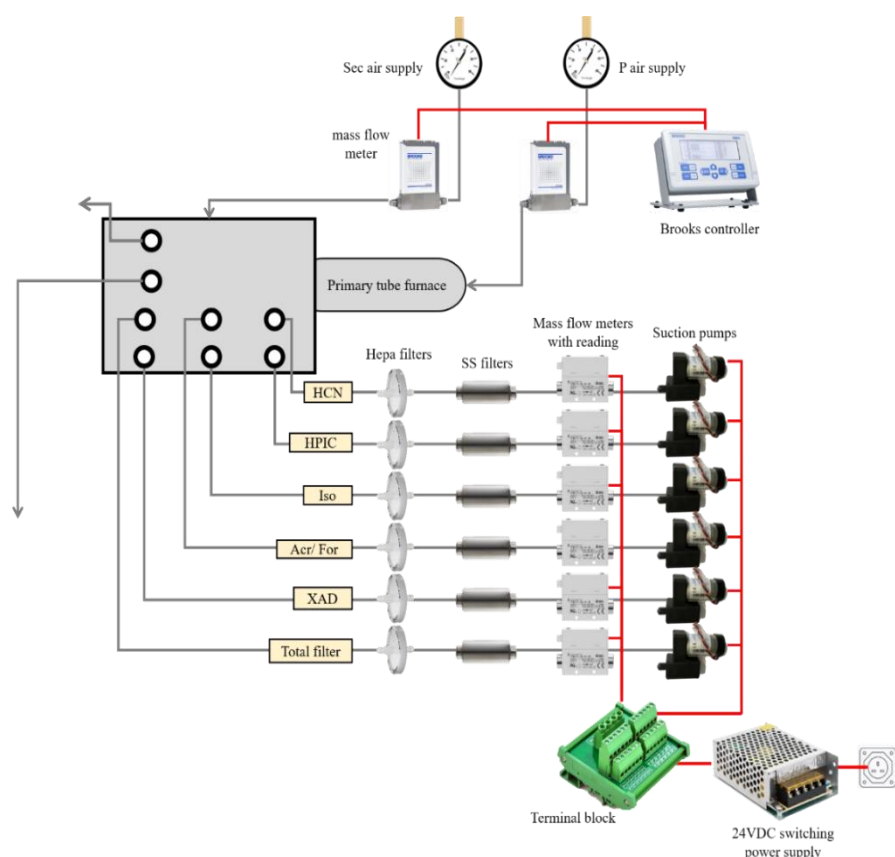


Figure 2: Set up of updated SSTF set up and additional gas sampling system.



Figure 3: Picture of the final set up of the additional gas sampling system used on the SSTF.

All electronics were powered by a 24 V DC power supply block, purchased from RS Components, connected to a terminal block, purchased from Amazon, to split power to 12 power supply lines.

Calibration of the steady state tube furnace

Standard operating procedures were followed for the following experiments. Details of the experimental procedures followed can be found in ISO/TS 19700.

The SSTF secondary air flow was calibrated in accordance with ISO/TS 19700. The results obtained from this calibration are shown in Table 10.

Table 10: Calibration of SSTF secondary air flow in accordance with ISO/TS 19700, including specified tolerance values used to test the calibration data obtained.

V_{N2} Primary flow L min⁻¹	V_{air} Secondary flow Lmin-1	Measured O₂ depletion	Standard specification tolerance		
			-0.0005	0.0005	Calibration pass/fail
10	40	0.0422	0.0415	0.0425	Pass
10	45	0.0384	0.0376	0.0386	Pass
10	47	0.0373	0.0363	0.0373	Pass
10	48	0.0361	0.0356	0.0366	Pass
3	47	0.0131	0.0121	0.0131	Pass

Appendix 4: ISO 5660 Cone calorimetry testing: standard methodology used

This appendix contains the methodology used for the cone calorimeter and details regarding the sample preparation for testing.

Cone calorimetry methodology and sample preparation

Samples were analysed using a Govmark model CC-2 cone calorimeter and tested in accordance with ISO 5660. A diagram of the cone calorimeter is shown in Figure 4.



Figure 4: Photograph of the ISO 5660 Cone Calorimeter.

Materials were cut to 100 mm x 100 mm and wrapped in aluminium foil with the surface exposed and placed onto a lead sample holder without the case on. Tests conducted on cables were prepared by cutting cables into 10 cm strips and laid closely together on the sample holder with the ends slightly exposed (approximately 0.5 mm). Plasterboard samples were tested with the paper still on. For each test the sample was weighed, and relevant information inputted into the cone calorimeter software.

Samples were subjected to a heat of 50 kW and time to ignition, mass loss, rate of heat release and smoke production were measured.

The test was measured from time to ignition to the when flaming ceased within the material. All samples were ran in duplicate.

Appendix 5: Microscale Combustion Calorimetry: Standard testing methodology

This appendix contains details regarding calibration testing and the methodologies used for sample testing.

Prior to testing, a pellet of polystyrene (weighing between 0.21 to 0.25 mg) was placed in a crucible and used to run a pre-set calibration test.

Approximately 1 to 3 mg of sample was weighed out and placed into a ceramic crucible. The sample was then loaded into the MCC. A pre-set method to measure heat of combustion was selected. The material information was placed into the software and the MCC test was set to run.

The tests were ran in accordance with the ASTM D7309-21b¹²³ test method standard. The sample was placed in a ceramic crucible and placed on the specimen holder. It is then inserted into the specimen chamber. The sample is then heated in an inert atmosphere of nitrogen by use of a controlled temperature program, heating the sample at 1 Ks^{-1} . As the sample pyrolyses, any volatiles produced but the sample rise into the combustion chamber where the volatiles mix rapidly with oxygen (set to $900 \text{ }^\circ\text{C}$). A diagram of the MCC is shown in Figure 5¹¹³.

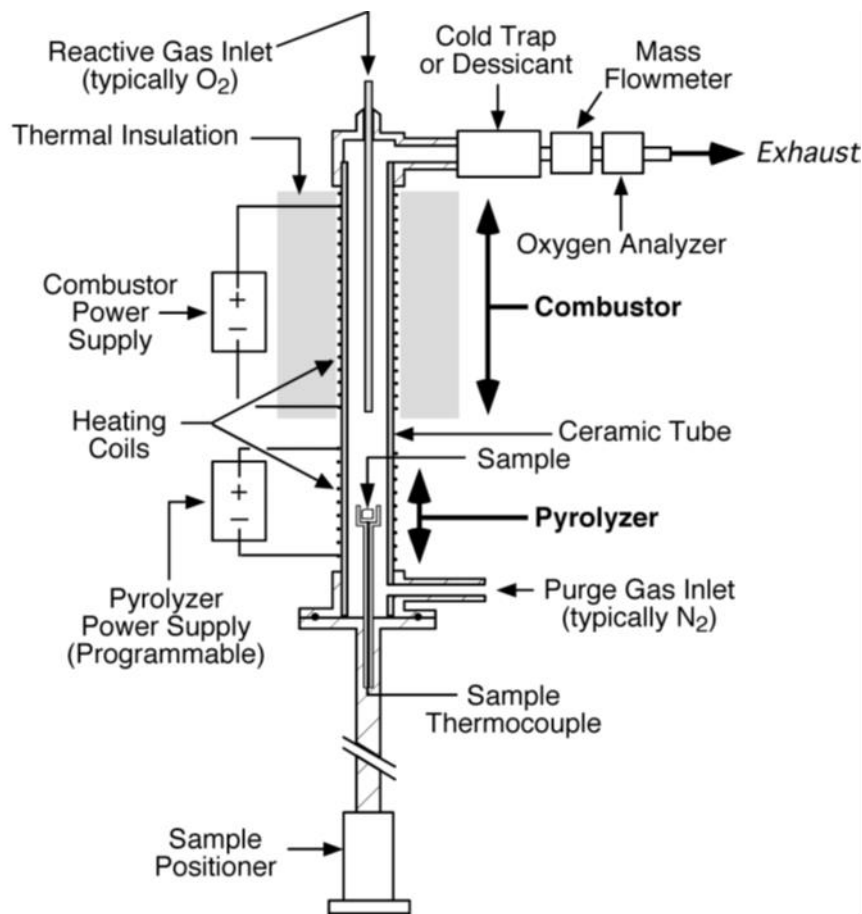


Figure 5: Schematic diagram of Microscale Combustion Calorimetry¹¹³.

Appendix 6: Using the McCaffrey probe data to calculate air velocity

This appendix contains information and details about the pressure transducers used for the measurement of air velocity in the McCaffrey probes, as well as details regarding the calculations from the voltage measurements to air velocity.

The McCaffrey probe was connected to a SDP1000-L05 Pressure transducer purchased from Sensirion.

Table 11: Summary of the information obtained from the pressure transducer data sheet

Parameter	Information
Pressure range	-5 Pa to 125 Pa
0 Pa voltage output	0.25 V
Maximum voltage output	4 V
I factor	125 Pa

The information collected from the data sheet, shown in Table 11, was used in the following equations.

The pressure transducer has a linear output, and so equation 14 can be used to calculate the pressure.

$$P = \frac{I_{factor} \times (voltage - 0.250)}{3.750} \quad \text{Equation 14}$$

The value of 3.75 is the maximum voltage output of the pressure transducer – the voltage output at 0 Pa (4 V – 0.25 V).

As the air density changes with temperature, the density was calculated using the thermocouple reading that was in closest proximity to the probe. The density was calculated using equation 15.

$$\frac{\rho_{298 K}}{\rho_{actual}} = \frac{T_{298 K}}{T_{actual}} \quad \text{Equation 15}$$

This was then used to calculate the velocity using the calculated pressure and air density for equation 16.

$$v = \sqrt{\frac{2\Delta P}{\rho}} \quad \text{Equation 16}$$

The McCaffery probe at the bottom of the door were added to allow for estimation of the air flow into the room. The probes at the top of the door can be used to estimate the flow out of the room.

Where: P is pressure (pa), ρ is density (in kg m⁻³), v is velocity (in ms⁻¹), T is temperature (in K).

Appendix 7: Calculation of volume flow of gas using McCaffrey probe measurements.

This appendix contains information regarding the use of air velocity measurements alongside temperature measurements to calculate volume flow of gas in an opening.

Calculation of volume flow of gas

At ambient conditions the air flow in is equal to the airflow out of the room by mass or volume at 298 K. Using the area of the door, and assuming the flow is even across the door area, in or out, the upper McCaffrey probe can be used to estimate the velocity of the effluent going out of the room, and the lower McCaffrey probe to estimate the velocity of air entering the room.

The data obtained from the thermocouple tree in the centre of the doorway can then be used to estimate the height of the neutral plane, and the temperature of the effluent leaving the room.

Assuming constant pressure, and using mass flow rates (or by corrected volume flow to 298 K), equation 17 can be used.

$$\frac{V_{298\text{ K}}}{V_{\text{actual}}} = \frac{298\text{ K}}{T_{\text{actual}}} \quad \text{Equation 17}$$

The three measurements can be split into upper and lower values. The upper values are those measured above the neutral plane: Upper area (A_u), Upper temperature (T_u) and velocity (V_u). The lower values are those measured below the neutral plane: Lower area (A_l), lower temperature (T_l) and velocity (V_l). It should be noted that A_l is smaller than A_u as T_u is greater than T_l , although the mass flow or volume flow at 298 K should be equal.

Equation 18 is for the lower volume flow calculation.

$$\text{Volume flow lower} = V_{\text{actual}} = AL \times vL \quad \text{Equation 18}$$

The upper volume flow can be calculated using Equation 19 and 20.

$$V_{\text{Actual}} = A_u \times v_u \quad \text{Equation 19}$$

$$v_{298} = \frac{298}{T_{\text{Actual}}} \times A_u \times v_u \quad \text{Equation 20}$$

Appendix 8: ISO/TS 19700 Steady State Tube Furnace manual and user guide

This appendix contains the SSTF user manual written and created for this work.

Important note:

This guide has been written specifically for the ISO/TS SSTF at UCLan.

Setting up the SSTF

As there are several individual components to set up on the SSTF, please use the check-list attached at the end of this document to ensure you have set up all components of the SSTF before running a test.

The process to set up the SSTF is as followed:

Step 1: Turning everything on.

There are 6 sets of plug sockets that need to be turned on (essentially anything with a plug in the socket on the wall from the computer downwards will need to be switched on).

Turn on the computer and log in (Login: administrator Password: steadystate).

Plug in the plug for the sensors (it is white and should be next to the computer plug on an extension lead). The light on the box next to the oxygen analysers should be on. Behind the computer on the wall, there is a box with a switch on it. Flip the switch to turn the smoke laser on.

Turn on the pump that is next to the computer.

Turn on the primary furnace and set to your desired temperature.

Put the primary air flow into the end of the SSTF tube.

If you do not do this, the tube will get **very hot** while the furnace is heating.

Ensure there is quartz wool in the centre of the secondary furnace tube. Turn on the secondary furnace and set to 900 °C.

Turn on the air flow controller (to set this up see details below)

Turn on the primary and secondary air flow at the wall (only the black gas tap needs to be turned, they are set to the correct output).

Turn on the vacuum line and drive mechanism. For the vacuum line, it should turn on automatically after turning the plug on (if not, press the on button). Press start on the vacuum. It is ready for use.

Once everything is turned on, put the glass door onto the mixing chamber and clamp in place. If you are planning to run an under-ventilated test, ensure you place the glass plug into the end of the tube (where it protrudes into the mixing chamber) prior to clamping the glass door in place.

Step 2: Setting up your desired test.

The main components you will need to set for a test method are: **Primary and secondary air flows** and **feed rate**.

Setting up the correct air flow:

After turning on the air flow controller (small white box with a screen), turn on the primary gas tap and the secondary gas tap at the wall.

On the screen, go to “1. PV rate, SP rate”, press set and enter. This is for your primary air flow.

Scroll down until you are on “PV Full scale”. Input the value for desired conditions (see table below).

Go back to the main screen.

Scroll down to “2. PV rate, SP rate”, press set and enter.

Scroll down until you are on “PV full scale” and input the desired value. This is for your secondary air flow.

Your air flow is set.

Condition required	PV full scale value for primary l min ⁻¹	PV full scale for secondary L min ⁻¹
Well-ventilated	10	40
Under-ventilated	3.2	46.7

These values are *rough guides* for the desired condition. Typically they will provide the desired condition, however they may need adjusting depending on the burning behaviour of the material. If so, calculate the primary air flow required and set the secondary flow accordingly (based on your desired equivalence ratio) (the total of your air flows needs to = 50).

NOTE: During a run, if it looks like the flame is being blown out (wispy flaming), your primary air flow may need reducing.

How to check the air flow you have set is what is being produced:

There are 2 yellow flow meters on the end of the bench of the SSTF. To check the air flow, you will need to plug the line you would like to check into the flow meter (there are arrows to show you which is the inlet and which is the outlet).

Grab a timer

Turn on the flow meter

Press start on the flow meter and on the stop watch (at the same time).

After 1 minute, check the value of the flow meter. If the value is the same as what you have set it to, then your flow is correct. If it is not, the tap on the wall may need adjusting. Adjust the tap accordingly and repeat steps 2-4 until the correct flow is reached.

Alternatively, connect a flow meter to the end of the primary air inlet. Turn on the flow meter and check it reads the same as what has been set up.

2 bar of air- don't change the flow on the wall, need to be confident in flow meter if checking this.

Setting up the correct feed rate:

Generally, the feed rate should be set to introduce the sample at 1g a minute. The feed rate will vary with your sample weight. To calculate the correct feed rate, use the equation below:

$$\text{Feed rate} = \frac{\text{Sample length in mm}}{\text{Sample mass in g}}$$

As an example:

A sample weighing 20 g that is 800 mm long will require a feed rate of 40 (800/20).

Setting up your primary line:

To do this, you will need:

Grease

Glass wool

Two bubbler traps for water (optional)

1 bubbler trap for silica

Silica (kept in the oven)

Ascarite

Medium size tubing

Get your a bubbler trap and fill it to around 1/3 full with water. Lightly grease the tops of the bubbler before putting the top on (this will prevent them sticking together).

Label "trap 1".

Place trap 1 on a stand close to the mixing chamber. Trap 1 will draw directly from the mixing chamber. Use the tubing to connect trap 1 to the silica trap. Remember the gas must go down into the water. The exit of trap 1 should be connected to the entrance to the silica trap. You need to make sure they are connected in the correct direction so that the pump does not draw in water. Always double check you have connected them in the correct way otherwise the pump will break.

These traps are optional. if you are expecting a very sooty run or a significant volume of irritants to be produced, it is advised to use at least 1 trap.

Get your silica bubbler trap. Fill the trap with silica to around 1/5th of the size of the bubbler. Then place around a tablespoon amount of glass wool (roughly ball shaped) on top of the silica. Lightly grease the top of the trap and place the top onto the trap. Connect this to trap 2 and clamp in place.

There will be a circular tube directly attached to the pump. Remove this tube and fill this with glass wool. Reconnect to the pump. Before you connect this, check if there are any stray pieces of the

glass wool sticking out. Try to ensure there are none sticking out as this will potentially cause a leak in your connection. Then connect the line exiting the silica trap to this. This connection should be tight. At this point you should see bubbles in trap 1 and 2.

Check the flow meters on the wall. They should be within the marked ranges. If they are not, adjust the flow until they are. They should both sit around 1 L min^{-1} .

Follow the gas line until you reach another circular tube. Remove them and place a glass wool plug in one end. Loosely fill the rest of the tube with silica, then place a glass wool plug on the other end. Connect this in the same manner you have in step 5.

Follow the gas line until you reach the ascarite tube close to the oxygen analyser. Remove the glass tube. In one end, place a glass wool plug. Loosely fill the tube with ascarite (it should not be tightly packed and should look like a layer of ascarite taking up around half the volume of the tube when lying down. Plug the other end with glass wool and reconnect tightly.

This will need replacing if the ascarite goes white. This can happen during the day if numerous tests have been carried out.

If there is ascarite *already in the tube* you will need to remove this. To do so, take the tube to the sink. Remove the glass wool plug and throw this away. To remove the ascarite, run cold water through the tube. **Do this slowly as the tube will get hot.** Once it is dissolved, remove the glass wool from the bottom and dry the tube well.

Setting up your secondary line:

Connect a soot filter to the beginning of the secondary line (this is the line that goes directly to the secondary furnace).

Setting up the computer:

Open the SSTF recording software on the computer (labelled pDAQView).

Turn on the extraction.

The SSTF is now ready for a calibration run.

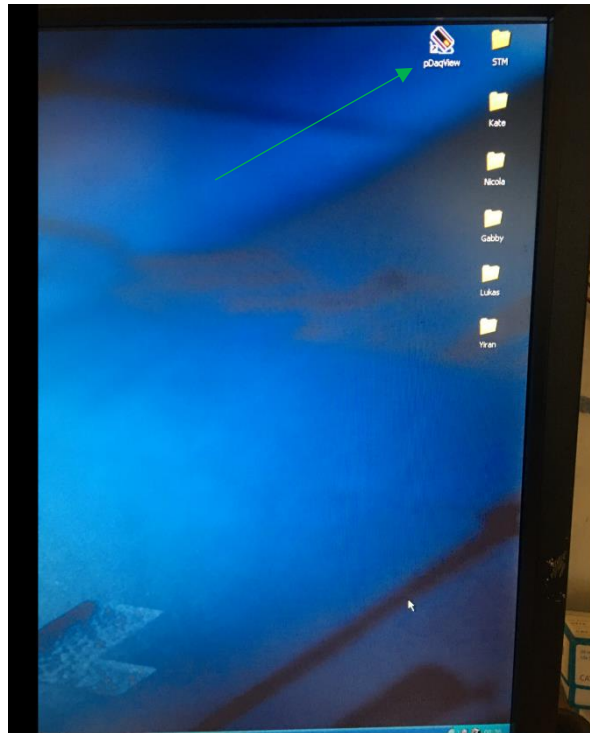
Note: When using the software, always remember to rename the file prior to starting and select the file destination. If you do not do this, the file will over-ride the previous one and you will lose your data.

Running a test

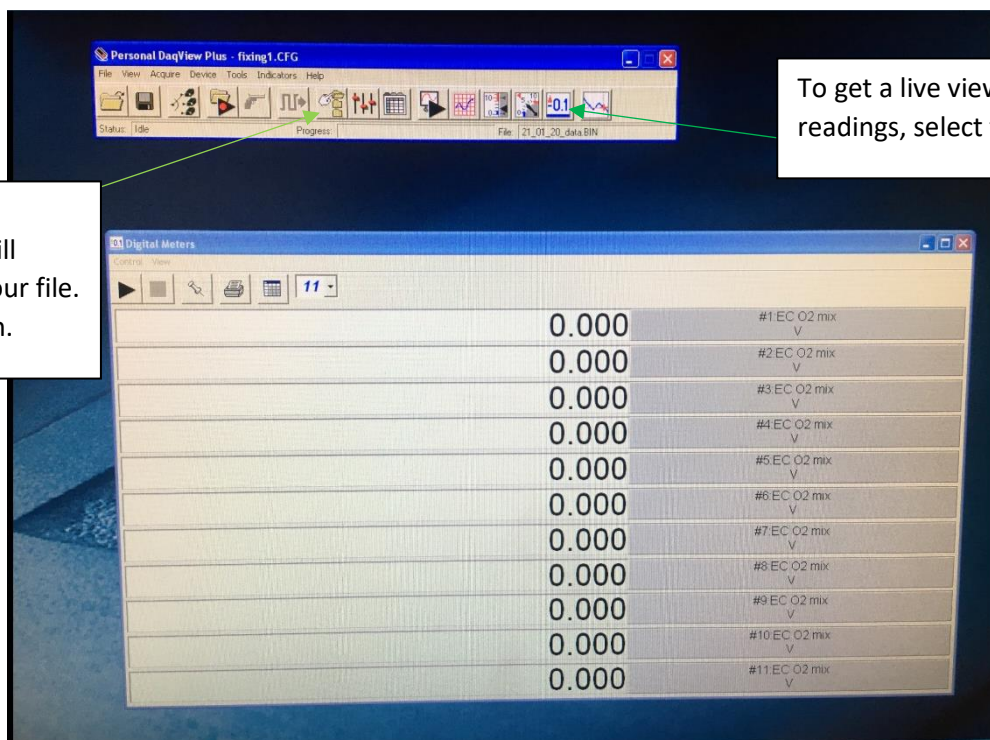
Using the SSTF software

Step 1: Login to the computer (username: administrator Password: steadystate)

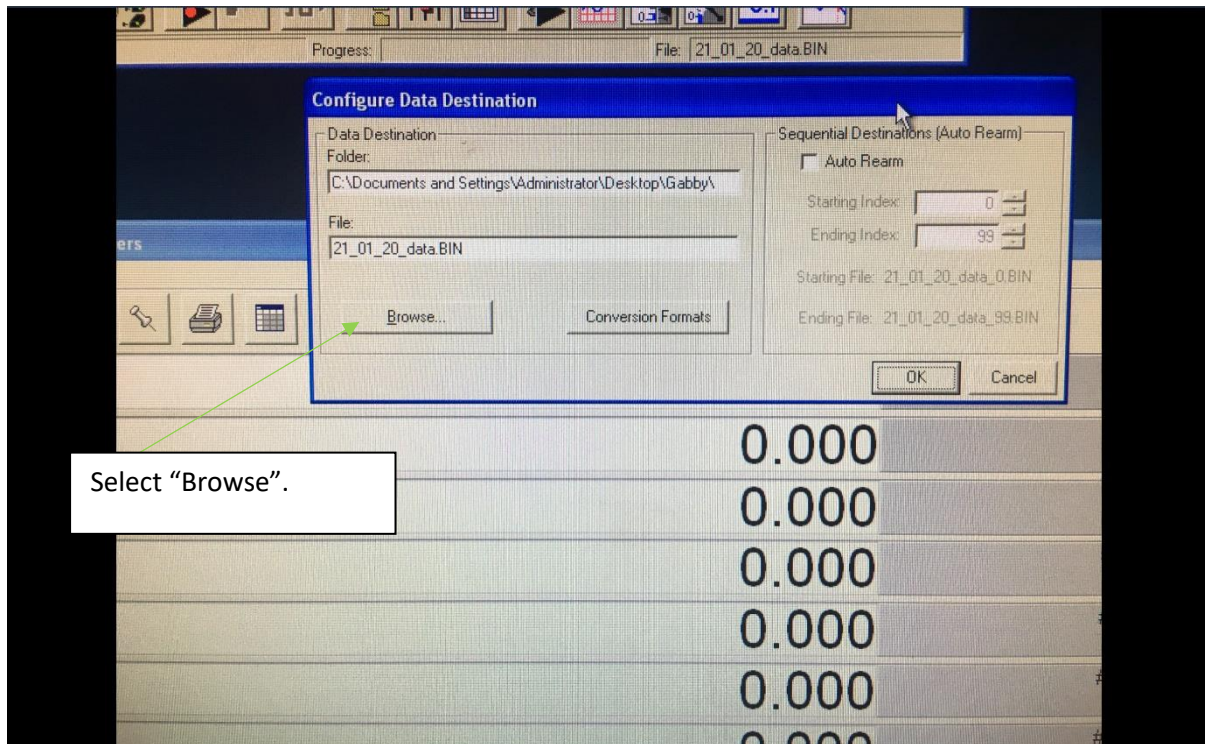
Step 2: Open pDaqView shown below.



Step 3: Set up your test.

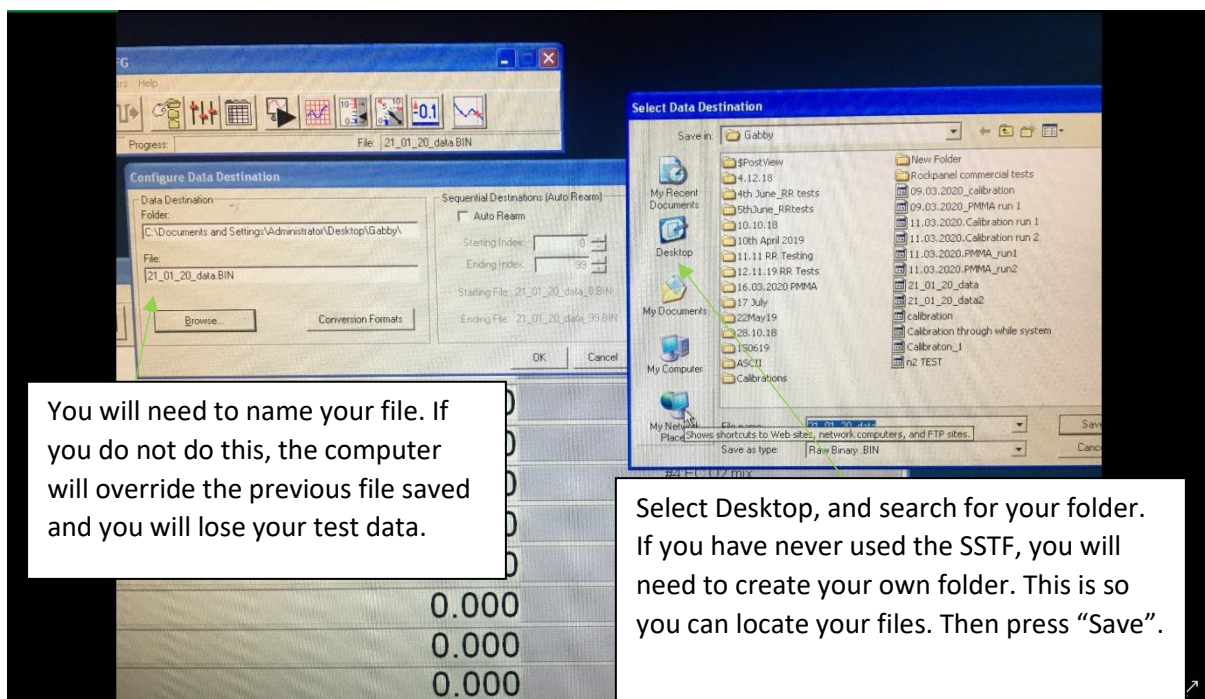


This will show up on the screen.



Select "Browse".

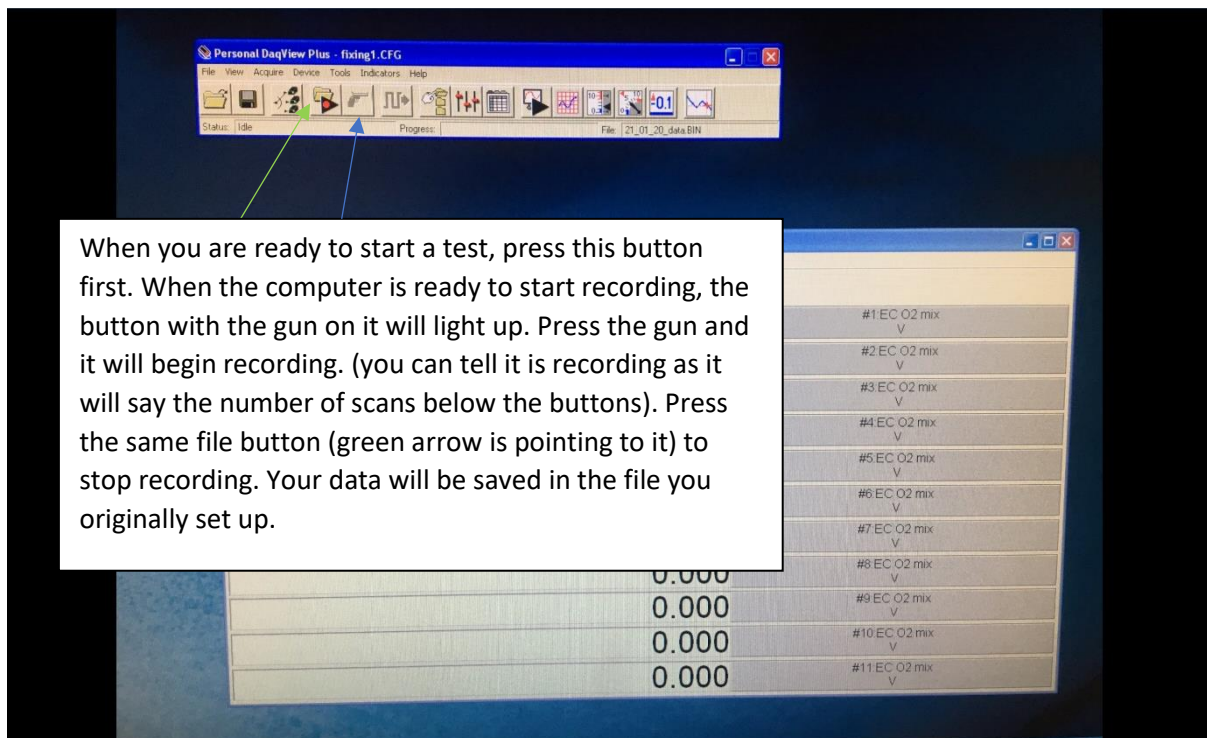
This will open next.



You will need to name your file. If you do not do this, the computer will override the previous file saved and you will lose your test data.

Select Desktop, and search for your folder. If you have never used the SSTF, you will need to create your own folder. This is so you can locate your files. Then press "Save".

Press OK once you have done this.



When you are ready to start a test, press this button first. When the computer is ready to start recording, the button with the gun on it will light up. Press the gun and it will begin recording. (you can tell it is recording as it will say the number of scans below the buttons). Press the same file button (green arrow is pointing to it) to stop recording. Your data will be saved in the file you originally set up.

The data will now be recording. You are ready to begin your calibration or test.

To collect your data, you will need to open the file you created. Open the **ASCII file** and take this file. This will open on your computer as a notepad file. The **other file types will not work.**

You are now ready to begin your data analysis.

Shut down procedure:

Close the program using the red X button in the top right corner. The computer will ask if you would like to save your current configuration. **Always select NO** (unless you have been working on renewing the SSTF data recording methodology and configuration).

If you save your current configuration, **please let the other SSTF users know** as this impacts how the SSTF runs and records data.

Calibrating the SSTF.

Before you run a test, the SSTF will need to be calibrated. This needs to be done at the start of every day before you run a test. If you are doing a significant amount of testing in one day, it is worth running a second calibration halfway through to ensure everything is still working correctly (and to accommodate for any drift the analysers may experience).

Calibrating the laser

To calibrate the laser, you will need a dense material (typically a coffee jar lid is suitable, however optical filters from the cone calorimeter are more ideal).

Set the computer to record data.

Record the voltage of the laser with no obstruction.

Record the voltage of the laser with 100% obstruction.

If using optical filters, make a note of the voltage for each filter.

Calibrating the sensors

What you'll need:

Nitrogen gas bag

CO/CO₂ gas bag

Vacuum line

Connect the gas bag to the vacuum line near the NFX. Make sure the gas bag tap is open.

Draw all the gas out of the bag. Once empty, turn off the vacuum line and close the tap on the bag.

Connect the bag to the gas line. Open the tap of the gas bag (make sure it is open!)

Fill the gas bag. Once full, turn off the gas and close the tap of the bag. Disconnect the bag.

Do this for the other gas bag.

Note: when using the CO/CO₂ gas you will need to go into the gas storage room and turn on the cylinder. Turn the gas tap on the cylinder about 90° clockwise to open it. Do not forget to turn it off when you are finished.

Leak checking the SSTF:

Open a gas bag and connect it to the primary or secondary line (you will need to do both).

Leave the gas bag on the line and monitor the oxygen sensor. If there are no leaks in the line, the oxygen sensor will read 0.0.

If it does not, go through the line and tighten each connection, this is usually where the leak occurs. The larger connections are most prone to leaks.

If there are no leaks, be sure to check there is not a leak in the gas bag. This can happen and will prevent you from leak checking the SSTF correctly. If the bag is leaking, use a new one. Also be sure to vacuum the bag out fully, this can also cause the SSTF to not reach 0.0.

Running a calibration:

Make sure there is no gas bag attached to the primary and secondary lines.

Start recording the test on the computer.

Start a timer at the same time as the test.

After around 5 minutes connect the nitrogen bag to one line and the CO/CO₂ bag to the other. **Make sure the bag tap is open!**

Once the oxygen sensor reaches 0.0, record data for around 7-10 minutes to give time for the sensors to plateau.

After you have done this, switch the bags over so they are on the other line (e.g. if you used N₂ on the primary line first, put the CO/CO₂ on second). Make a note of which gas you used first on each line and when you changed them over. This will be useful when looking at your calibration data.

Once you have finished your calibration, stop data recording.

Running a calibration direct to the sensor:

There can be a delay in the gases reaching the sensors. To avoid this, you can place the bag as close to the sensor as possible by detaching a line of tubing as close to the sensors as possible and placing the gas bag there.

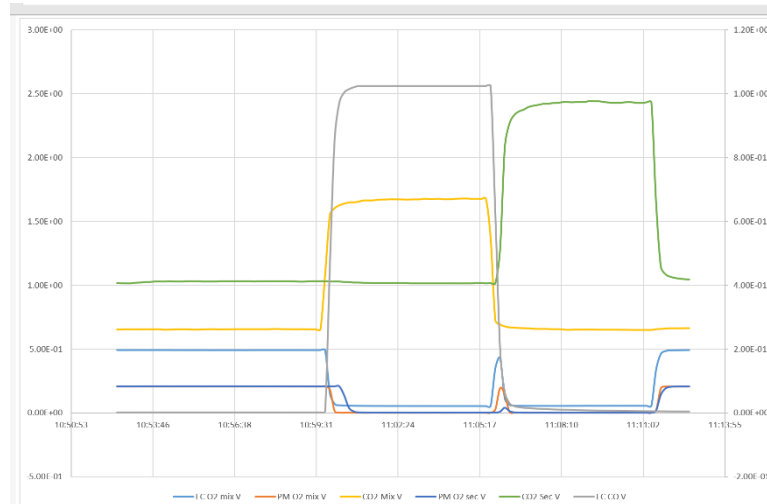
Repeat the previous steps for running the calibration, but press on the bags as there will not be a pump drawing the gas in.

Note: If you do your calibration this way, be sure to leak check the lines once you have re-connected them to ensure you have made the connection tight.

Calibration data:

Here is an example of acceptable calibration data. The data shown is in the raw voltages obtained from the SSTF data prior to processing. The key points to look for are highlighted below.

The calibration run should produce “top hat” shaped peaks. The green peak (CO₂ sec) shows more of a curve than a flat top. To avoid this, leave the calibration running for longer to give the sensor time to plateau. Below is ideally what your calibration will look like.



You are now ready to start testing.

Guide for sample preparation

When using the SSTF, you are likely to be testing a range of materials. Some materials will need different preparation than others. Please find the section your material fits into for guidance prior to running a test.

As a general rule, your sample should be:

800 mm in length

20 g in mass

Be aware that if you alter the length or mass of a sample considerably, your test time will vary. Take this into consideration when choosing gas sampling times as your steady period of burning will occur at slightly different time.

Test guidance for pellets:

When testing pellets, they will usually melt and pool in the boat. Be aware of this you expect there to be residual material after your test. You must also ensure the SSTF tube is flat, otherwise the material will run and pool during the test.

Preparing the sample for testing:

Weigh out your pellets using a weighing boat.

Distribute the pellets evenly across the sample boat. The easiest method for this is to roughly spread the pellets over the boat, then shake the boat vertically to evenly distribute the material. There is little difference in specifically placing sections of material on the boat as the material will typically pool when you put it in the furnace.

Burning behaviour of pellets is typically smooth and steady. There should be little difficulty in obtaining steady burning from pellet materials.

Test guidance for rigid foams:

When testing rigid foams such as PIR and phenolic foam, be aware that the foam may swell upon heating. To avoid this, try to ensure there is room between the sample and the top of the furnace tube. There has been instances where the foam has become stuck in the tube due to its size. If possible, use the larger (non-standardized) quartz tube.

If the foam becomes stuck in the furnace, use a rod to pull the material out when it is safe to do so. Do not use the drive unit! (the boat holder on the front of the drive unit is made from aluminium. If you use this to remove a sample from the furnace, you will melt it.

Foams typically warp when exposed to heat. This often means part of the sample will lift up and reach the top of the tube. Be aware of this as it can potentially get stuck in the tube. It is not a common problem unless you are using a large sample.

Risk of back burning:

Some foams are significantly more flammable than others. When no flame retardants are present in the foam the flame spread will often overtake the rate of sample introduction. This can result in back burning. If you expect your material to burn back (high flammability noticed during cone

calorimetric testing will be an indicator), keep an eye on the right hand side of the tube for flaming. Typically it will settle down, however in the event of rapid flame spread **turn the primary air flow off at the wall** (using the black gas tap). This will stop any burning from occurring. At this point, set the drive mechanism to reverse to remove the sample from the furnace.

Foam preparation:

Cut the foam to 800 mm in length. It is often easiest to use a bread knife.

Using a sharp knife, cut the foam to fit the shape of the boat (curved). This will allow the foam to sit better in the boat.

Cut the foam down as evenly as possible until you have reached your desired mass.

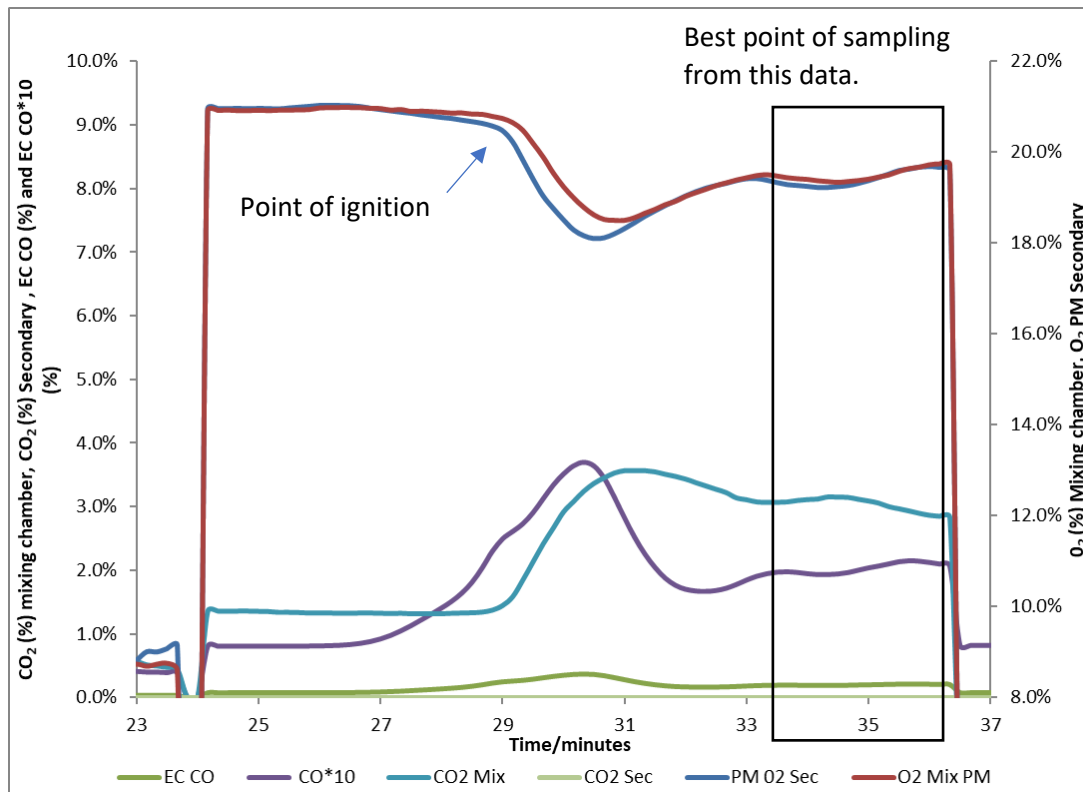
Once cut, it is often best to cut the foam into 2 or 3 separate pieces, and use pins to hold the pieces together. In the event of warping, it will allow the foam to move without disrupting your entire sample or block air flow. This is not necessary to do. If you choose to prepare your sample in this way, ensure you weigh the pins you use so that it does not implicate your measurements of the residue after the test.

Guidance for achieving steady burning:

Often with foams, it can be difficult to achieve a prolonged period of steady burning. If your sample struggles to burn steadily, increase the temperature by 25°C.

Here is an example of SSTF foam data where steady burning was not achieved. When obtaining data like this, it can be difficult to select a point of steady burning to begin your sampling. Increasing the temperature will typically improve your burning behaviour.

In the cases where increasing your temperature does not improve the period of steady burning, it may be necessary to sample for extended periods of time and use the data as an average result.



Using this example data, the best sampling point would be the area highlighted.

Guidance for wood-based products

Example materials that should follow this guidance include: MDF, High Pressure Laminate and wood samples.

Wood-based samples can be difficult to achieve steady burning due to their structure. Wood-based products will typically show a delayed ignition (approximately 4-6 minutes into the test).

In addition to this delayed ignition, there is usually a pressure build up inside the tube, leading to rapid ignition after a prolonged period. Due to the pressure build up, it is advised **not to use a plug** for under-ventilated testing. Often, the plug will shoot out due to the increased pressure at ignition. This has potential to break the glass door on the mixing chamber.

Sample preparation:

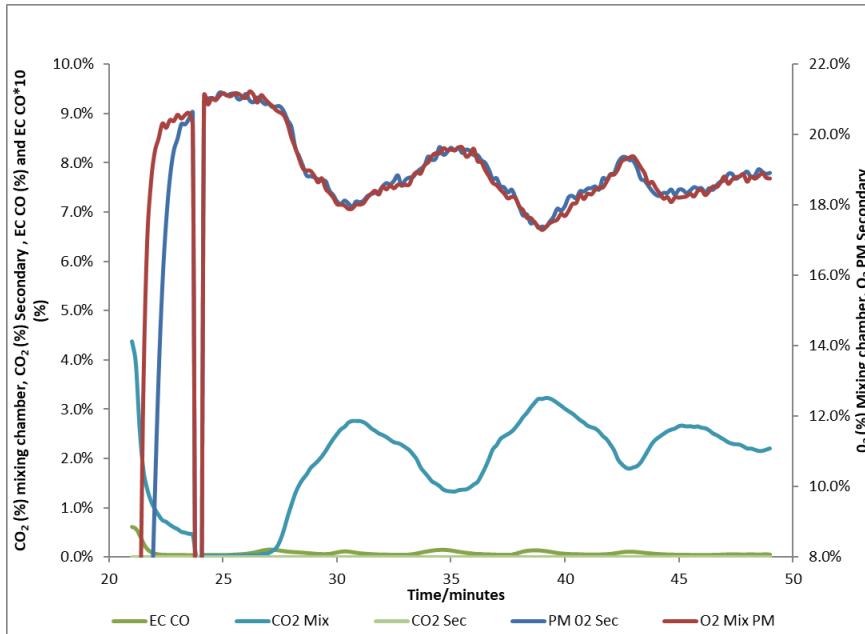
Due to wood based products being hard materials, it is advised to calculate the dimensions required for your desired mass of sample and get this cut in engineering using a bandsaw. This will result in the cleanest cut possible for your test.

Note: Be sure to know what your material is prior to getting it cut. This will help determine what kind of saw will be used to cut your material in the best way possible when in engineering.

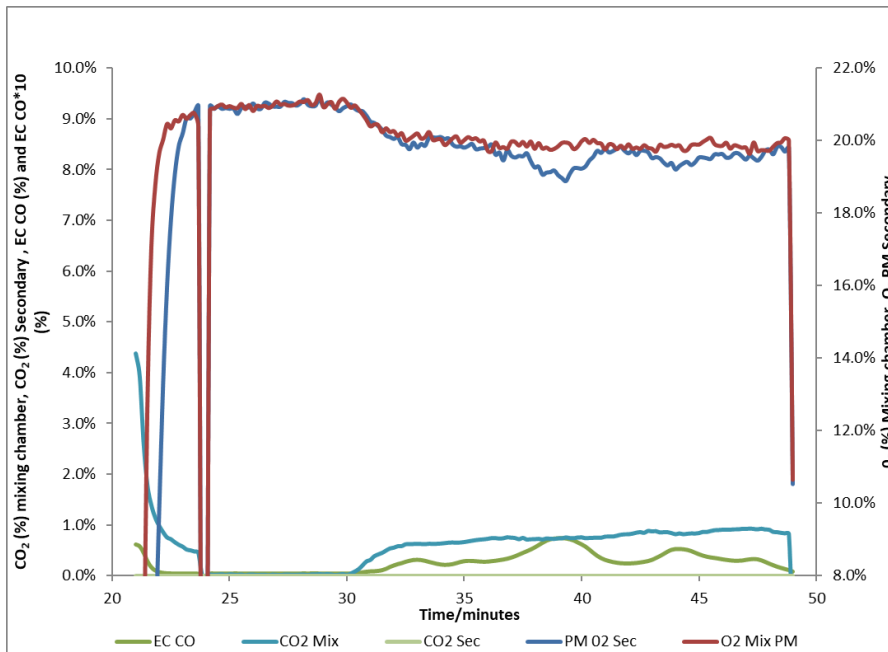
Guidance for steady burning:

It has proven difficult to obtain steady burning in these materials, particularly for solid wood. The burning behaviour is often sporadic. To mitigate this, it is advised to increase the temperature by 50 °C prior to running the test (this is particularly the case when attempting 650 °C tests).

An example of a solid wood test can be seen below.



The flaming in this test was very sporadic. No period of steady burning was achieved. The test was improved by increasing the temperature from 650 °C to 700 °C, seen below. A much more usable set of data will be obtained this way.



Guidance for non-combustible materials

For materials that are deemed non-combustible, it is recommended to run the test at 900 °C.

Guidance for materials containing chlorine

After testing materials containing high contents of chlorine based fire retardants, be sure to clean the sampling lines in case of Cl residue.

When testing materials such as PVC, you must place steel wool into the tube of the secondary furnace to prevent Cl entering the secondary line and reaching any analysers. The **steel wool should be placed at the exit of the secondary furnace**. There should be enough wool to loosely cover the tube.

Emergency procedures

Always wear heat proof gloves when handling anything coming out of the furnace.

If a material is burning while the drive mechanism is reversing and shows no sign of stopping, turn off the primary air at the wall. This will stop flaming.

If a material burns upon leaving the furnace (upon contact with fresh air):

In the case of a large uncontrollable flame: Place the sample back into the furnace and turn the furnace off and let it cool down. Try and remove after cooling.

In the case of a small flame: use the water spray bottle and quench the flames. If it is smoking, place the sample underneath an extraction point with the extraction on.

If a material is producing a significant amount of smoke upon leaving the furnace, place the sample and boat underneath an extraction point.

If a material becomes stuck in the furnace upon reversing at the end of a test, use a rod to pull the material out of the tube.

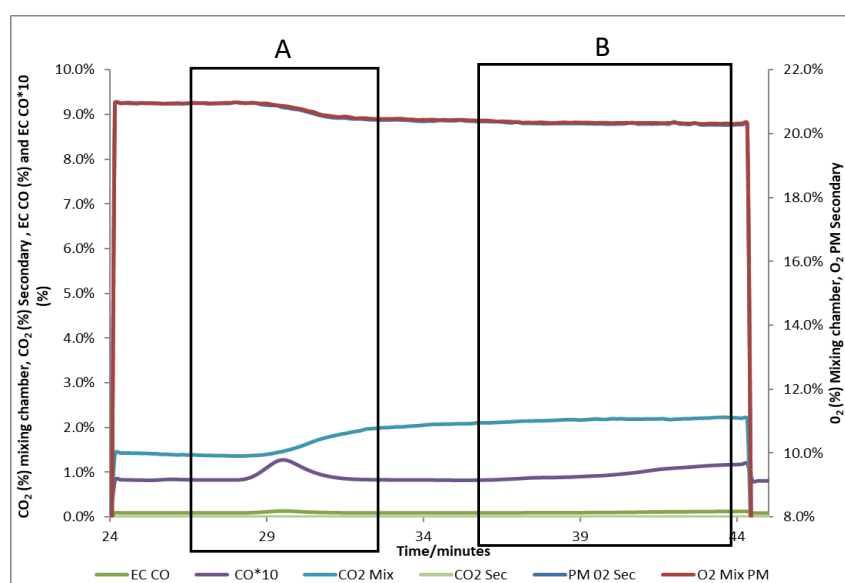
Gas sampling

The steady state tube furnace forces the sustained steady burning of a material at a constant rate. During the point of steady burning, the rate of production of free radicals is equal to the rate of free radical recombination. This means that any toxicants produced during this period will be produced at a constant rate. This is why gas sampling must take place during a period of steady burning in order to obtain a repeatable result.

How to find the period of steady burning:

The easiest means of identifying the steady period of a test is to run a trial test first. After doing this, you will be able to identify where gas concentrations are relatively constant.

Here is some example data:



You would not select point A as a sampling point. The test is starting, oxygen levels are in the process of dropping and not stabilising. At point B, the gases are much more constant. This is what you look for to determine the best point of sampling. The oxygen concentrations can also be monitored to determine a point at which combustion is steady. As a rule of thumb, when they remain stable, it is an appropriate time to begin sampling. **During the point of sampling, your flow rate must be kept constant.** Be sure to note the flow rate you used during each test.

Sampling time:

The minimum amount of time you should sample for is 5 minutes. However, it is ideal to sample for as long as possible during a steady period.

Specific sampling methods

Sampling for HCN

To sample for HCN you will need:

2x glass bubblers with tops

Grease

Clamps

0.1M NaOH (to prepare this, weigh out 4 mg of NaOH and dilute with deionised water in a 1000 ml volumetric flask).

Flow meter and vacuum line

Measure out 150 ml of 0.1 M NaOH into each glass bubbler. Lightly grease the top of the bubbler then put the top of the bubbler in place.

Connect bubbler 1 to bubbler 2 (in the same way you set up traps 1 and 2) and label the bottles. Clamp these in place next to the mixing chamber and have a line ready to be connected to the mixing chamber.

Switch on the flow meter. Set your desired flow rate on the flow meter and open the vacuum line. Make a note of the flow rate used. **This should be kept constant.**

When you are ready to begin sampling, connect the line from the flow meter to the end of bubbler 2. An additional drying tube can be added before the filter and mass flow controller to dry the fire effluent prior to it entering the mass flow controller and pump.

Connect the line from bubbler 1 to the mixing chamber to begin sampling. Make a note of the time you began sampling, and for the duration you have sampled for.

Once you are ready to stop sampling, disconnect the line from the mixing chamber and vacuum line. Be sure to cover the mixing chamber sampling port used to prevent gas from leaving the chamber.

Once you are ready, transfer the NaOH solution to a sample bottle and label with the name of the test, HCN sample number (1 and 2), the date and your name.

Ideally these samples should be stored in the fridge, however the solution is stable at room temperature and can be stored in a cupboard.

These samples are ready for HCN analysis.

Sampling for acid gases

To sample for HCN you will need:

2x glass bubblers with tops

Grease

Clamps

Deionised water

Flow meter and vacuum line

Measure out 100 ml of deionised water into each glass bubbler. Lightly grease the top of the bubbler then put the top of the bubbler in place.

Connect bubbler 1 to bubbler 2 (in the same way you set up traps 1 and 2) and label the bottles. Clamp these in place next to the mixing chamber and have a line ready to be connected to the mixing chamber.

Switch on the flow meter. Set your desired flow rate on the flow meter and open the vacuum line. Make a note of the flow rate used.

When you are ready to begin sampling, connect the line from the flow meter to the end of bubbler 2. **This should be kept constant.** An **additional drying tube** can be added before the filter and mass flow controller to dry the fire effluent prior to it entering the mass flow controller and pump.

Connect the line from bubbler 1 to the mixing chamber to begin sampling. Make a note of the time you began sampling, and for the duration you have sampled for.

Once you are ready to stop sampling, disconnect the line from the mixing chamber and vacuum line. Be sure to cover the mixing chamber sampling port used to prevent gas from leaving the chamber.

Once you are ready, transfer the bubbler solution to a sample bottle and label with the name of the test, HPIC sample number (1 and 2), the date and your name.

Ideally these samples should be stored in the fridge, however the solution is stable at room temperature and can be stored in a cupboard.

These samples are ready for HPIC analysis.

Sampling for soot

Pre-weigh a dried filter paper. Record the mass.

Place the filter paper into a cassette filter and connect to a sampling line.

After the filter, there should be some form of drying agent. A tube of silica can be used after the filter to dry the effluent.

This should be connected to a mass flow controller. **Be sure to keep this flow constant.**

Then connect to a pump and set up an exhaust line going into the extraction hood.

After a run, place your filter into a desiccator or the oven for a few hours to dry the filter paper.

Once dry, record the mass of the filter.

Sampling for alternative gases

The sampling procedure using any liquid trapping agents follows the aforementioned procedures. Be sure to make note of the flow rate and sampling time used.

Use of XAD tubes can be directly connected to the sampling line using flexible tubing.

Procedure for running multiple tests

At the end of each test, disconnect the primary and secondary line from the mixing chamber and cover the sampling ports. This will allow for clean air to be drawn through the lines and through the mixing chamber. Ideally do this for a minimum of 5 minutes.

If the test is particularly sooty, you may need to clean the mixing chamber and clean the sampling ports. To clean the sampling ports, run a pipe cleaner through the sampling ports used.

If the material contains a significant amount of Cl, the mixing chamber and lines may need a deeper clean.

Be sure to check the glass wool, silica and ascarite throughout the primary and secondary lines. They may need replacing between tests. (the silica will turn an orange colour if it needs replacing, the glass wool will be dirty and the ascarite will turn white).

Cleaning and maintenance

The SSTF needs to be cleaned on a regular basis for measurements to be accurate. This includes keeping the tube clean, as well as sampling lines and pumps. The cleaning procedure will be divided into daily cleaning, weekly maintenance and deep cleaning processes.

Daily cleaning

After a day of testing, the SSTF will require cleaning. Keep clean air drawing through the primary and secondary lines to allow clean air through the system. The time required for this will depend on the state of the test conducted. Particularly messy tests should be left longer, meanwhile clean tests may only require 5 minutes.

Shut down procedure

Turn off the primary and secondary furnace.

Turn off the primary and secondary air at the wall.

Turn off the air flow controller, vacuum and drive mechanism.

Remove the glass door from the mixing chamber.

Shut down the computer. Turn off all plugs and close all vacuum taps.

The main area that will need to be cleaned is the mixing chamber.

To clean the glass door, use methanol and paper towels to remove any residue until clean.

If the door is sooty, it may be necessary to vacuum the soot from the door. Clean the door with methanol and paper towels.

To clean the mixing chamber, use methanol and paper towels. If it is particularly sooty, you may need to vacuum the soot from the chamber. Be sure to clean the corners of the chamber properly.

To clean the sampling ports, run a pipe cleaner through the sampling ports. It may be necessary to put a light amount of methanol onto the pipe cleaner if they are particularly dirty.

Check the filters through the system to check if they need replacing.

Be sure everything is off and put away prior to leaving the lab. Remember to turn off the extraction when you are finished.

Regular maintenance and deep cleaning

The SSTF should undergo maintained and deep cleaning regularly.

Sensors

Sensors and filters should be checked regularly. The voltage output of the electrochemical cells should be monitored regularly to notice any changes. In the case of drastic voltage changes during calibration, the cell may need replacing.

The filters within the CO₂ analyser box should be regularly checked and changed if necessary.

The filters in the back of the paramagnetic O₂ analysers should be checked regularly for soot build up. Replace them if they are dirty.

Pumps

The sstf uses several pumps. These need to be regularly opened and cleaned. A build up of soot can impair the pumps function and can cause the pump to over-heat.

Cleaning sample boats and furnace tube

The sample boats will need regular cleaning.

Ensure the glass door of the mixing chamber is off.

Turn the primary furnace to 900 °C.

Once the furnace has reached temperature, turn the extraction on

From the front end of the mixing chamber, slowly insert the boat into the tube.

Slowly feed the boat into the furnace. Allow time for each section of the boat to sit in the furnace to allow it to clean.

Do this for as many boats required.

Cleaning the furnace tube

Protocol for the long standard size tube

Ensure the glass door of the mixing chamber is off.

Loosen the clamp on the quartz tube (there is a circular clamp that holds the quartz tube in place on the mixing chamber. This will need loosening).

Turn the primary furnace to 900 °C.

Once the furnace has reached temperature, turn the extraction on

Slowly feed the quartz tube into the furnace (it will need to be pulled in both directions to clean both ends). Be careful not to move the tube vertically as it will break. **The mixing chamber and furnace are slightly different heights.** You must use a tool, such as a spanner, to lift the end of the quartz tube down from the mixing chamber and when you put it back. This will help avoid any breakages.

Clamp the tube back in place once cool.

If the tube is particularly dirty, **flaming may occur.** To prevent this, wrap the end of the tube closest to the drive mechanism loosely in glass wool to make a seal between the furnace and the tube. This will prevent any gas from blowing into the lab.

Protocol for the non-standardised tube

Ensure the glass door of the mixing chamber is off.

Remove the glass tube from the far end of the furnace. Clean this using methanol and a brush.

Loosen the clamp on the quartz tube (there is a circular clamp that holds the quartz tube in place on the mixing chamber. This will need loosening).

Turn the primary furnace to 900 °C.

Once the furnace has reached temperature, turn the extraction on

Slowly feed the quartz tube into the furnace (it will need to be pulled in both directions to clean both ends). Be careful not to move the tube vertically as it will break.

Clamp the tube back in place once cool. Replace the glass tube on the end of the quartz tube.

The process for cleaning the secondary furnace tube is the same as above. Be sure to use the primary furnace as you will need the cleaning to take place under the extraction hood.

Tubing

Tubing on the SSTF must be regularly replaced. This will involve removing each connection and replacing it with fresh tubing. Be sure to do this systematically as it can prove difficult to replace all connections without a point of reference. There is guidance for the layout of the SSTF tubing lines should you forget where a connection should go.

Any changes and replacements to the SSTF should be documented in the designated SSTF folder to ensure all users are able to see what has been done.

This will also aid troubleshooting if there are problems after maintenance routines.

Appendix 9: Box analyser

This appendix contains information about the program designed for the analysers, the details of sampling times and a set of instructions created for operation of the analysers. Final photographs of the analyser are also shown.

Arduino controlled solenoid switch:

The solenoids for the box analyser are controlled using electronic switches programmed into the Arduino. The current set up for the solenoid switch is summarised in Table 12.

Table 12: Programmed time intervals for the solenoid sampling switches.

Solenoid	Time delay until solenoid opens from time Arduino is powered on /min	Time solenoid valve will be open for after delay /min
1	10	5
2	15	5
3	20	5
4	25	5
5	30	5
6	35	5
7	40	5
8	45	5

Note: The program will begin running as soon as you power up the Arduino. The 10 min delay will happen as soon as you power on the Arduino, so be ready to start your test before you power on.

How to modify the Arduino code to alter the timed switches:

The Arduino is coded in **C++**. Below is the code used for the switches. The time is in milliseconds, so to determine what value to put in, use the formula **min x 60 x 1000**. Any code uploaded to the Arduino will replace the previous code.

To modify the code the Arduino runs, you will need to download Arduino IDE (<https://www.arduino.cc/en/software>)

Open Arduino IDE and copy the code seen below (Notes have been added to describe the function of each line of the code to help with reading and modifications).

The highlighted areas are what you will need to change if you wish to change the times. Yellow sections are the delay times, green sections are how long the solenoid will be on for. Be sure to check the =no at the start is the correct pin on the Arduino board.

If you need to remove one of the switches you will need to delete the entire segment to avoid causing errors in the code. Errors in the code means that it wont function. A full section can be Shown in the text box. **This is the only thing you should change out of the code.**

The Arduino will run whichever code was uploaded to it last, so once you make any changes you will need to upload the code to the Arduino.

To reset the Arduino, upload this code and it will be reset:

```
Void setup() {}
```

```
Void loop() {}
```

CODE:

```
void setup() {  
  int solenoidPin = 2;  
  pinMode(solenoidPin, OUTPUT);  
  digitalWrite (solenoidPin, LOW  
  delay(0);  
  digitalWrite(solenoidPin, HIGH  
  delay(300000);  
  digitalWrite(solenoidPin, LOW);
```

The code above was used for each solenoid pin connected to the circuit.

How to operate the analyser:

Plug it in

After a short while you will see the screen load up

Login to the analyser (you will need to plug in a keyboard to the USB hub).

The password is 240296

Once the analyser has loaded up, click on the file labelled 'NDIR Software'.

This will open the file that contains the software.

Click on the 'Hostsoftware' file. It will begin to load.

Open 'file' then click new file

Set the desired location and file name.

Tick the boxes of the gases you want to log

Make sure the box 'append to file' is clicked.

Press start when you are ready to begin

The values should read 0 for a bit at the start, then it should begin to read the actual values (20.95 for O₂).

Connect a bag of N₂ to the gas line connected to the NDIR

When you see the values drop to close to 0, press 'Zero' on the software.

Remove the gas bag, let the NDIR values go back to normal.

Connect 4% CO/CO₂ to the gas line for 3-5 mins while logging the data, do the same for N₂.

Once you are done, stop the log by pressing 'stop'.

Click on file, new file and put in the name of your test in.

Make a note of the file name and location prior.

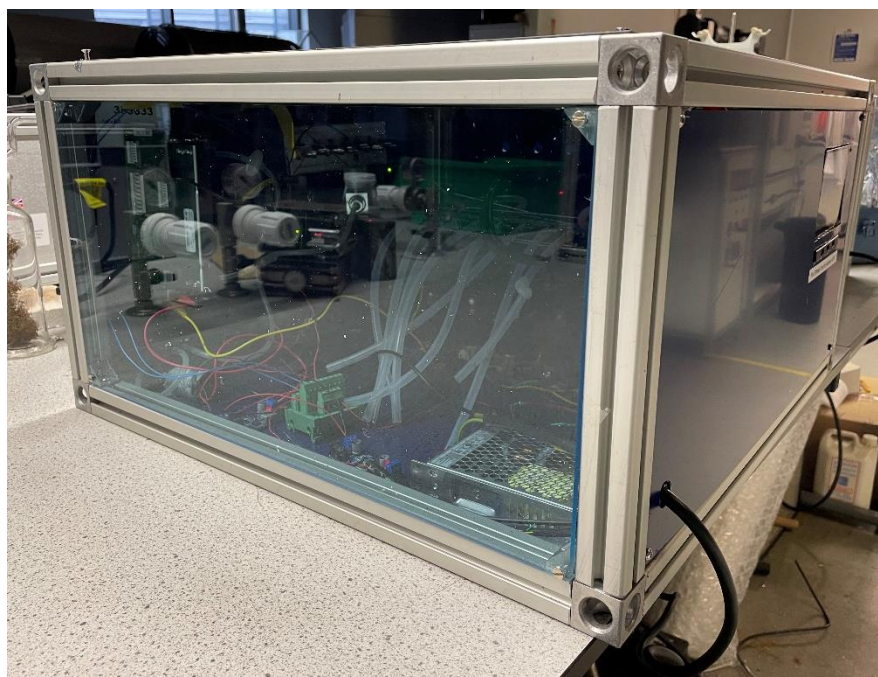
Repeat steps 10-13.

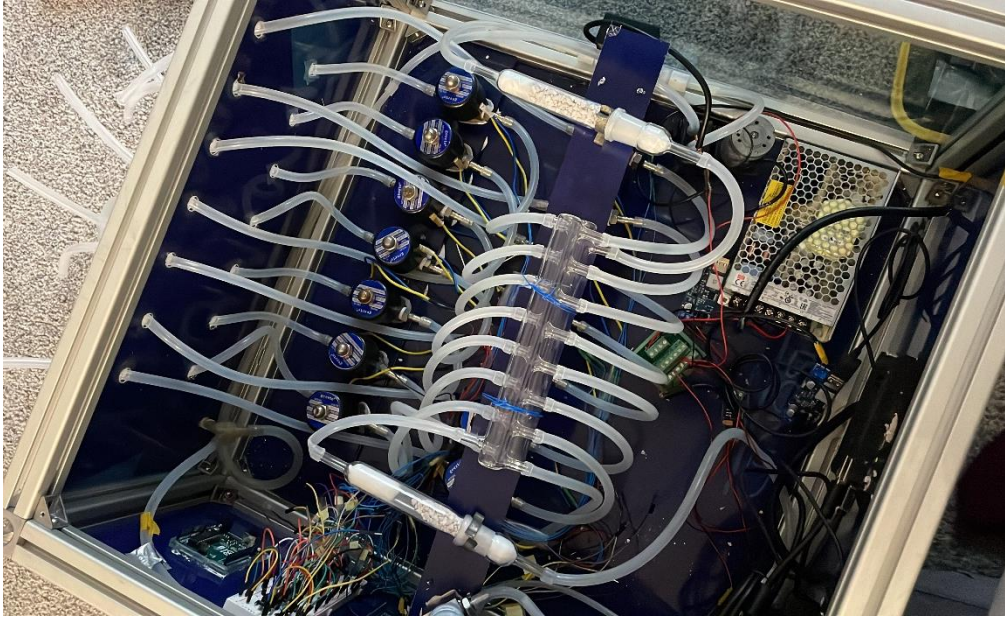
How to connect to your phone or laptop:

Download VNC viewer on your phone or laptop

Input the IP address of the analyser (ask for the code- this differs depending on internet source used for the analyser).

Final photographs of the analyser





Appendix 10: Bench-scale data

This appendix contains the validity assessments of the data obtained during SSTF testing of proposed round robin materials, calculated using the original methodology in the ISO/TS 19700 standard, as well as the assessment made using the longest steady state period possible.

Bench-scale data:

The data obtained from the validity assessments made using the ISO/TS 19700 standard is shown in this section. The data shown is the calculated validity, and therefore contains no units.

Key:

*= 1g of organic loading per sec.

Table 13: Validity assessment of SSTF data from proposed round robin materials.

Material	Condition	long term trend						short term fluctuation					
		CO	Valid	CO ₂	Valid	O ₂	Valid	CO	Valid	CO ₂	Valid	O ₂	Valid
HPL non FR	650 WV	0.019	✓	0.018	✓	-0.005	✓	0.007	✓	0.005	✓	0.001	✓
		0.002	✓	0.003	✓	0.001	✓	0.005	✓	0.003	✓	0.002	✓
		0.010	✓	0.018	✓	0.002	✓	0.006	✓	0.005	✓	0.002	✓
		Total	3/3	Total	3/3	Total	3/3	Total	3/3	Total	3/3	Total	3/3
	650 UV	0.120	X	0.006	✓	-0.007	✓	0.040	✓	0.006	✓	0.0004	✓
		0.001	✓	0.019	✓	-0.001	✓	0.002	✓	0.005	✓	0.0003	✓
		0.061	X	0.012	✓	-0.005	✓	0.021	✓	0.005	✓	0.0004	✓
		Total	1/3	Total	3/3	Total	3/3	Total	3/3	Total	3/3	Total	3/3
	825 UV	0.081	X	0.021	X	0.060	✓	0.005	✓	0.006	✓	0.001	✓
		0.081	X	0.021	X	0.060	✓	0.005	✓	0.006	✓	0.001	✓
		0.081	X	0.010	✓	0.060	✓	0.005	✓	0.005	✓	0.001	✓
		Total	0/3	Total	1/3	Total	3/3	Total	3/3	Total	3/3	Total	3/3
HPL FR	650 WV	0.124	X	0.025	X	-0.001	✓	0.039	✓	0.007	✓	0.001	✓
		0.115	X	0.027	X	-0.194	✓	0.041	X	0.019	✓	0.001	✓
		0.119	X	0.026	X	-0.098	✓	0.040	✓	0.013	✓	0.001	✓
		Total	0/3	Total	0/3	Total	3/3	Total	2/3	Total	3/3	Total	3/3
	650 UV	0.001	✓	0.018	✓	0.001	✓	0.002	✓	0.005	✓	0.002	✓
		0.001	✓	0.018	✓	0.001	✓	0.002	✓	0.005	✓	0.002	✓

		0.001	✓	0.018	✓	0.001	✓	0.002	✓	0.005	✓	0.002	✓
		Total	3/3	Total	3/3	Total	3/3	Total	3/3	Total	3/3	Total	3/3
	825 UV	0.001	✓	0.025	X	0.001	✓	0.001	✓	0.007	✓	0.001	✓
		0.002	✓	0.021	X	0.178	X	0.005	✓	0.006	✓	0.001	✓
		0.242	X	0.019	✓	0.001	✓	0.009	✓	0.006	✓	0.001	✓
		Total	2/3	Total	1/3	Total	2/3	Total	3/3	Total	3/3	Total	3/3
Cables	650 WV	0.044	X	0.031	X	-0.002	✓	0.016	✓	0.008	✓	0.001	✓
		0.044	X	0.013	✓	0.01	✓	0.025	✓	0.012	✓	0.001	✓
		0.044	X	0.022	X	0.004	✓	0.020	✓	0.011	✓	0.001	✓
		Total	0/3	Total	1/3	Total	3/3	Total	3/3	Total	3/3	Total	3/3
	650 UV	0.104	X	0.009	✓	0.006	✓	0.008	✓	0.003	✓	0.002	✓
		0.097	X	0.005	✓	0.001	✓	0.004	✓	0.001	✓	0.002	✓
		0.100	X	0.007	✓	0.003	✓	0.006	✓	0.002	✓	0.002	✓
		Total	0/3	Total	3/3	Total	3/3	Total	3/3	Total	3/3	Total	3/3
	825 UV	0.100	X	0.007	✓	0.003	✓	0.006	✓	0.002	✓	0.002	✓
		0.080	X	0.014	✓	0.001	✓	0.008	✓	0.005	✓	0.002	✓
		0.063	X	0.017	✓	0.004	✓	0.016	✓	0.008	✓	0.002	✓
		Total	0/3	Total	3/3	Total	3/3	Total	3/3	Total	3/3	Total	3/3
Plasterboard	650 UV	- 0.143	✓	0.003	✓	0.001	✓	0.022	✓	0.001	✓	0.001	✓
		- 0.044	✓	0.150	X	-0.002	✓	0.011	✓	0.004	✓	0.001	✓

		0.158	X	0.159	X	-0.0001	✓	0.019	✓	0.004	✓	0.0003	✓
		Total	2/3	Total	1/3	Total	3/3	Total	3/3	Total	3/3	Total	3/3
	900 WV	-0.010	✓	0.010	✓	-0.0004	✓	0.017	✓	0.003	✓	0.001	✓
		0.035	X	0.014	✓	-0.001	✓	0.016	✓	0.004	✓	0.001	✓
		0.013	✓	0.026	✓	-0.001	✓	0.007	✓	0.004	✓	0.001	✓
		Total	2/3	Total	3/3	Total	3/3	Total	3/3	Total	3/3	Total	3/3
Flexible polyurethane	650 WV	-0.014	✓	-0.031	✓	-0.000	✓	0.041	X	0.016	✓	0.0004	✓
		0.057	X	-0.044	✓	-0.001	✓	0.016	✓	0.012	✓	0.0003	✓
		0.021	X	-0.038	✓	-0.000	✓	0.028	✓	0.014	✓	0.0003	✓
		Total	1/3	Total	3/3	Total	3/3	Total	2/3	Total	3/3	Total	3/3
	650 UV	0.061	X	-0.002	✓	-0.000	✓	0.023	✓	0.002	✓	0.001	✓
		-0.014	✓	0.008	✓	0.001	✓	0.007	✓	0.003	✓	0.001	✓
		0.324	X	0.041	X	-0.000	✓	0.100	X	0.015	✓	0.001	✓
		Total	1/3	Total	2/3	Total	3/3	Total	2/3	Total	3/3	Total	3/3
	825 UV	0.034	X	-0.011	✓	-0.001	✓	0.017	✓	0.003	✓	0.001	✓
		0.110	X	0.010	✓	-0.001	✓	0.034	✓	0.003	✓	0.001	✓
		0.068	X	0.038	X	-0.001	✓	0.0329	✓	0.011	✓	0.001	✓
		Total	0/3	Total	2/3	Total	3/3	Total	3/3	Total	3/3	Total	3/3
		650 WV	0.008	✓	0.026	X	-0.001	✓	0.008	✓	0.016	✓	0.001

		0.007	✓	0.020	X	0.060	X	0.041	X	0.019	✓	0.003	✓
		0.021	x	0.019	✓	0.000	✓	0.039	X	0.031	✓	0.001	✓
		Total	2/3	Total	1/3	Total	2/3	Total	1/3	Total	3/3	Total	3/3
	650 UV	0.061	X	0.093	X	0.005	✓	0.003	✓	0.028	✓	0.001	✓
		0.008	✓	0.013	✓Ply w	0.012	✓	0.008	✓	0.027	✓	0.000	✓
		0.020	✓	0.014	✓	0.001	✓	0.008	✓	0.020	✓	0.002	✓
		Total	2/3	Total	2/3	Total	3/3	Total	3/3	Total	3/3	Total	3/3
	825 UV	0.008	✓	0.011	✓	0.005	✓	0.008	✓	0.016	✓	0.002	✓
		0.240	X	0.020	✓	0.010	✓	0.002	✓	0.030	✓	0.001	✓
		0.004	✓	0.019	✓	0.014	✓	0.009	✓	0.024	✓	0.001	✓
		Total	2/3	Total	3/3	Total	3/3	Total	3/3	Total	3/3	Total	3/3

Table 14: Validity assessment of SSTF data from proposed round robin materials using longest steady state period possible.

Material	Condition	long term trend						short term fluctuation						
		CO	Valid	CO ₂	Valid	O ₂	Valid	CO	Valid	CO ₂	Valid	O ₂	Valid	
HPL non FR	650 WV	0.019	✓	0.018	✓	0.077	X	0.007	✓	0.005	✓	0.001	✓	
		0.002	✓	0.003	✓	0.0002	✓	0.005	✓	0.003	✓	0.001	✓	
		0.010	✓	0.018	✓	0.003	✓	0.006	✓	0.005	✓	0.0002	✓	
		Total	3/3	Total	3/3	Total	2/3	Total	3/3	Total	3/3	Total	3/3	
	650 UV	0.120	X	0.006	✓	-0.000	✓	0.040	✓	0.006	✓	0.000	✓	
		0.001	✓	0.019	✓	-0.007	✓	0.002	✓	0.005	✓	0.000	✓	
		0.061	X	0.012	✓	-0.0005	✓	0.021	✓	0.005	✓	0.000	✓	
		Total	1/3	Total	3/3	Total	3/3	Total	3/3	Total	3/3	Total	3/3	
	825 UV	0.081	X	0.021	X	-0.044	✓	0.005	✓	0.006	✓	0.000	✓	
		0.081	X	0.021	X	-0.0005	✓	0.005	✓	0.006	✓	0.000	✓	
		0.081	X	0.010	✓	-0.0225	✓	0.005	✓	0.005	✓	0.000	✓	
		Total	0/3	Total	1/3	Total	3/3	Total	3/3	Total	3/3	Total	3/3	
	HPL FR	650 WV	0.124	X	0.025	X	-0.000	✓	0.039	✓	0.007	✓	0.001	✓
			0.115	X	0.027	X	-0.000	✓	0.041	X	0.019	✓	0.001	✓
			0.119	X	0.026	X	-0.000	✓	0.040	✓	0.013	✓	0.000	✓
			Total	0/3	Total	0/3	Total	3/3	Total	2/3	Total	3/3	Total	3/3
650 UV		0.001	✓	0.018	✓	0.001	✓	0.002	✓	0.005	✓	0.001	✓	
		0.001	✓	0.018	✓	0.001	✓	0.002	✓	0.005	✓	0.001	✓	
		0.002	✓	0.018	✓	0.001	✓	0.002	✓	0.005	✓	0.001	✓	

		0.001	✓	0.018	✓	0.001	✓	0.002	✓	0.005	✓	0.001	✓
		Total	3/3	Total	3/3	Total	3/3	Total	3/3	Total	3/3	Total	3/3
	825 UV	0.001	✓	0.025	X	-0.089	✓	0.001	✓	0.007	✓	0.001	✓
		0.002	✓	0.021	X	-0.001	✓	0.005	✓	0.006	✓	0.001	✓
		0.242	X	0.019	✓	-0.000	✓	0.009	✓	0.006	✓	0.000	✓
		Total	2/3	Total	1/3	Total	3/3	Total	3/3	Total	3/3	Total	3/3
Cables	650 WV	0.044	X	0.031	X	-0.000	✓	0.016	✓	0.008	✓	0.000	✓
		0.044	X	0.013	✓	-0.000	✓	0.025	✓	0.012	✓	0.000	✓
		0.044	X	0.022	X	-0.000	✓	0.020	✓	0.011	✓	0.001	✓
		Total	0/3	Total	1/3	Total	3/3	Total	3/3	Total	3/3	Total	3/3
	650 UV	0.104	X	0.009	✓	-0.000	✓	0.008	✓	0.003	✓	0.000	✓
		0.097	X	0.005	✓	0.000	✓	0.004	✓	0.001	✓	0.000	✓
		0.100	X	0.007	✓	-0.000	✓	0.006	✓	0.002	✓	0.001	✓
		Total	0/3	Total	3/3	Total	3/3	Total	3/3	Total	3/3	Total	3/3
	825 UV	0.100	X	0.007	✓	0.000	✓	0.006	✓	0.002	✓	0.001	✓
		0.080	X	0.014	✓	0.000	✓	0.008	✓	0.005	✓	0.000	✓
		0.063	X	0.017	✓	0.000	✓	0.016	✓	0.008	✓	0.001	✓
		Total	0/3	Total	3/3	Total	3/3	Total	3/3	Total	3/3	Total	3/3
	Plasterboard	650 UV	-0.143	✓	0.003	✓	-0.000	✓	0.022	✓	0.001	✓	0.001
-0.044			✓	0.150	X	-0.000	✓	0.011	✓	0.004	✓	0.001	✓
0.158			X	0.159	X	-0.002	✓	0.019	✓	0.004	✓	0.001	✓

		Total	2/3	Total	1/3	Total	3/3	Total	3/3	Total	3/3	Total	3/3
	900 WV	-0.010	✓	0.010	✓	0.001	✓	0.017	✓	0.003	✓	0.000	✓
		0.035	X	0.014	✓	-0.001	✓	0.016	✓	0.004	✓	0.000	✓
		0.013	✓	0.026	✓	-0.001	✓	0.007	✓	0.004	✓	0.000	✓
		Total	2/3	Total	3/3	Total	3/3	Total	3/3	Total	3/3	Total	3/3
Flexible polyurethane	650 WV	-0.014	✓	-0.031	✓	-0.000	✓	0.041	X	0.016	✓	0.001	✓
		0.057	X	-0.044	✓	0.000	✓	0.016	✓	0.012	✓	0.001	✓
		0.021	X	-0.038	✓	0.000	✓	0.028	✓	0.014	✓	0.000	✓
		Total	1/3	Total	3/3	Total	3/3	Total	2/3	Total	3/3	Total	3/3
	650 UV	0.061	X	-0.002	✓	0.000	✓	0.023	✓	0.002	✓	0.000	✓
		-0.014	✓	0.008	✓	0.000	✓	0.007	✓	0.003	✓	0.000	✓
		0.324	X	0.041	X	0.000	✓	0.100	X	0.015	✓	0.001	✓
		Total	1/3	Total	2/3	Total	3/3	Total	2/3	Total	3/3	Total	3/3
	825 UV	0.034	X	-0.011	✓	0.002	✓	0.017	✓	0.003	✓	0.000	✓
		0.110	X	0.010	✓	0.000	✓	0.034	✓	0.003	✓	0.000	✓
		0.068	X	0.038	X	0.000	✓	0.0329	✓	0.011	✓	0.000	✓
		Total	0/3	Total	2/3	Total	3/3	Total	3/3	Total	3/3	Total	3/3
	Plywood	650 WV	0.008	✓	0.026	X	-0.007	✓	0.008	✓	0.016	✓	0.001
0.007			✓	0.020	X	0.000	✓	0.041	X	0.019	✓	0.001	✓
0.021			x	0.019	✓	-0.002	✓	0.039	X	0.031	✓	0.000	✓
Total			2/3	Total	1/3	Total	3/3	Total	1/3	Total	3/3	Total	3/3

	650 UV	0.061	X	0.093	X	0.001	✓	0.003	✓	0.028	✓	0.002	✓
		0.008	✓	0.013	✓	-0.002	✓	0.008	✓	0.027	✓	0.001	✓
		0.020	✓	0.014	✓	0.001	✓	0.008	✓	0.020	✓	0.002	✓
		Total	2/3	Total	2/3	Total	3/3	Total	3/3	Total	3/3	Total	3/3
	825 UV	0.008	✓	0.011	✓	-0.002	✓	0.008	✓	0.016	✓	0.000	✓
		0.240	X	0.020	✓	0.000	✓	0.002	✓	0.030	✓	0.000	✓
		0.004	✓	0.019	✓	-0.003	✓	0.009	✓	0.024	✓	0.001	✓
		Total	2/3	Total	3/3	Total	3/3	Total	3/3	Total	3/3	Total	3/3

Appendix 11: Large-scale test data

This appendix contains the smoke toxicity data obtained from the large-scale tests. This includes the acid gas analysis and HCN analysis conducted using HPIC.

Sample codes used

The data obtained from analysing the samples collected for acid gases and HCN during the large-scale testing is presented below. Each test has been given a code which is explained below.

IC represents Ion Chromatography.

Sample initial	Sample name
C	Cables
F	Polyurethane Foam
G	Plasterboard (gypsum board)
H	Heptane calibrations
P	OSB

Initial	Sample condition
W	Well-ventilated
U	Under-ventilated

Code	Sample Location
1	Door
2	Exhaust duct

Code	Sample time /min
1	0 to 5
2	5 to 10
3	10 to 15
4	15 to 20
5	20 to 25
6	25 to 30

Acid gas analysis

Table 15: HPIC data obtained from large-scale testing.

Sample Code	Fluoride mg/L	Chloride mg/L	Nitrite mg/L	Bromide mg/L	Nitrate mg/L	Phosphate mg/L	Sulphate mg/L
C-U-1-IC-1	0.005	0.195					0.167
C-U-1-IC-1	0.002	0.159			0.013		0.135
C-U-1-IC-2	0.001	0.174					0.151
C-U-1-IC-2		0.137	0.003		0.003		0.107
C-U-1-IC-3		0.165		0.005			
C-U-1-IC-3		0.128			0.003		0.098
C-U-1-IC-4	0.003	0.168		0.005		0.047	0.111
C-U-1-IC-4	0.001	0.140	0.003		0.003	0.025	0.107
C-U-1-IC-5	0.001	0.067		0.005		0.110	0.039
C-U-1-IC-5	0.001	0.140			0.003		0.112
C-U-2-IC-1	0.004	0.215					0.153
C-U-2-IC-1	0.004	0.223			0.004		0.178
C-U-2-IC-2	0.003	0.204					0.130
C-U-2-IC-2	0.001	0.203	0.003	0.005			0.162
C-U-2-IC-3	0.001	0.190			0.009		0.125
C-U-2-IC-3	0.004	0.196		0.005	0.009	0.008	0.153
C-U-2-IC-4	0.003	0.204			0.004		0.132
C-U-2-IC-4	0.004	0.212			0.004		0.172
C-U-2-IC-5	0.003	0.190	0.003		0.004	0.007	0.125
C-U-2-IC-5	0.003	0.196					0.137
C-W-1-IC-1	0.001	0.052	0.026		0.013	0.008	0.049
C-W-1-IC-1		0.050	0.026		0.013		0.072
C-W-1-IC-3	0.003	0.023	0.003		0.004	0.008	0.028
C-W-1-IC-3	0.001	0.027	0.007		0.004		0.029
C-W-1-IC-4	0.005	0.025	0.003		0.004	0.015	0.026
C-W-1-IC-4	0.003	0.023	0.003		0.004		0.039
C-W-1-IC-5	0.001	0.025					0.013
C-W-1-IC-5		0.023	0.003			0.008	0.026
CW-2-IC-1		0.023					0.023
C-W-2-IC-1		0.021			0.003		0.016
C-W-2-IC-2	0.001	0.036	0.007		0.009		0.046
C-W-2-IC-2	0.001	0.030	0.003	0.005			0.020
C-W-2-IC-2		0.034	0.007		0.004		0.055
CW-2-IC-3	0.004	0.025					0.023
C-W-2-IC-3	0.001	0.019					0.019
CW-2-IC-5	0.004	0.034			0.004		0.029
C-W-2-IC-5	0.002	0.028	0.003				0.023
C-W-3-IC-4	0.003	0.030					0.016
C-W-3-IC-4	0.001	0.022			0.003		0.019
F-- 1-IC-3	0.003	0.085	0.003	0.005	0.009		0.066
F2-U-2-IC-2	0.003	0.051		0.005			0.033
F2-U-2-IC-2	0.002	0.036				0.006	0.030

F2-U-2-IC-3		0.025	0.003	0.005			0.020
F2-U-2-IC-3		0.017					0.009
F2-U-2-IC-4	0.004	0.055		0.005	0.004		0.033
F2-U-2-IC-4	0.003	0.047					0.035
F2-U-2-IC-5	0.004	0.046	0.003	0.005	0.009	0.016	0.052
F2-U-2-IC-5		0.035					0.037
F2-U-2-IC-6	0.003	0.032	0.007	0.005			0.033
F2-U-2-IC-6		0.024					0.014
F2-U-2-IC-7	0.003	0.028	0.003		0.009		0.016
F2-U-2-IC-7		0.019					0.019
F-W-1-IC-1	0.003	0.080	0.024	0.011	0.017		0.111
F-W-1-IC-1	0.001	0.066	0.015		0.010		0.079
F-W-1-IC-2		0.051	0.007		0.009	0.016	0.085
F-W-1-IC-2	0.001	0.043	0.009				0.063
F-W-1-IC-3		0.041	0.003			0.016	0.072
F-W-1-IC-3		0.031	0.003				0.051
F-W-1-IC-4	0.001	0.034		0.005	0.004		0.095
F-W-1-IC-4		0.038	0.003				0.079
F-W-1-IC-5	0.003	0.041	0.003	0.005	0.004		0.095
F-W-1-IC-5		0.041					0.089
F-W-1-IC-6	0.004	0.037					0.043
F-W-1-IC-6	0.002	0.029					0.033
F-W-1-IC-7	0.005	0.039	0.003	0.005	0.009	0.016	0.029
F-W-1-IC-7	0.001	0.031					0.019
F-W-2-IC-1		0.034					0.052
F-W-2-IC-1	0.001	0.036			0.004		0.078
F-W-2-IC-2	0.001	0.039		0.005			0.057
F-W-2-IC-2	0.003	0.041			0.004		0.075
F-W-2-IC-3		1.045					0.057
F-W-2-IC-3	0.003	0.043					0.062
F-W-2-IC-4	0.037	0.045					0.054
F-W-2-IC-4	0.001	0.041	0.003				0.078
F-W-2-IC-5		0.041	0.003				0.070
F-W-2-IC-5	0.001	0.043				0.008	0.095
F-W-2-IC-6		0.023					0.018
F-W-2-IC-6		0.020	0.003				0.033
F-W-2-IC-7							
F-W-2-IC-7							
F-W-2-IC-7		0.051				0.008	0.007
F-W-2-IC-7		0.057					0.010
G-1-IC-1	0.003	0.052	0.007	0.005	0.013		0.067
G-1-IC-1	0.003	0.057	0.003		0.013		0.101
G-1-IC-2	0.001	0.027					0.031
G-1-IC-2	0.001	0.032			0.008	0.008	0.039
G-1-IC-3	0.003	0.032			0.004	0.008	0.023
G-1-IC-3		0.029					0.042
G-1-IC-4		0.029					0.031

G-1-IC-4		0.034					0.042
G-1-IC-5		0.025					0.031
G-1-IC-5		0.029			0.004		0.036
G-1-IC-6	0.004	0.036	0.003				0.018
G-1-IC-6	0.003	0.038					0.029
G-1-IC-7	0.003	0.036	0.003		0.009	0.023	0.059
G-1-IC-7		0.041	0.003		0.008	0.008	0.085
G-2-IC-1		0.032					0.065
G-2-IC-1	0.001	0.036	0.003			0.008	0.079
G-2-IC-2	0.003	0.011			0.004		0.022
G-2-IC-2	0.001	0.014					0.030
G-2-IC-3	0.001	0.011			0.004		0.073
G-2-IC-3		0.011					0.086
G-2-IC-4	0.003	0.014					0.040
G-2-IC-4	0.004	0.014	0.003	0.005	0.004		0.043
G-2-IC-5	0.003	0.066			0.013		0.100
G-2-IC-5	0.004	0.068			0.009		0.115
G-2-IC-6	0.001	0.014					0.024
G-2-IC-6		0.014			0.004		0.036
G-2-IC-7		0.011					0.032
G-2-IC-7	0.001	0.014					0.026
H-1-IC-1	0.003	0.041	0.003		0.013		0.075
H-1-IC-1	0.001	0.043		0.005	0.030		0.069
H-1-IC-1	0.003	0.043			0.021		0.076
H-1-IC-2	0.001	0.014					0.003
H-1-IC-2		0.011			0.004	0.008	0.016
H-1-IC-2	0.003	0.018			0.004	0.008	0.020
H-1-IC-3		0.009				0.008	0.013
H-1-IC-3	0.001	0.009	0.007		0.004		0.007
H-1-IC-3	0.001	0.009					0.010
H-1-IC-4		0.011			0.022	0.008	0.003
H-1-IC-4		0.009			0.017		0.010
H-1-IC-4	0.001	0.007			0.021		0.007
H-1-IC-5	0.001	0.021	0.003		0.009		0.452
H-1-IC-5		0.027	0.003		0.021		0.438
H-1-IC-5	0.001	0.023	0.003		0.017		0.458
H-1-IC-6		0.011	0.003	0.011	0.004		0.066
H-1-IC-6		0.009	0.003		0.013	0.016	0.059
H-1-IC-6	0.001	0.007			0.004		0.069
H-1-IC-7	0.001	0.007					0.010
H-1-IC-7	0.001	0.009	0.003		0.004		0.003
H-1-IC-7	0.001	0.007					0.003
H-2-IC-1		0.007	0.003		0.009		
H-2-IC-1	0.001	0.007			0.004		0.010
H-2-IC-2	0.004	0.007			0.022		
H-2-IC-2	0.001	0.005			0.026	0.008	0.003
H-2-IC-3	0.001	0.002	0.003		0.004		

H-2-IC-3		0.005					
H-2-IC-4		0.002	0.003		0.009		0.007
H-2-IC-4		0.005		0.005			0.003
H-2-IC-5	0.001	0.002	0.003	0.005	0.009		0.003
H-2-IC-5		0.007				0.008	0.010
H-2-IC-6		0.007				0.008	0.007
H-2-IC-6	0.003	0.007	0.003				0.020
H-2-IC-7		0.005			0.004	0.016	0.007
H-2-IC-7	0.001	0.005			0.004		0.003
P1-U-IC-6	0.009	0.043	0.003		0.004	0.015	0.023
P1-U-IC-6	0.009	0.041	0.003	0.011	0.004		0.029
P1-U-1-IC-1	0.004	0.059	0.286		0.030	0.015	0.062
P1-U-1-IC-1	0.001	0.059	0.294		0.030		0.082
P1-U-1-IC-2	0.005	0.052	0.117		0.013		0.031
P1-U-1-IC-2	0.004	0.048	0.111	0.005	0.004		0.036
P1-U-1-IC-3		0.045	0.016		0.004		0.041
P1-U-1-IC-3	0.003	0.045	0.013	0.011	0.008		0.033
P1-U-1-IC-4	0.005	0.059	0.003		0.026	0.008	0.031
P1-U-1-IC-4	0.004	0.054			0.034	0.008	0.046
P1-U-1-IC-5	0.003	0.048		0.005			0.044
P1-U-1-IC-5	0.001	0.048		0.005	0.004		0.039
P1-U-1-IC-6	0.001	0.036	0.003				0.026
P1-U-1-IC-6		0.041					0.029
P1-U-1-IC-7	0.001	0.041			0.004		0.026
P1-U-1-IC-7		0.038			0.004		0.036
P1-U-2-IC-1		0.036					0.023
P1-U-2-IC-1	0.001	0.032					0.022
P1-U-2-IC-2		0.027					0.020
P1-U-2-IC-2		0.027	0.003		0.009		0.013
P1-U-2-IC-3	0.001	0.029					0.025
P1-U-2-IC-3	0.001	0.032					0.029
P1-U-2-IC-4		0.029		0.005			0.010
P1-U-2-IC-4		0.034	0.003				0.016
P1-U-2-IC-5	0.001	0.034					0.018
P1-U-2-IC-5	0.001	0.036	0.003				0.019
P1-U-2-IC-6	0.001	0.036			0.004	0.007	0.025
P1-U-2-IC-6		0.036					0.029
P1-U-2-IC-7		0.043	0.003			0.007	0.010
P1-U-2-IC-7		0.045				0.008	0.022
P1-W-2-IC-1	0.003	0.034			0.009		0.030
P1-W-2-IC-1		0.042	0.003				0.035
P1-W-2-IC-2		0.030				0.008	0.038
P1-W-2-IC-2		0.033			0.008		0.038
P1-W-2-IC-3		0.034			0.004	0.008	0.213
P1-W-2-IC-3	0.001	0.033			0.008	0.008	0.260
P1-W-2-IC-4	0.001	0.037		0.005	0.004		0.040
P1-W-2-IC-4		0.036			0.004		0.036

P1-W-2-IC-5		0.037			0.004		0.024
P1-W-2-IC-5		0.036		0.005			0.032
P1-W-2-IC-6	0.004	0.041					0.024
P1-W-2-IC-6	0.001	0.042		0.005			0.026
P1-W-2-IC-7		0.030					0.024
P1-W-2-IC-7	0.001	0.034			0.004		0.043
P1-W-IC-2		0.045		0.005		0.008	0.031
P1-W-IC-2		0.048	0.003		0.004	0.008	0.039
P1-W-IC-3	0.001	0.048			0.009	0.008	0.052
P1-W-IC-3		0.052					0.065
P1-W-IC-4		0.036		0.005	0.004		0.052
P1-W-IC-4		0.038	0.003				0.072
P1-W-IC-5	0.008				0.004		0.015
P1-W-IC-5	0.006	0.043	0.003	0.005	0.004	0.008	0.029
P1-W-IC-7		0.020			0.004		0.005
P1-W-IC-7	0.003	0.029		0.005	0.004		0.036
P1-W-IC-7		0.020	0.003				0.016
P1-W-IC-7	0.001	0.034	0.003		0.008	0.008	0.049
P-W-1-IC-1	0.001	0.057	0.003		0.004		0.059
P-W-1-IC-1		0.059			0.004		0.075
P-W-1-IC-2		0.041					
P-W-1-IC-2		0.043				0.008	0.062
P-W-1-IC-3		0.045			0.004		0.026
P-W-1-IC-3	0.001	0.048	0.007		0.008		0.042
P-W-1-IC-5	0.001	0.032			0.004		0.013
P-W-1-IC-5		0.034		0.005		0.015	0.033
P-W-1-IC-6	0.004	0.034					0.085
P-W-1-IC-6		0.055			0.003	0.111	0.030
P-W-1-IC-7	0.003	0.048	0.114		0.004		0.031
P-W-1-IC-7	0.001	0.045	0.114		0.004		0.042
P-W-2-IC-1		0.028	0.003				0.024
P-W-2-IC-1		0.025		0.005	0.004		0.022
P-W-2-IC-2		0.041	0.007		0.009	0.008	0.038
P-W-2-IC-2		0.042	0.003				0.048
P-W-2-IC-3	0.001	0.078					0.038
P-W-2-IC-3	0.001	0.076			0.004		0.035
P-W-2-IC-4	0.001	0.064			0.004		0.032
P-W-2-IC-4	0.001	0.065		0.005			0.042
P-W-2-IC-5	0.003	0.041			0.004	0.008	0.032
P-W-2-IC-5	0.001	0.036					0.019
P-W-2-IC-6	0.001	0.050			0.004		0.035
P-W-2-IC-6		0.051					0.042
P-W-2-IC-7		0.028		0.005	0.004		0.019
P-W-2-IC-7		0.029					0.029

HCN data analysis

Table 16: HCN data obtained from large-scale testing.

Sample name	Total air through bubbler (L)	Bubble vol (L)	Sample dilution	mg/L (ppm)	g/L	g/L of gas	HCN ppm gas
F2-U1-CN-1	5	0.15	1	28.28781	0.028288	0.000881	782.2
F2-U-1-CN-1 10x dilution	5	0.15	10	1.419733	0.014197	0.000442	392.6
F2-U-1-CN-1 10x dilution	5	0.15	10	1.470895	0.014709	0.000458	406.7
F2-U1-CN-2	5	0.15	1	3.658426	0.003658	0.000114	101.2
F2-U1-CN-2	5	0.15	1	3.40007	0.0034	0.000106	94.0
F2-U1-CN-3	5	0.15	1	0.381188	0.000381	1.19E-05	10.5
F2-U1-CN-3	5	0.15	1	0.338008	0.000338	1.05E-05	9.3
F2-U1-CN-4	5	0.15	1	0	0	0	0.0
F2-U1-CN-4	5	0.15	1	0	0	0	0.0
F2-U1-CN-5	5	0.15	1	0	0	0	0.0
F2-U1-CN-5	5	0.15	1	0	0	0	0.0
F2-U1-CN-6	5	0.15	1	0	0	0	0.0
F2-U1-CN-6	5	0.15	1	0	0	0	0.0
F2-U1-CN-7	5	0.15	1	0	0	0	0.0
F2-U1-CN-7	5	0.15	1	0	0	0	0.0
F2-U2-CN-1	5	0.15	1	0	0	0	0.0
F2-U2-CN-1	5	0.15	1	0	0	0	0.0
F2-U2-CN-2	5	0.15	1	0	0	0	0.0
F2-U2-CN-2	5	0.15	1	0	0	0	0.0
F2-U2-CN-3	5	0.15	1	0	0	0	0.0
F2-U2-CN-3	5	0.15	1	0	0	0	0.0
F2-U2-CN-4	5	0.15	1	0	0	0	0.0
F2-U2-CN-4	5	0.15	1	0	0	0	0.0
F2-U2-CN-5	5	0.15	1	0	0	0	0.0
F2-U2-CN-5	5	0.15	1	0	0	0	0.0
F2-U2-CN-6	5	0.15	1	0	0	0	0.0
F2-U2-CN-6	5	0.15	1	0	0	0	0.0
F2-U2-CN-7	5	0.15	1	0	0	0	0.0
F2-U2-CN-7	5	0.15	1	0	0	0	0.0
F-W-1-CN-1	5	0.15	1	12.09505	0.012095	0.000377	334.5
F-W-1-CN-1	5	0.15	1	9.509028	0.009509	0.000296	262.9
F-W-1-CN-1 2x dilution	5	0.15	2	4.355589	0.008711	0.000271	240.9
F-W-1-CN-1 2x dilution	5	0.15	2	4.329589	0.008659	0.00027	239.4
F-W-1-CN-2	5	0.15	1	0.90408	0.000904	2.82E-05	25.0
F-W-1-CN-2	5	0.15	1	0.930805	0.000931	2.9E-05	25.7
F-W-1-CN-3	5	0.15	1	0.124964	0.000125	3.89E-06	3.5
F-W-1-CN-3	5	0.15	1	0.044537	4.45E-05	1.39E-06	1.2

F-W-1-CN-4	5	0.15	1	0.066923	6.69E-05	2.08E-06	1.9
F-W-1-CN-4	5	0.15	1	0	0	0	0.0
F-W-1-CN-5	5	0.15	1	0	0	0	0.0
F-W-1-CN-5	5	0.15	1	0	0	0	0.0
F-W-1-CN-6	5	0.15	1	0	0	0	0.0
F-W-1-CN-6	5	0.15	1	0	0	0	0.0
F-W-1-CN-7	5	0.15	1	0	0	0	0.0
F-W-1-CN-7	5	0.15	1	0	0	0	0.0
F-W-2-CN-1	5	0.15	1	0	0	0	0.0
F-W-2-CN-1	5	0.15	1	0	0	0	0.0
F-W-2-CN-2	5	0.15	1	0	0	0	0.0
F-W-2-CN-2	5	0.15	1	0	0	0	0.0
F-W-2-CN-3	5	0.15	1	0	0	0	0.0
F-W-2-CN-3	5	0.15	1	0	0	0	0.0
F-W-2-CN-4	5	0.15	1	0	0	0	0.0
F-W-2-CN-4	5	0.15	1	0	0	0	0.0
F-W-2-CN-5	5	0.15	1	0	0	0	0.0
F-W-2-CN-5	5	0.15	1	0	0	0	0.0
F-W-2-CN-6	5	0.15	1	0	0	0	0.0
F-W-2-CN-6	5	0.15	1	0	0	0	0.0
F-W-2-CN-7	5	0.15	1	0	0	0	0.0
F-W-2-CN-7	5	0.15	1	0	0	0	0.0
G-1-CN-1	5	0.15	1	0	0	0	0.0
G-1-CN-1	5	0.15	1	0	0	0	0.0
G-1-CN-2	5	0.15	1	0	0	0	0.0
G-1-CN-2	5	0.15	1	0	0	0	0.0
G-1-CN-3	5	0.15	1	0	0	0	0.0
G-1-CN-3	5	0.15	1	0	0	0	0.0
G-1-CN-4	5	0.15	1	0	0	0	0.0
G-1-CN-4	5	0.15	1	0	0	0	0.0
G-1-CN-5	5	0.15	1	0	0	0	0.0
G-1-CN-5	5	0.15	1	0	0	0	0.0
G-1-CN-6	5	0.15	1	0	0	0	0.0
G-1-CN-6	5	0.15	1	0	0	0	0.0
G-1-CN7	5	0.15	1	0	0	0	0.0
G-1-CN7	5	0.15	1	0	0	0	0.0
G-2-CN-1	5	0.15	1	0	0	0	0.0
G-2-CN-1	5	0.15	1	0	0	0	0.0
G-2-CN-2	5	0.15	1	0	0	0	0.0
G-2-CN-2	5	0.15	1	0	0	0	0.0
G-2-CN-3	5	0.15	1	0	0	0	0.0
G-2-CN-3	5	0.15	1	0	0	0	0.0
G-2-CN-4	5	0.15	1	0	0	0	0.0
G-2-CN-4	5	0.15	1	0	0	0	0.0
G-2-CN-5	5	0.15	1	0	0	0	0.0
G-2-CN-5	5	0.15	1	0	0	0	0.0
G-2-CN-6	5	0.15	1	0	0	0	0.0

G-2-CN-6	5	0.15	1	0	0	0	0.0
G-2-CN-7	5	0.15	1	0	0	0	0.0
G-2-CN-7	5	0.15	1	0	0	0	0.0
H-1-CN-1	5	0.15	1	0	0	0	0.0
H-1-CN-1	5	0.15	1	0	0	0	0.0
H-1-CN-2	5	0.15	1	0	0	0	0.0
H-1-CN-2	5	0.15	1	0	0	0	0.0
H-1-CN-3	5	0.15	1	0	0	0	0.0
H-1-CN-3	5	0.15	1	0	0	0	0.0
H-1-CN-4	5	0.15	1	0	0	0	0.0
H-1-CN-4	5	0.15	1	0	0	0	0.0
H-1-CN-5	5	0.15	1	0	0	0	0.0
H-1-CN-5	5	0.15	1	0	0	0	0.0
H-1-CN-6	5	0.15	1	0	0	0	0.0
H-1-CN-6	5	0.15	1	0	0	0	0.0
H-1-CN-7	5	0.15	1	0	0	0	0.0
H-1-CN-7	5	0.15	1	0	0	0	0.0
H-2-CN-1	5	0.15	1	0	0	0	0.0
H-2-CN-1	5	0.15	1	0	0	0	0.0
H-2-CN-2	5	0.15	1	0	0	0	0.0
H-2-CN-2	5	0.15	1	0	0	0	0.0
H-2-CN-3	5	0.15	1	0	0	0	0.0
H-2-CN-3	5	0.15	1	0	0	0	0.0
H-2-CN-4	5	0.15	1	0	0	0	0.0
H-2-CN-4	5	0.15	1	0	0	0	0.0
H-2-CN-5	5	0.15	1	0	0	0	0.0
H-2-CN-5	5	0.15	1	0	0	0	0.0
H-2-CN-6	5	0.15	1	0	0	0	0.0
H-2-CN-6	5	0.15	1	0	0	0	0.0
H-2-CN-7	5	0.15	1	0	0	0	0.0
H-2-CN-7	5	0.15	1	0	0	0	0.0
P-W-1-CN-1	5	0.15	1	0	0	0	0.0
P-W-1-CN-1	5	0.15	1	0	0	0	0.0
P-W-1-CN-2	5	0.15	1	0	0	0	0.0
P-W-1-CN-2	5	0.15	1	0	0	0	0.0
P-W-1-CN-3	5	0.15	1	0	0	0	0.0
P-W-1-CN-3	5	0.15	1	0	0	0	0.0
P-W-1-CN-4	5	0.15	1	0	0	0	0.0
P-W-1-CN-4	5	0.15	1	0	0	0	0.0
P-W-1-CN-5	5	0.15	1	0	0	0	0.0
P-W-1-CN-5	5	0.15	1	0	0	0	0.0
P-W-1-CN-6	5	0.15	1	0	0	0	0.0
P-W-1-CN-6	5	0.15	1	0	0	0	0.0
P-W-1-CN-7	5	0.15	1	0	0	0	0.0
P-W-1-CN-7	5	0.15	1	0	0	0	0.0
P-W-2-CN-1	5	0.15	1	0	0	0	0.0
P-W-2-CN-1	5	0.15	1	0	0	0	0.0

P-W-2-CN-2	5	0.15	1	0	0	0	0.0
P-W-2-CN-2	5	0.15	1	0	0	0	0.0
PW-2-CN-3	5	0.15	1	0	0	0	0.0
PW-2-CN-3	5	0.15	1	0	0	0	0.0
P-W-2-CN-4	5	0.15	1	0	0	0	0.0
P-W-2-CN-4	5	0.15	1	0	0	0	0.0
P-W-2-CN-5	5	0.15	1	0	0	0	0.0
P-W-2-CN-5	5	0.15	1	0	0	0	0.0
P-W-2-CN-6	5	0.15	1	0	0	0	0.0
P-W-2-CN-6	5	0.15	1	0	0	0	0.0
P-W-2-CN-7	5	0.15	1	0	0	0	0.0
P-W-2-CN-7	5	0.15	1	0	0	0	0.0

-
- 1 Stec. A.A., Hull. T.R. *Fire Toxicity*, Elsevier/Woodhead Publishing, Cambridge. 2010.
- 2 GB Fire Statistics 2021 and preceding editions, Home Office, London,
3 <https://www.gov.uk/government/collections/fire-statistics>
- 4 McKenna. S. T., Birtles. R., Dickens. K., et al. *Flame retardants in UK furniture increase smoke toxicity more than they reduce fire growth rate* (2018), *Chemosphere* (196), pp. 429-439
- 5 Bisby. L. *Grenfell tower inquiry*, Phase 1- Final Expert Report (2018), University Of Edinburgh
6 <https://www.grenfelltowerinquiry.org.uk/evidence/witness-statements-sharon-haley> Date
7 accessed: 03/08/2019
- 8 Molyneux. S., Hull. T., Stec. A.A. *The correlation between carbon monoxide and hydrogen cyanide in fire effluents of flame retarded polymers* (2014), *Fire Safety Science*, pp. 389-403.
- 9 ISO TS 19706:2011- Guidelines for assessing the fire threat to people.
- 10 Stec. A.A. *Fire Toxicity- The elephant in the room* (2017), *Fire Safety Journal* (91), pp. 79-90.
- 11 UK. Gov. UK Fire statistics, 1955-2017.
- 12 Purser. D., Hull. T. R. *Prediction of CO evolution from small-scale polymer fires* (2000), *Polymer International* (49), pp. 1259-1265.
- 13 Hirschler. M. M. *Safety, health and environmental aspects of flame retardants* (2013), *The Handbook of Fire Retarded textiles- Woodhead publishing limited*, pp. 117-119.
- 14 Chief fire & Rescue Adviser. *Generic Risk Assessment 5.8- Flashover, backdraught and fire gas ignitions* (2009), *Fire and Rescue Service Operational Guidance*, pp. 5-7.
- 15 Purser. D. *Fire Toxicity and Toxic Hazard Analysis* (2011), *Sixth International Seminar on Fire and Explosion Hazards*, pp. 721-734.
- 16 Purser. D. A. *Toxic combustion product yields as a function of equivalence ratio and flame retardants in under-ventilated fires: Bench-Large-Scale comparisons* (2016) *Polymers* (8), 330.
- 17 Pitts. W. M. *The global equivalence ratio concept and the formation mechanisms of carbon monoxide in enclosure fires* (1995), *Progress in Energy and Combustion science* (21), pp. 197-237.
- 18 Babrauskas. V., Parker. W. J., Mulholand. G., Twilley. W. H., *The phi meter: A simple, fuel-dependant instrument for monitoring combustion equivalence ratio* (1994), *Review of Scientific Instruments* (65), 7, pp. 2367-2375.
- 19 Hull. T. R., Stec. A. A. *Polymers and Fire* (2009), *Fire Retardancy of Polymers: New Strategies and Mechanisms*, Edited by T. R Hull and B. K. Kandola, pp. 1-14
- 20 Grand. A. F., Wilkie. C. A. *Chemical Aspects of Thermal Decomposition* (2012), *Fire retardancy of polymeric materials*, pp. 45-52.
- 21 Witkowski. A., Stec. A. A., Hull. T. R. *Thermal decomposition of polymeric materials* (2016), *SFPE handbook of fire protection engineering*, pp. 167-254.
- 22 Drysdale. D. *An introduction to Fire dynamics (second edition) (book)*, John Wiley & Sons.
- 23 McKenna. S. T. Thesis, *The fire hazards of insulation materials* (2019), University of Central Lancashire.
- 24 *Air quality in Europe -2020 report*, European Environment Agency.
- 25 Pilling. M. J., Seakins. P.W. *Reaction kinetics* (1995), Oxford university press, pp. 248-249.
- 26 Purser D.A. and Purser, J.A., *HCN yields and fate of fuel nitrogen for materials under different combustion conditions in the ISO 19700 tube furnace and large-scale fires* (2009), *Fire Safety Science*, pp. 1117-1128.
- 27 Stec. A. A. *Fire Toxicity- The elephant in the room?* (2017), *Fire Safety Journal* (91), pp. 79-90
- 28 McKenna. S. T., Birtles. R., et al. *Flame retardants in UK furniture increase smoke toxicity more than they reduce fire growth rate* (2017), *Chemosphere*.
- 29 Levin. B. *New Approaches to toxicity: a seven-gas predictive model and toxicant suppressants* (1997), *Drug and chemical toxicology* (4), pp. 271-280.
- 30 ISO 13571:2012 Life-threatening components of fire- Guidelines for the estimation of time to compromised tenability in fires

- 28 Tsuchiya. Y., Sumi. K. *Evaluation of the toxicity of combustion products* (1972), Journal of Fire and
Flammability (3), pp 46-50
- 29 ISO 13344:2015 Estimation of lethal toxic potency of fire effluents.
- 30 Greenberg. M. I., et al. *Occupational, Industrial and Environmental Toxicology* (2003), Elsevier
Health Sciences, pp. 369-371.
- 31 Environmental Protection Agency. *Toxicological review of hydrogen cyanide and cyanide salts*
(2010), U. S. Environmental Protection Agency, Washington, DC, pp. 7-19.
- 32 Aimeonova. F. P., Fishbein. L. *Hydrogen cyanide and cyanides: Human health aspects* (2004), World
Health Organisation Geneva, pp. 1-73
- 33 Lawson-smith. P., Janssen. E., Hyldegaard. O. *Cyanide intoxication as part of smoke inhalation- a
review on diagnosis and treatment from the emergency perspective* (2011), Scandinavian Journal of
Trauma, Resuscitation and Emergency Medicine (19), pp. 1-5.
- 34 Walsh. D. W., Eckstein. M. *Hydrogen cyanide in fire smoke: an underappreciated threat* (2004),
Emergency medical services (22), pp. 160-163.
- 35 Layton. M., Roper. D. *Investigation of the Hereditary Haemolytic Anaemias* (2017), Dacie and Lewis
Practical Haematology (12), pp. 228-253.
- 36 Goldstein. M. *Carbon Monoxide Poisoning* (2007), Journal Of Emergency Medicine (6), pp. 538-542.
- 37 Srisont. S., Chirachariyavej. T., Peonim. A. *A carbon dioxide fatality from dry ice* (2009), Journal of
Forensic Science (54), 4, pp. 961-962.
- 38 Langford. N.J. *Carbon dioxide poisoning* (2005), Toxicological reviews (24), 4, pp. 229-235.
- 39 Permentier. K., Vercammen. S., et al. *Carbon dioxide poisoning: a literature review of an often
forgotten cause of intoxication in the emergency department* (2017), International Journal of
Emergency Medicine (10), pp. 1-4.
- 40 Brand. G., Jacquot. L., Regnier. M. *Toxicity of Carbon Dioxide: A review* (2011), Chemical Research
in Toxicology (24), pp. 2061-2070
- 41 Purser. D. A. *Hazards from smoke and irritants- Chapter 3* (2010), Fire Toxicity, Woodhead
Publishing.
- 42 National Research Council. *Acrolein, Acute exposure guideline levels* (2010), Acute Exposure
Guideline levels for selected airborne chemicals (8), pp. 13-48.
- 43 World Health Organisation. *Chapter 5.8 Formaldehyde* (2001), Air Quality Guidelines- Second
edition, pp. 2-25.
- 44 Jayalaksmi. K., Ravikumar. H., Naidu. J., et al. *Review Article: A silent killer- Formaldehyde: review of
effects and management* (2011), International Journal of Oral and Maxillofacial pathology, pp.
2231-2250.
- 45 Roberts. A., Johnson. N., Cudkowicz. M., et al. *Job-related formaldehyde exposure and ALS
mortality in the USA* (2016), Neurology, Neurosurgery and Psychiatry (87), 7, pp. 786-788.
- 46 TOXNET. *Formaldehyde*, Toxicology Data Network. Date accessed: 10/08/2019
- 47 Al-Sayegh. W., Aljumaiah. O., et al. *Wood crib with PVC cables: Compartment fire toxicity* (2016),
Proceedings 8th International Seminar on Fire and Explosion Hazards.
- 48 Hull. T., Stec. A., Paul. K. *Hydrogen chloride in Fires* (2009), Fire Safety Science (9), pp. 665-676.
- 49 Agabiti. N., Ancona. C., et al. *Short term respiratory effects of acute exposure to chlorine due to a
swimming pool accident* (2001), Occupational and Environmental Medicine (58), pp. 399-404.
- 50 National Research Council (US) Sub-committee on Rocket-emission toxicants. *Assessment of
Exposure-Response Functions for Rocket Emission Toxicants* (1998), National Academies Press (US),
pp.
- 51 Heath protection Agency. *Hydrogen Chloride- A Toxicological Overview* (2007), Toxicological
Overview, pp. 1-9.
- 52 E. A. Higgins., V. Fiorca., A. A. Thomas., et al. *Acute toxicity of brief exposures to HF, HCl, NO2 and
HCN with and without CO* (1972), Fire Technology (8), pp. 120-130.
- 53 Salem. H., Katz. S.A. *Toxicology of fire and smoke* (2006), Inhalation Toxicity, CRC Press Taylor and
Francis Group pp. 207-231.

-
- 54 Pavelka. S. *Metabolism of Bromide and Its Interference with the Metabolism of Iodine* (2004),
Physiological Research (53), pp. 81-90
- 55 Young. J. D., Dyar. O., Xiong. L., Howell. S. *Methamoglobin production in normal adults inhaling low
concentrations of nitric oxide* (1994), Intensive Care Medicine (20), pp. 581-584.
- 56 Cohen. R. A., Adachi. T. *Nitric-oxide-induced vasodilation: regulation by physiologic s-
glutathiolation and pathologic oxidation of the sarcoplasmic endoplasmic reticulum calcium ATPase*
(2006), Trends In Cardiovascular Medicine (4), pp. 109-114.
- 57 Hull. T., Carman. J. M., Purser. D. A. *Prediction of CO evolution from small-scale polymer fires* (2000), Polymer
International (49), pp. 1259-1265.
- 58 Richter, H., Howard, J.B. Formation of polycyclic aromatic hydrocarbons and their growth to soot-a
review of chemical reaction pathways, 2000, Progress in Energy and Combustion Science,
26(4):565-608.
- 59 Blomqvist P. Emissions from Fires. Ph. D thesis, Lund University; 2005
- 60 Miller. K. P., Ramos. K. S. *Impact of Cellular metabolism on the biological effects of benzo[a]pyrene
and related hydrocarbons* (2001), Drug Metabolism Reviews (1), pp. 1-35.
- 61 Yang. P., Ma. J., Zhang. B., et al. *CpG site-specific hypermethylation of p16INK4a in peripheral blood
lymphocytes of PAH-exposed Workers* (2012), Cancer Epidemiol Biomarkers and Prevention (21),
pp. 182-190.
- 62 Sparkman. O. D., Kitson. F., et al. *Isocyanates* (2011), Gas chromatography and Mass Spectrometry
(second edition): A practical guide, Elsevier, pp. 341-344.
- 63 Malo. J., Ghezzi. H., Elie. R. *Occupational Asthma caused by isocyanates patters of asthmatic
reactions to increasing day to day doses* (1999), American journal of respiratory and critical care
medicine (6), pp. 1879- 1883.
- 64 Wisnewski. A., Lemus. R., et al. *Isocyanate-conjugated human lung epithelial cell proteins: A link
between exposure and asthma* (1999), The Journal Of Allergy and Clinical Immunology (104), pp.
341-347.
- 65 Harries. M. G., Burge. S., et al. *Isocyanate asthma: respiratory symptoms due t 1,5-naphthylene di-
isocyanate* (1979), Official journal of the British Thoracic Society (34), pp. 762-766.
- 66 Vallero. D. *Chapter 6: Inherent properties of air pollutants* (2014), Fundamentals of Air Pollution
(5th edition), pp. 139-195.
- 67 Mckenna. S. T., Jones. N., Peck. G., Hull. T., et al. *Fire behaviour of modern façade materials –
Understanding the Grenfell Tower fire* (2019), Journal of hazardous materials (368), pp. 115-123
- 68 ISO 16312-2: *Guidance for assessing the validity of physical fire models for obtaining fire effluent
toxicity data for fire hazard risk assessment- Part 2: Evaluation of individual physical fire models*
(2017), ISO Geneva.
- 69 ISO 5659-2 *Plastics- Smoke Generation Part 2: Determination of optical density by a single-chamber
test* (2017) International Standard Fourth Edition.
- 70 2010 Fire test Procedure Code, Maritime Safety Committee, (MSC 87/26/Add.3) Annex 34, Part 2
Smoke and Toxicity Test, International Maritime Organisation, London.
- 71 EN 45545-2:2013 Railway Applications. Fire Protection on railway vehicles. Requirements for fire
behaviour of materials and components.
- 72 EN 2826:2011 Aerospace series- Burning behaviour of non metallic materials under the influence
of radiating heat and flames- Determination of gas components in the smoke; ABD 0031 Fire-
Smoke-Toxicity (FST) Test specification (Airbus industries); Boeing BSS
- 73 Hull. T. R., Stec. A. A., Kaczorek-Chrobak. K. *Carbon monoxide generation in fires: Effects of temperature on
halogenated aromatic* (2011), Fire Safety Science, pp. 253-263.
- 74 ISO 5660: 2020 Reaction-to-fire tests — Heat release, smoke production and mass loss rate — Part
5: Heat release rate (cone calorimeter method) and smoke production rate (dynamic
measurement) under reduced oxygen atmospheres.
- 75 Hull. T. R. *Challenges in fire testing: reaction to fire tests and assessment of fire toxicity* (2008),
Advances In Fire Retardant Materials, Woodhead Publishing, Cambridge, pp. 255-290.

-
- ⁷⁶ Hietaniemi, J., Kallonen, R., Mikkola, E. *Burning characteristics of selected substances: Production of heat, smoke and chemical species*. Fire and Materials, (1999) 23, pg. 171-185
[http://dx.doi.org/10.1002/\(SICI\)1099-1018\(199907/08\)23:4<171::AID-FAM680>3.0.CO;2-C](http://dx.doi.org/10.1002/(SICI)1099-1018(199907/08)23:4<171::AID-FAM680>3.0.CO;2-C)
- ⁷⁷ BS 7990:2003 *Tube furnace method for the determination of toxic product yields in fire effluents*
- ⁷⁸ LeTallec, Y., Smith, D. A., Hunter, J., and Groenfeld, F.R., Evaluation of toxicants for materials used in military vehicles and equipment, 10th International Fire Science and Engineering Conference (Interflam) 631-637, (2004).
- ⁷⁹ ISO/TS 19700:2016 Controlled equivalence ratio method for the determination of hazardous components of fire effluents — Steady-state tube furnace
- ⁸⁰ Purser, D. A., Hull, T. R., Blomqvist, P., et al. *Repeatability and reproducibility of the ISO /TS 19700 steady state tube furnace* (2012), Fire Safety Journal (55), pp. 22-34.
- ⁸¹ J.A. Purser, D.A. Purser, A.A. Stec, C. Moffatt, T.R. Hull, J.Z. Su, M. Bijloos, P. Blomqvist. *Repeatability and reproducibility of the ISO/TS 19700 steady state tube furnace* (2013), Fire Safety Journal (55), pp. 22-34.
- ⁸² ISO 12136:2011, Reaction to fire tests - Measurement of material properties using a fire propagation apparatus.
- ⁸³ ASTM E2058 - 19 Standard Test Methods for Measurement of Material Flammability Using a Fire Propagation Apparatus (FPA)
- ⁸⁴ Tewarson, A., *Generation of heat and chemical compounds in fires* (2002), SFPE handbook of fire protection engineering (3), pp. 3-82.
- ⁸⁵ ASTM E1678; NFPA 265: Combustion Toxicity Test Apparatus
- ⁸⁶ McKenna, S. T. Thesis, *The fire hazards of insulation materials* (2019), University of Central Lancashire.
- ⁸⁷ ISO 19701:2013 – Methods for Sampling and Analysis of Fire Effluents
- ⁸⁸ Blomqvist, P., Sandinge, A. *Experimental evaluation of fire toxicity test methods* (2018), Research Institute of Sweden, Safety and transport fire research, pp. 1-134.
- ⁸⁹ Hull, T. R., Purser, D. A., Stec, A. A. *Fire toxicity assessment: Comparison of asphyxiant yields from laboratory and large-scale flaming fires* (2014), Fire Safety Science (11), pp
- ⁹⁰ Gersen, S., Mokhov, A. V., Levinsky, H. B. *Diode laser absorption measurement and analysis of HCN in atmospheric-pressure, fuel-rich premixed methane/air flames* (2008), Combustion and Flame (155), pp. 267-276.
- ⁹¹ ASTM EN1678-15. *Standard test method for measuring smoke toxicity for use in fire hazard analysis* (2015), ASTM international
- ⁹² Marsh, N. D., Gann, R. G. NIST Technical note 1760: Smoke Component Yields from Bench-scale Fire Tests: 1. NFPA 269/ ASTM EN 1678 (2013), NIST Fire Research Division Engineering Laboratory, pp 1-57.
- ⁹³ Marsh, N. D., Gann, R. G. NIST Technical note 1761: Smoke component yields from bench-scale fire tests: 2. ISO 19700 Controlled Equivalence ratio tube furnace (2013), NIST Fire Research Division Engineering Laboratory, pp. 1-45.
- ⁹⁴ Marsh, N. D., Gann, R. G. NIST Technical note 1762: Smoke Component yields from bench-scale fire tests: 3. ISO 5660-1 /ASTM E 1354 with Enclosure and variable oxygen concentration (2013), NIST Fire Research Division Engineering Laboratory, pp. 1-37
- ⁹⁵ Marsh, N. D., Gann, R. G. NIST Technical note 1763: Smoke Component yields from bench-scale fire tests: 4. Comparison with room fire results (2013), NIST Fire Research Division Engineering Laboratory, pp. 1-35.
- ⁹⁶ Kaplan, H.L., Grand, A.F., Switzer, W.G., Mitchell, D.S., Rogers, W.R., Hartzell, G.E. Effects of Combustion Gases on Escape Performance of the Baboon and the Rat (1985), Journal of Fire Sciences (3), pp. 228-244.

-
- ⁹⁷ ISO/TS 19700:2016 Controlled equivalence ratio method for the determination of hazardous components of fire effluents — Steady-state tube furnace
- ⁹⁸ ISO 5660:2015 Reaction-to-fire tests — Heat release, smoke production and mass loss rate — Part 1: Heat release rate (cone calorimeter method) and smoke production rate (dynamic measurement)
- ⁹⁹ Marsh. N. D., Gaan. R. G., Nyden. M. R. *Observations on the generation of toxic products in the NFPA/ISO Smoke Density Chamber* (2010), Proceedings of the 12th international conference on fire science and engineering, (Interflam), Nottingham, UK.
- ¹⁰⁰ Technical Bulletin 133: Flammability test procedure for seating furniture for use in public occupancies (1991): State of California, USA.
- ¹⁰¹ *Regulation No 305/2011 of the European Parliament and of the Council: Harmonised conditions for the marketing of construction products* (2011). Official Journal of the European Union.
- ¹⁰² The Commission of The European Communities. *2006/751/EC: Commission Decision of 27 October 2006 amending Decision 2000/147/EC implementing Council Directive 89/106/EEC as regards the classification of the reaction-to-fire performance of construction products (notified under document number C(2006) 5063)* (2006), Official Journal of the European Union, pp. 1-5.
- ¹⁰³ ISO 9705:1993 Fire tests- Full-scale room test for surface products
- ¹⁰⁴ Messerschmidt. B. *The Capabilities and imitations of the Single Burning Item (SBI) Test* (2005), Rockwool International A/S, Denmark, Fire and Building Safety in the Single European Market, pp. 70-81.
- ¹⁰⁵ Björn Sundström, *The development of a European Fire Classification System for Building Products Test Methods and Mathematical Modelling*, Doctoral Thesis, Department of Fire Safety Engineering, Lund University, Sweden, 2007
- ¹⁰⁶ BS ISO 29903:2012. *Guidance for comparison of toxic gas data between different physical fire models and scales.*
- ¹⁰⁷ Babrauskas. V., Parker. W. J., et al. *The Phi meter: A simple, fuel-independent instrument for monitoring combustion equivalence ratio* (1994), Review of Scientific Instruments, 65 (7), pp. 2367-2375.
- ¹⁰⁸ Lonnermark. A., Blomqvist. P., Mansson. M., Persson. H. *TOXFIRE-Fire characteristics and smoke gas analysis in under-ventilated large-scale combustion experiments* (1996), SP Report. Pp. 1-129.
- ¹⁰⁹ Blomqvist. P., Sandinge. A. *Experimental evaluation of fire toxicity test methods* (2018), Research Institute of Sweden, Safety and transport fire research, pp. 1-134.
- ¹¹⁰ Hull. T. R., Stec. A. A. *Chapter 5: Generation, Sampling and Quantification of Toxic combustion Products* (2016) Toxicology, Survival and Health Hazards of Combustion Products, Issues in Toxicology (23), Royal Society of Chemistry, pp. 108-138. Edited by Purser. D., Maynard. R and Wakefield. J.
- ¹¹¹ Blomqvist, P., Hertzberg, T. and Tuovinen, H. *A small-scale controlled equivalence ratio tube furnace method – Experience of the method and link to large-scale fires* (2007), Proceedings of the 11th International Interflam Conference, Interscience Communications Ltd., London, pp. 391-402.
- ¹¹² Stec, A. A., Hull, T. R., Lebek, K., Purser, J. A., and Purser, D. A. *The effect of temperature and ventilation condition on the toxic product yields from burning polymers* (2008), Fire and Materials (32), pp. 49-60.
- ¹¹³ Babrauskas. V., Parker. W. J., Mulholand. G., Twilley. W. H., *The phi meter: A simple, fuel-dependant instrument for monitoring combustion equivalence ratio* (1994), Review of Scientific Instruments (65), 7, pp. 2367-2375.
- ¹¹⁴ Liu. X., Hao. J., Gaan. S. *Recent studies on the decomposition and strategies of smoke and toxicity suppression of polyurethane based materials* (2016), Royal Society of Chemistry Advances (22), pp. 74742-74756.

-
- ¹¹⁵ Hull. T. R., Paul. K. T., Stec. A. A. *Hydrogen chloride in fires* (2008). Fire Safety Science- Proceedings of the ninth international symposium, pp. 665-676.
- ¹¹⁶ Ma J, Purnendu KD (2010) Recent Developments in Cyanide Detection: A Review, *Analytica Chimica Acta*, 673 (2), p117-125
- ¹¹⁷ Hull TR, Stec AA (2015) Generation, Sampling and Quantification of Toxic Combustion Products. In: Purser DA, Maynard RL, Wakefield, JC (eds.) *Toxicology, Survival and Health Hazards of Combustion Products*, RSC, ISBN: 1849735697
- ¹¹⁸ Delgado A, et al (2008) Cyanide Management through Proper Measurement, *Hydrometallurgy, Proceedings of the Sixth International Symposium*, ISBN: 0873352661
- ¹¹⁹ Schneider. M. E., Kent. L. A. *The design and application of bi-directional velocity probes for measurements in large-scale pool fires* (1987) Instrument Society of America (26) 4, pp. 2-9.
- ¹²⁰ Steckler. K. D., Quintiere. J. G., Rinkinen. W. J. *Flow induced by Fire in a compartment*, 19th symposium (Intl.) on combustion (1982), The Combustion Institute, Pittsburg, pp. 913-920
- ¹²¹ Sundstrom. B., Wickstrom. U. *FIRE: Full Scale Tests; Calibration of Test Room -Part 1* (1981), Technical Report SP-RAPP, Boras, Sweden
- ¹²² Babrauskas. V. *Upholstered furniture room measurements, comparison with furniture calorimeter data, and flashover predictions* (1984), *Journal of Fire Sciences* (2), pp. 5-19.
- ¹²³ ASTM D7309-21b: 2021- Standard test method for determining flammability characteristics of plastics and other solid materials using microscale combustion calorimetry.